Spatio-Temporal Numerical Modelling of Whooping Cough Dynamics

A thesis submitted for the degree of Doctor of Philosophy

by

Wirawan Piyawong

Department of Mathematical Sciences, Brunel University

May 2001

Abstract

The *SIR* (Susceptible/Infectious/Recovered) whooping cough model involving non-linear ordinary differential equations is studied and extended to incorporate (i) diffusion (ii) convection and (iii) diffusion-convection in one-space dimension. First- and second-order finite-difference methods are developed to obtained the numerical solutions of the ordinary differential equations. Though implicit in nature, with the resulting improvements in stability, the methods are applied explicitly. The proposed methods are economical and reliable in comparison to classical numerical methods. When extended to the numerical solutions of the partial differential equations, the solutions are found by solving a system of linear algebraic equations at each time step, as opposed to solving a non-linear system, which often happens when solving non-linear partial differential equations.

Acknowledgements

I would like to express my gratitude to my supervisor Professor E.H. Twizell for his invaluable suggestions, continuous encouragement and for always having an open door throughout the period of my thesis. I have learned a great deal from him and, for all that he has done, I am deeply grateful.

This is a pleasant opportunity to thank Miss M. A. Grubb and Dr J.-E. Furter for their lectures on dynamical systems. I would like to take the opportunity also to thank Mr P. Kaewtrakulpong for his help with the computer package Matlab. I wish to express my gratitude to King Mongkut's University of Technology Thonburi for the scholarship and support provided throughout the duration of this thesis. I also would like to thank the staff in the Department of Mathematical Sciences here at Brunel and my friends both in academia and elsewhere for making my research time enjoyable.

Finally, I wish to dedicate this thesis to the memory of my father and my sincere thanks also go to my family who have been not only supportive but also encouraging and understanding at all times; this could not have been done without you.

TO THE MEMORY OF
MY FATHER

Contents

List of Figures

List of Tables

Chapter 1

Introduction

The study of epidemics has a long history with a large variety of models and explanations for the spread and cause of epidemic outbreaks. The study of disease occurrence is called epidemiology. An epidemic is an unusually large, short-term outbreak of a disease. A disease is called endemic if it persists in a population. Mathematical models of the population dynamics of disease can contribute to a better understanding of epidemiological patterns and disease control. Much of the theoretical discussion of the dynamics of epidemics of childhood diseases has been modelled mathematically using the *SIR* (Susceptible-Infective-Recovered) model (Anderson & May [3]). This model is a simple model of epidemic spread in which disease is transmitted by direct contact between hosts who become immune after a single infection, and are thus ideally suited to the testing of the mathematical model and numerical methods developed for the solution of the model equations.

Chaotic behaviour can be found in many areas of the chemical, physical and biological sciences and in many areas of engineering. Epidemiology is one of the areas of the bio-medical sciences in which chaotic behaviour is believed to be possible (Schaffer & Kot [26]); it is one of the profusion of examples given in the popular book by Gleick [11].

The examples given above are of dynamic behaviour, though it must be emphasized that not all dynamic systems in bio-medical system exhibits chaos. In recent times the phenomenon of chaos has brought about beneficial collaboration between bio-medical researchers and mathematicians. Such collaboration has often resulted

in the mathematical modelling of a bio-medical system by a non-linear ordinary or partial equations or by a system of such equations. Often, the intention in compiling such a model is to reproduce observations before using the model to make predictions.

Careful analysis, therefore, must be carried out to ensure that the mathematical model does not predict chaos in the system under investigation, when chaos is not a feature of that system. Further care must be taken to ensure that a numerical method chosen to solve the model equations does not predict chaos when chaos is not a feature of either the bio-medical system or the theoretical solution of the associated model equations. Such chaos was described as *contrived chaos* in the article by Twizell *et al.* [30].

In this thesis, the *SIR* model of whooping cough dynamics is studied. The model equation will be a system of ordinary differential equations (ODEs) which is extended to three types of system of partial differential equations (PDEs), namely reaction-diffusion, reaction-convection and reaction-convection-diffusion types. The aim of the thesis is to develop finite-difference schemes for the numerical solution of the ordinary and partial differential equations in which chaotic behaviour is not inherent.

The efficient numerical integration of systems of non-linear differential equations over long time intervals necessitates the use of time steps which are the largest possible, bearing in mind accuracy and stability. Explicit methods, such as the Euler method or Runge-Kutta methods, are extensively used in solving systems of ODEs. These methods, however, may lead to chaotic or spurious solutions which are not a feature of the differential equation nor of the physical processes being modelled, see Ablowitz & Herbst [1] and Corless *et al.* [6]. Explicit methods are also well known to be inexpensive to implement when used to compute the solutions of non-linear PDEs but they have poor numerical-stability properties (see, for instance, Lambert [15] and Twizell [28]). To avoid contrived chaos, while retaining efficiency and stability, the user may need to discard explicit numerical methods and turn instead to implicit methods. The numerical schemes to be developed are implicit in nature but are applied explicitly; therefore they are convenient, appropriate and

easy to implement for the solution of various problems of non-linear PDEs.

Solving systems of non-linear ODEs and PDEs requires the solution of a non-linear algebraic system using, say, the well-known Newton-Raphson method for a system. In order to obviate the need to use a relatively expensive, non-linear, algebraic solver such as the Newton-Raphson method for a system, while continuing to benefit from the superior stability properties of implicit methods, Twizell *et al.* [30] proposed numerical methods for the solution of differential equations of the forms

$$\mathrm{d}w/\mathrm{d}t = f(w)$$

and

$$\partial u/\partial t = \partial^2 u/\partial x^2 + g(u)$$

in which $w = w(t)$ and $u = u(x,t)$ are real-valued functions, $x \in \mathbb{R}$ is a space variable and $t \in \mathbb{R}^+$ represents time. Twizell *et al.* [30] approximated the non-linear functions $f(w)$ and $g(u)$ by splitting them and evaluating terms in the splitting at different time levels. This idea will be employed in subsequent chapters of this thesis in ways with permit the solutions of ODEs to be determined *explicitly* from what appear to be *implicit* numerical methods and the solution of non-linear PDEs to be obtain by solving a linear algebraic system at each time step.

The numerical methods developed in this thesis can be applied by using several processors working in parallel. This is an important feature in terms of efficiency and speed in computing. Programs are designed and written in the FORTRAN 77 programming language. The software package Matlab v5.2 is used to plot all figures in this thesis.

In Chapter 2 various preliminary definitions and theorems needed in the development and analyses of the numerical methods in later chapters are given.

Chapter 3 deals with the *SIR* whooping cough model. This model consists of a system of non-linear ordinary differential equations which is studied qualitatively and numerically by using first- and second-order finite-difference schemes. Four numerical methods are developed, analysed and tested to solve the *SIR* whooping

cough model. The first method is the well-known first-order explicit Euler method. The others are first-order numerical methods and a second-order numerical method. The introduction of seasonal variation into the *SIR* whooping cough model leading to periodic and chaotic dynamics is presented by numerical simulations.

In Chapters 4, 5, 6, the *SIR* whooping cough model is extended to the three types of one-space dimension partial differential equation models, which are reaction-diffusion equations, reaction-convection equations and reaction-diffusion-convection equations, respectively.

Chapter 4 has added a space dimension into the *SIR* whooping cough model and considered the corresponding reaction-diffusion equations. A family of finite-difference schemes are analysed and used to solve the reaction-diffusion equations. The numerical results will be investigated for different values of the diffusion rate using two experiments.

Chapter 5 introduces a one-dimensional whooping cough model of reaction-convection type. Two numerical methods are analysed and tested to approximate the equations of the model. The von Neumann method is used to examine stability of the proposed methods and numerical solutions are given for the numbers of susceptible and infectious individuals.

Chapter 6 will study the whooping cough dynamics in the case where reaction, diffusion and convection terms are present. A family of methods are analysed for the solution of the reaction-convection-diffusion equations. The maximum principle analysis is used to prove convergence of the proposed method. The numerical results for different values of diffusion and convection rates are obtained and discussed.

Part of the contents of Chapter 3 have been contained in a technical report by Piyawong and Twizell [21].

Chapter 2

Mathematical Preliminaries

2.1 The Mean Value Theorem and Taylor's Theorem

The following theorems are of fundamental importance in deriving methods for error estimation that will be needed in later chapters.

Theorem 2.1 (Mean Value Theorem) If $f(x)$ is a continuous function on $[a, b]$ and differentiable on (a, b), then a number c in (a, b) exits with

$$f(b) - f(a) = f'(c)(b - a). \tag{2.1.1}$$

Theorem 2.2 (Mean Value Theorem in two variables) If $f(x, y)$ is differentiable, then there exists a point (x_0, y_0) on the line connecting the points (x_1, y_1) and (x_2, y_2) such that

$$f(x_2, y_2) - f(x_1, y_1) = \frac{\partial f}{\partial x}(x_0, y_0)(x_2 - x_1) + \frac{\partial f}{\partial y}(x_0, y_0)(y_2 - y_1). \tag{2.1.2}$$

The proofs of these theorems can be found in any standard text (see, for example, Sandefur [25]). One of the most important tools of numerical analysis is Taylor's theorem and the associated Taylor series and may be founded in Burden & Faires [5].

Theorem 2.3 (Taylor, one-dimensional) Assume that f has continuous derivatives of order $n+1$ in an interval (a, b) containing x_0. Then, for every $x \in [a, b]$ there

exists a number ξ between x_0 and x with

$$f(x) = P_n(x) + R_n(x), \tag{2.1.3}$$

where

$$\begin{aligned} P_n(x) &= f(x_0) + f'(x_0)(x - x_0) + \frac{1}{2}f''(x_0)(x - x_0)^2 + \ldots + \frac{f^{(n)}(x_0)}{n!}(x - x_0)^n \\ &= \sum_{k=0}^{n} \frac{f^{(k)}(x_0)}{k!}(x - x_0)^k, \end{aligned} \tag{2.1.4}$$

and

$$R_n(x) = \frac{f^{(n+1)}(\xi)}{(n+1)!}(x - x_0)^{n+1}. \tag{2.1.5}$$

Here $P_n(x)$ is called the ***n*th Taylor polynomial** for f about x_0 and $R_n(x)$ is called the **remainder term** (or **truncation error**) associated with $P_n(x)$. The size of the remainder depends on how close x_0 is to x, the order of the Taylor polynomial, and on the size of $f^{(n+1)}$ on (a, b). The infinite series obtained by taking the limit of $P_n(x)$ as $n \to \infty$ is called the **Taylor series** for f about x_0.

Theorem 2.4 (Taylor, two-dimensional) Suppose $f(x, y)$ and all its partial derivatives of order less than or equal to $n + 1$ are continuous on $D = \{(x, y) | a \leq x \leq b, c \leq y \leq d\}$, and let $(x_0, y_0) \in D$. For every $(x, y) \in D$, there exists ξ between x and x_0 and η between y and y_0 with

$$f(x, y) = P_n(x, y) + R_n(x, y), \tag{2.1.6}$$

where

$$\begin{aligned} P_n(x, y) &= f(x_0, y_0) + \left[(x - x_0)\frac{\partial f}{\partial x}(x_0, y_0) + (y - y_0)\frac{\partial f}{\partial x}(x_0, y_0)\right] \\ &\quad + \frac{1}{2!}\left[(x - x_0)^2\frac{\partial^2 f}{\partial x^2}(x_0, y_0) + 2(x - x_0)(y - y_0)\frac{\partial^2 f}{\partial x \partial y}(x_0, y_0)\right. \\ &\quad \left. + (y - y_0)^2\frac{\partial^2 f}{\partial y^2}(x_0, y_0)\right] + \ldots \\ &\quad + \frac{1}{n!}\sum_{k=0}^{n} \binom{n}{k} (x - x_0)^{n-k}(y - y_0)^k \frac{\partial^n f}{\partial x^{n-k} \partial y^k}(x_0, y_0) \end{aligned} \tag{2.1.7}$$

and

$$R_n(x,y) = \frac{1}{(n+1)!}\sum_{k=0}^{n+1}\binom{n+1}{k}(x-x_0)^{n+1-k}(y-y_0)^k\frac{\partial^{n+1}f}{\partial x^{n+1-k}\partial y^k}(\xi,\eta). \tag{2.1.8}$$

The function $P_n(x,y)$ is called the **nth Taylor polynomial in two variables** for f about (x_0,y_0), and $R_n(x,y)$ is the remainder term associated with $P_n(x,y)$.

2.2 Finite-Difference Methods

The mathematical modelling of many problem in physics, engineering, chemistry, biology etc. are formulated in terms of differential equations. Much of the analysis of the solution behaviour of a given differential equation is done by constructing numerical solutions. The finite-difference method is a numerical method for solving differential equations. The idea of the method is to replace the derivative in the equation using finite-difference approximations. Applying Taylor's theorem 2.3, the function-value $u(x)$ is expressed as series

$$u(x+h) = u(x) + hu'(x) + \frac{h^2}{2!}u''(x) + \ldots \tag{2.2.1}$$

and

$$u(x-h) = u(x) - hu'(x) + \frac{h^2}{2!}u''(x) - \ldots, \tag{2.2.2}$$

where $h > 0$ is called an *increment* in x and taking the first two term of the right-hand side of (2.2.1) and (2.2.2) gives

$$u(x+h) = u(x) + hu'(x) + O(h^2) \tag{2.2.3}$$

and

$$u(x-h) = u(x) - hu'(x) + O(h^2) \tag{2.2.4}$$

where the expression $O(h^2)$ indicates that the error $R_2(x)$ has *principle part* proportion to h^2 as $h \to 0$. The first and second derivative replacements of a function $u(x)$, then, can be derived as follows ($h > 0$):

First-order backward-difference replacement, $u \in C^2[x-h, x]$

$$\frac{\mathrm{d}u}{\mathrm{d}x} = \frac{u(x) - u(x-h)}{h} + O(h), \quad \text{as} \quad h \to 0. \tag{2.2.5}$$

First-order forward-difference replacement, $u \in C^2[x, x+h]$

$$\frac{\mathrm{d}u}{\mathrm{d}x} = \frac{u(x+h) - u(x)}{h} + O(h), \quad \text{as} \quad h \to 0. \tag{2.2.6}$$

Second-order central-difference replacement, $u \in C^3[x-h, x+h]$

$$\frac{\mathrm{d}u}{\mathrm{d}x} = \frac{u(x+h) - u(x-h)}{2h} + O(h^2), \quad \text{as} \quad h \to 0. \tag{2.2.7}$$

Second-order central-difference replacement, $u \in C^4[x-h, x+h]$

$$\frac{\mathrm{d}^2u}{\mathrm{d}x^2} = \frac{u(x-h) - 2u(x) + u(x+h)}{h^2} + O(h^2), \quad \text{as} \quad h \to 0. \tag{2.2.8}$$

Depending on which approximations for first and second derivatives are chosen, a differential equation can be transformed into an m-step discrete dynamical system of the form (Herges [13])

$$x_{k+m} = F(x_{k+m-1}, x_{k+m-2}, \ldots, x_k), \ k = 0, 1, 2, \ldots \tag{2.2.9}$$

with $F : \mathbb{R}^{m.n} \to \mathbb{R}^n$ and initial values $x_0, x_1, \ldots, x_{m-1} \in \mathbb{R}^n$.

When solving numerically an initial-value problem of the form

$$\frac{\mathrm{d}x}{\mathrm{d}t} = f(t, x), \ a \le t \le b, \ x(a) = x_0, \tag{2.2.10}$$

with $x : [a, b] \to \mathbb{R}^n$ and $f : [a, b] \times \mathbb{R}^n \to \mathbb{R}^n$, the approximating discrete dynamical system is often only a one-step difference equation of the form

$$x_{k+1} - x_k = hG(t, x_k; h) \tag{2.2.11}$$

with $h > 0$ the step length of the equidistant grid points $t_i = a + ih$ $(i = 1, 2, \ldots, N)$, $N = (b-a)/h$. The solution $x(t)$ of equation (2.2.10) at $t = t_i$ $(i = 1, 2, \ldots, N)$ is approximated by the numerical solution $x_i \in \mathbb{R}^n$ $(i = 1, 2, \ldots, N)$ obtained by iterating the difference equation (2.2.11), where $G : [a, b] \times \mathbb{R}^n \to \mathbb{R}^n$ and $x_0 \in \mathbb{R}^n$

is the initial value. Scheme (2.2.11) is a special case of the general one-step discrete dynamical system.

The local truncation error at a specified grid point measures the amount by which the exact solution of the differential equation (2.2.10) fails to satisfy the difference equation. Hence, the local truncation error $\mathcal{L}[x(t_i); h]$ at $t_i = a + ih$, $i = 1, 2, \ldots, N$ for scheme (2.2.11) is defined by

$$\mathcal{L}[x(t_i); h] = x(t_i) - x(t_{i-1}) - hG(t, x(t_{i-1}); h),\ i = 1, 2, \ldots, N \qquad (2.2.12)$$

and gives the accuracy of the numerical method at grid point t_i, $i = 1, 2, \ldots, N$ assuming the method was exact the previous step.

Definition 2.5 (Order of a one-step difference method) Let the solution $x(t)$ of equation (2.2.10) be $(p+1)$-times continuously differentiable, $p \in \mathbb{N}$, then the local truncation error $\mathcal{L}[x(t_i); h]$, $i = 1, 2, \ldots, N$ can be expressed in term of a finite Taylor series of the form

$$\mathcal{L}[x(t_i); h] = \sum_{k=0}^{p+1} c_k h^k \frac{\mathrm{d}^k x(t_{i-1})}{\mathrm{d}t^k},\ i = 1, 2, \ldots, N. \qquad (2.2.13)$$

The local truncation errors and with them the associated one-step difference method is said to be of order p if $c_0 = c_1 = \ldots = c_p = 0$ and $c_{p+1} \neq 0$.

Definition 2.6 (Consistency of a one-step difference method) A one-step difference method with local truncation error $\mathcal{L}[x(t_i); h]$, $i = 1, 2, \ldots, N$ is said to consistent with the differential equation it approximates if

$$\lim_{h \to 0} \max_{1 \leq i \leq N} \frac{\|\mathcal{L}[x(t_i); h]\|}{h} = 0. \qquad (2.2.14)$$

A one-step difference method is consistent precisely when the function $G(t, x; h)$ in (2.2.11) approaches $f(t, x)$, the right-hand side of the differential equation (2.2.10), as the step size h goes to zero; that is, the local truncation error approaches zero as the step size approaches zero. Clearly, a one-step difference method is consistent if it is of order $p \geq 1$ and $\mathrm{d}^{(p+1)} x / \mathrm{d}\, t^{(p+1)}$ is bounded on $[a, b]$.

Definition 2.7 (Convergence of a one-step difference method) A one-step difference method is said to be convergent with respect to the differential equation it approximates if

$$\lim_{h\to 0} \max_{1\le i\le N} \|x_i - x(t_i)\| = 0, \tag{2.2.15}$$

where $x(t_i)$ is the value of the solution of the differential equation at $t_i = a + ih$ and x_i is the approximation obtained from the difference method at the ith step.

A one-step difference method is convergent precisely when the solution to the difference equations approaches the solution to the differential equation as the step size go to zero.

Another type of error, known as round-off error, is introduced to the solution obtained when implementing a numerical scheme on a computer. As computers can store only a finite number of digits to represent each number, round-off errors can occur at each step of the computation. For a practical computation, the cumulative growth of the round-off errors must not swamp the true difference equation. If the growth of these errors is reasonable or controlled, the computation is stable. Thus, a numerical model with consistent equations, convergent solution, and stable error propagation yields a computationally stable scheme whose results can closely approximate the exact solution to the mathematical model. The following theorem (see Burden & Faires [5]) connects the notations of consistency, convergence and stability of a one-step difference method and states an error bound of the numerical solution.

Theorem 2.8 Suppose the initial-value problem (2.2.10) is approximated by the one-step difference method (2.2.11). Suppose also $\exists\, c > 0, \exists\, h_0 > 0$ such that $G(t, x; h)$ is continuous and satisfies a *Lipschitz condition* with respect to $x \in \mathbb{R}^n$ with *Lipschitz constant* L on the set $D = \{(t, x, h) | a \le t \le b, \|x - x_0\| < c, 0 \le h \le h_0\}$. Then

(i) the one-step difference method depends continuously on the initial value;

(ii) the one-step difference method is convergent if and only if it is consistent; that is, if and only if

$$G(t, x; 0) = f(t, x), \ \forall \ t \in [a, b]; \tag{2.2.16}$$

(iii) if a function $g : [0, h_0] \to \mathbb{R}$, and for each $i = 1, 2, \ldots, N$, the local truncation error $\mathcal{L}[x(t_i); h]$ satisfies $\|\mathcal{L}[x(t_i); h]\| \leq g(h)$ for $0 \leq h \leq h_0$, then

$$\|x(t_i) - x_i\| \leq \frac{g(h)}{L} \exp(L(t_i - a)). \tag{2.2.17}$$

2.3 First-Order Systems of Ordinary Differential Equations

Consider the initial-value problem for a first-order system of the form

$$\frac{\mathrm{d}\mathbf{x}}{\mathrm{d}t} = \mathbf{f}(t, \mathbf{x}), \quad t > t_0, \quad \mathbf{x}(t_0) = \mathbf{x}_0 \in \mathbb{R}^n \tag{2.3.1}$$

where $\mathbf{x} = [x_1, x_2, \ldots, x_n]^T$ and $\mathbf{f} = [f_1, f_2, \ldots, f_n]^T$ and $\mathbf{f}$ is a sufficiently well-behaved function that maps $\mathbb{R} \times \mathbb{R}^n$ to $\mathbb{R}^n$. Equation (2.3.1) is said to be *autonomous* if $\mathbf{f}$ is independent of t, and to be *non-autonomous* otherwise.

The analytical solution of (2.3.1) is usually so complicated that it is more efficient to solve it numerically for $t > t_0$. Before attempting to approximate the solution numerically, however, it is assumed that the hypotheses of the following theorem are satisfied (Lambert [15]).

Theorem 2.9 Let $\mathbf{f}(t, \mathbf{x})$, where $\mathbf{f} : \mathbb{R} \times \mathbb{R}^n \to \mathbb{R}^n$, be defined and continuous for all $(t, \mathbf{x})$ in the region D defined by $a \leq t \leq b$, $-\infty < x_i < \infty$, $i = 1, 2, \ldots . n$, where a and b are finite, and let there exit a constant L such that

$$|\mathbf{f}(t, \mathbf{x}) - \mathbf{f}(t, \mathbf{x}^*)| \leq L|\mathbf{x} - \mathbf{x}^*| \tag{2.3.2}$$

holds for every $(t, \mathbf{x}), (t, \mathbf{x}^*) \in D$ (L is called the *Lipschitz constant*). Then for any $\mathbf{x}_0 \in \mathbb{R}^n$, there exists a unique solution $\mathbf{x}(t)$ of (2.3.1), where $\mathbf{x}(t)$ is continuous and differentiable for all $(t, \mathbf{x}) \in D$.

The use of either differential or difference equations to represent dynamical behaviour corresponds, respectively, to whether the behaviour is viewed as occurring in continuous or discrete time. The following definitions and theorems are the necessary tools to study the qualitative analysis of experimental dynamical systems.

Definition 2.10 A vector $\overline{\mathbf{x}}$ is an equilibrium point or critical point of a dynamic system if it has the property that once the system state vector is equal to $\overline{\mathbf{x}}$ it remains equal to $\overline{\mathbf{x}}$ for all future time.

In particular, if a system is described by a set of differential equations (continuous-time system) as in (2.3.1), a critical point is a state $\overline{\mathbf{x}}$ satisfying

$$\mathbf{f}(t, \mathbf{x}) = \mathbf{0}$$

for all t. If the vector function $\mathbf{f}$ does not depend explicitly on time, the system is said to be time-invariant, in which case the critical point is a point $\overline{\mathbf{x}}$ such that

$$\mathbf{f}(\overline{\mathbf{x}}) = \mathbf{0}.$$

Definition 2.11 (Stable critical point) A critical point $\overline{\mathbf{x}}$ is said to be asymptotically stable if there exists a number $\varepsilon > 0$ such that $\forall\ \mathbf{x}_0 \in \mathbb{R}^n$ satisfying $\|\overline{\mathbf{x}} - \mathbf{x}_0\| < \varepsilon$, then

$$\lim_{t \to \infty} \mathbf{x}(t) = \overline{\mathbf{x}}.$$

In order to determine the stability of $\overline{\mathbf{x}}$ it is necessary to understand the nature of solution near $\overline{\mathbf{x}}$. Let

$$\mathbf{x}(t) = \overline{\mathbf{x}} + \mathbf{y}(t). \tag{2.3.3}$$

Substituting (2.3.3) into (2.3.1) expanding as a Taylor series about $\overline{\mathbf{x}}$ gives

$$\frac{\mathrm{d}\mathbf{x}}{\mathrm{d}t} = \frac{\mathrm{d}\mathbf{y}}{\mathrm{d}t} = \mathbf{f}(\overline{\mathbf{x}}) + \frac{\partial \mathbf{f}(\overline{\mathbf{x}})}{\partial \mathbf{x}} \mathbf{y}(t) + \text{ higher order terms.} \tag{2.3.4}$$

Since $\mathbf{f}(\overline{\mathbf{x}}) = \mathbf{0}$, equation (2.3.4) becomes

$$\frac{\mathrm{d}\mathbf{y}}{\mathrm{d}t} \approx \frac{\partial \mathbf{f}(\overline{\mathbf{x}})}{\partial \mathbf{x}} \mathbf{y}(t), \tag{2.3.5}$$

which is a constant coefficient, linear system for $\mathbf{y}(t)$. The matrix $J = \dfrac{\partial \mathbf{f}}{\partial \mathbf{x}}$ is referred to as the *Jacobian* of $\mathbf{f}$. The long-term behaviour of (2.3.1) is determined by the eigenvalues of the Jacobian as in the following theorem (Luenberger [17]).

Theorem 2.12 A necessary and sufficient condition for a critical point $\overline{\mathbf{x}}$ of (2.3.1) to be *asymptotically stable* is that the eigenvalues of matrix J evaluated at $\overline{\mathbf{x}}$ all have negative real part. If at least one eigenvalue has positive real part, the point is *unstable.*

The difference equation

$$\mathbf{x}_{k+1} = \mathbf{F}(\mathbf{x}_k),\ k = 0, 1, 2, \ldots \tag{2.3.6}$$

is a one-step discrete dynamical system with $\mathbf{F} : \mathbb{R}^n \to \mathbb{R}^n$ and the initial value $\mathbf{x}_0 \in \mathbb{R}^n$. The notation of stable fixed point is similar to those of continuous systems. Here, the definition of a fixed point of a one-step discrete dynamical system and the criteria to test whether a fixed point of a one-step discrete dynamical system is stable or not, will be given (Luenberger [17] and Sandefur [25]).

Definition 2.13 (Fixed point) If $\overline{\mathbf{x}} \in \mathbb{R}^n$ satisfies $\mathbf{F}(\overline{\mathbf{x}}) = \overline{\mathbf{x}}$ then $\overline{\mathbf{x}}$ is called a fixed point of the dynamical system (2.3.6).

Theorem 2.14 Let $\overline{\mathbf{x}}$ be a fixed point of the one-step discrete dynamical system, $J = \dfrac{\partial \mathbf{F}}{\partial \mathbf{x}}$ be the Jacobian of $\mathbf{F}$ at $\overline{\mathbf{x}}$ with eigenvalues $\lambda_1, \lambda_1, \ldots, \lambda_n \in \mathbb{C}$, and the spectral radius ρ of J is defined by $\rho(J) = \max\limits_{1 \le i \le n} |\lambda_i|$. Then a fixed point $\overline{\mathbf{x}}$ is said to be asymptotically stable if $\rho(J) < 1$ and unstable if $\rho(J) > 1$.

2.4 Numerical Solutions to Partial Differential Equations

Many problem in the bio-medical sciences requiring numerical solution involve special cases of the linear parabolic differential equation

$$\sigma(x,t)\frac{\partial u}{\partial t} = \frac{\partial}{\partial x}\left(a(x,t)\frac{\partial u}{\partial x}\right) + b(x,t)\frac{\partial u}{\partial x} - c(x,t)u, \tag{2.4.1}$$

which holds within some described region R of the (x,t) space. Within this region, the functions σ, a are strictly positive and c is non-negative (Twizell [29]).

The most common method of solution of partial differential equations is the finite-difference method. The partial derivatives in the equation are replaced by difference quotients, converting the differential equation to a difference equation. The difference equation and the given data are used to determine the function values at a grid of discrete mesh points that cover the original domain of the mathematical model. There is no best method for obtaining approximating difference formulae. The only requirement is that the formulae, having been obtained, must pass certain tests of the adequacy of the difference equations, namely, the *consistency, convergence*, and *stability* of the numerical model.

The concept of stability is concerned with boundedness of the solution of the finite-difference equations and is examined by finding conditions under which the difference between the theoretical and numerical solution of the difference equation given at the mesh point $(mh, n\ell)$ by

$$Z_m^n = U_m^n - \widehat{U}_m^n$$

remains bounded as n increases, for fixed h and ℓ. The following methods are used in this thesis for examining the stability of finite-difference schemes in Chapters 4, 5 and 6 (see, for full detail, Mitchell and Griffiths [19], Douglas [8], Lees [16] and Rose [24]).

The von Nuemann method is the most widely-used method for determining the stability (or instability) of a finite difference approximation. Here, a harmonic decomposition is made of the error Z at the grid points on a given time level, leading to the error function

$$E(x) = \sum_j A_j \, e^{i\,\beta_j\,x}$$

where $|\beta_j|$ is the frequency of the error, j are arbitrary and i is the complex number $\sqrt{-1}$. It is necessary to consider only the single term $e^{i\beta x}$ where β is any real number. For convenience, suppose that the time level being considered corresponds to $t = 0$.

To investigate the error propagation as t increases, it is necessary to find a solution of the finite-difference equation which reduces to $e^{i\beta x}$ when $t = 0$. Let such a solution be

$$E(t, x) \approx e^{\alpha t}\, e^{i\beta x}$$

where $\alpha = \alpha(\beta)$ is, in general, complex. The original error component $e^{i\beta x}$ will not grow with time if

$$|e^{\alpha l}| \leq 1$$

for all α. This is von Neumann's criterion for stability, sometimes called the von Neumann necessary condition for stability. In order to allow for exponentially growing solutions of the partial differential equation itself, a more general form is

$$|e^{\alpha l}| \leq 1 + O(l).$$

The following important points should be noted concerning the von Neumann method of examining stability, Mitchell and Griffiths [19].

(i) The method which is based on Fourier series applies only if the coefficients of the linear difference equation are constant. If the difference equation has variable coefficients, the method can still be applied locally and it might be expected that a method will be stable if the von Neumann condition, derived as though the coefficients were constant, is satisfied at every point of the field. There is much numerical evidence to support this contention.

(ii) For two level difference schemes with *one dependent variable* and any number of independent variables, the von Neumann condition is sufficient as well as necessary for stability. Otherwise, the condition is *necessary* only.

(iii) Boundary conditions are neglected by the von Neumann method which applies in theory only to pure initial-value problems with periodic initial data. It does, however, provide necessary conditions for stability of constant coefficient problems regardless of the type of boundary condition.

The von Neumann method is applied to prove the stabilities of numerical methods which are developed in Chapters 4 and 5.

The maximum principle is one of the most useful and best known tools employed in the study of partial differential equations. This principle is a generalization of the elementary fact of calculus that any function $f(x)$ which satisfies the inequality $f'' > 0$ on an interval $[a, b]$ achieves its maximum value at one of the endpoints of the interval. The solutions of the inequality $f'' > 0$ are said to satisfy a *maximum principle.* More generally, functions which satisfy a differential inequality in a domain D and, because of it, achieve their maxima on the boundary of D are said to possess a maximum principle (Protter and Weinberger [22]). The maximum principle enables information about the solutions of differential equations without any explicit knowledge of the solutions themselves. In particular, the maximum principle is a useful tool in the approximation of solutions, a subject of great interest to many scientists.

In the following, convergence of solutions of mixed initial/boundary-value problems for a certain class of non-linear parabolic equations will be estimated using the maximum principle analysis. Similar estimations will be used to analyse the stabilities of numerical methods developed in Chapters 4 and 6. Consider the non-linear parabolic differential equation

$$\frac{\partial^2 u}{\partial x^2} = F\left(x, t, u, \frac{\partial u}{\partial x}, \frac{\partial u}{\partial t}\right). \tag{2.4.2}$$

in the strip $0 < t \leq T$, $0 < x < L$, with the initial condition

$$-\beta_0(x)u(x,0) = f_0(x) \tag{2.4.3}$$

and the boundary conditions

$$\alpha_1(t)\,\frac{\partial u}{\partial x}(0,t) - \beta_1(t)\,u(0,t) = f_1(t) \tag{2.4.4}$$

$$-\alpha_2(t)\,\frac{\partial u}{\partial x}(L,t) - \beta_2(t)\,u(L,t) = f_2(t), \tag{2.4.5}$$

assuming that the solution $u(x,t)$ is unique and exists with suitable regularity properties in the strip.

The non-linear parabolic operator of (2.4.2) is of the form

$$L[u] \equiv \frac{\partial^2 u}{\partial x^2} - F(x, t, u, u_x, u_t), \tag{2.4.6}$$

where $F(x, t, u, u_x, u_t)$ denotes a fixed continuous function of its variables for (x, t) in a region Ω in the (x, t)-plane and for all u, u_x, u_t. Assume that the partial derivative F_u, F_{u_x}, F_{u_t} exist, are continuous, and satisfy the inequalities

$$0 < a_0 \leq F_{u_t} \leq a_1 < \infty, \tag{2.4.7}$$

$$|F_{u_x}| \leq b < \infty, \tag{2.4.8}$$

$$0 \leq c_0 \leq F_u \leq c_1 < \infty, \tag{2.4.9}$$

where a_0, a_1, b, c_0 and c_1 are fixed constants. Let Ω be a domain bounded by the coordinate lines $x = 0$, $t = 0$ and the lines $x = L$, $t = T$; the closure of Ω will be denoted by $\overline{\Omega}$. The set composed of the segments $\partial\Omega_0\,(0 < x < L,\ t = 0)$, $\partial\Omega_1\,(x = 0,\ 0 < t < T,)$ and $\partial\Omega_2\,(x = L,\ 0 < t < T)$ will be denoted by $\partial\Omega$ and called the boundary of Ω.

The boundary operators, Λ_0, Λ_1, Λ_2, are defined by

$$\begin{aligned}
\Lambda_0[u] &= -\beta_0\, u(x, 0) \quad \text{on } \partial\Omega_0, \\
\Lambda_1[u] &= \alpha_1(t)\, \frac{\partial u}{\partial x}(0, t) - \beta_1(t)\, u(0, t) \quad \text{on } \partial\Omega_1, \\
\Lambda_2[u] &= -\alpha_2(t)\, \frac{\partial u}{\partial x}(L, t) - \beta_2(t)\, u(L, t) \quad \text{on } \partial\Omega_2;
\end{aligned} \tag{2.4.10}$$

here, β_0, β_1, β_2 are continuous positive functions and α_1, α_2 are continuous non-negative functions on Ω_0, Ω_1, Ω_2. Let f_0, f_1, f_2 be fixed functions defined on Ω_0, Ω_1, Ω_2, respectively.

A mixed initial/boundary-value problem $\mathcal{P}$ may be formulated as follows: for fixed T, determine a function $u(x, t)$ defined in Ω with certain regularity properties satisfying the equation

$$L[u] = 0 \quad \text{on } \Omega$$

and the initial and boundary conditions (see (2.4.10))

$$\Lambda_i[u] = f_i \quad \text{on } \partial\Omega_i, \quad i = 0, 1, 2.$$

It is assumed that this problem has at most one solution which exists with suitable regularity properties under appropriate regularity conditions on the operators L, Λ and on the initial and boundary data. Specifically, it is assumed that u_{xxxx}, u_{xxt}, u_{tt} and lower-order mixed partial derivatives exist and are continuous in Ω.

Let $\overline{\Omega}_h$ be the rectangular lattice covering $\overline{\Omega}$ given by lines

$$\begin{aligned} x &= mh, \quad m = 0, 1, \ldots, M, \\ t &= n\ell, \quad n = 0, 1, \ldots, N, \end{aligned}$$

where $h = L/M$ and $\ell = T/N$. The boundary of the lattice $\overline{\Omega}_h$ denoted by $\partial\Omega_h$ is the union of three set

$$\partial\Omega_{h,i} = \partial\Omega_i \cap \overline{\Omega}_h, \quad i = 0, 1, 2.$$

The interior of the lattice is the set $\Omega_h = \overline{\Omega}_h - \partial\Omega_h$. Then the mixed initial-boundary value problem $\mathcal{P}_h$ consists in finding a function u^h defined on Ω_h which satisfies the equation

$$L_h[u^h] = 0 \quad \text{on } \Omega_h$$

and the initial and boundary conditions (see (2.4.10))

$$\Lambda_{h,i}[u^h] = f_{h,i} \quad \text{on } \partial\Omega_{h,i},$$

where $f_{h,i}$ is a given function on $\partial\Omega_{h,i}$.

Rose [24] approximated the differential equation (2.4.6) by the family of implicit difference equations

$$\begin{aligned} \theta \bigtriangledown_x^2 \varphi(x,t) + (1-\theta) \bigtriangledown_x^2 \varphi(x, t-\ell) = F[x, t, \varphi(x,t), \theta \bigtriangledown_x \varphi(x,t) \\ + (1-\theta) \bigtriangledown_x \varphi(x, t-\ell), \bigtriangledown_t \varphi(x,t)], \quad (2.4.11) \end{aligned}$$

where $0 \leq \theta \leq 1$ and $\bigtriangledown_x^2$, $\bigtriangledown_x$, $\bigtriangledown_t$ are defined by

$$\begin{aligned} \bigtriangledown_x^2 \varphi(x,t) &= \frac{1}{h^2}[\varphi(x-h,t) - 2\varphi(x,t) + \varphi(x+h,t)], \\ \bigtriangledown_x \varphi(x,t) &= \frac{1}{2h}[\varphi(x+h,t) - \varphi(x-h,t)], \\ \bigtriangledown_t \varphi(x,t) &= \frac{1}{\ell}[\varphi(x,t) - \varphi(x,t-k)]. \end{aligned}$$

Rose showed that

$$\|u - \varphi\|_\infty = O(\ell + h^2)$$

for any value of the mesh ratio $\lambda = \ell/h^2$ provided that

$$0 \leq 2(1-\theta)\lambda \leq a_0.$$

The following convergence theorem which can be found in Rose [24] and Lee [16] will be used in the analyses in Chapter 4 and Chapter 6.

Theorem 2.15 Let problem $\mathcal{P}$ be approximated by problems $\mathcal{P}_h$ in the sense that

$$\max_i \max_{\partial\Omega_i} |f_i - f_{h,i}| = \begin{cases} \alpha^* O(h) & \text{if } \alpha^* \neq 0, \\ O(h^2) & \text{if } \alpha^* = 0, \end{cases} \tag{2.4.12}$$

where $\alpha^* = \max_i \max_{\partial\Omega_i} |\alpha_i|$ $(i = 1, 2)$. Then, if h, $\ell \to 0$ in such a way that

$$\lambda = \frac{\ell}{h^2} \leq \frac{a_0}{2\theta}, \tag{2.4.13}$$

the solutions u^h of $\mathcal{P}_h$ approximates the solution u of problem $\mathcal{P}$ uniformly in $\overline{\Omega}$; that is,

$$|u - u^h| = \alpha^* O(h) + O(h^2) + O(\ell). \tag{2.4.14}$$

Chapter 3

Oscillatory Dynamics of Whooping Cough

3.1 Introduction

Whooping cough is mainly a childhood disease, although it may affect people of all ages. This disease is most severe and the incidence of mortality is highest in young children, most fatal cases being in infants in their first year of life. The dynamics of whooping cough is described by the *SIR* model and is studied in this chapter. The long-term dynamics of the model are analysed to determine a threshold condition in which the critical points are stable. Periodicity and other oscillatory behaviours can be sustained in the model if the contact rate is allowed to vary seasonally. When the model is seasonally forced, a wide range of the complex dynamic behaviour is seen, including chaos and co-existing cycles of different periods (London & Yorke [18], Dietz [7] and Duncan *et al.* [10]).

This chapter is organized as follows. In §3.2, the compartmental model is described. The mathematical model of the transmission of whooping cough and its dynamics are given in §3.3 and §3.4, respectively. The *SIR* model with seasonal forcing is discussed in §3.5. A linearized model of the dynamics of epidemics shows that the inter-epidemic interval is determined by the product of population (N) and susceptibility (β) and that the system will settle at its steady-state unless triggered by external factors. Many mathematical models involving non-linear differential equations usually cannot be solved analytically and thus one has to rely on numeri-

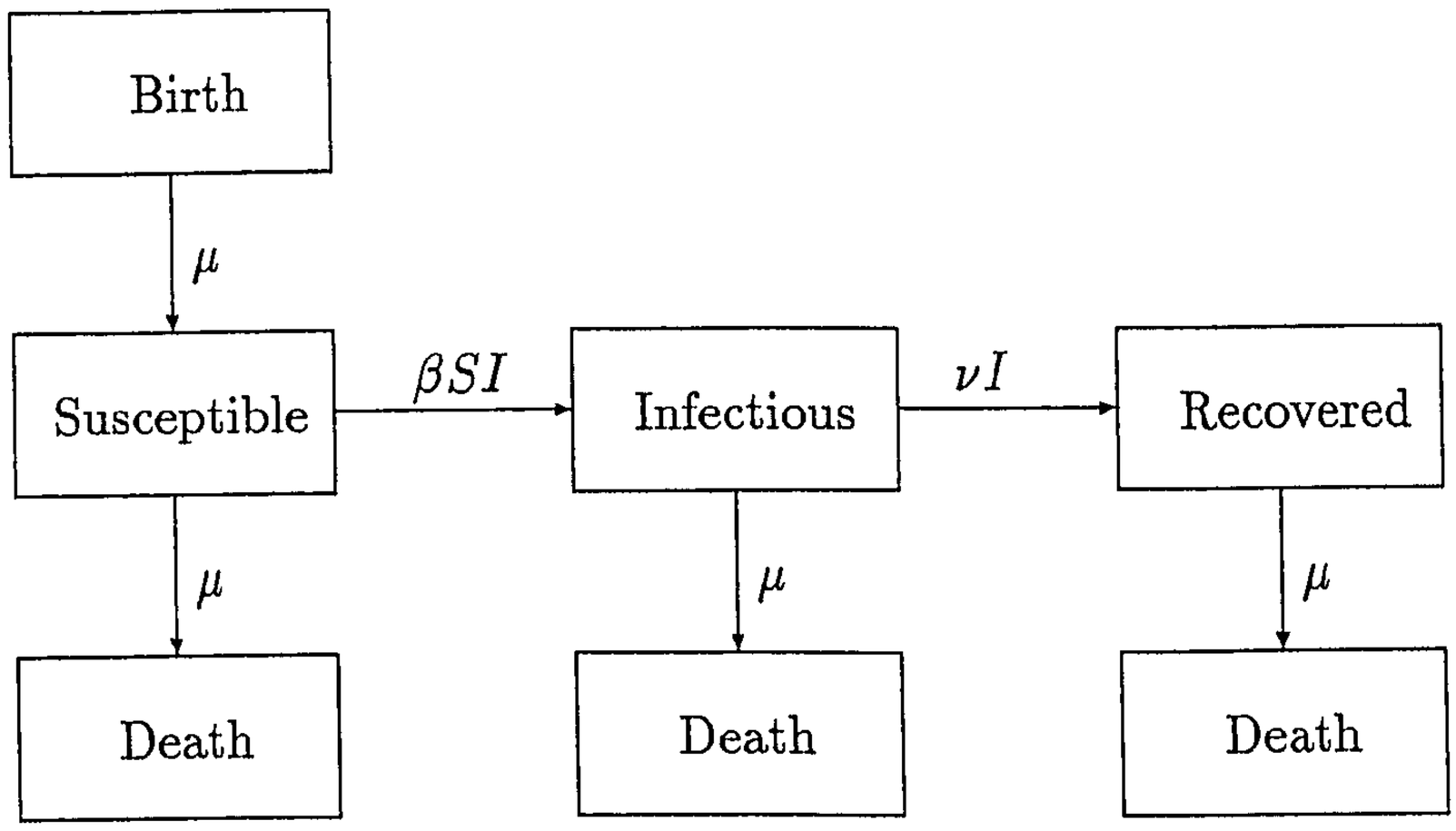

Figure 3.1: The compartmental diagram for the *SIR* model of whooping cough.

cal methods. First- and second-order methods for solving the differential equations will be developed and analysed in §3.6 and §3.7. The dynamics of the *SIR* model and *SIR* with seasonal forcing using the proposed method are tested in numerical simulations and will be reported in §3.8.

3.2 Compartmental Models

The impact of parasitic infection on the dynamics of host population growth can be described using compartmental models (see for example Anderson & May [3]). The population in the epidemic model of this study is divided into three classes: susceptible, infectious and recovered, with sizes S, I and R, respectively. In this deterministic model the rate of transition from susceptible to infectious is assumed to be proportional to S and I with rate constant β. The rate of transition from infectious to recovered is proportional to I with rate constant ν. A latent period after becoming infected, but before becoming infectious, is ignored. New susceptibles are introduced at a constant rate, μ, by birth and all classes experience the same constant death rate, μ. A diagram of the model is shown in figure 3.1. It is assumed that nobody dies of whooping cough: therefore, the infected hosts do not experience a higher mortality rate. Recovered individuals do not flow back into the susceptible

compartment, as lifelong immunity is supposed.

3.3 The *SIR* Whooping Cough Model

The *SIR* (susceptible-infective-recovered) whooping cough model is obtained by translating the compartmental model proposed above into mathematical terms. It consists of three coupled, non-linear ordinary differential equations

$$\frac{\mathrm{d}S}{\mathrm{d}t} = \mu N - \mu S - \beta SI, \tag{3.3.1}$$

$$\frac{\mathrm{d}I}{\mathrm{d}t} = -(\mu + \nu)I + \beta SI, \tag{3.3.2}$$

$$\frac{\mathrm{d}R}{\mathrm{d}t} = \nu I - \mu R \tag{3.3.3}$$

with $t \geq 0$, subject to the initial conditions

$$S(0) = S_0, \quad I(0) = I_0, \quad R(0) = R_0, \tag{3.3.4}$$

in the domain

$$\mathcal{D} = \{(S, I, R) \in \mathbb{R}^3_+ \mid S + I + R \leq N\},$$

in which $S(t)$, $I(t)$ and $R(t)$ represent the number of susceptible, infective and recovered individuals at time t, respectively. The model assumes a population of constant size, so that $S(t)+I(t)+R(t) = N$. The parameters μ, ν and β denote the death rate (life expectancy$= 1/\mu$), the rate of recovery from disease (infectious period$= 1/\nu$) and the transmission coefficient (susceptibility to disease), respectively. All model parameters are assumed to be positive.

Without loss of generality, equations (3.3.1)-(3.3.3) may be written in terms of the fraction of the population in each class by defining three new variables

$$x = \frac{S}{N}, \quad y = \frac{I}{N}, \quad z = \frac{R}{N}. \tag{3.3.5}$$

Incorporation of these changes reduces the differential equations to

$$\frac{\mathrm{d}x}{\mathrm{d}t} = \mu - \mu\, x - N\beta\, x\, y; \qquad x(0) = x_0, \tag{3.3.6}$$

$$\frac{\mathrm{d}y}{\mathrm{d}t} = N\beta\, x\, y - (\mu + \nu)\, y; \quad y(0) = y_0, \tag{3.3.7}$$

$$\frac{\mathrm{d}z}{\mathrm{d}t} = \nu\, y - \mu\, z; \qquad z(0) = z_0. \tag{3.3.8}$$

The population has a constant size, which is normalized to unity: $x(t)+y(t)+z(t)=1$. Note that it is necessary to solve only two equations because $z(t)$ can always be found from $x(t)$ and $y(t)$ by using $z(t)=1-x(t)-y(t)$. It is sufficient, therefore, to consider the IVP {(3.3.6),(3.3.7)} in the x-y phase plane. The dynamical behaviour of {(3.3.6),(3.3.7)} will be studied in the region

$$\overline{\mathcal{D}}=\{(x,y)\mid x\geq 0,\ y\geq 0,\ x+y\leq 1\}. \tag{3.3.9}$$

3.4 Qualitative Analysis

3.4.1 Critical points

The first thing to investigate when analysing a dynamical system is the existence of critical points. The steady state of (3.3.6) and (3.3.7) is determined when the time derivatives vanish giving the critical points

$$x=1,\ y=0 \tag{3.4.1}$$

and

$$x_s=\frac{\mu+\nu}{N\beta},\quad y_s=\frac{\mu}{\mu+\nu}\left(1-\frac{\mu+\nu}{N\beta}\right). \tag{3.4.2}$$

The first is trivial in the sense that it corresponds to the case of the existence of no infectious individuals. The second, non-trivial, critical point is equivalent to

$$(x_s,y_s)=\left(\frac{1}{\mathcal{R}_0},\frac{\mu}{\mu+\nu}\left(1-\frac{1}{\mathcal{R}_0}\right)\right)$$

which varies significantly with $\mathcal{R}_0$. Here, $\mathcal{R}_0$ is the basic reproductive rate of the infection, defined, as in Anderson & May [3], to be

$$\mathcal{R}_0=\frac{N\beta}{\mu+\nu},$$

since it is the average number of secondary infections that occur when one infective is introduced into a completely susceptible host population.

3.4.2 Stability analysis

The pair of equations (3.3.6) and (3.3.7) can be written in the form

$$\frac{\mathrm{d}x}{\mathrm{d}t} = f(x,y), \tag{3.4.3}$$

$$\frac{\mathrm{d}y}{\mathrm{d}t} = g(x,y), \tag{3.4.4}$$

where

$$f(x,y) = \mu - \mu\, x - N\beta\, x\, y,$$

$$g(x,y) = N\beta\, x\, y - (\mu+\nu)\, y.$$

The local stabilities of the critical points are determined by the eigenvalues of the Jacobian which correspond to each of the two critical points. The Jacobian associated with {(3.4.3),(3.4.4)} is the matrix

$$J = \begin{bmatrix} -\mu - N\beta y & -N\beta x \\ N\beta y & -(\mu+\nu) + N\beta x \end{bmatrix}, \tag{3.4.5}$$

the determinant of which vanishes when

$$\mathcal{R}_0 \equiv \frac{N\beta}{\mu+\nu} = 1. \tag{3.4.6}$$

This unique value of $\mathcal{R}_0$ will be regarded as a bifurcation parameter of the model equations.

At the trivial critical point $x = 1$ and $y = 0$ and the eigenvalues, λ_1, λ_2, of the associated Jacobian are

$$\lambda_1 = -\mu, \quad \lambda_2 = -(\mu+\nu)(1-\mathcal{R}_0) \tag{3.4.7}$$

from which it follows that the eigenvalues are real and negative whenever $\mathcal{R}_0 < 1$. On the other hand the eigenvalues are real and of opposite sign if $\mathcal{R}_0 > 1$. Therefore, the trivial critical point is asymptotically stable whenever $\mathcal{R}_0 < 1$ and unstable whenever $\mathcal{R}_0 > 1$.

Similarly, the eigenvalues of the Jacobian at the non-trivial critical point given in (3.4.2) are the roots of the characteristic equation $P(\lambda) = 0$, where

$$P(\lambda) = \lambda^2 + A\lambda + B \tag{3.4.8}$$

Table 3.1: Stability properties of critical points

	critical points	
	trivial	non-trivial
$\mathcal{R}_0 < 1$	stable	unstable
$\mathcal{R}_0 > 1$	unstable	stable
$\mathcal{R}_0 = 1$	saddle-node bifurcation	

and

$$A = \mu\mathcal{R}_0, \quad B = \mu(\mu + \nu)(\mathcal{R}_0 - 1).$$

It follows from the Routh-Hurwitz criterion (Lambert [15], p.14) that all eigenvalues have negative real part if $A > 0$ and $B > 0$. This holds if $\mathcal{R}_0 > 1$ and all model parameters are assumed to be positive. The non-trivial critical point, therefore, is asymptotically stable whenever $\mathcal{R}_0 > 1$ and unstable for $\mathcal{R}_0 < 1$.

For $\mathcal{R}_0 = 1$, there is only one critical point since the non-trivial critical point coincides with the trivial critical point (see equations (3.4.1) and (3.4.2)). This critical point is non-hyperbolic (Wiggins [31]) as one of the eigenvalues of the Jacobian becomes zero while the other $(-\mu)$ is real and negative. This presents the point at which a node (stable or unstable depending on the sign of μ) is just changing to a saddle point or *vice versa*. The parameter μ, however, is non-negative and this critical point is a stable node, and $\mathcal{R}_0$ will be called a saddle-node bifurcation (Gray & Scott [12]). Furthermore, both critical points of the system {(3.3.6),(3.3.7)} exchange their stability properties as $\mathcal{R}_0$ passes through unity (see table 3.1).

The asymptotic behaviours of solution paths in the x-y phase plane are described in the following theorem (Hethcote [14]).

Theorem 3.1 *If* $\mathcal{R}_0 \leq 1$, *then the triangle* $\overline{\mathcal{D}}$ *defined by* (3.3.9) *is an asymptotic stability region for the critical point* (1,0). *If* $\mathcal{R}_0 > 1$, *then* $\overline{\mathcal{D}} - \{(x,0) \mid 0 \leq x \leq 1\}$ *is an asymptotic stability region for the critical point given in* (3.4.2).

3.5 The Seasonal *SIR* Model

The dynamics of the *SIR* model are determined by the model's two steady states (see §3.4). In the absence of external perturbation, all variables x, y and z eventually reach a constant steady-state. The epidemiological data on whooping cough (Duncan *et al.* [9]), however, often demonstrate periodic or irregular outbreaks of the epidemic dynamics which the *SIR* model fails to capture. Then, more realistic dynamics may be achieved by taking into account the seasonal nature of the epidemic. London & Yorke [18], for example, showed the importance of considering the contact rate, β, as a periodic (annual) function of time. Sources of seasonal variation in the contact rate have been attributed to social behaviour, such as the timing of the school year, and seasonal changes in the weather conditions (Bolker & Grenfell [4], Duncan *et al.* [9],[10], London & Yorke [18]).

In this section, the seasonal *SIR* model is studied by adding a forcing term $\beta(t)$ to equations (3.3.6) and (3.3.7) to give the initial-value problem

$$\frac{\mathrm{d}x}{\mathrm{d}t} = \mu - \mu x - N\beta(t)xy, \quad x(0) = x_0, \tag{3.5.1}$$

$$\frac{\mathrm{d}y}{\mathrm{d}t} = -(\mu+\nu)y + N\beta(t)xy, \quad y(0) = y_0, \tag{3.5.2}$$

in which $\beta(t)$ is given by (Duncan *et al.* [9])

$$\beta(t) = \beta_0(1 + \delta\sin(\omega t)), \tag{3.5.3}$$

where the parameter δ is the force of the infection (equivalent to fractional variation in susceptibility) and ω is the angular frequency of oscillation in susceptibility (ω=2π/period of oscillation). It will be assumed that δ is a real number between zero and unity.

The critical points of the system {(3.5.1),(3.5.2)} are obtained as in (3.4.1) and (3.4.2), respectively, but the infection rate β is replaced by $\beta_0(1+\delta\sin(\omega t))$, giving

$$C_1^* = (1,0) \qquad \text{and} \qquad C_2^* = (x_s, y_s), \tag{3.5.4}$$

where

$$x_s = \frac{\mu+\nu}{N\beta_0(1+\delta\sin(\omega t))} \quad \text{and} \quad y_s = \frac{\mu}{\mu+\nu}(1-x_s).$$

It is found that the trivial critical point C_1^* coincides with the trivial critical point of the *SIR* whooping cough model while the non-trivial critical point C_2^* is now time dependent. Thus, the oscillation-behaviour can be expected whenever the non-trivial critical point is attracting. The non-trivial critical point should be asymptotically stable if $\mathcal{R}_0(t) = N\beta(t)/(\mu+\nu) > 1$.

When $\delta > 0$ is small, equations (3.5.1) and (3.5.2) can be approximated by a linearized model by defining

$$x = x_s + \eta, \tag{3.5.5}$$

$$y = y_s + \xi, \tag{3.5.6}$$

where η and ξ represent the variations in x and y from their steady-state values.

Substituting equations (3.5.5) and (3.5.6) into equations (3.5.1) and (3.5.2) and ignoring higher-order terms gives

$$\frac{\mathrm{d}\eta}{\mathrm{d}t} \approx -(N\beta_0 y_s + \mu)\eta - (\mu+\nu)\xi - (\mu+\nu)y_s\delta\sin(\omega t), \tag{3.5.7}$$

$$\frac{\mathrm{d}\xi}{\mathrm{d}t} \approx N\beta_0 y_s\eta + (\mu+\nu)y_s\delta\sin(\omega t). \tag{3.5.8}$$

These equations describe a forced second-order linear system where the forcing function is the periodic driving term $(\mu+\nu)y_s\delta\sin(\omega t)$: that is, oscillations in susceptibility, δ, can act as a driver for the system (Olsen & Schaffer [20], Rand & Wilson [23], Tidd *et al.* [27]). In the absence of seasonal oscillations, $\delta = 0$, eliminating η from (3.5.7) and (3.5.8) gives

$$\frac{\mathrm{d}^2\xi}{\mathrm{d}t^2} + \mu\frac{N\beta_0}{\mu+\nu}\frac{\mathrm{d}\xi}{\mathrm{d}t} + \mu(N\beta_0 - \mu - \nu)\xi = 0 \tag{3.5.9}$$

which is a form representing the equation of motion of an unforced, damped linear oscillator. For the disease under consideration the human life expectancy, $1/\mu$, is much longer than the infectious period, $1/\nu$, so that under this situation there exist damped oscillations around the equilibrium for $\mathcal{R}_0 > 1$. The oscillation has a period (T) defined as

$$T = \frac{2\pi}{\sqrt{\mu(N\beta_0 - \mu - \nu)}}. \tag{3.5.10}$$

Thus, the inter-epidemic interval (Duncan *et al.* [10], [9]), T, is determined by $N\beta_0$.

Therefore, the dynamics of the seasonal *SIR* model are then dependent on the amplitude of the variation in susceptibility, δ. When $\delta = 0$, equations (3.3.6) and (3.3.7) are considered as a non-linear system that is driven by variations in $N\beta$. For small amplitudes of the variation, δ, the response is approximately linear; thus the output is sinusoidal for a sinusoidal variation in δ at the same frequency but with different amplitude and phase. As δ is increased, the non-linear effects come to dominate and the response becomes non-sinusoidal, as will be shown in §3.8.2.

3.6 Numerical methods

The numerical methods are based on the replacement of $\mathrm{d}x/\mathrm{d}t$ and $\mathrm{d}y/\mathrm{d}t$ in (3.3.6) and (3.3.7) by the first-order approximations

$$\frac{\mathrm{d}x(t)}{\mathrm{d}t} = \frac{x(t+\ell) - x(t)}{\ell} + O(\ell) \quad \text{as} \quad \ell \to 0 \tag{3.6.1}$$

and

$$\frac{\mathrm{d}y(t)}{\mathrm{d}t} = \frac{y(t+\ell) - y(t)}{\ell} + O(\ell) \quad \text{as} \quad \ell \to 0, \tag{3.6.2}$$

where $\ell > 0$ is an increment in t (time step), associated with the discretization of the interval $t \geq 0$ at the points $t_n = n\ell$, with $t_{n+1} - t_n = \ell$, $n = 0, 1, 2, \ldots$. The theoretical solutions of the initial-value problem (3.3.6) and (3.3.7) at any typical point $t = t_n$ are denoted by $x(t_n)$, $y(t_n)$, while the solution of an approximating numerical method will be denoted by X^n and Y^n, respectively, at the same point t_n.

3.6.1 First-order methods

Euler's method

Replacing $\mathrm{d}x/\mathrm{d}t$ and $\mathrm{d}y/\mathrm{d}t$ in (3.3.6) and (3.3.7) by (3.6.1) and (3.6.2), respectively, and evaluating all terms on the right-hand sides of (3.3.6) and (3.3.7) at time t_n gives

Method $\mathcal{M}_1$

$$X^{n+1} = X^n + \ell\{\mu - \mu X^n - N\beta X^n Y^n\}, \tag{3.6.3}$$

$$Y^{n+1} = Y^n + \ell\{-(\mu+\nu)Y^n + N\beta X^n Y^n\}, \tag{3.6.4}$$

$n = 0, 1, 2, \ldots$, which is the familiar Euler explicit method.

Alternative first-order methods

The alternative first-order methods are obtained again by approximating the derivatives in (3.3.6) and (3.3.7) by (3.6.1) and (3.6.2), respectively, and evaluating the variables on the right-hand sides of (3.3.6) and (3.3.7) at time t_n and t_{n+1} as in the following two ways

Method $\mathcal{M}_2$

$$\frac{X^{n+1} - X^n}{\ell} = \mu - \mu X^{n+1} - N\beta X^{n+1} Y^n, \tag{3.6.5}$$

$$\frac{Y^{n+1} - Y^n}{\ell} = -(\mu+\nu) Y^{n+1} + N\beta X^n Y^n. \tag{3.6.6}$$

After rearranging, these give the explicit formulations

$$X^{n+1} = \frac{\ell\mu + X^n}{1 + \ell\mu + \ell N\beta Y^n}, \tag{3.6.7}$$

$$Y^{n+1} = \frac{Y^n + \ell N\beta X^n Y^n}{1 + \ell\mu + \ell\nu}, \tag{3.6.8}$$

for $n = 0, 1, 2, \ldots$.

Method $\mathcal{M}_3$

$$\frac{X^{n+1}-X^n}{\ell} = \mu - \mu X^{n+1} - N\beta X^n Y^n, \tag{3.6.9}$$

$$\frac{Y^{n+1}-Y^n}{\ell} = -(\mu+\nu)Y^{n+1} + N\beta X^{n+1} Y^n. \tag{3.6.10}$$

Substituting for X^{n+1} from (3.6.9) into (3.6.10) and rearranging, gives the explicit formulations

$$X^{n+1} = \frac{\ell\mu + X^n - \ell N\beta X^n Y^n}{1+\ell\mu}, \tag{3.6.11}$$

$$Y^{n+1} = \frac{(1+\ell\mu+\ell^2\mu N\beta)Y^n + \ell N\beta X^n Y^n(1-\ell N\beta Y^n)}{(1+\ell\mu)(1+\ell\mu+\ell\nu)}, \tag{3.6.12}$$

for $n = 0, 1, 2, \ldots$.

The local truncation errors

Method $\mathcal{M}_1$ The local truncation errors (LTEs) of this method may be determined (see for example, Lambert [15]) from (3.6.3) and (3.6.4) and are given by

$$\mathcal{L}_x^1[x(t), y(t); \ell] = x(t+\ell) - x(t) - \ell\{\mu - \mu x(t) - N\beta x(t)y(t)\}$$

and

$$\mathcal{L}_y^1[x(t), y(t); \ell] = y(t+\ell) - y(t) + \ell\{(\mu+\nu)\, y(t) - N\beta\, x(t)\, y(t)\}.$$

Using Taylor expansions of $x(t+\ell)$ and $y(t+\ell)$ about t lead to

$$\mathcal{L}_x^1[x(t), y(t); \ell] = \frac{\ell^2}{2}x''(t) + O(\ell^3) \quad \text{as} \quad \ell \to 0 \tag{3.6.13}$$

and

$$\mathcal{L}_y^1[x(t), y(t); \ell] = \frac{\ell^2}{2}y''(t) + O(\ell^3) \quad \text{as} \quad \ell \to 0, \tag{3.6.14}$$

at some point $t = t_n$, verifying that this familiar numerical method is first-order accurate.

Similarly, the local truncation errors $\mathcal{L}_x[x(t), y(t); \ell]$ and $\mathcal{L}_y[x(t), y(t); \ell]$ associated with the family of the methods $\mathcal{M}_2$ and $\mathcal{M}_3$ are seen to be

(i) for family $\mathcal{M}_2$

$$\mathcal{L}_x^2[x(t),y(t);\ell] \;=\; \ell^2\left\{\frac{x''(t)}{2}+\mu x'(t)+N\beta x'(t)y(t)\right\}+O(\ell^3) \quad \text{as} \quad \ell\to 0, \tag{3.6.15}$$

$$\mathcal{L}_y^2[x(t),y(t);\ell] \;=\; \ell^2\left\{\frac{y''(t)}{2}+(\mu+\nu)y'(t)\right\}+O(\ell^3) \quad \text{as} \quad \ell\to 0, \tag{3.6.16}$$

(ii) for family $\mathcal{M}_3$

$$\mathcal{L}_x^3[x(t),y(t);\ell] \;=\; \ell^2\left\{\frac{x''(t)}{2}+\mu x'(t)+\right\}+O(\ell^3) \quad \text{as} \quad \ell\to 0, \tag{3.6.17}$$

$$\mathcal{L}_y^3[x(t),y(t);\ell] \;=\; \ell^2\left\{\frac{y''(t)}{2}+(\mu+\nu)y'(t)-N\beta x'(t)y(t)\right\}+O(\ell^3) \quad \text{as} \quad \ell\to 0, \tag{3.6.18}$$

at some time $t=t_n$. Hence, the methods $\mathcal{M}_2$ and $\mathcal{M}_3$ are first-order accurate.

3.6.2 Second-order method

The second-order method is based on a linear combination of first-order numerical methods. To achieve second-order accuracy when solving the non-linear ODEs in (3.3.6) and (3.3.7), the second-order methods for functions $x=x(t)$ and $y=y(t)$ will be developed differently. Three first-order methods were mentioned in §3.6.1, and a new first-order method will be introduced; a linear combination of them will lead to the second-order numerical method. It will be assumed that $x(t)$ and $y(t)$, the solutions of the initial-value problem {(3.3.6),(3.3.7)}, are twice continuously differentiable for all $t\geq 0$.

Second-order Method for X^{n+1}

To obtain second-order accuracy for $x=x(t)$, take equation (3.3.6) in the form

$$x'(t)-\mu+\mu\,x(t)+N\beta\,x(t)\,y(t)=0. \tag{3.6.19}$$

Differentiating equation (3.6.19) with respect to time, t, gives

$$x''(t) + \mu\, x'(t) + N\beta\, x'(t)\, y(t) + N\beta\, x(t)\, y'(t) = 0. \tag{3.6.20}$$

The first-order methods previously discussed are given below along with the new first-order method,

$$\mathcal{M}_{1x}: \quad \frac{X^{n+1} - X^n}{\ell} = \mu - \mu\, X^n - N\beta\, X^n\, Y^n, \tag{3.6.21}$$

$$\mathcal{M}_{2x}: \quad \frac{X^{n+1} - X^n}{\ell} = \mu - \mu\, X^{n+1} - N\beta\, X^{n+1}\, Y^n, \tag{3.6.22}$$

$$\mathcal{M}_{3x}: \quad \frac{X^{n+1} - X^n}{\ell} = \mu - \mu\, X^{n+1} - N\beta\, X^n\, Y^n, \tag{3.6.23}$$

$$\mathcal{M}_{4x}: \quad \frac{X^{n+1} - X^n}{\ell} = \mu - \mu X^{n+1} - N\beta X^n Y^{n+1} \tag{3.6.24}$$

and their associated LTEs

$$\mathcal{L}_x^1[x(t), y(t); \ell] = \frac{\ell^2}{2} x''(t) + O(\ell^3) \quad \text{as} \quad \ell \to 0, \tag{3.6.25}$$

$$\mathcal{L}_x^2[x(t), y(t); \ell] = \ell^2 \left\{ \frac{x''(t)}{2} + \mu\, x'(t) + N\beta\, x'(t)\, y(t) \right\} + O(\ell^3) \quad \text{as} \quad \ell \to 0, \tag{3.6.26}$$

$$\mathcal{L}_x^3[x(t), y(t); \ell] = \ell^2 \left\{ \frac{x''(t)}{2} + \mu\, x'(t) \right\} + O(\ell^3) \quad \text{as} \quad \ell \to 0, \tag{3.6.27}$$

$$\mathcal{L}_x^4[x(t), y(t); \ell] = \ell^2 \left\{ \frac{x''(t)}{2} + \mu\, x'(t) + \ell N\beta\, x(t)\, y'(t) \right\} + O(\ell^3) \quad \text{as} \quad \ell \to 0. \tag{3.6.28}$$

Using equations (3.6.25)-(3.6.28) leads to the local truncation error of a second-order numerical method for $x = x(t)$, denoted by $\mathcal{L}_x^s[x(t), y(t); \ell]$, as being defined by

$$\mathcal{L}_x^s = \mathcal{L}_x^1 + \mathcal{L}_x^2 - \mathcal{L}_x^3 + \mathcal{L}_x^4. \tag{3.6.29}$$

It is easy to see that

$$\mathcal{L}_x^s = \ell^2 \Big(x''(t) + \mu\, x'(t) + N\beta\, x'(t)\, y(t) + N\beta x(t) y'(t) \Big) + O(\ell^3) \quad \text{as} \quad \ell \to 0, \tag{3.6.30}$$

so that, using (3.6.20),

$$\mathcal{L}_x^s \;=\; O(\ell^3) \quad \text{as} \quad \ell \to 0. \tag{3.6.31}$$

To construct the associated second-order method for $x = x(t)$, it follows from (3.6.29) that equations (3.6.21)-(3.6.24) must be arranged to give

$$\begin{aligned}
\mathcal{M}_{1,x}: &\quad X^{n+1} - X^n - \ell\mu + \ell\mu X^n + \ell N\beta X^n Y^n = 0,\\
\mathcal{M}_{2,x}: &\quad X^{n+1} - X^n - \ell\mu + \ell\mu X^{n+1} + \ell N\beta X^{n+1} Y^n = 0,\\
\mathcal{M}_{3,x}: &\quad X^{n+1} - X^n - \ell\mu + \ell\mu X^{n+1} + \ell N\beta X^n Y^n = 0,\\
\mathcal{M}_{4,x}: &\quad X^{n+1} - X^n - \ell\mu + \ell\mu X^{n+1} + \ell N\beta X^n Y^{n+1} = 0,
\end{aligned}$$

following which the second-order method for $x = x(t)$ is seen to be

$$\left[2 + \mu\ell + \ell N\beta Y^n\right] X^{n+1} = 2X^n + 2\mu\ell - \ell\{\mu + N\beta Y^{n+1}\} X^n. \tag{3.6.32}$$

Second-order Method for Y^{n+1}

To determine the second-order method for $y = y(t)$, consider equation (3.3.7) which can be written as

$$y'(t) + (\mu + \nu)\, y(t) - N\beta\, x(t)\, y(t) = 0. \tag{3.6.33}$$

Then, differentiating equation (3.6.33) with respect to t gives

$$y''(t) + (\mu + \nu)\, y'(t) - N\beta\, x(t)\, y'(t) - N\beta\, x'(t)\, y(t) = 0. \tag{3.6.34}$$

The first-order approximations to equation (3.3.7) with their LTEs can be given by

$$\mathcal{M}_{1y}: \quad \frac{Y^{n+1} - Y^n}{\ell} \;=\; -(\mu + \nu)\, Y^n + N\beta\, X^n\, Y^n, \tag{3.6.35}$$

$$\mathcal{L}_y^1[x(t), y(t); \ell] \;=\; \frac{\ell^2}{2} y''(t) + O(\ell^3) \quad \text{as} \quad \ell \to 0, \tag{3.6.36}$$

$$\mathcal{M}_{2y}: \quad \frac{Y^{n+1} - Y^n}{\ell} \;=\; -(\mu + \nu)\, Y^{n+1} + N\beta\, X^n\, Y^n, \tag{3.6.37}$$

$$\mathcal{L}_y^2[x(t),y(t);\ell] = \ell^2\left\{\frac{y''(t)}{2}+(\mu+\nu)\,y'(t)\right\} + O(\ell^3) \quad \text{as} \quad \ell\to 0, \tag{3.6.38}$$

$$\mathcal{M}_{3y}: \quad \frac{Y^{n+1}-Y^n}{\ell} = -(\mu+\nu)Y^{n+1}+N\beta X^{n+1}Y^n, \tag{3.6.39}$$

$$\mathcal{L}_y^3[x(t),y(t);\ell] = \ell^2\left\{\frac{y''(t)}{2}+(\mu+\nu)\,y'(t)-N\beta x'(t)y(t)\right\} + O(\ell^3) \quad \text{as} \quad \ell\to 0, \tag{3.6.40}$$

$$\mathcal{M}_{4y}: \quad \frac{Y^{n+1}-Y^n}{\ell} = -(\mu+\nu)Y^{n+1}+N\beta X^{n}Y^{n+1}, \tag{3.6.41}$$

$$\mathcal{L}_y^4[x(t),y(t);\ell] = \ell^2\left\{\frac{y''(t)}{2}+(\mu+\nu)y'(t)-N\beta x(t)\,y'(t)\right\} + O(\ell^3) \quad \text{as} \quad \ell\to 0. \tag{3.6.42}$$

It follows from equations (3.6.36), (3.6.38), (3.6.40) and (3.6.42) that $\mathcal{L}_y^s[x(t),y(t);\ell]$ defined by

$$\begin{aligned}\mathcal{L}_y^s &= \mathcal{L}_y^1-\mathcal{L}_y^2+\mathcal{L}_y^3+\mathcal{L}_y^4\\ &= \ell^2\Big(y''(t)+(\mu+\nu)\,y'(t)-N\beta\,x'(t)\,y(t)-N\beta x(t)y'(t)\Big)\\ &\quad +O(\ell^3) \quad \text{as} \quad \ell\to 0\end{aligned} \tag{3.6.43}$$

and, using (3.6.34), yields

$$\mathcal{L}_y^s = O(\ell^3) \quad \text{as} \quad \ell\to 0. \tag{3.6.44}$$

Thus, the second-order method for $y=y(t)$ may be constructed in the same way as described for $x=x(t)$ in the previous section and is easily shown to be

$$\left[2+\ell(\mu+\nu)-\ell N\beta X^n\right]Y^{n+1}=2Y^n+\ell\{-(\mu+\nu)+N\beta X^{n+1}\}Y^n. \tag{3.6.45}$$

To solve the linear algebraic system (3.6.32) and (3.6.45) for X^{n+1} and Y^{n+1}, the system may be written for simplicity in the forms

$$AX^{n+1}-(2-\ell\mu)X^n+\ell N\beta X^nY^{n+1}-2\ell\mu = 0, \tag{3.6.46}$$

$$\mathcal{B}Y^{n+1} - (2 - \ell\mu - \ell\nu)Y^n - \ell N\beta X^{n+1}Y^n = 0 \tag{3.6.47}$$

where

$$\mathcal{A} = 2 + \ell\mu + \ell N\beta Y^n, \tag{3.6.48}$$

$$\mathcal{B} = 2 + \ell\mu + \ell\nu - \ell N\beta X^n. \tag{3.6.49}$$

Solving the equations (3.6.46) and (3.6.47), give

$$X^{n+1} = \frac{(2 - \ell\mu)\mathcal{B}X^n + 2\mu\ell\mathcal{B} - \ell(2 - \ell\mu - \ell\nu)N\beta X^nY^n}{\mathcal{C}}, \tag{3.6.50}$$

$$Y^{n+1} = \frac{(2 - \ell\mu - \ell\nu)\mathcal{A}Y^n + 2\mu\ell^2 N\beta Y^n + \ell(2 - \ell\mu)N\beta X^nY^n}{\mathcal{C}} \tag{3.6.51}$$

where $\mathcal{A}$, $\mathcal{B}$ are as in (3.6.48) and (3.6.49) and

$$\mathcal{C} = \mathcal{A}\mathcal{B} + (\ell N\beta)^2 X^nY^n. \tag{3.6.52}$$

Therefore, a second-order solution to the first-order IVP system {(3.3.6),(3.3.7)} may be computed using (3.6.50) and (3.6.51) with $n = 0, 1, 2, \ldots$.

3.7 Analyses of the methods

Finding the fixed points of the finite-difference methods is equivalent to finding the critical points of the initial-value problem {(3.3.6),(3.3.7)}, see for example Luenberger [17]. It can be shown that the fixed points of each finite-difference method, as $n \to \infty$, are the same as the critical points of the ODE system.

All the numerical methods which were mentioned in §3.6 are of the form of the two one-point iteration functions given by

$$X^{n+1} := g_1(X_n, Y_n) \quad \text{and} \quad Y^{n+1} := g_2(X_n, Y_n) \tag{3.7.1}$$

and all have steady-state solutions (fixed points), which will be denoted by

$$\mathbf{u}_1^* = (X_1^*, Y_1^*) = (1, 0) \qquad \text{and} \qquad \mathbf{u}_2^* = (X_2^*, Y_2^*) \tag{3.7.2}$$

where

$$X_2^* = \frac{\mu+\nu}{N\beta} \quad \text{and} \quad Y_2^* = \frac{\mu}{\mu+\nu}(1-X_2^*). \tag{3.7.3}$$

To analyse the stability of these fixed points, it is necessary to consider the associated functions

$$X \equiv g_1(X,Y) \quad \text{and} \quad Y \equiv g_2(X,Y) \tag{3.7.4}$$

where, for {(3.6.3),(3.6.4)},

$$g_1(X,Y) = X + \ell\mu - \ell\{\mu + N\beta Y\}X, \tag{3.7.5}$$

$$g_2(X,Y) = Y + \ell\{-(\mu+\nu) + N\beta X\}Y, \tag{3.7.6}$$

for {(3.6.5),(3.6.6)},

$$g_1(X,Y) = \frac{\ell\mu + X}{1 + \ell\mu + \ell N\beta Y}, \tag{3.7.7}$$

$$g_2(X,Y) = \frac{Y + \ell N\beta XY}{1 + \ell\mu + \ell\nu}, \tag{3.7.8}$$

for {(3.6.9),(3.6.10)},

$$g_1(X,Y) = \frac{\ell\mu + X - \ell N\beta XY}{1+\ell\mu}, \tag{3.7.9}$$

$$g_2(X,Y) = \frac{Y}{1+\ell\mu+\ell\nu} + \frac{\ell N\beta Y(X + \ell\mu - \ell N\beta XY)}{(1+\ell\mu)(1+\ell\mu+\ell\nu)}, \tag{3.7.10}$$

and for {(3.6.50),(3.6.51)},

$$g_1(X,Y) = \frac{(2-\ell\mu)\mathcal{B}X + 2\mu\ell\mathcal{B} - \ell N\beta(2-\ell\mu-\ell\nu)XY}{\mathcal{C}}, \tag{3.7.11}$$

$$g_2(X,Y) = \frac{(2-\ell\mu-\ell\nu)\mathcal{A}Y + 2\mu\ell^2 N\beta Y + \ell N\beta(2-\ell\mu)XY}{\mathcal{C}} \tag{3.7.12}$$

where

$$\begin{aligned} \mathcal{A} &= 2 + \mu\ell + N\ell\beta Y, \\ \mathcal{B} &= 2 + \ell(\mu+\nu) - \ell N\beta X, \\ \mathcal{C} &= (2+\mu\ell)(2+\ell\mu+\ell\nu) - (2+\ell\mu)\ell N\beta X + (2+\ell\mu+\ell\nu)\ell N\beta Y. \end{aligned} \tag{3.7.13}$$

A sequence generated by the numerical method converges to a fixed point if and only if the spectral radius, $\rho(J)$, at the fixed point of the Jacobian, J, given by

$$J = \begin{bmatrix} \partial g_1/\partial x & \partial g_1/\partial y \\ \\ \partial g_2/\partial x & \partial g_2/\partial y \end{bmatrix} \tag{3.7.14}$$

satisfies the condition (see theorem 2.14)

$$\rho(J) < 1. \tag{3.7.15}$$

3.7.1 Stability of the fixed points of Method $\mathcal{M}_1$

To analyse the stability of this method, the Jacobian appropriate to equations (3.7.5) and (3.7.6) is

$$J = \begin{bmatrix} 1-\ell(\mu+N\beta Y) & -\ell N\beta X \\ \ell N\beta Y & 1+\ell\{N\beta X-(\mu+\nu)\} \end{bmatrix}. \tag{3.7.16}$$

At the trivial critical point, $\mathbf{u}_1^* = (1,0)$, the characteristic polynomial of the Jacobian J from (3.7.16) is given by

$$\lambda^2 - \{2-\ell\mu+\ell(\mu+\nu)(\mathcal{R}_0-1)\}\lambda + (1-\ell\mu)\{1+\ell(\mu+\nu)(\mathcal{R}_0-1)\} = 0. \tag{3.7.17}$$

The eigenvalues are

$$\lambda_{1,2} = \frac{2-\ell\mu+\ell(\mu+\nu)(\mathcal{R}_0-1) \pm \sqrt{\ell^2\{\mu+(\mu+\nu)(\mathcal{R}_0-1)\}^2}}{2} \tag{3.7.18}$$

so that

$$\lambda_1 = 1+\ell(\mu+\nu)(\mathcal{R}_0-1), \quad \lambda_2 = 1-\ell\mu \quad \text{if} \quad \mathcal{R}_0 > 1 \tag{3.7.19}$$

and

$$\lambda_1 = 1-\ell(\mu+\nu)(1-\mathcal{R}_0), \quad \lambda_2 = 1-\ell\mu \quad \text{if} \quad \mathcal{R}_0 < 1. \tag{3.7.20}$$

From (3.7.19) and (3.7.20), it is clear that, for $\mathcal{R}_0 > 1$, the spectral radius is strictly greater than unity for all ℓ. For $\mathcal{R}_0 < 1$, the spectral radius is strictly less than unity if

$$\ell < \frac{2}{(\mu+\nu)(1-\mathcal{R}_0)} \quad \text{and} \quad \ell < 2/\mu. \tag{3.7.21}$$

Therefore, the trivial fixed point is conditionally stable for $\mathcal{R}_0 < 1$ and unstable for $\mathcal{R}_0 > 1$.

At the non-trivial fixed point in (3.7.3), the characteristic polynomial of the Jacobian J is given by

$$\lambda^2 - (2 - \ell\mu\mathcal{R}_0)\lambda + 1 - \ell\mu\mathcal{R}_0 + \ell^2\mu(\mu+\nu)(\mathcal{R}_0 - 1) = 0 \tag{3.7.22}$$

and the associated eigenvalues are

$$\lambda_{1,2} \;=\; 1 - \frac{\ell}{2}\left\{\mu\mathcal{R}_0 \pm \sqrt{(\mu\mathcal{R}_0)^2 - 4\mu(\mu+\nu)(\mathcal{R}_0 - 1)}\right\}. \tag{3.7.23}$$

If $\mathcal{R}_0 < 1$, $\lambda_{1,2}$ are real and positive since the discriminant is always positive. Moreover,

$$\mu\mathcal{R}_0 < \sqrt{(\mu\mathcal{R}_0)^2 - 4\mu(\mu+\nu)(\mathcal{R}_0 - 1)}$$

so that one of the roots of equation (3.7.23) is greater than unity. This shows that the spectral radius is strictly greater than unity for all values of ℓ.

For $\mathcal{R}_0 > 1$, the spectral radius will be considered as follows:

Case i Suppose that $(\mu\mathcal{R}_0)^2 - 4\mu(\mu+\nu)(\mathcal{R}_0 - 1) < 0$, the eigenvalues are complex numbers with

$$|\lambda_{1,2}|^2 = 1 - \ell\mu\mathcal{R}_0 + \ell^2\mu(\mu+\nu)(\mathcal{R}_0 - 1)$$

and the spectral radius is strictly less than unity if $0 < |\lambda_{1,2}|^2 < 1$ so that

$$0 < \ell\mu(\mathcal{R}_0 - 1) < \frac{1 - \ell\mu}{1 - \ell\mu - \ell\nu}. \tag{3.7.24}$$

Case ii Suppose that $(\mu\mathcal{R}_0)^2 - 4\mu(\mu+\nu)(\mathcal{R}_0 - 1) = 0$ then $\lambda_{1,2} = \dfrac{(2 - \ell\mu\mathcal{R}_0)}{2}$ and the spectral radius is strictly less than unity if $-1 < \lambda_{1,2} < 1$ so that

$$0 < \ell\mu(\mathcal{R}_0 - 1) < 4 - \ell\mu. \tag{3.7.25}$$

Case iii Suppose that $(\mu\mathcal{R}_0)^2 - 4\mu(\mu+\nu)(\mathcal{R}_0-1) > 0$ then the two eigenvalues are real and are given by

$$\lambda_1 = 1 - \frac{\ell}{2}\left\{\mu\mathcal{R}_0 + \sqrt{(\mu\mathcal{R}_0)^2 - 4\mu(\mu+\nu)(\mathcal{R}_0-1)}\right\}, \tag{3.7.26}$$

$$\lambda_2 = 1 - \frac{\ell}{2}\left\{\mu\mathcal{R}_0 - \sqrt{(\mu\mathcal{R}_0)^2 - 4\mu(\mu+\nu)(\mathcal{R}_0-1)}\right\}. \tag{3.7.27}$$

The spectral radius is, therefore, strictly less than unity if

$$\ell\mu\mathcal{R}_0 < 2 \quad \text{or} \quad \ell\mu(\mathcal{R}_0-1) < 2 - \ell\mu. \tag{3.7.28}$$

From cases i-iii, it is found that equations (3.7.24), (3.7.25) and (3.7.28) are the conditions under which the numerical method $\mathcal{M}_1$ will converge to the non-trivial fixed point (3.7.3) whenever $\mathcal{R}_0 > 1$.

3.7.2 Stability of the fixed points of Method $\mathcal{M}_2$

The Jacobian, for {(3.7.7),(3.7.8)}, is the matrix

$$J = \begin{pmatrix} \dfrac{1}{1+\ell\mu+\ell N\beta Y} & \dfrac{-\ell N\beta(\ell\mu+X)}{(1+\ell\mu+\ell N\beta Y)^2} \\ \dfrac{\ell N\beta Y}{1+\ell\mu+\ell\nu} & \dfrac{1+\ell N\beta X}{1+\ell\mu+\ell\nu} \end{pmatrix}. \tag{3.7.29}$$

The stability of the trivial fixed point is determined by the eigenvalues of the matrix J, given by

$$|J-\lambda I| = \begin{vmatrix} \dfrac{1}{1+\ell\mu} - \lambda & \dfrac{-\ell N\beta}{1+\ell\mu} \\ 0 & \dfrac{1+\ell N\beta}{1+\ell\mu+\ell\nu} - \lambda \end{vmatrix} = 0 \tag{3.7.30}$$

so that

$$\lambda_1 = \frac{1}{1+\ell\mu}, \quad \lambda_2 = \frac{1+\ell N\beta}{1+\ell\mu+\ell\nu}. \tag{3.7.31}$$

Clearly, the spectral radius is strictly less than unity for all ℓ if $\mathcal{R}_0 < 1$. Condition (3.7.15), therefore, is satisfied and the numerical method {(3.6.7),(3.6.8)} will

converge unconditionally from any starting values $x_0,\ y_0$ to the trivial fixed point $x = 1,\ y = 0$ whenever $\mathcal{R}_0 < 1$.

For the non-trivial fixed point given in (3.4.2), the Jacobian is the matrix

$$J = \begin{pmatrix} \dfrac{\mu+\nu}{\mu+\nu+\mu\ell N\beta} & \dfrac{-\ell(\mu+\nu)^2}{\mu+\nu+\mu\ell N\beta} \\ \dfrac{\mu\ell(N\beta-\mu-\nu)}{(\mu+\nu)(1+\ell\mu+\ell\nu)} & 1 \end{pmatrix}. \tag{3.7.32}$$

The eigenvalues of matrix J, λ_1 and λ_2, are the roots of the equation

$$\phi(\lambda) \equiv \lambda^2 - a\,\lambda + b = 0 \tag{3.7.33}$$

where

$$a \;=\; \frac{2(\mu+\nu)+\mu\ell N\beta}{\mu+\nu+\mu\ell N\beta} > 0$$

and

$$b \;=\; \frac{(\mu+\nu)\Big(1+\ell\mu+\ell\nu+\ell^2\mu(\mu+\nu)(\mathcal{R}_0-1)\Big)}{(\mu+\nu+\mu\ell N\beta)(1+\ell\mu+\ell\nu)} > 0$$

whenever $\mathcal{R}_0 > 1$.

The eigenvalues, λ_1 and λ_2, of matrix J are complex conjugates if $a^2 - 4b < 0$, and it is then easy to show that $|\lambda_i| < 1$ $(i = 1, 2)$ for all ℓ because

$$b - 1 = -\ell\mu N\beta - \ell^2\mu(\mu+\nu)^2 < 0 \quad \text{for all } \ell > 0.$$

The eigenvalues λ_1 and λ_2 are real if $a^2 - 4b \geq 0$. The properties of a quadratic function can be employed to show that $\lambda_{1,2} \in (-1, 1)$. The function $\phi(\lambda)$ is evaluated at $\lambda = -1, 0, 1$, giving

$$\phi(-1) = a + b + 1 > 0,\ \phi(0) = b > 0 \text{ and } \phi(1) = \frac{\ell^2\mu(\mu+\nu)^2(\mathcal{R}_0-1)}{(\mu+\nu+\mu\ell N\beta)(1+\ell\mu+\ell\nu)}.$$

Because $\phi(-1) > \phi(0) > 0$, the function ϕ has a minimum value at some point $\lambda = \lambda_{\mathtt{min}}$ between 0 and 1 since

$$\phi'(\lambda) = 2\lambda - a = 0 \quad \text{if} \quad \lambda = \frac{a}{2}$$

and

$$\phi''(\lambda) = \phi''(\lambda_{\mathtt{min}}) > 0, \quad \text{when} \quad \lambda_{\mathtt{min}} = \frac{a}{2}.$$

Clearly $\lambda_{\mathtt{min}} > 0$ and $\lambda_{\mathtt{min}} < 1$ when $a - 2 < 0$. It is easy to show that

$$\begin{aligned} a - 2 &= \frac{2(\mu+\nu) + \mu\ell N\beta - 2(\mu+\nu) - 2\ell\mu N\beta}{\mu + \nu + \mu\ell N\beta} \\ &= \frac{-\ell\mu N\beta}{\mu + \nu + \mu\ell N\beta} \end{aligned}$$

so that $\lambda_{\mathtt{min}} < 1$. Overall, $\phi(\lambda)$ has two real positive zeros which are less than unity in modulus, irrespective of the size of ℓ, when $\mathcal{R}_0 > 1$.

It can be concluded, therefore, that the non-trivial fixed point is unconditionally stable (with respect to ℓ), whenever $\mathcal{R}_0 > 1$.

3.7.3 Stability of the fixed points of Method $\mathcal{M}_3$

The elements of the Jacobian associated with the method, from {(3.7.9),(3.7.10)}, are given by

$$\begin{aligned} \frac{\partial g_1}{\partial X} &= \frac{1 - \ell N\beta Y}{1 + \ell\mu}, \\ \frac{\partial g_1}{\partial Y} &= \frac{-\ell N\beta X}{1 + \ell\mu}, \\ \frac{\partial g_2}{\partial X} &= \frac{\ell N\beta Y(1 - \ell N\beta Y)}{(1+\ell\mu)(1+\ell\mu+\ell\nu)}, \\ \frac{\partial g_2}{\partial Y} &= \frac{1}{1+\ell\mu+\ell\nu} + \frac{\ell N\beta(\ell\mu + X - 2\ell N\beta XY)}{(1+\ell\mu)(1+\ell\mu+\ell\nu)}. \end{aligned} \tag{3.7.34}$$

The Jacobian, at the trivial fixed point, $X_1^* = 1$, $Y_1^* = 0$, is the matrix

$$J = \begin{pmatrix} \dfrac{1}{1+\ell\mu} & \dfrac{-\ell N\beta}{1+\ell\mu} \\ 0 & \dfrac{1+\ell N\beta}{1+\ell\mu+\ell\nu} \end{pmatrix}, \tag{3.7.35}$$

and so

$$\lambda_1 = \frac{1}{1+\ell\mu}, \quad \lambda_2 = \frac{1+\ell N\beta}{1+\ell\mu+\ell\nu}$$

are as in (3.7.31). Therefore, the trivial fixed point is unconditionally stable for $\mathcal{R}_0 < 1$ and unstable for $\mathcal{R}_0 > 1$.

The Jacobian evaluated at the non-trivial fixed point given in (3.7.3) is given by

$$J = \begin{pmatrix} \frac{\mu+\nu+\ell\mu(\mu+\nu-N\beta)}{(1+\ell\mu)(\mu+\nu)} & \frac{-\ell(\mu+\nu)}{1+\ell\mu} \\ \\ \frac{\ell\mu(N\beta-\mu-\nu)(\mu+\nu+\ell\mu(\mu+\nu-N\beta))}{(\mu+\nu)^2(1+\ell\mu)(1+\ell\mu+\ell\nu)} & \frac{1+2\ell\mu+\ell\nu+\ell^2\mu(2\mu+2\nu-N\beta)}{(1+\ell\mu)(1+\ell\mu+\ell\nu)} \end{pmatrix}. \tag{3.7.36}$$

The eigenvalues of matrix J, λ_1 and λ_2, are the roots of the equation

$$\lambda^2 - (2-p-q)\,\lambda + 1 - q = 0 \tag{3.7.37}$$

so that

$$\lambda_1 = 1 - \frac{1}{2}\left\{(p+q) + \sqrt{(p+q)^2 - 4p}\right\}, \tag{3.7.38}$$

$$\lambda_2 = 1 - \frac{1}{2}\left\{(p+q) - \sqrt{(p+q)^2 - 4p}\right\} \tag{3.7.39}$$

where $p = \dfrac{\ell^2\mu(\mu+\nu)(\mathcal{R}_0-1)}{(1+\ell\mu)(1+\ell\mu+\ell\nu)} > 0$ for all $\mathcal{R}_0 > 1$ and $q = \dfrac{\ell\mu\mathcal{R}_0}{1+\ell\mu} > 0$.

Case i Suppose that $(p+q)^2 - 4p < 0$ then $|\lambda_{1,2}|^2 = 1-q$ and the spectral radius is strictly less than unity whenever $0 < 1-q < 1$, that is

$$\ell\mu(\mathcal{R}_0 - 1) < 1. \tag{3.7.40}$$

Case ii Suppose that $(p+q)^2 - 4p = 0$ then $\lambda_{1,2} = \dfrac{2-(p+q)}{2}$ and the spectral radius is strictly less than unity if

$$0 < p+q < 4$$

that is

$$0 < \ell\mu(\mathcal{R}_0 - 1) < \frac{4 + 7\ell\mu + 4\ell\nu + 3\ell^2\mu(\mu+\nu)}{1 + 2\ell\mu + 2\ell\nu}. \tag{3.7.41}$$

Case iii If $(p+q)^2 - 4p > 0$ then the two eigenvalues are real and are given by

$$\lambda_{1,2} = 1 - \frac{1}{2}\left\{(p+q) \pm \sqrt{(p+q)^2 - 4p}\right\}.$$

It is clear that the spectral radius is strictly less than unity whenever $a + b < 2$ or

$$0 < \ell\mu(\mathcal{R}_0 - 1) < \frac{2 + 3\ell\mu + 2\ell\nu + \ell^2\mu(\mu+\nu)}{1 + 2\ell\mu + 2\ell\nu}. \tag{3.7.42}$$

These, therefore, are the conditions under which the numerical method $\mathcal{M}_3$ will converge to the non-trivial fixed point (3.7.3).

3.7.4 Stability of the fixed points of the second-order method

The stability of the fixed point is again determined by the Jacobian, J, which for {(3.7.11), (3.7.12)}, is

$$J = \begin{bmatrix} \partial g_1/\partial X & \partial g_1/\partial Y \\ \\ \partial g_2/\partial X & \partial g_2/\partial Y \end{bmatrix} \tag{3.7.43}$$

where

$$\begin{aligned}
\frac{\partial g_1}{\partial X} &= \frac{(2-\mu\ell)(-\ell N\beta X + \mathcal{B}) - 2\mu N\beta\ell^2 - \ell N\beta(2-\ell\mu-\ell\nu)Y}{\mathcal{C}} \\
&\quad + \frac{(2+\mu\ell)\ell N\beta g_1(X,Y)}{\mathcal{C}}, \\
\frac{\partial g_1}{\partial Y} &= \frac{-\ell N\beta(2-\ell\mu-\ell\nu)X - (2+\mu\ell+\nu\ell)\ell N\beta g_1(X,Y)}{\mathcal{C}}, \\
\frac{\partial g_2}{\partial X} &= \frac{\ell N\beta(2-\ell\mu)Y + (2+\mu\ell)\ell N\beta g_2(X,Y)}{\mathcal{C}}, \\
\frac{\partial g_2}{\partial Y} &= \frac{(2-\mu\ell-\nu\ell)(\ell N\beta Y + \mathcal{A}) + 2\mu\ell^2 N\beta + \ell N\beta(2-\ell\mu)X}{\mathcal{C}} \\
&\quad - \frac{(2+\mu\ell+\nu\ell)\ell N\beta g_2(X,Y)}{\mathcal{C}}
\end{aligned} \tag{3.7.44}$$

and $\mathcal{A}$, $\mathcal{B}$ and $\mathcal{C}$ are as in (3.7.13).

Substituting the trivial fixed point, $X_1^* = 1$, $Y_1^* = 0$, into (3.7.43), the matrix J becomes

$$J(\mathbf{u}_1) = \begin{pmatrix} \frac{2-\mu\ell}{2+\ell\mu} & \frac{-4\ell N\beta}{(2+\ell\mu)(2-\ell N\beta+\ell\mu+\nu\ell)} \\ 0 & \frac{-2+\ell(-N\beta+\mu+\nu)}{-2+\ell(N\beta-\mu-\nu)} \end{pmatrix} \tag{3.7.45}$$

which has eigenvalues

$$\lambda_1 = \frac{2-\ell\mu}{2+\ell\mu} \quad \text{and} \quad \lambda_2 = \frac{2-\ell(\mu+\nu)(1-\mathcal{R}_0)}{2+\ell(\mu+\nu)(1-\mathcal{R}_0)}. \tag{3.7.46}$$

Obviously, $|\lambda_{1,2}| < 1$, if $\mathcal{R}_0 < 1$ for every value of ℓ, and the trivial fixed point is unconditionally stable for $\mathcal{R}_0 < 1$ and unstable for all ℓ if $\mathcal{R}_0 > 1$.

The elements of matrix J in (3.7.44), at the non-trivial fixed point in (3.7.3), are

$$\frac{\partial g_1}{\partial X} = \frac{4(\mu+\nu) - 2\ell\mu N\beta - \ell^2\mu(\mu+\nu)(N\beta-\mu-\nu)}{4(\mu+\nu) + 2\ell\mu N\beta + \ell^2\mu(\mu+\nu)(N\beta-\mu-\nu)},$$

$$\frac{\partial g_1}{\partial Y} = \frac{-4\ell(\mu+\nu)^2}{4(\mu+\nu) + 2\ell\mu N\beta + \ell^2\mu(\mu+\nu)(N\beta-\mu-\nu)},$$

$$\frac{\partial g_2}{\partial X} = \frac{4\ell\mu(N\beta-\mu-\nu)}{4(\mu+\nu) + 2\ell\mu N\beta + \ell^2\mu(\mu+\nu)(N\beta-\mu-\nu)},$$

$$\frac{\partial g_2}{\partial Y} = \frac{4(\mu+\nu) + 2\ell\mu N\beta - \ell^2\mu(\mu+\nu)(N\beta-\mu-\nu)}{4(\mu+\nu) + 2\ell\mu N\beta + \ell^2\mu(\mu+\nu)(N\beta-\mu-\nu)}.$$

The matrix J has eigenvalues λ given by

$$\phi(\lambda) \equiv \lambda^2 - \mathcal{Q}_1\lambda + \mathcal{Q}_2 = 0 \tag{3.7.47}$$

where

$$\mathcal{Q}_1 = 2(a-b),$$

$$\mathcal{Q}_2 = a+b-c,$$

with

$$a = \frac{4(\mu+\nu)}{4(\mu+\nu) + 2\ell\mu N\beta + \ell^2\mu(\mu+\nu)^2(\mathcal{R}_0-1)},$$

$$b = \frac{\ell^2\mu(\mu+\nu)^2(\mathcal{R}_0-1)}{4(\mu+\nu)+2\ell\mu N\beta+\ell^2\mu(\mu+\nu)^2(\mathcal{R}_0-1)},$$

$$c = \frac{2\ell\mu N\beta}{4(\mu+\nu)+2\ell\mu N\beta+\ell^2\mu(\mu+\nu)^2(\mathcal{R}_0-1)},$$

so that $a,\ b,\ c$ are positive if $\mathcal{R}_0 > 1$. Necessary and sufficient conditions for stability are $|\lambda_i| < 1,\ i = 1, 2$. Since the eigenvalues are the roots of a quadratic equation, they can be real or complex numbers depending on the sign of the discriminant $\mathcal{Q}_1^2 - 4\mathcal{Q}_2$.

- The inequality $\mathcal{Q}_1^2 - 4\mathcal{Q}_2 < 0$ here means that the eigenvalues λ_1 and λ_2 are complex numbers. For stability, then, $|\lambda_{1,2}|^2 < 1$ implies $0 < a + b - c < 1$. Hence, the time step ℓ must be chosen, for given values of N, β, μ and ν, to satisfy the condition $|\lambda_i| < 1,\ i = 1, 2$.

- For $\mathcal{Q}_1^2 - 4\mathcal{Q}_2 \geq 0$, λ_1 and λ_2 are real numbers. Then, the property of a quadratic function is considered as follows:

  Now, $\phi(-1) = 4a$ and $\phi(1) = 4b$ are positive for all $\mathcal{R}_0 > 1$. Next, $\mathrm{d}\phi(\lambda)/\mathrm{d}\lambda = 2\lambda - 2(a-b)$ and $\mathrm{d}^2\phi(\lambda)/\mathrm{d}\lambda^2 = 2 > 0$ so that $\phi(\lambda)$ has a minimum value at

  $$\lambda = \lambda_{\mathtt{min}} = a - b.$$

  It is found that $\lambda_{\mathtt{min}} > -1$ and $\lambda_{\mathtt{min}} < 1$ when

  $$\begin{aligned} a - b + 1 &= 8(\mu+\nu) + 2\ell\mu N\beta > 0 \quad \text{and} \\ a - b - 1 &= -2\ell\mu N\beta - 2\ell^2\mu(\mu+\nu)^2(\mathcal{R}_0-1) < 0 \end{aligned}$$

  then $-1 < \lambda_{\mathtt{min}} < 1$ when $\mathcal{R}_0 < 1$. Finally the minimum value at $\lambda = \lambda_{\mathtt{min}}$ is

  $$\phi(\lambda_{\mathtt{min}}) = \frac{-4\ell^2\{(\mu N\beta)^2 - 4\mu(\mu+\nu)^3(\mathcal{R}_0-1)\}}{\{4(\mu+\nu)+2\ell\mu N\beta+\ell^2\mu(\mu+\nu)^2(\mathcal{R}_0-1)\}^2} < 0$$

  whenever $\mathcal{R}_0 > 1$ and $(\mu N\beta)^2 > 4\mu(\mu+\nu)^3(\mathcal{R}_0-1)$, irrespective of the size of the time step ℓ.

These, therefore, are the conditions under which the numerical method (3.6.50), (3.6.51) will converge to the non-trivial fixed point in (3.7.3).

In the case when $\mathcal{R}_0 = 1$ the non-trivial fixed point coincides with the trivial fixed point and the elements of the matrix J take the values given in (3.7.16), (3.7.29), (3.7.34) and (3.7.44) with $X = X_1^* = 1$ and $Y = Y_1^* = 0$. All numerical methods will, therefore, converge to the trivial fixed point, using an appropriate time step, when $R_0 = 1$.

3.8 Numerical Experiments

The initial-value problem given by equations {(3.3.6),(3.3.7)} and {(3.5.1),(3.5.2), (3.5.3)} are solved numerically by using the developed methods in § 3.6. All experiments are carried out with the parameter values

$$\begin{aligned} \mu &= 0.04 \quad \text{years}^{-1}, \\ \nu &= 24.0 \quad \text{years}^{-1}, \end{aligned} \tag{3.8.1}$$

which are considered by Duncan *et al.* [9]; these values of μ and ν refer to an average life expectancy of 25 years and an infectious period of approximately 15 days (approximately), respectively.

In the case of the *SIR* model in {(3.3.6),(3.3.7)}, the reproductive rate $\mathcal{R}_0$ will be serve as a bifurcation parameter. The product of population and susceptibility, $N\beta$, was chosen to be $N\beta = 23$ ($\mathcal{R}_0 = 0.96$) first and then $N\beta = 123$ ($\mathcal{R}_0 = 5$), hence testing values of $\mathcal{R}_0$ smaller and larger than unity. Therefore, for the first the trivial critical point should be attracting and for the other the system should converge to the non-trivial critical point. In the case of the seasonal *SIR* model given in equations (3.5.1)-(3.5.3), the infection rate is time dependent depending upon β, δ and ω. Following Duncan *et al.* [10], δ will be serve as the bifurcation parameter and the behaviour of this system will be reported in §3.8.2.

3.8.1 Numerical solutions of *SIR* model

The numerical experiments are performed for various values of ℓ to observe the behaviour of the numerical methods. All experiments are carried out with the parameter (3.8.1) and $N\beta = 23$ ($\mathcal{R}_0 < 1$) and $N\beta = 123$ ($\mathcal{R}_0 > 1$) and the initial data given by

$$\begin{aligned} X_0 &= 0.25, \\ Y_0 &= 0.0006. \end{aligned} \tag{3.8.2}$$

Method $\mathcal{M}_1$

Since restricting conditions on ℓ for asymptotic stability were found, convergence cannot be expected for every step length. For $\mathcal{R}_0 > 1$, the method was seen to give oscillatory convergence to the non-trivial fixed point until ℓ reached 0.0515. Steady oscillations appeared in the numerical solution: oscillatory, very slow convergence occurred for $\ell \in (0.04, 0.0515)$, and the method produced overflow for $\ell > 0.0515$. These findings are illustrated in figure 3.2 (a)-(c). Taking $\mathcal{R}_0 < 1$ the method gave monotonic convergence to the trivial fixed point when a time step $\ell \leq 0.125$ was used but overflow was produced for $\ell > 0.125$.

(a)

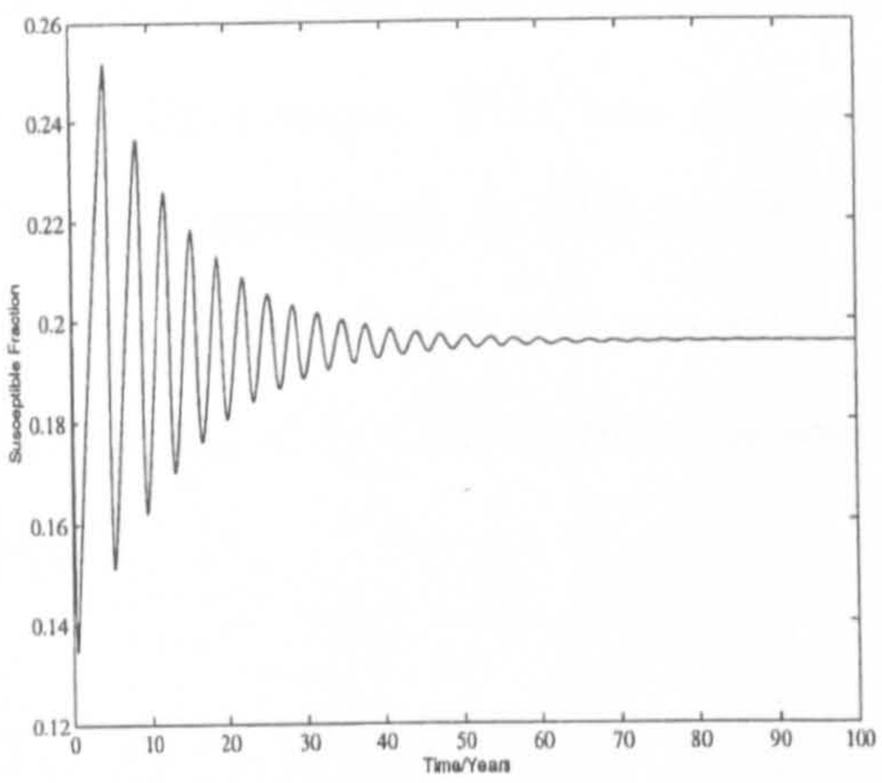

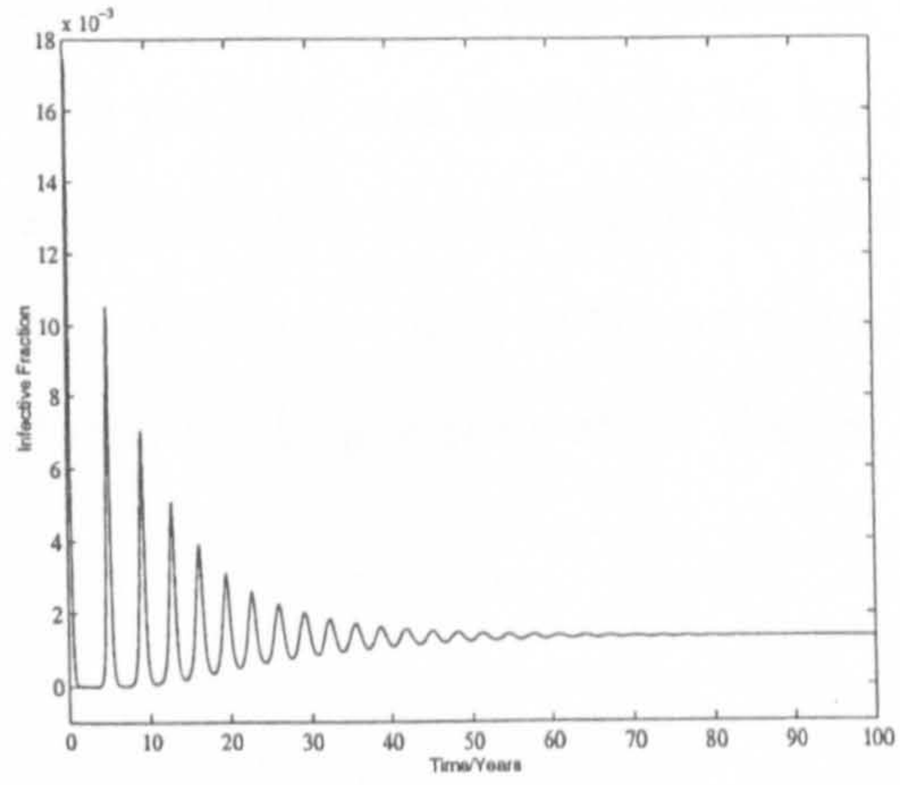

(b)

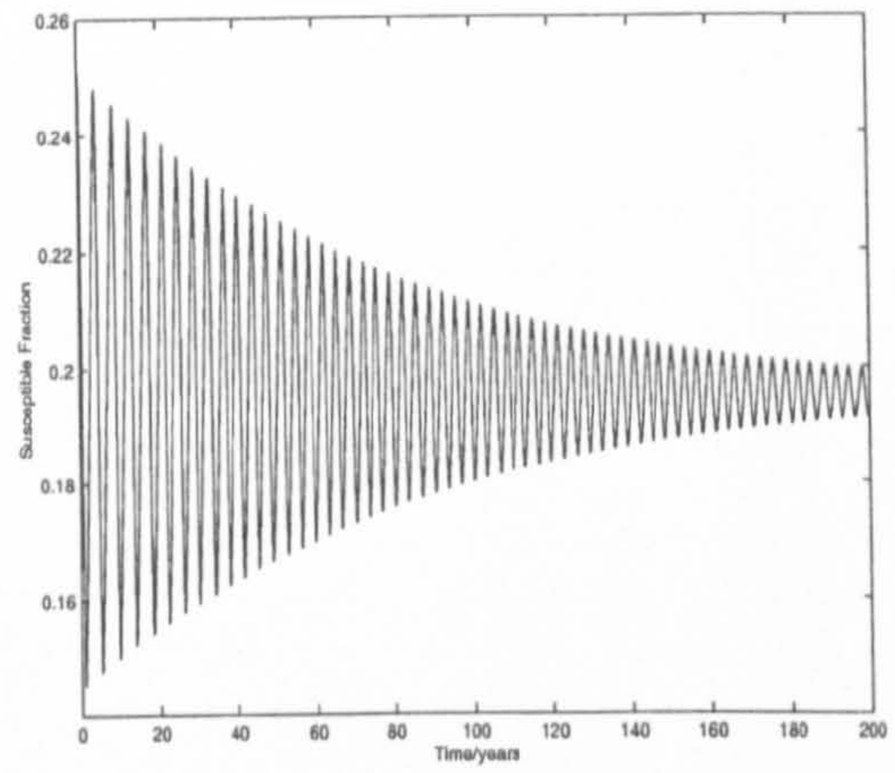

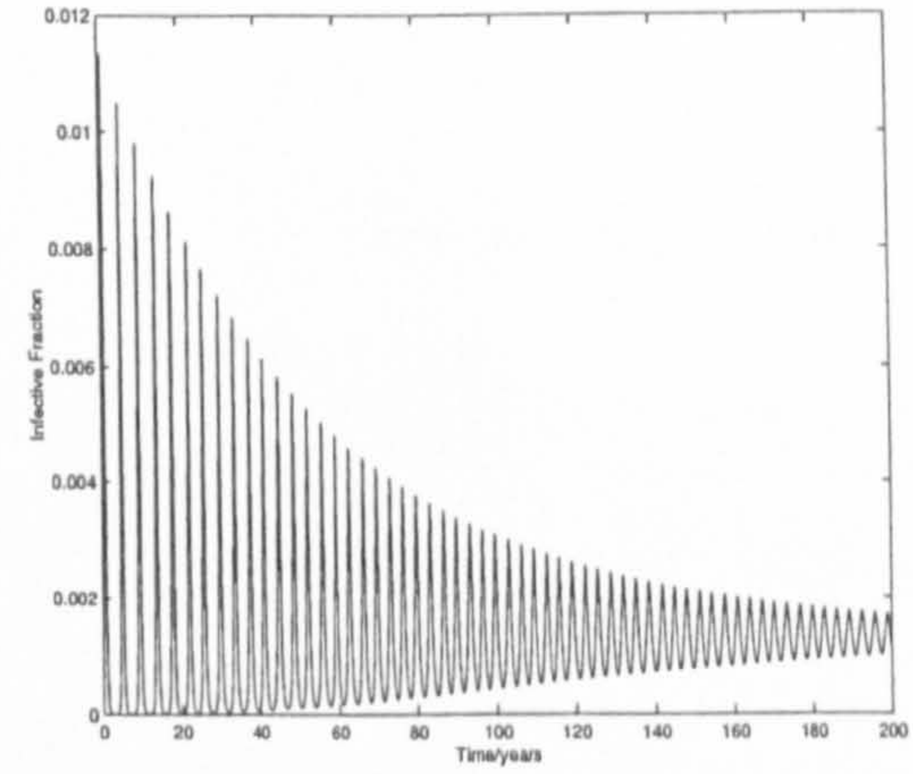

(c)

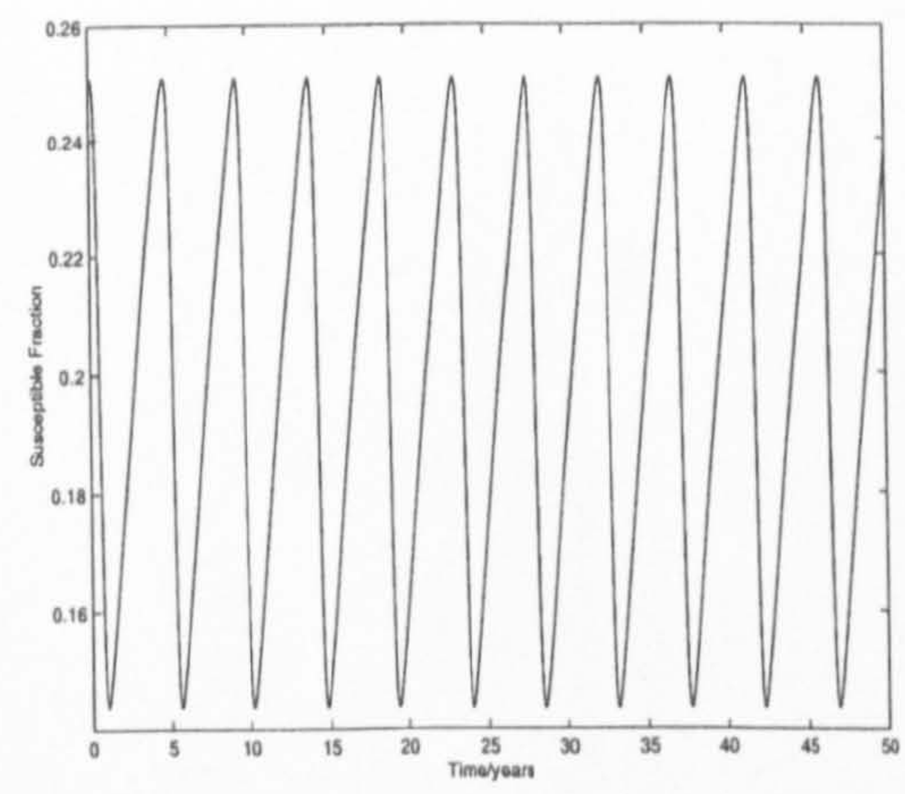

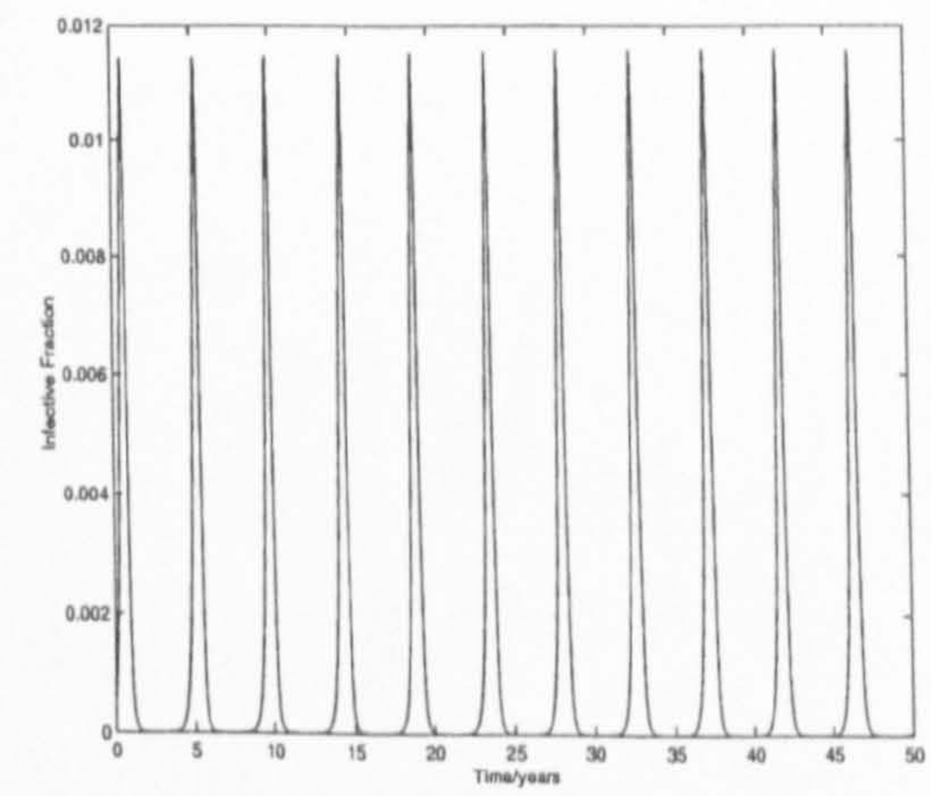

Figure 3.2: Time series using method $\mathcal{M}_1$ with $N\beta = 123$ ($\mathcal{R}_0 > 1$) and (a) $\ell = 0.01$, (b) $\ell = 0.05$, (c) $\ell = 0.0515$.

Method $\mathcal{M}_2$

This method never produced overflow and always converged to fixed points for all positive time steps. This was expected since the method was shown to be unconditionally convergent in §3.7.2. The method simulates the behaviour of the model correctly, converging to the non-trivial fixed point for $\mathcal{R}_0 > 1$ and to the trivial fixed point for $\mathcal{R}_0 < 1$. Convergence is seen to be slower for larger time steps (figure 3.3 (a)-(c)).

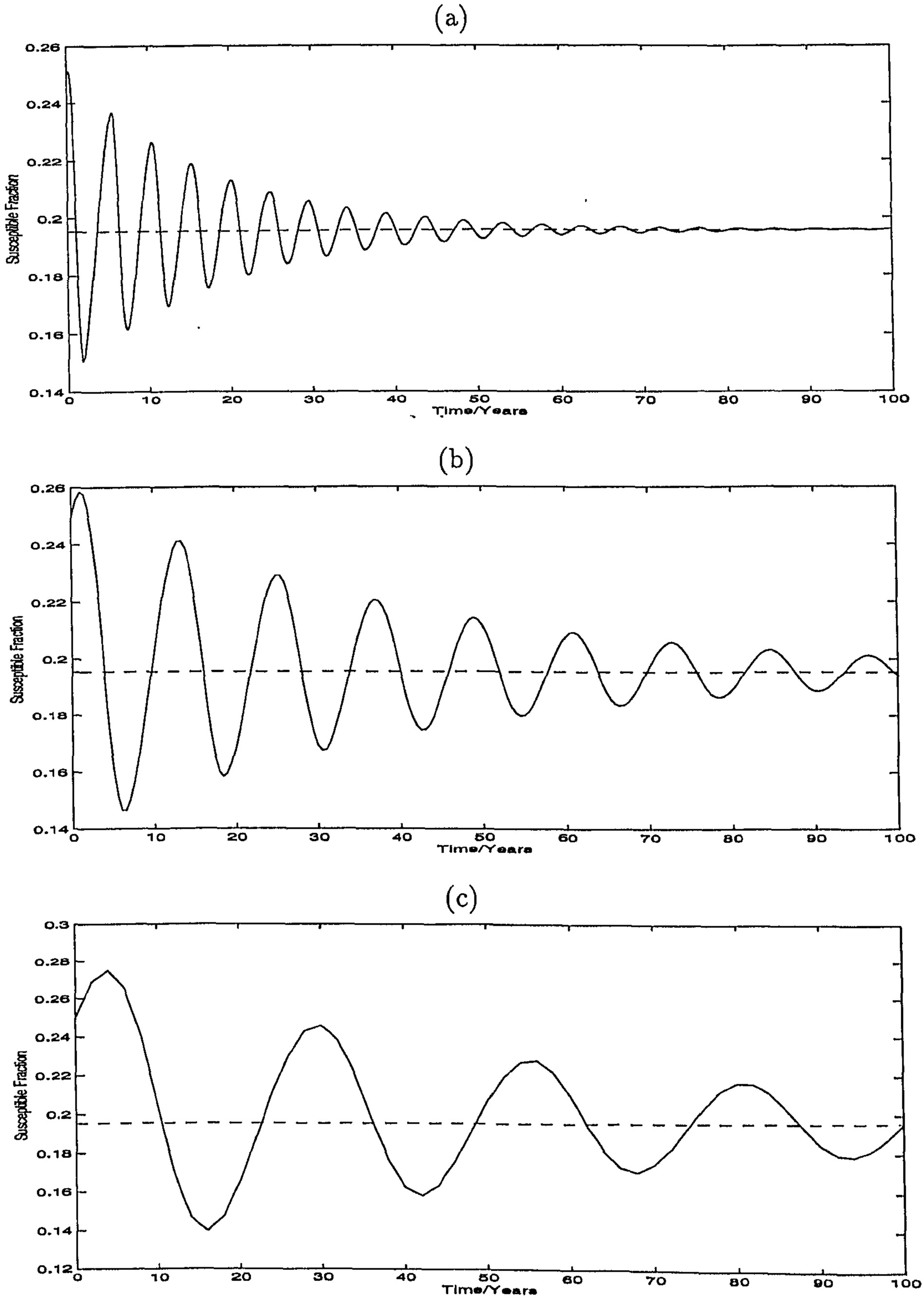

Figure 3.3: Time series of susceptible fraction produced by Method $\mathcal{M}_2$ with $N\beta = 123$; (a) $\ell = 0.05$, (b) $\ell = 0.5$ and (c) $\ell = 2.0$.

Method $\mathcal{M}_3$

When $\mathcal{R}_0 < 1$, this method gave monotonic convergence to the trivial fixed point for all $\ell > 0$. When $\mathcal{R}_0 > 1$, the method gave oscillatory convergence to the non-trivial fixed point for $\ell < 6$. Monotonic convergence took place whenever $\ell \in [6, 9.66)$. That is, the higher the value of ℓ, the quicker the non-trivial fixed point is reached, see figure 3.4. When $\ell \in (9.66, 16]$, the method produced periodic limit cycles around the non-trivial fixed point and chaos was observed. The method produced overflow for $\ell > 16$. Figure 3.5 shows the bifurcation diagram for this method as ℓ increases. In this diagram, it is seen that the period-1 originates from a single point, period-2, where there are two points and so on. Chaos occurs in the bands where the dots seem to be smeared at random. Such dynamic behaviour is usually very interesting but it is contrived.

(a)

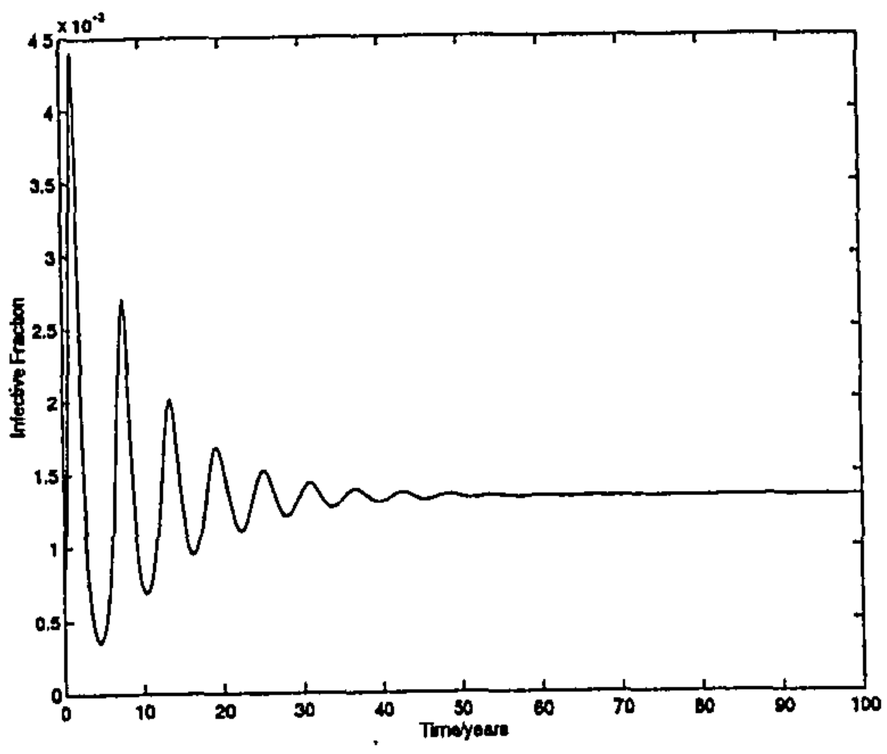

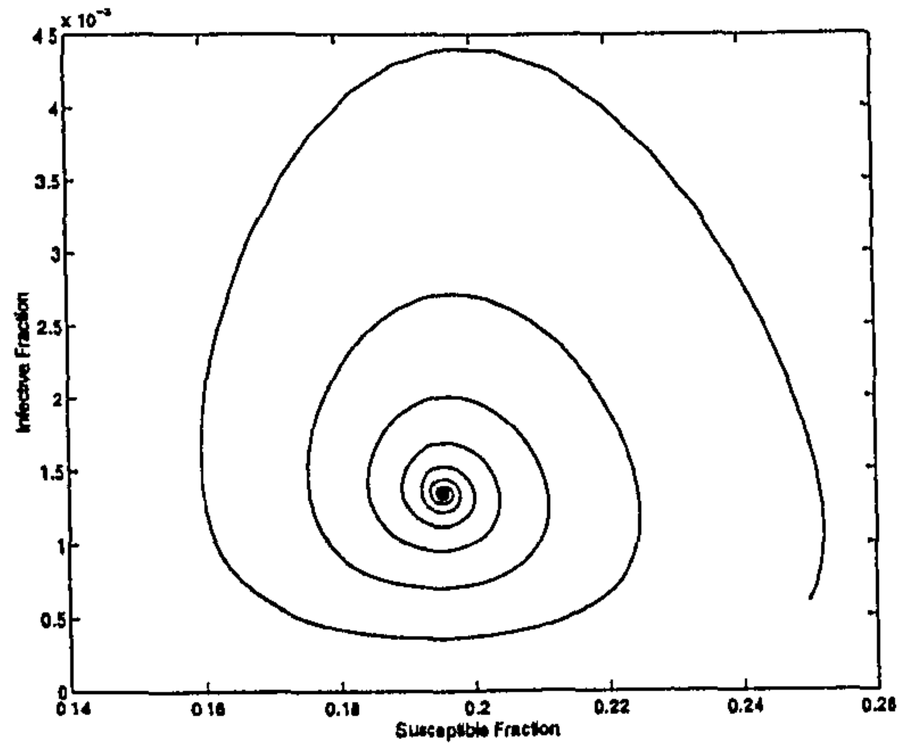

(b)

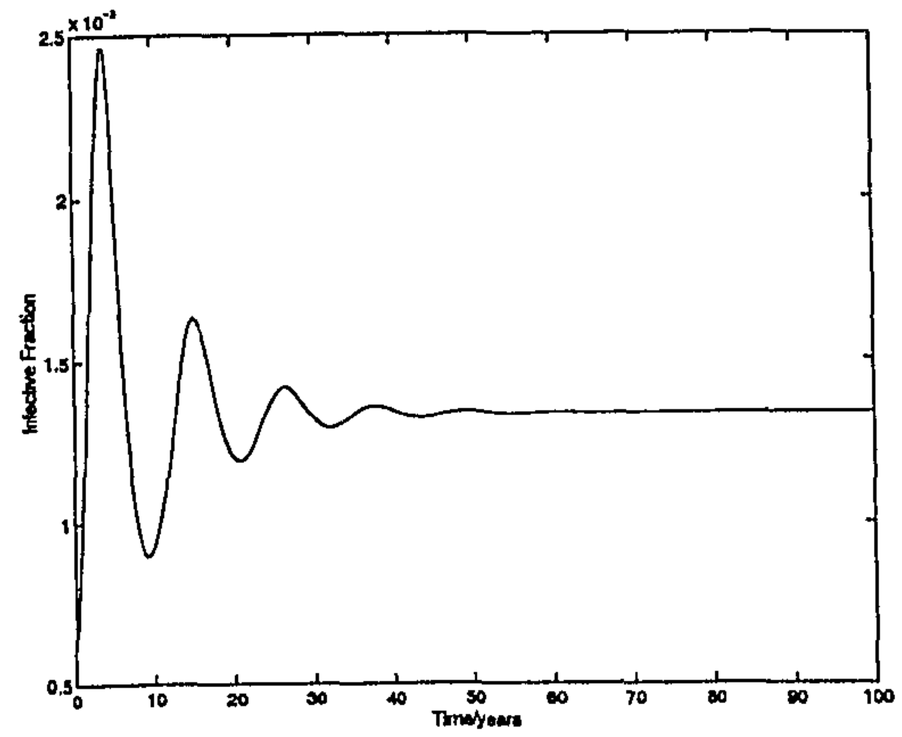

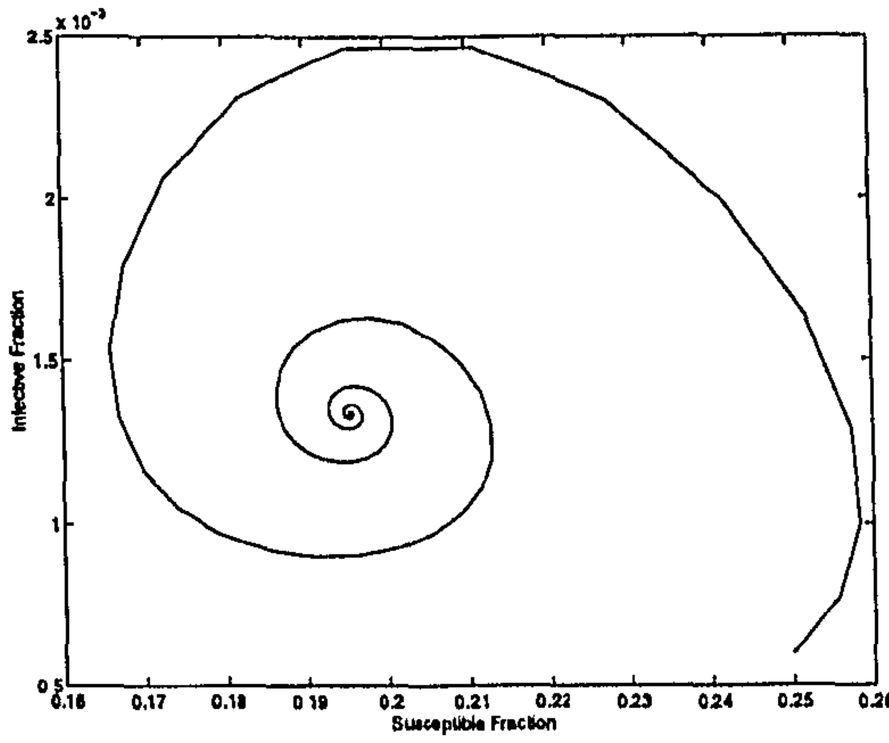

(c)

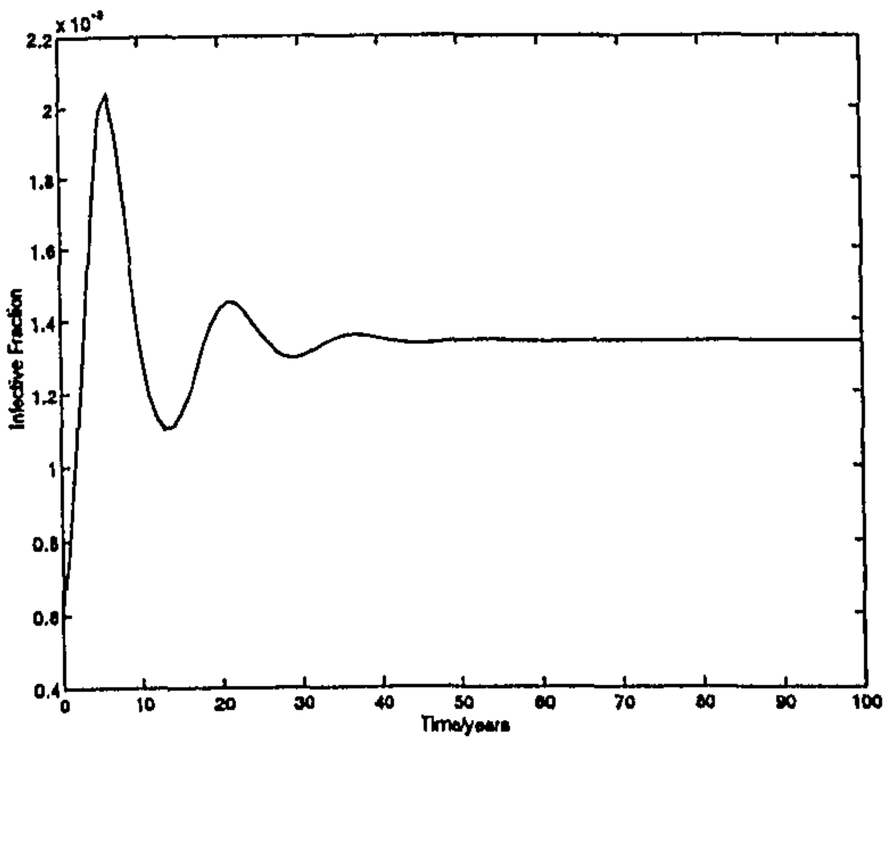

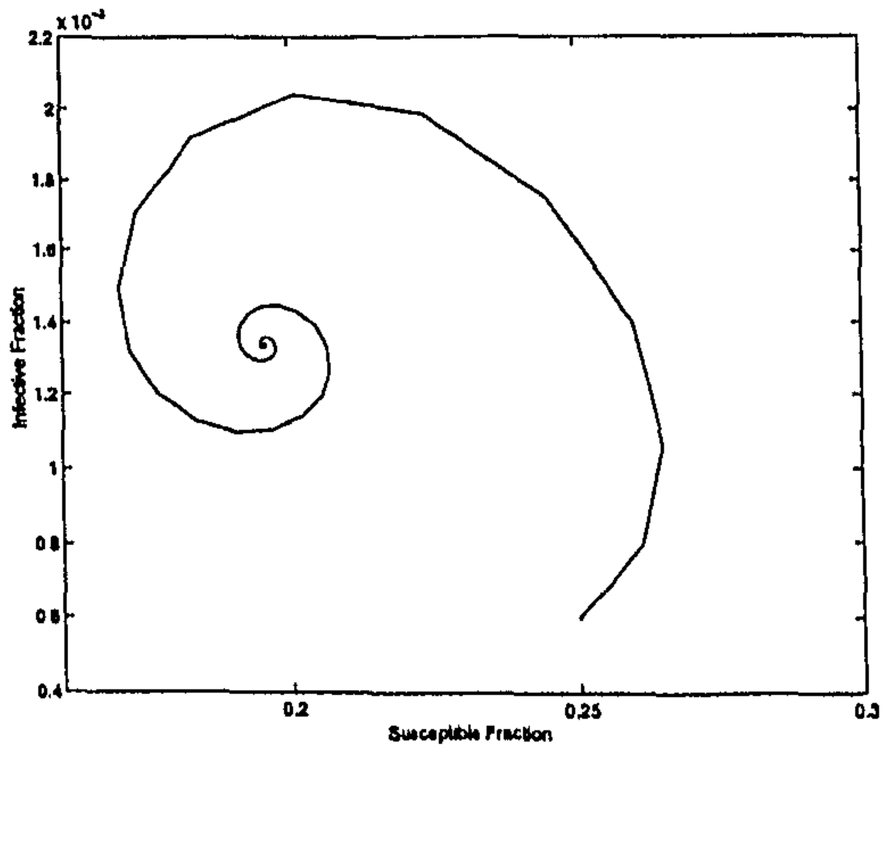

Figure 3.4: The time series of infective fractions for various ℓ (left-hand column) and the corresonding phase-plane (righ-hand column), the infective fraction *versus* the susceptible fraction, using method $\mathcal{M}_3$ with $N\beta = 123$ ($\mathcal{R}_0 > 1$) and (a) $\ell = 0.1$, (b) $\ell = 0.5$, (c) $\ell = 1$.

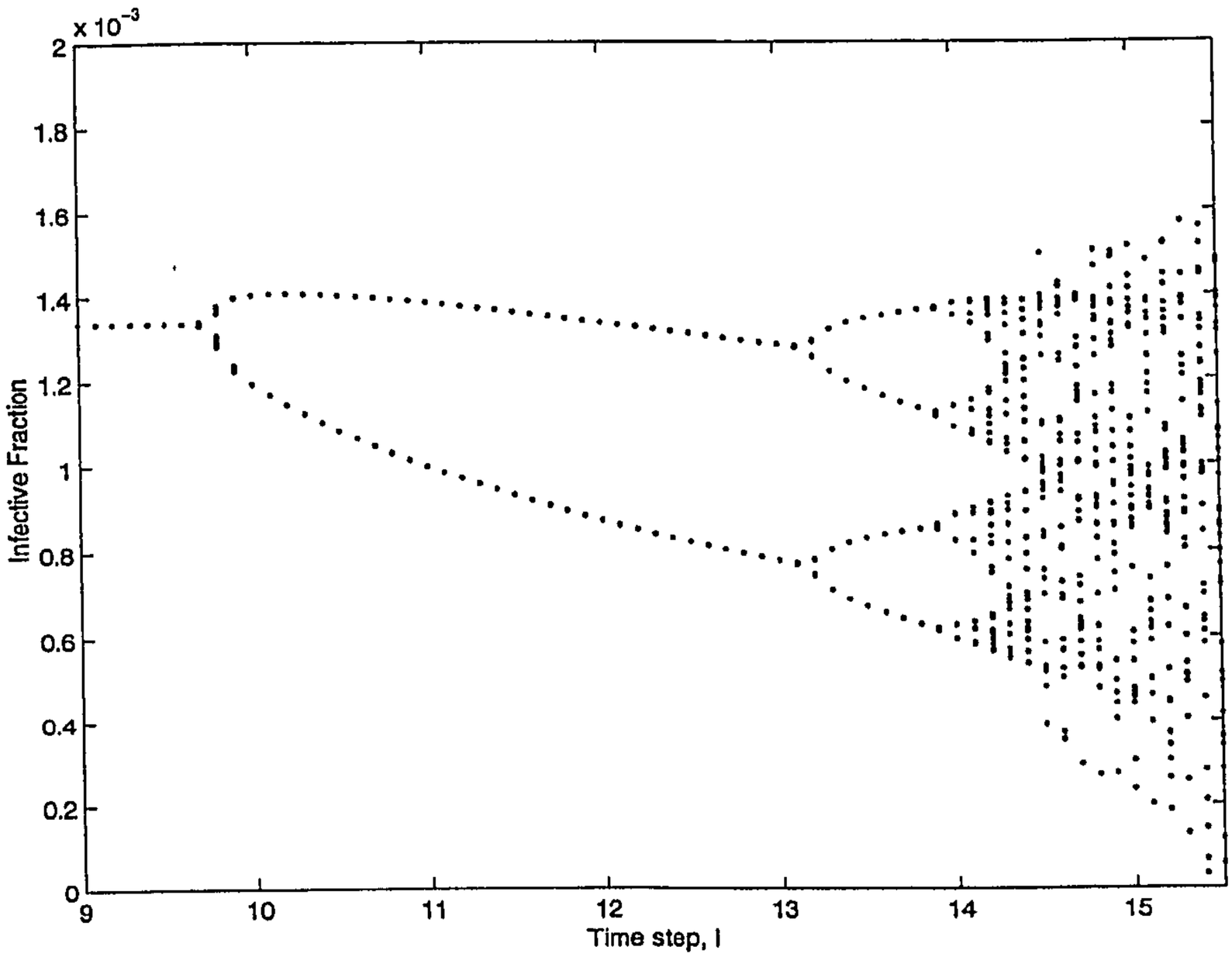

Figure 3.5: Bifurcation diagram of method $\mathcal{M}_3$

Second-order Method

This method is seen to be very restrictive on time step, ℓ; for $\mathcal{R}_0 > 1$ it produced overflow when $\ell > 0.394$. It gave oscillatory convergence to the non-trivial fixed point for $\ell < 0.292$. For $0.292 \leq \ell < 0.394$, oscillations appeared and some meaningless negative values were observed for the infective proportion before the solutions converged to the non-trivial fixed point. When $\mathcal{R}_0 < 1$, this method did not produce overflow but converged to the correct fixed point for $\ell < 1 \times 10^6$ with monotonic convergence for $\ell \leq 0.12$. For $0.12 < \ell \leq 100$, oscillations appeared in the infective proportion while for $100 < \ell < 1 \times 10^6$, oscillatory convergence occured in both the fraction of population susceptibles and infectives. When $\ell \geq 1 \times 10^6$, convergence did not take place; instead, this method produces periodic cycles around the fixed point. These findings are shown in figure 3.6 (a)-(c).

Overall, it was observed that using an appropriate time step ℓ, all methods converge to their theoretically-predicted fixed points in all cases.

(a)

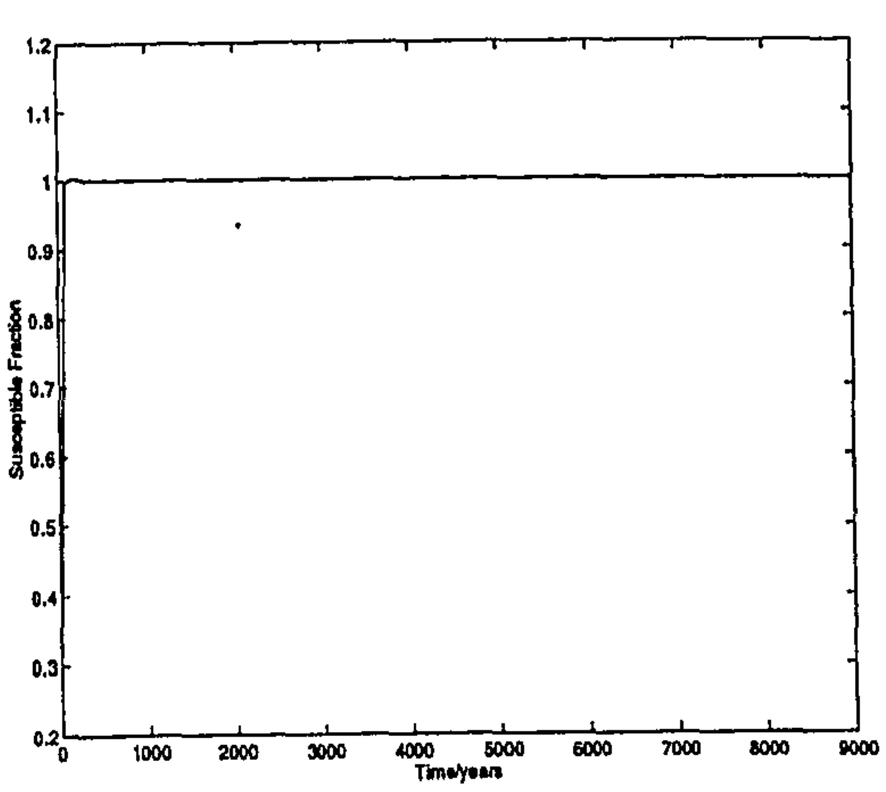

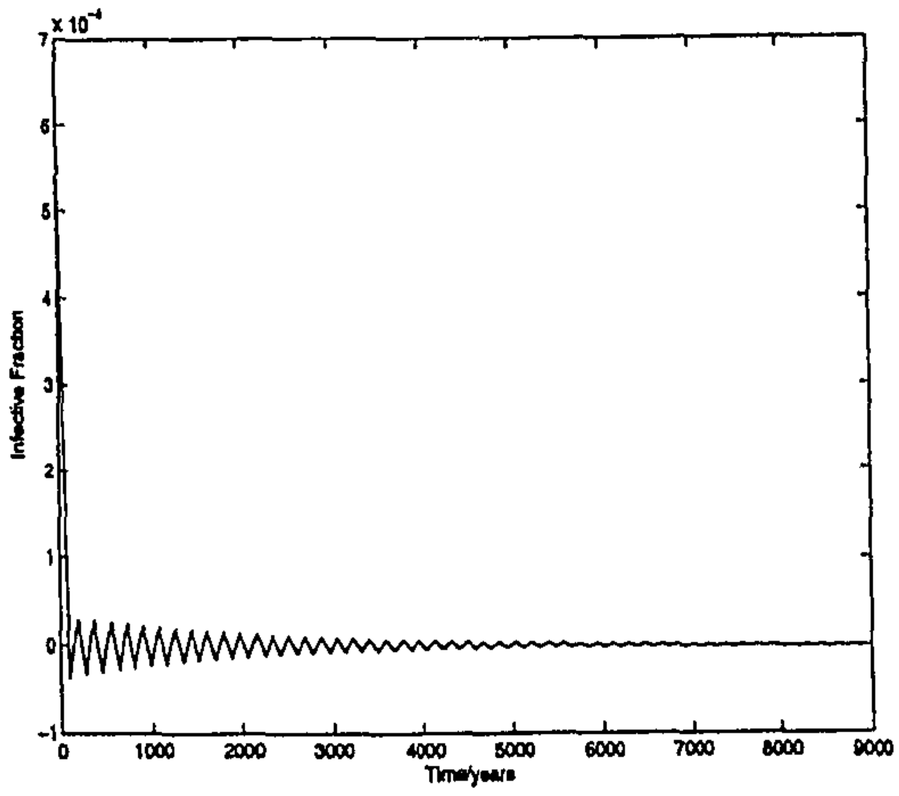

(b)

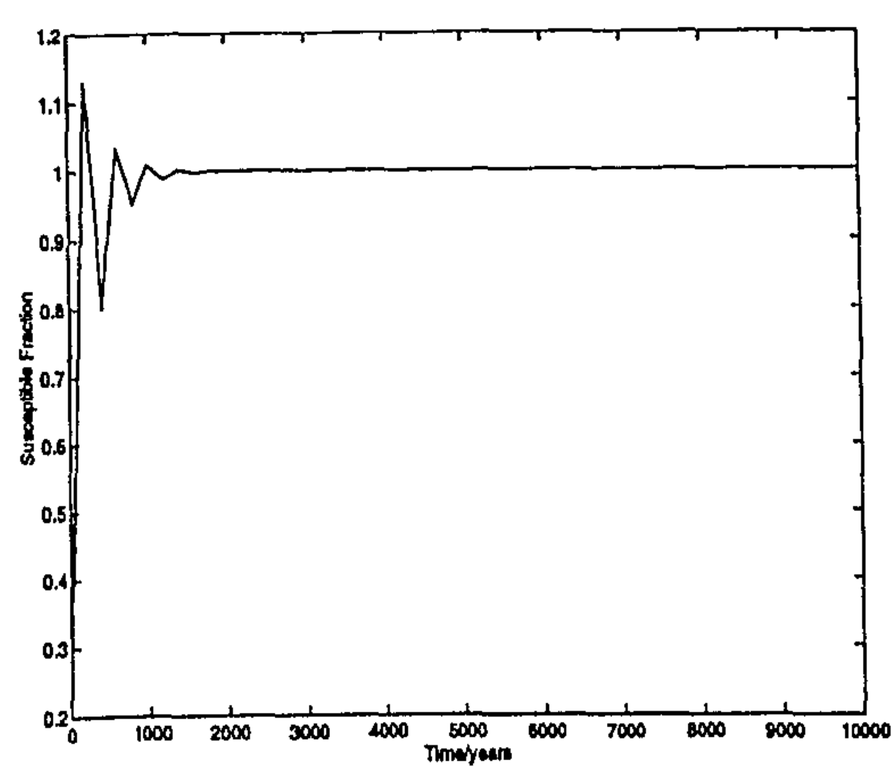

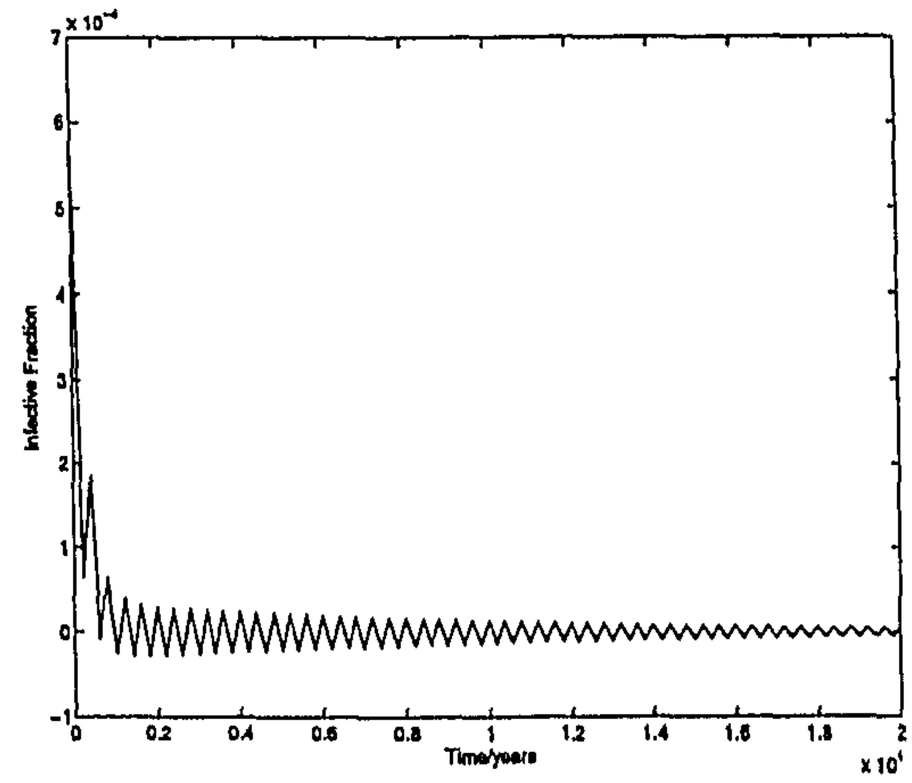

(c)

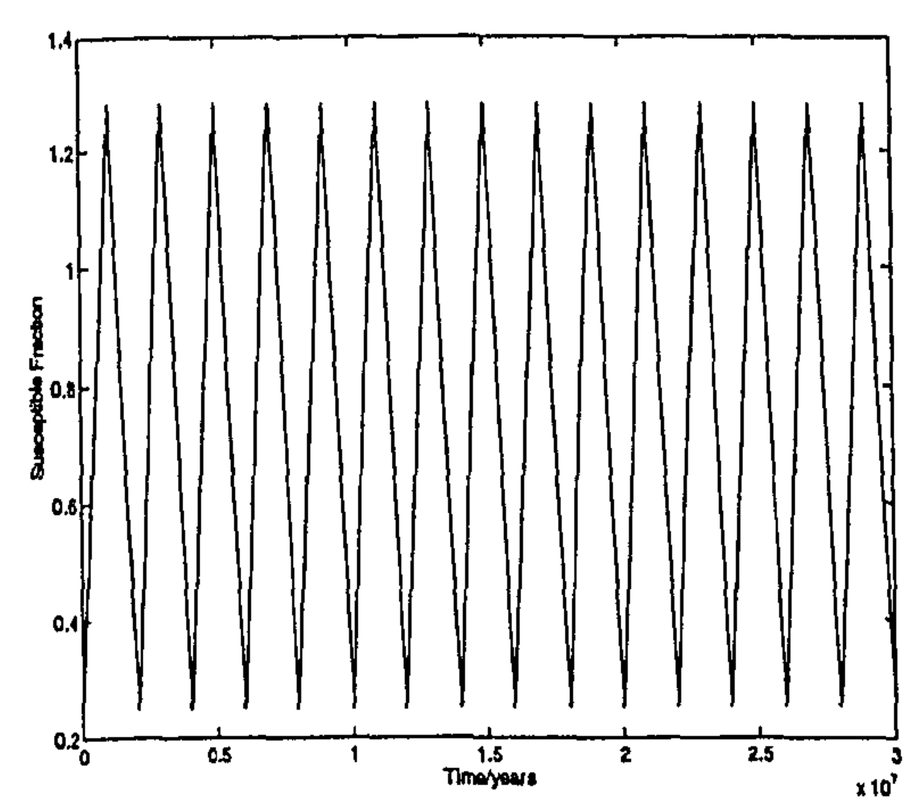

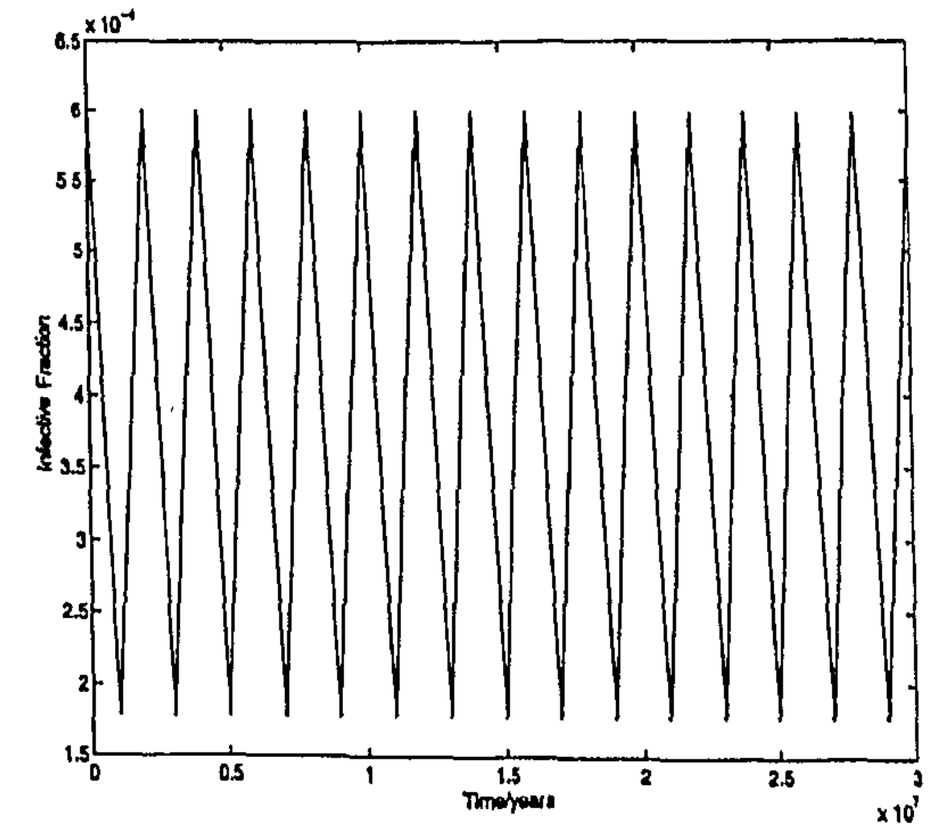

Figure 3.6: Time series produced by the second-order method with $N\beta = 23$ ($\mathcal{R}_0 < 1$) and (a) $\ell = 90$, (b) $\ell = 200$, (c) $\ell = 1 \times 10^6$.

3.8.2 Numerical solutions of the seasonal *SIR* model

In order to test the behaviour of the developed methods for solving the seasonal *SIR* model when the contract rate β is replacing by $\beta(t)$ as defined in (3.5.3), a second-order method is first chosen to illustrate some numerical results. The model will be considered with $N\beta_0 = 123$, $\omega = \frac{2}{3}\pi$ and $N\beta_0 = 270$, $\omega = 2\pi$, while δ will serve as a bifurcation parameter, as in Duncan *et al.* [10]. For all parameter values chosen, the model is run for 250 years and all figures show the results for the last 20 years. The numerical solutions of the seasonal *SIR* model is shown in Figures 3.7-3.12.

For $N\beta_0 = 123$ and $\delta = 0.1$, the numerical results of modelling are shown in Figures 3.7 (a)-(c). It is seen that the response is non-sinusoidal (Figures 3.7 (a),(b)). The infective fraction falls to zero in the inter-epidemic period (Figure 3.7 (a)), which means that the disease was not endemic. A corresponding simulation for the susceptible fraction shows a progressive build-up by new births during the inter-epidemic period and a dramatic fall during the epidemic, see figure 3.7 (b). The phase diagram of the susceptible fraction *versus* the infective fraction *versus* NB is shown in figure 3.7 (c). Here, NB is the ratio $(N\beta(t) - N\beta_0)/N\beta_0$ which is obtained from (3.5.3).

Repeating the calculations using the same parameters but with $N\beta_0 = 270$ and $\omega = 2\pi$ yields a very different result. Specifically, qualitatively different dynamics are obtained for different values of δ. As δ increases, the solution passes from a period-1-year cycle to a 2-year cycle and to chaotic behaviour *via* a sequence of the period-doubling bifurcations, see Figure 3.8 (a)-(f). The period-doubling sequence of the seasonal *SIR* model is shown in Figure 3.8 (c)-(f). The behaviour-solutions appear to be almost coincident with Duncan *et al.* [10] in their Table 1, showing that a second-order method gives a reliable representation of the numerical solutions associated with {(3.5.1),(3.5.2),(3.5.3)}. The fraction of the population infected does not drop to zero, indicating that the disease is epidemic.

The numerical experiment leading to Figure 3.8 (a) is repeated using Methods $\mathcal{M}_1$, $\mathcal{M}_2$, $\mathcal{M}_3$ and a second-order method with different time steps (see Figures

3.9-3.12). Figures 3.9 (a)-(c) show time series of infective fraction using method $\mathcal{M}_1$; these figures correspond to figure 2 (a) in Duncan *et al.* [10] but the profile of the infective fraction is lower. The numerical results using Methods $\mathcal{M}_2$ and $\mathcal{M}_3$ are very sensitive to the time step chosen so that different time steps give different cycles. It is seen that both methods give a biennial cycle for $\ell < 0.003$ and the profile of the infective fraction increases as the time step decreases, see figures 3.10 (b),(c) and 3.11 (b),(c), respectively. Figures 3.12 (a)-(c) are produced by a second-order method, the plots agree with Duncan *et al.* [10].

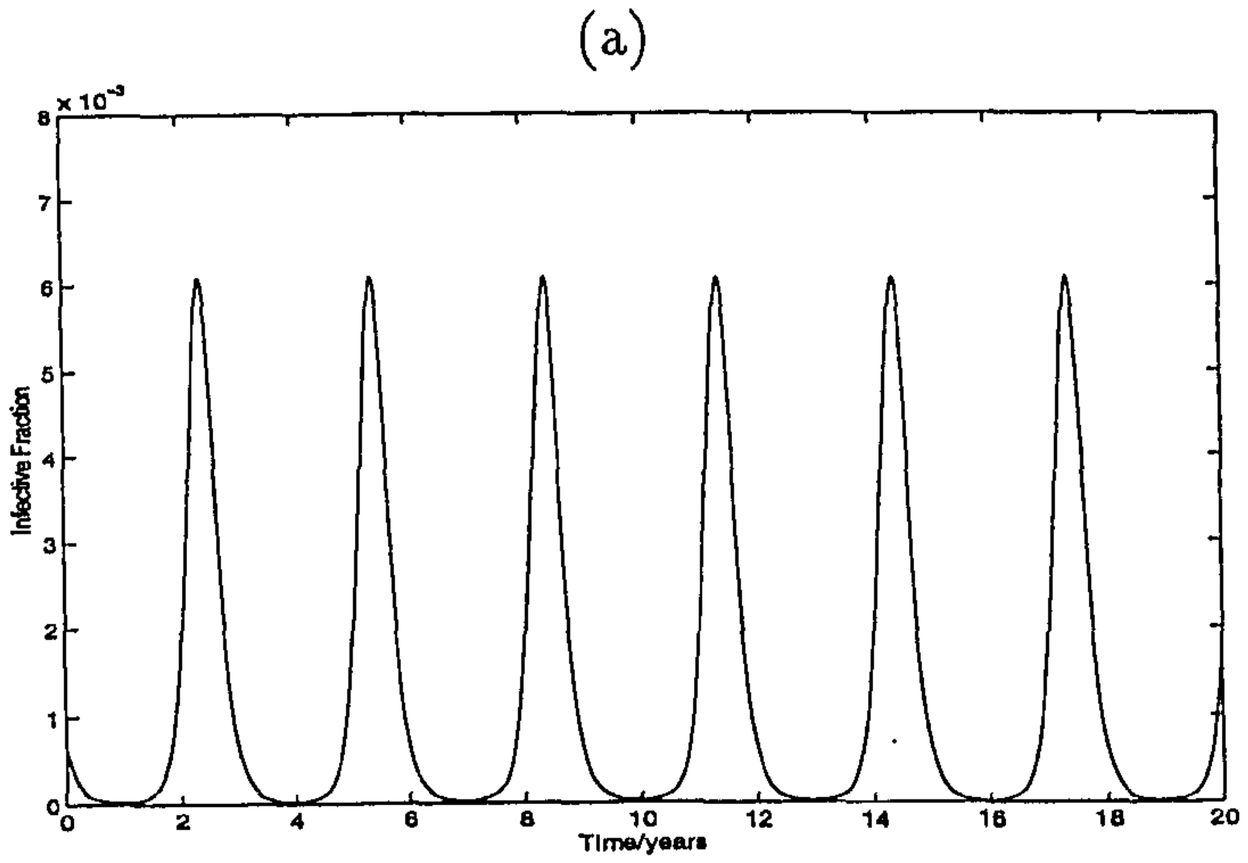

Figure 3.7: Numerical solution for the seasonal SIR model produced by the second-order method, $N\beta_0 = 123$, $\delta = 0.1$, $\omega = \frac{2}{3}\pi$ and $\ell = 0.01$: (a) the infective fraction *versus* time, (b) the susceptible fraction *versus* time, (c) phase diagram of susceptible fraction *versus* infective fraction *versus* NB.

(a)

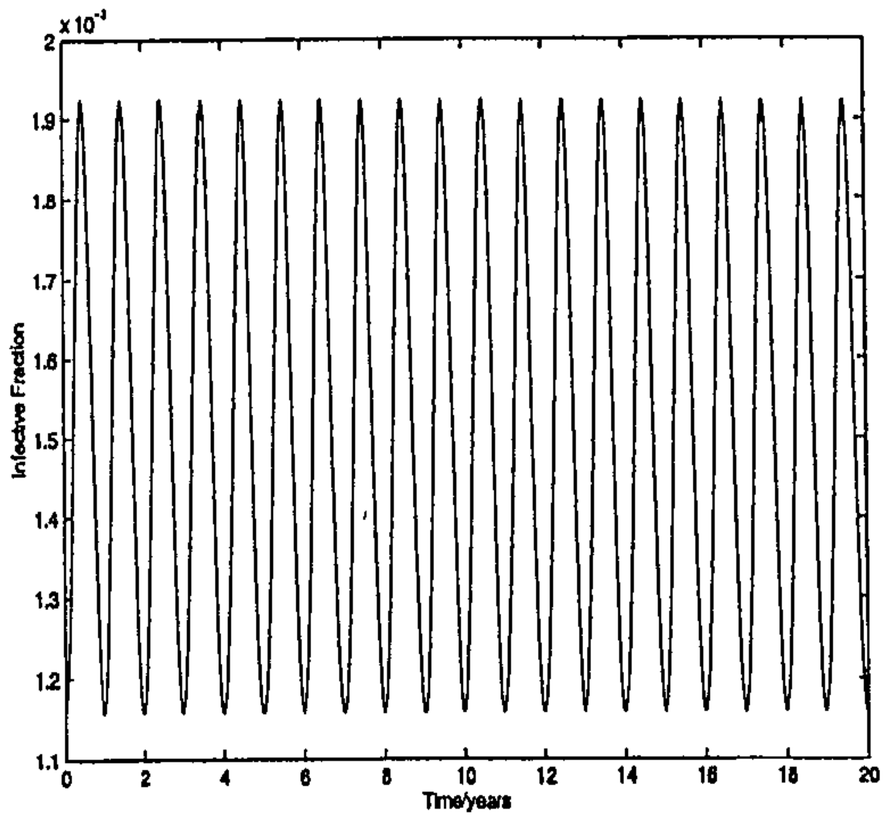

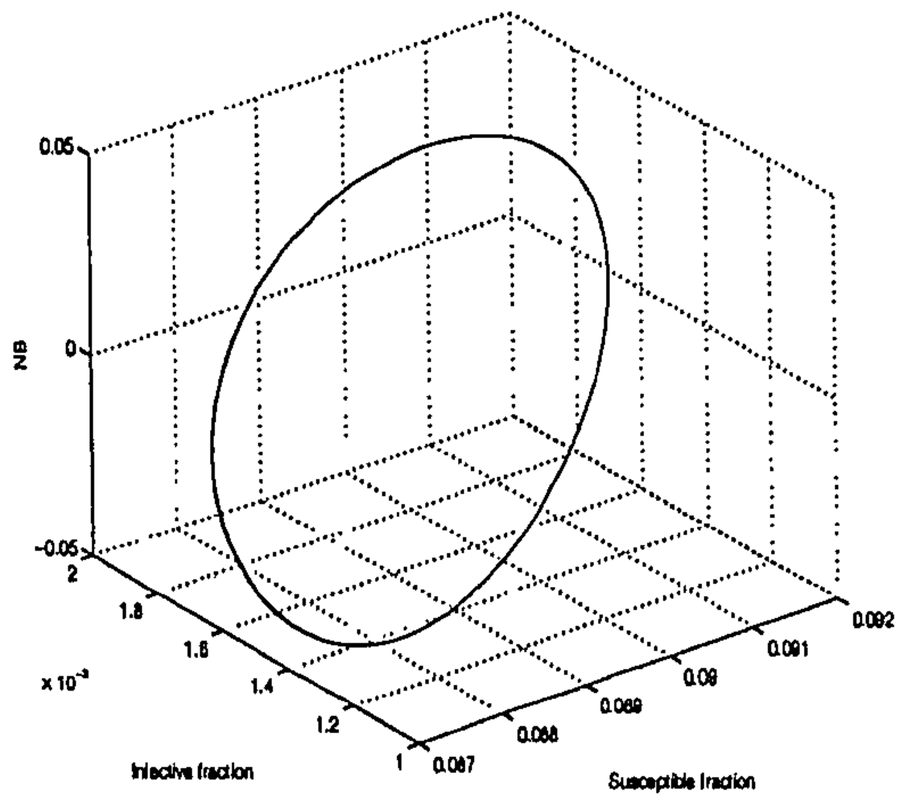

(b)

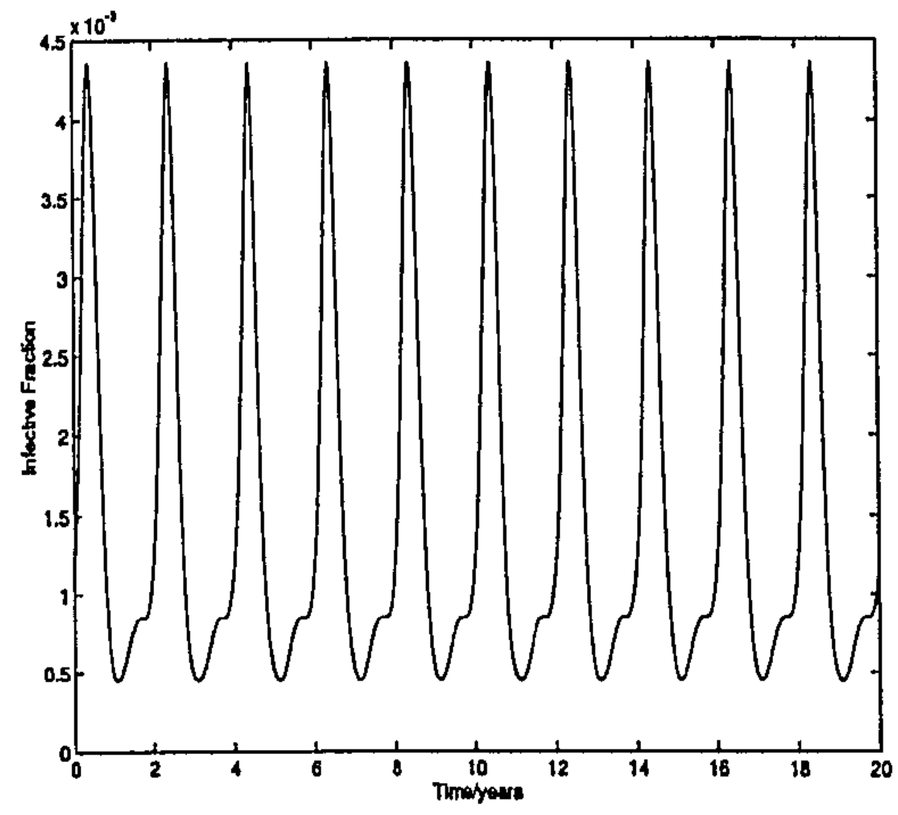

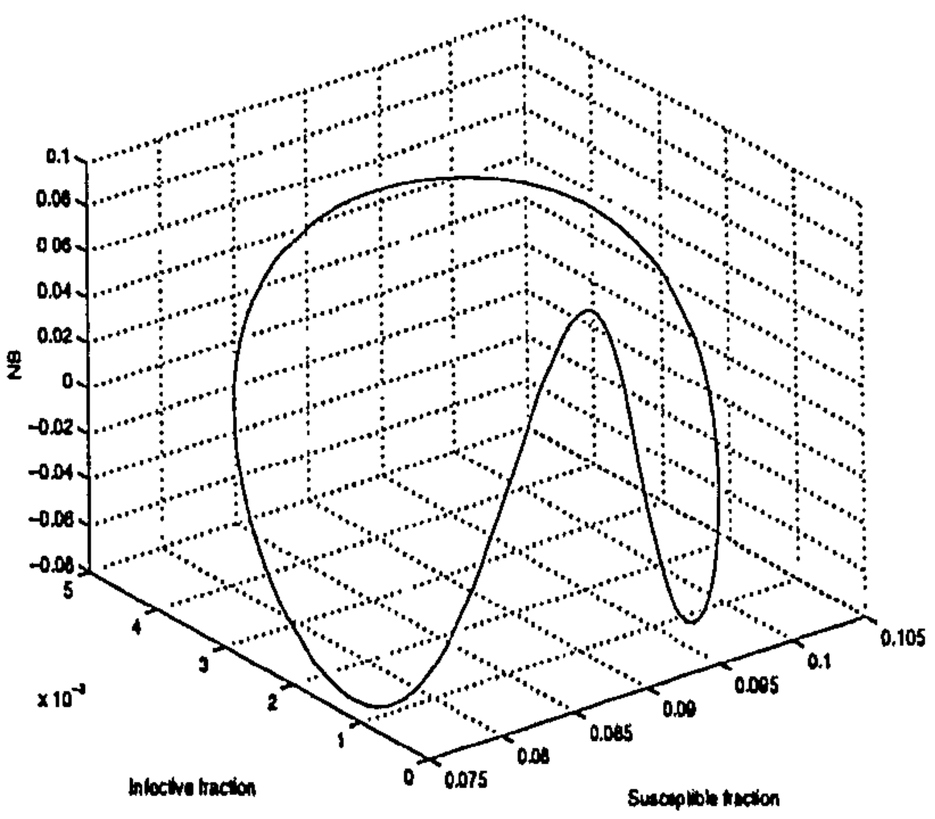

(c)

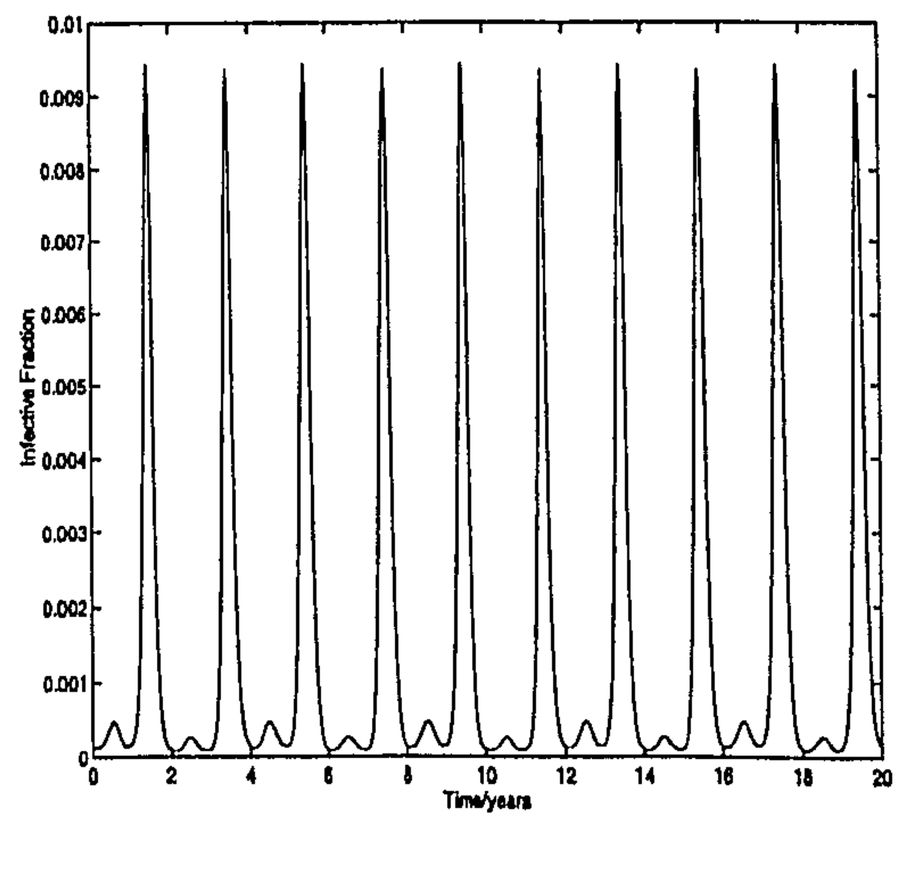

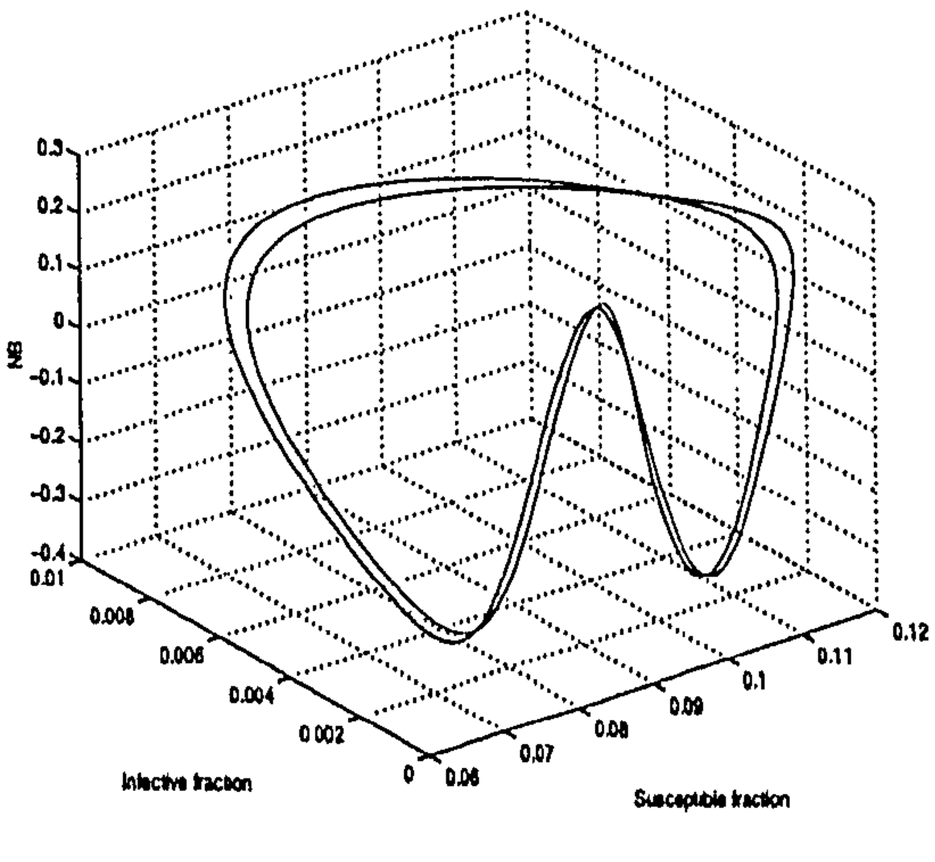

Figure 3.8

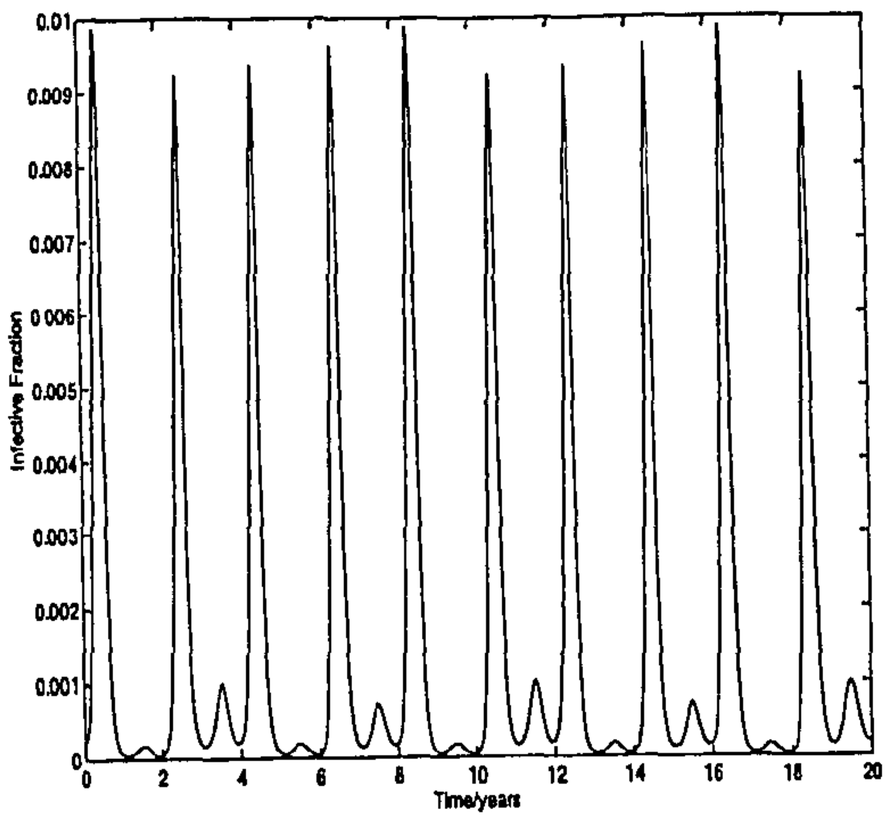

(d)

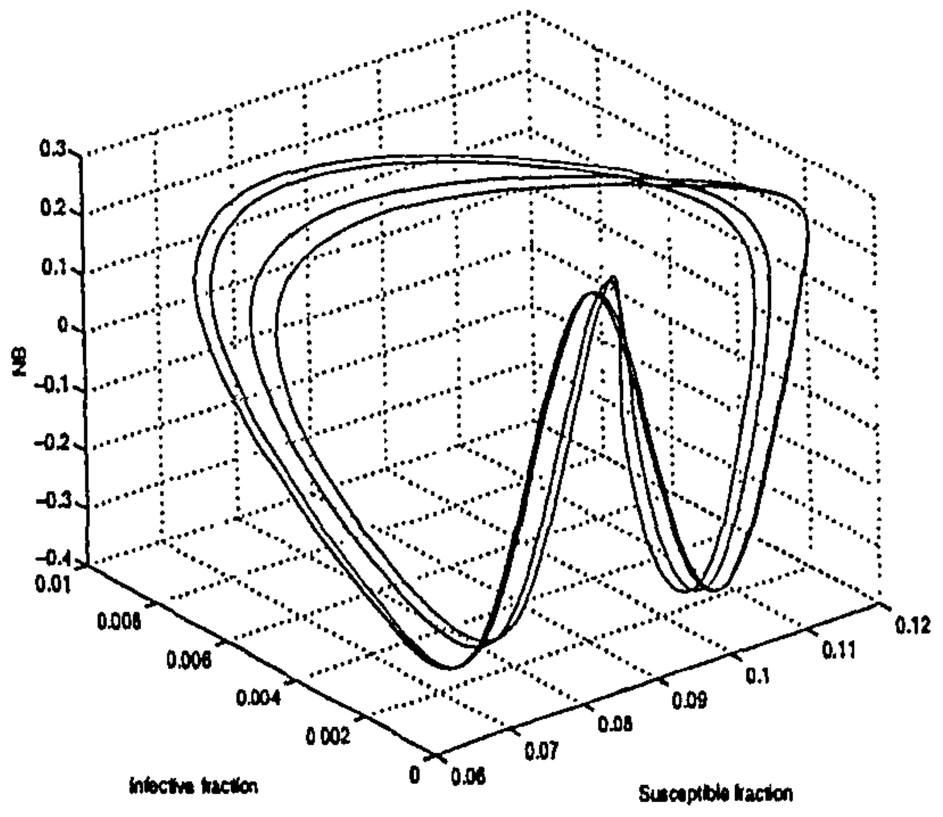

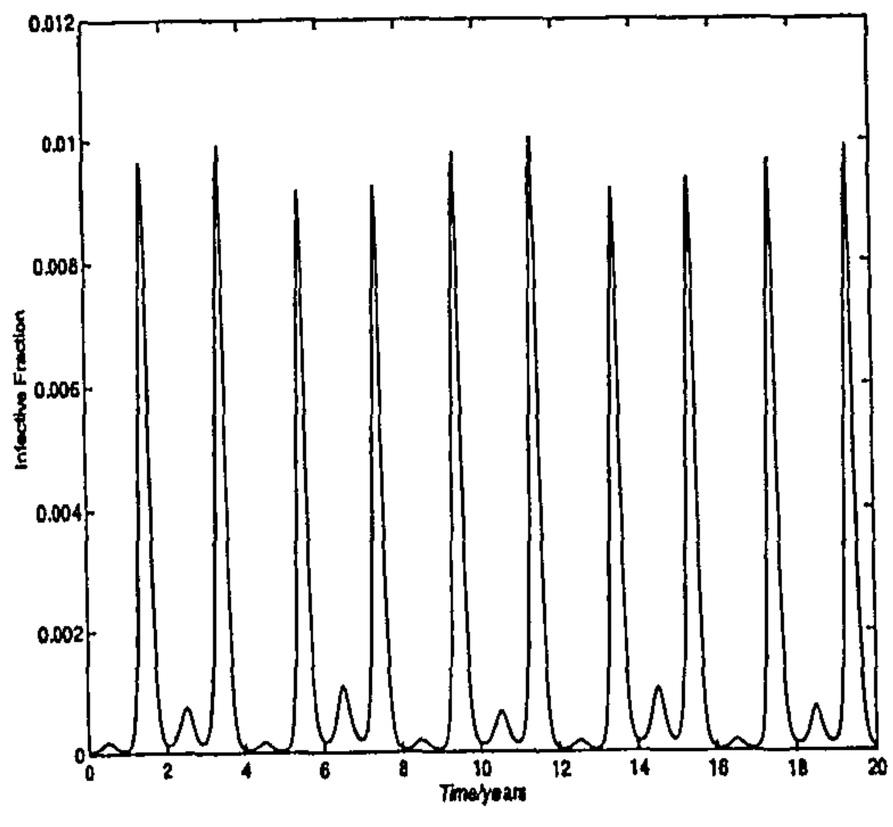

(e)

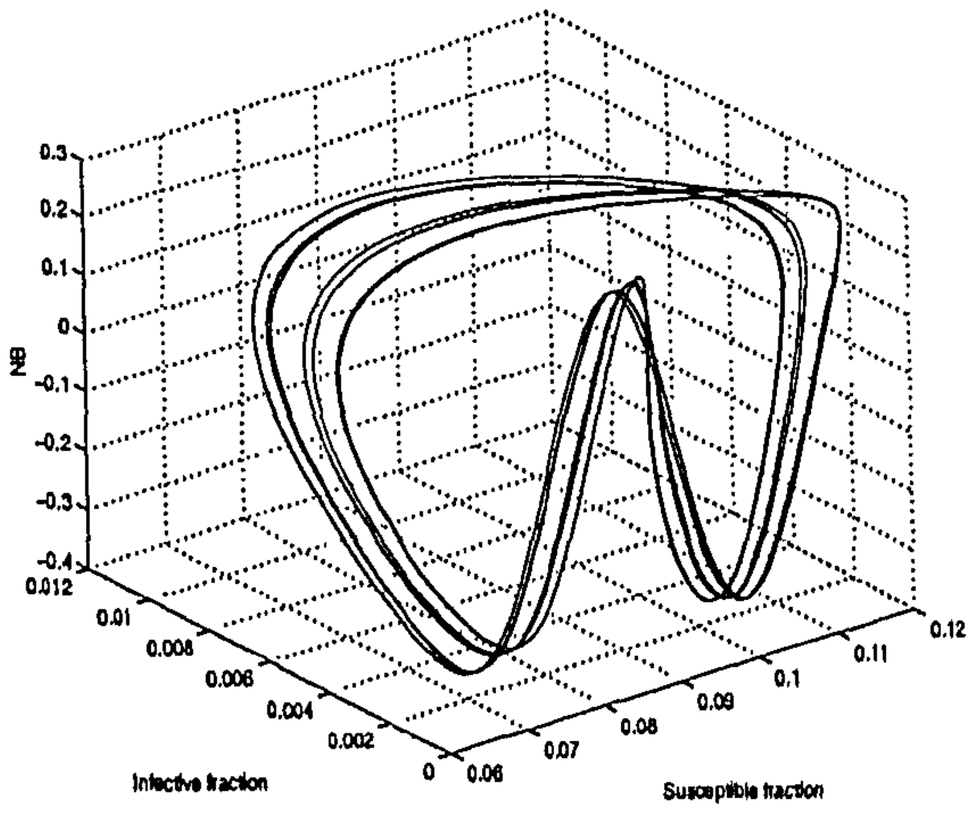

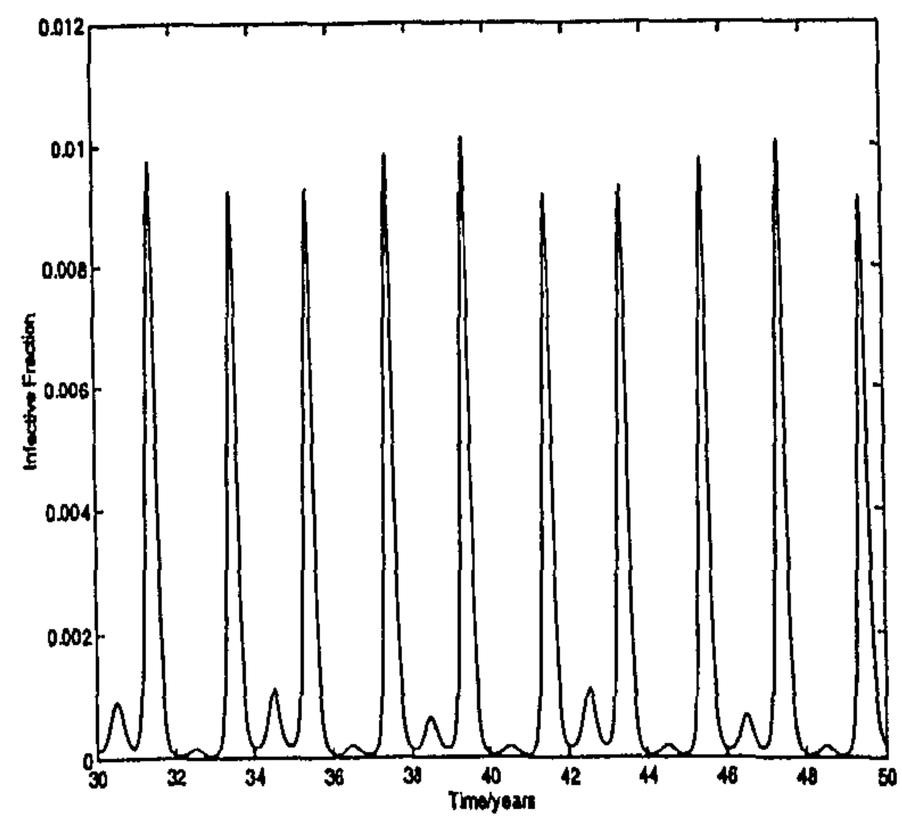

(f)

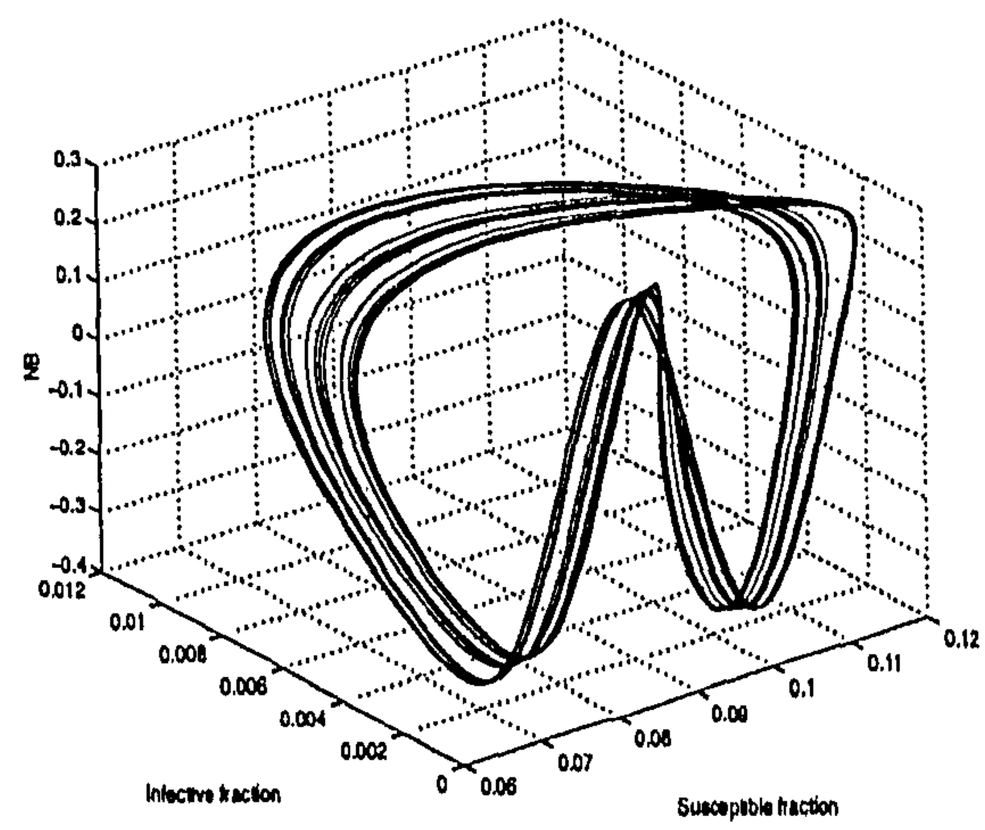

Figure 3.8: The time series of infective fractions (left-hand column) and the corresponding phase diagram (right-hand column), the infective fraction *versus* the susceptible fraction *versus* NB, using the second-order method with $N\beta_0 = 270$, $\ell = 0.005$ and (a) $\delta = 0.05$, (b) $\delta = 0.08$, (c) $\delta = 0.26$, (d) $\delta = 0.292$, (e) $\delta = 0.295$, (f) $\delta = 0.298$.

(a)

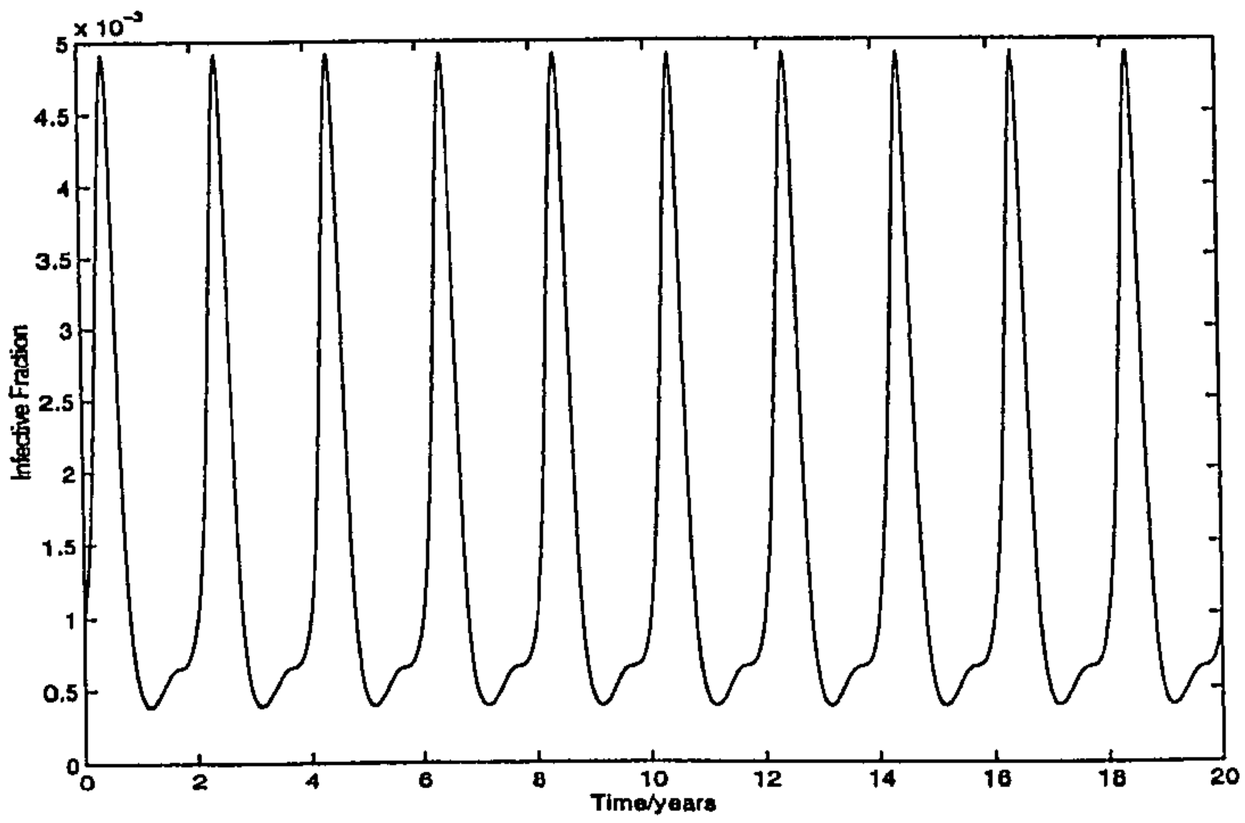

(b)

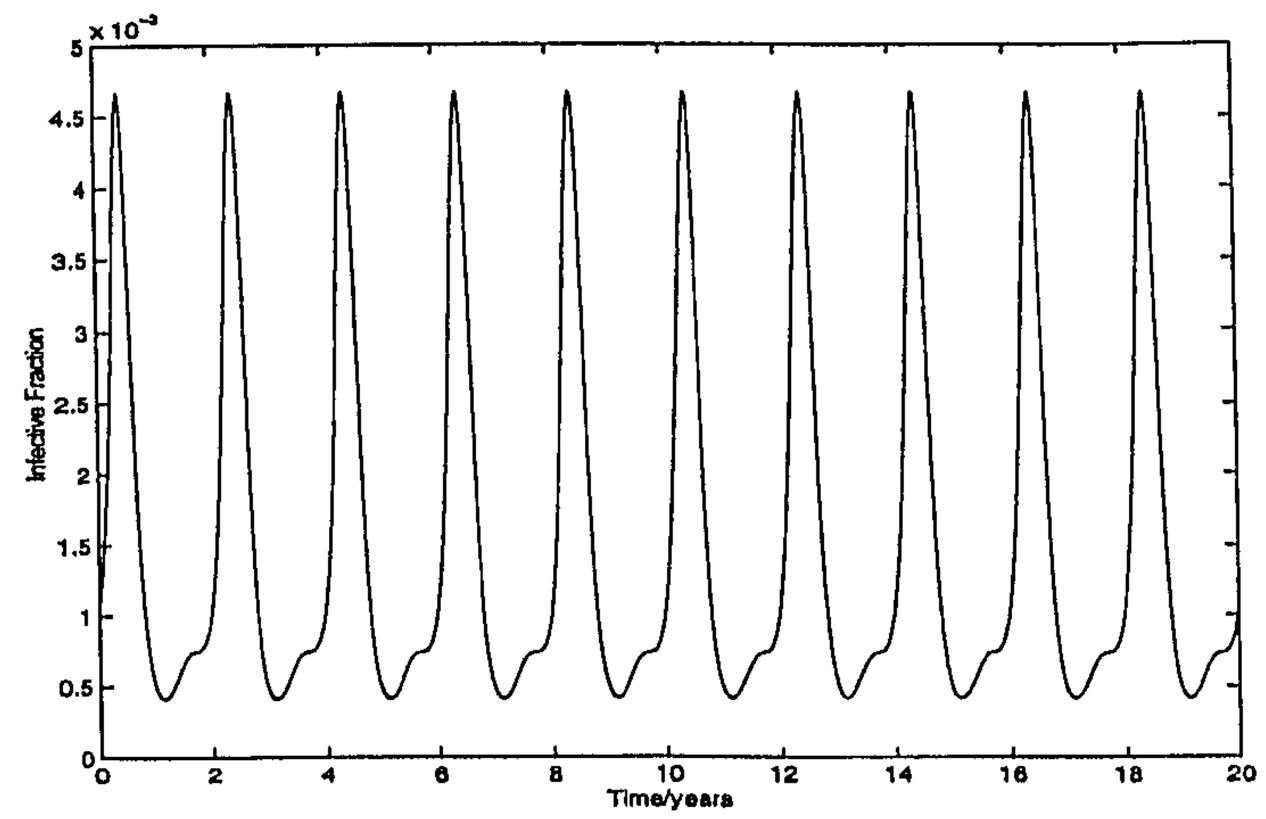

(c)

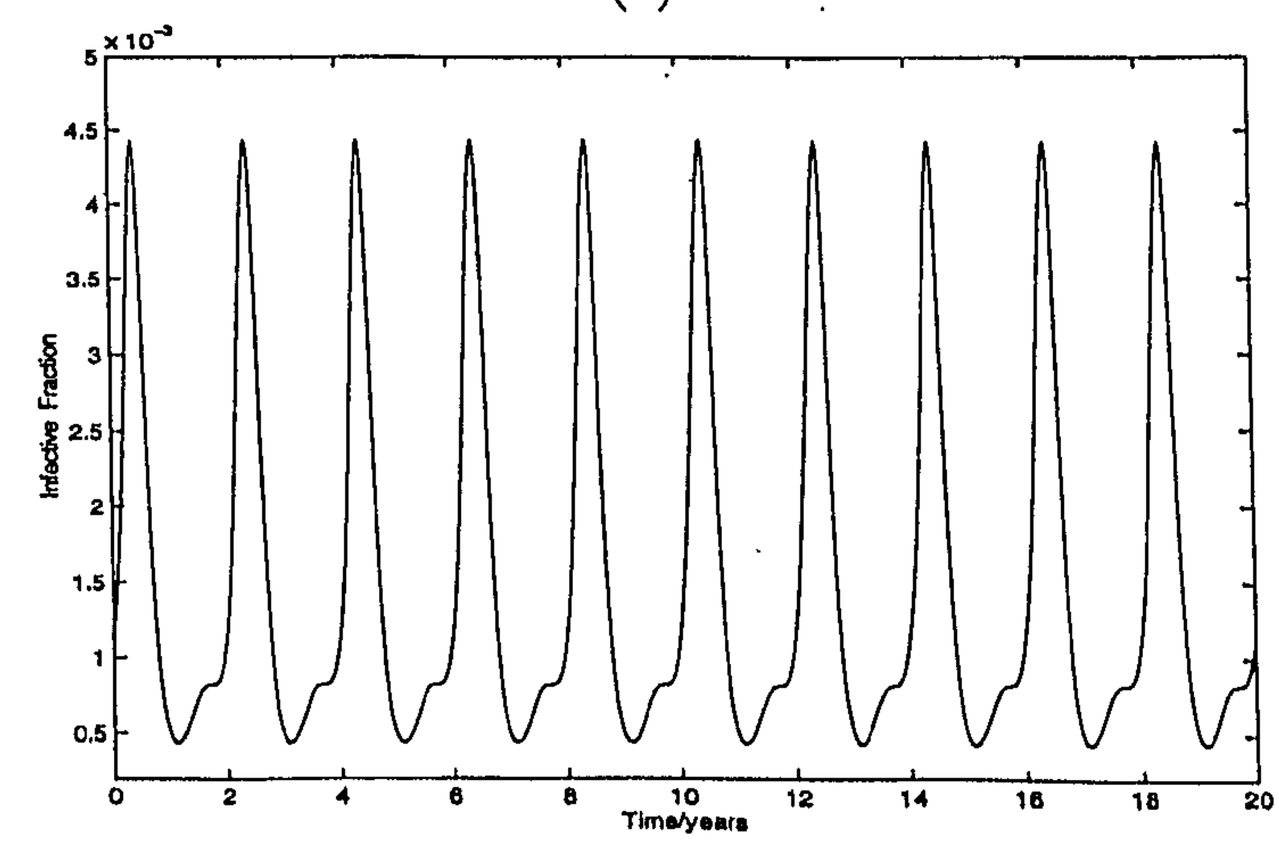

Figure 3.9: The infective fraction *versus* time using method $\mathcal{M}_1$ with $N\beta_0 = 270$, $\delta = 0.08$ and (a) $\ell = 0.01$, (b) $\ell = 0.005$, (c) $\ell = 0.001$.

(a)

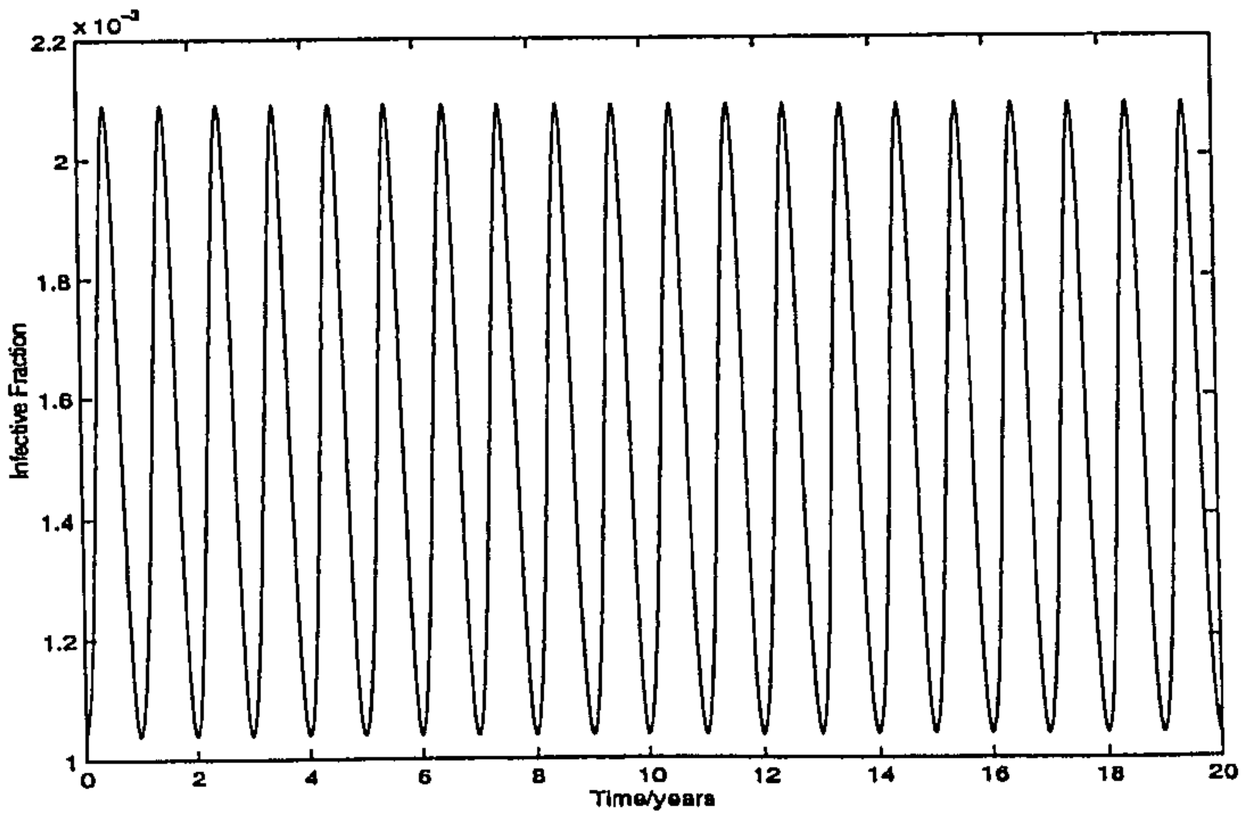

(b)

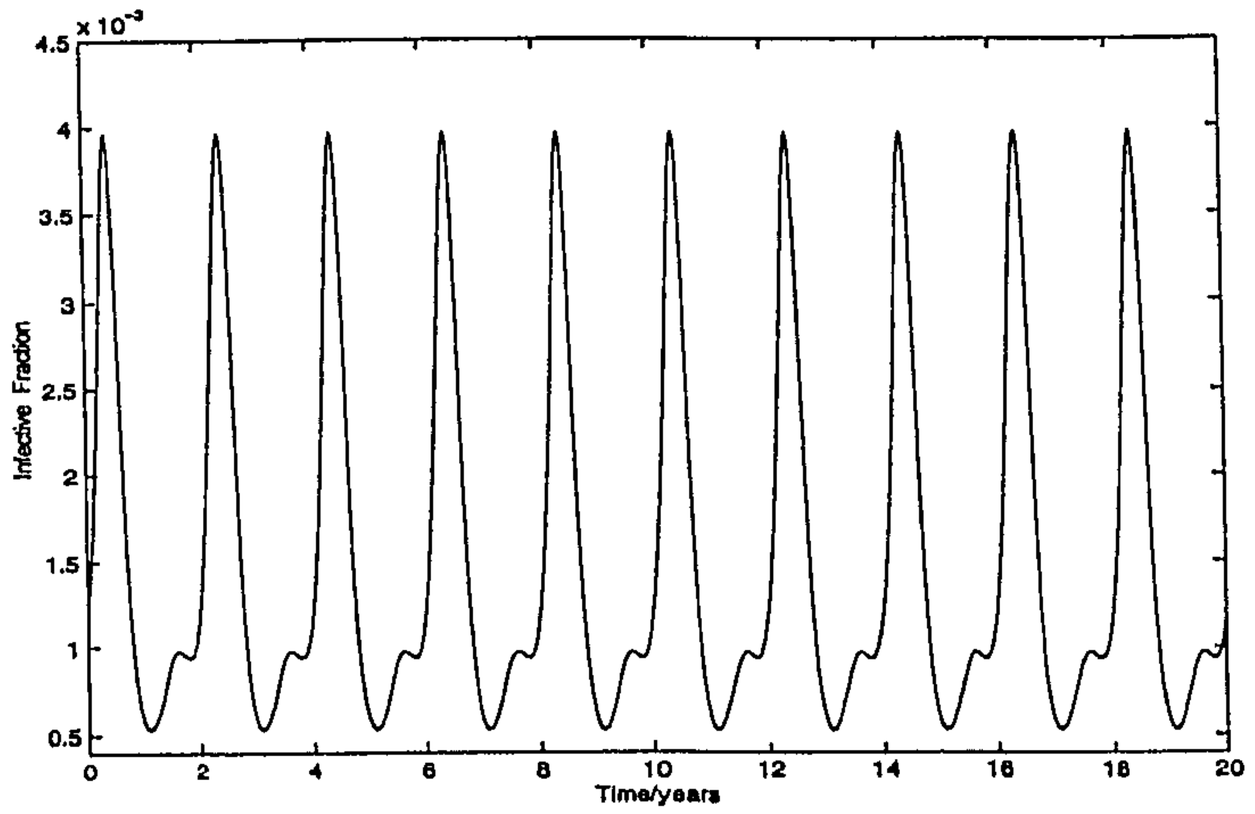

(c)

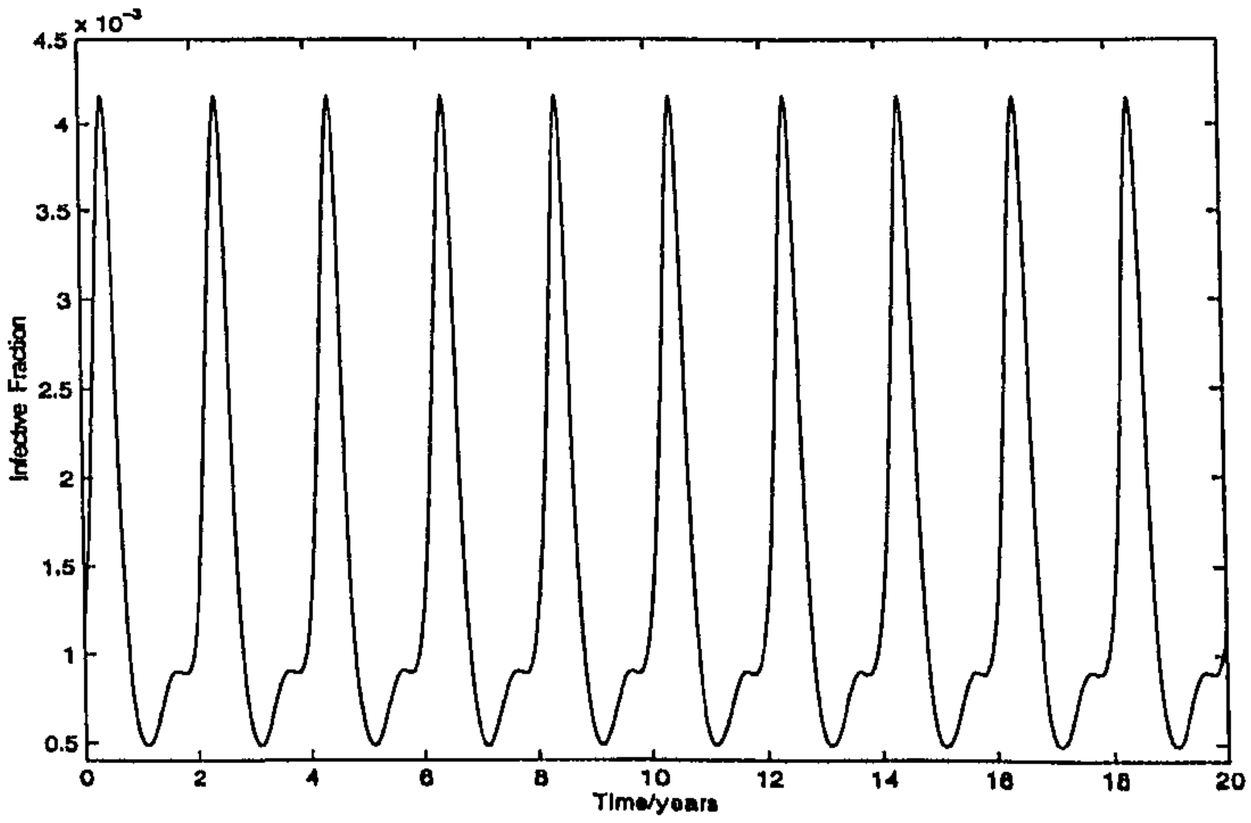

Figure 3.10: The infective fraction *versus* time using method $\mathcal{M}_2$ with $N\beta_0 = 270$, $\delta = 0.08$ and (a) $\ell = 0.005$, (b) $\ell = 0.001$, (c) $\ell = 0.0005$.

(a)

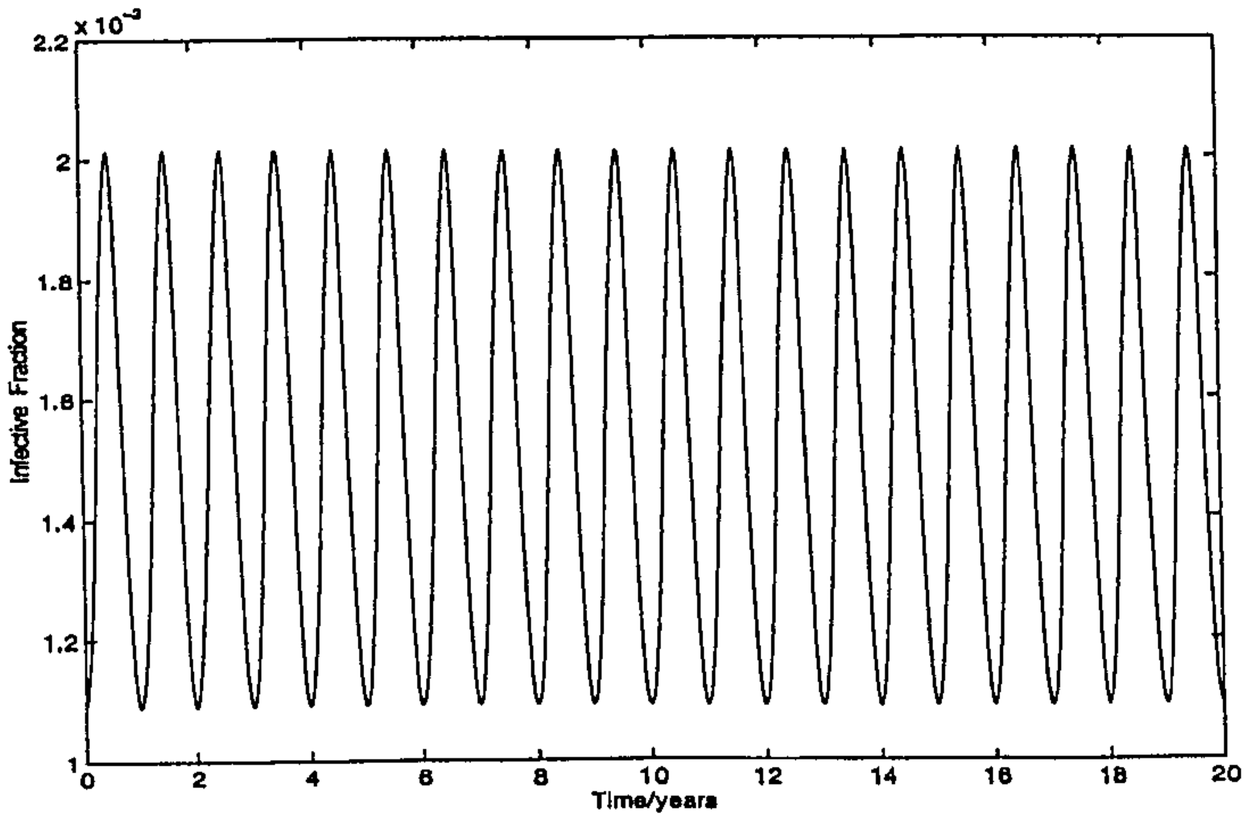

(b)

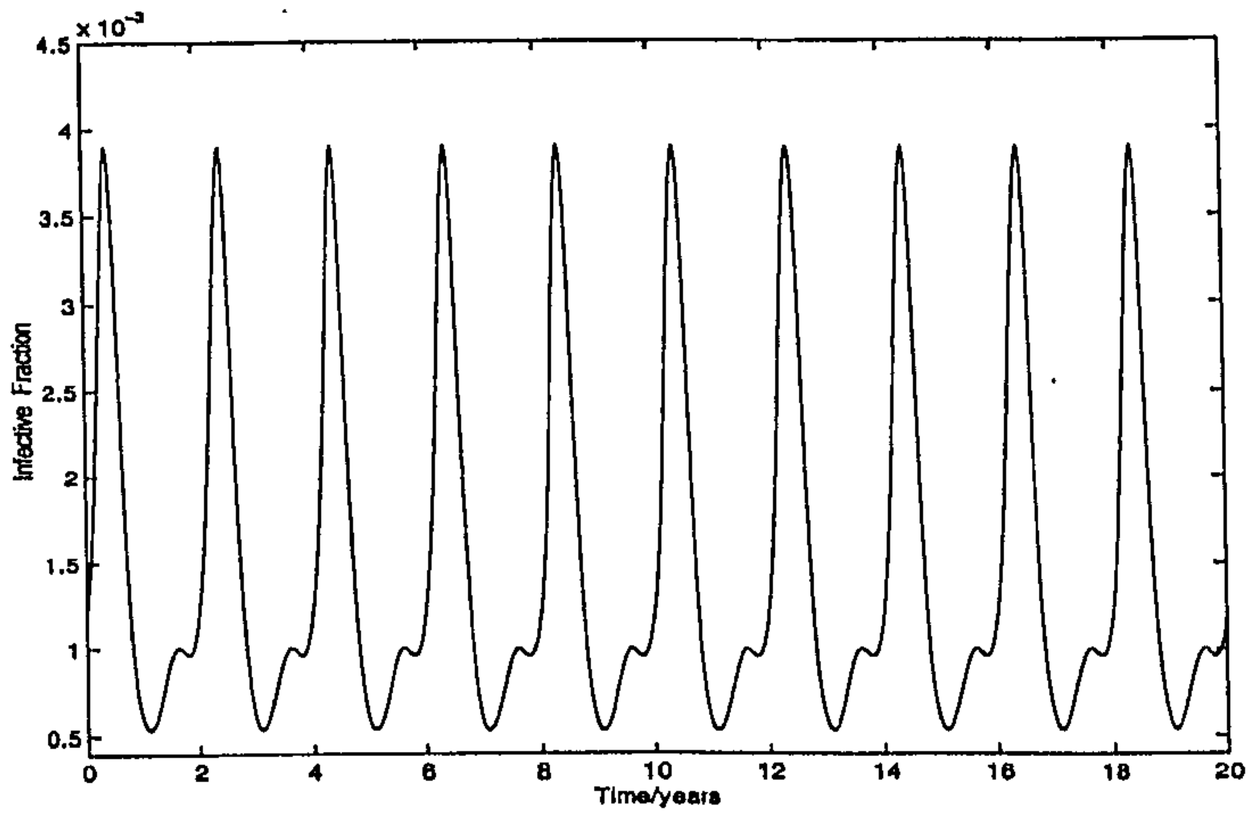

(c)

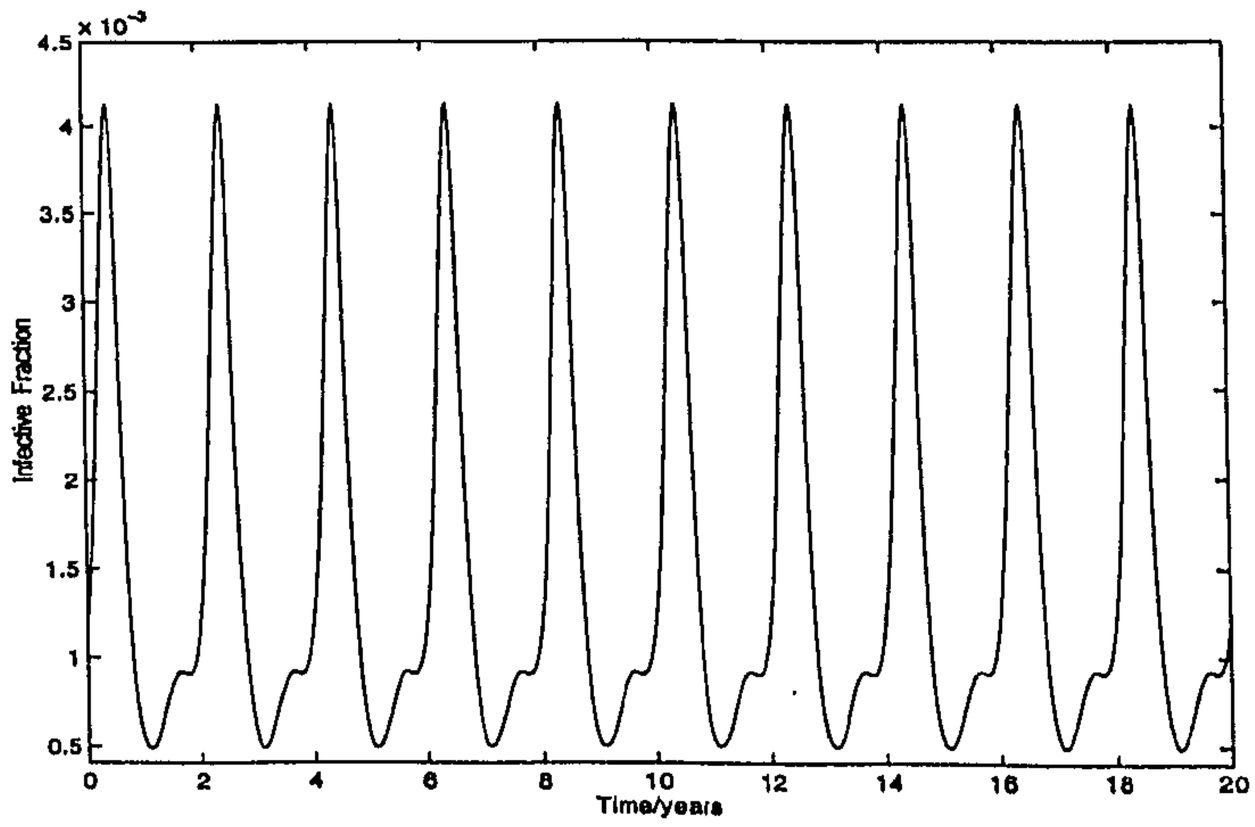

Figure 3.11: The infective fraction *versus* time using method $\mathcal{M}_3$ with $N\beta_0 = 270$, $\delta = 0.08$ and (a) $\ell = 0.005$, (b) $\ell = 0.001$, (c) $\ell = 0.0005$.

(a)

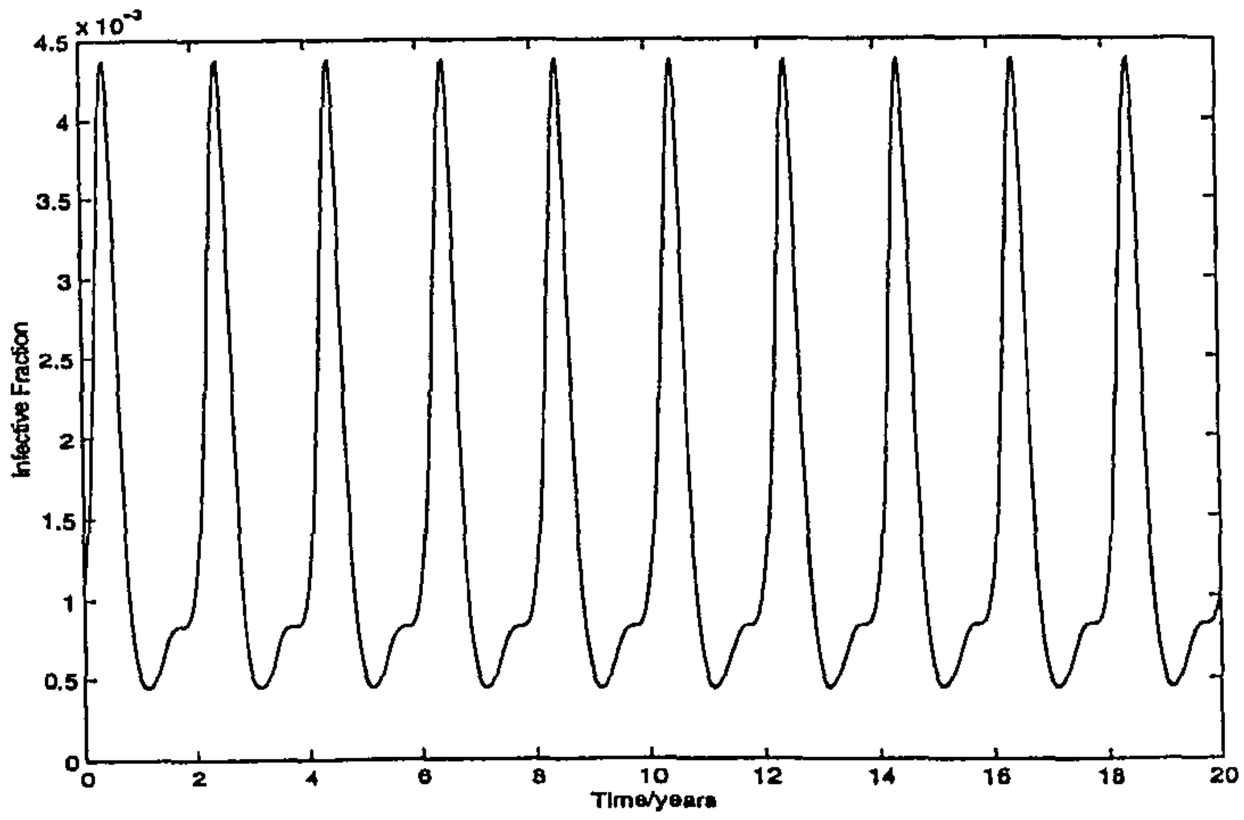

(b)

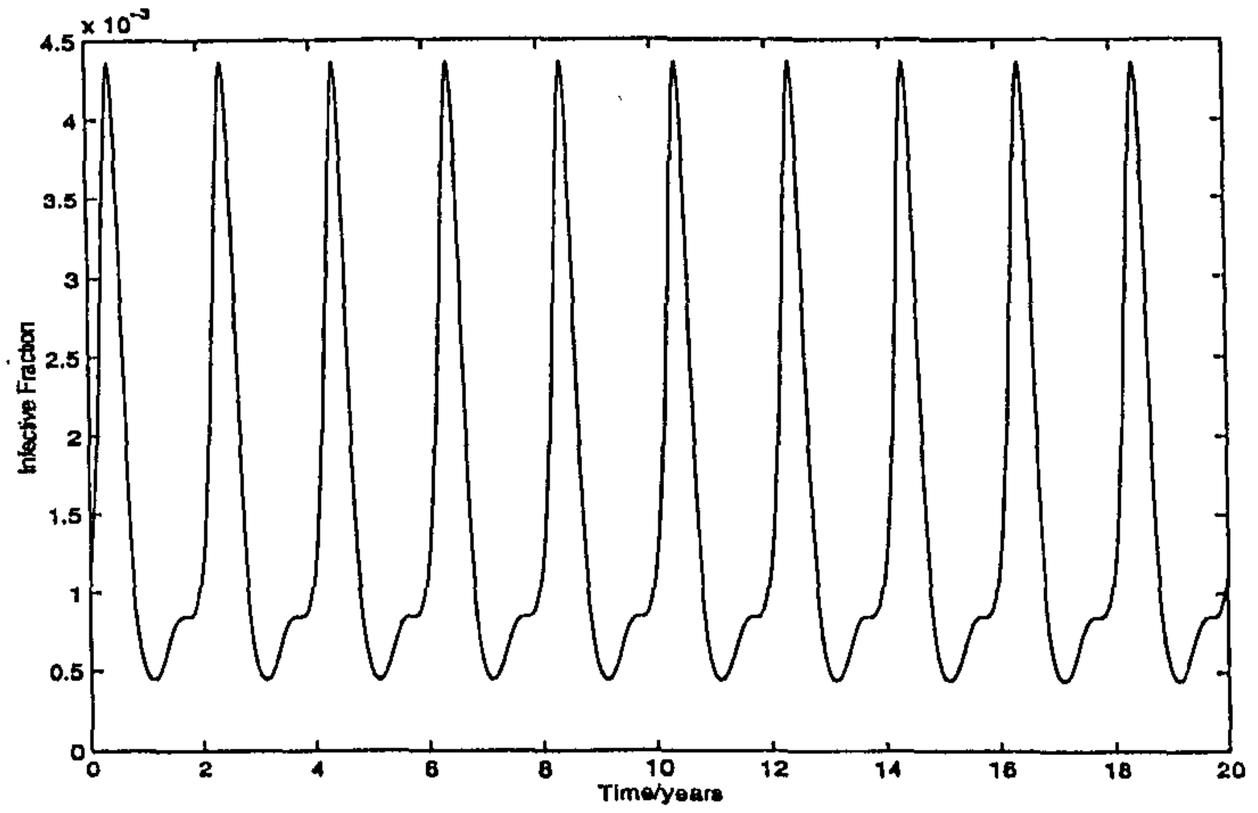

(c)

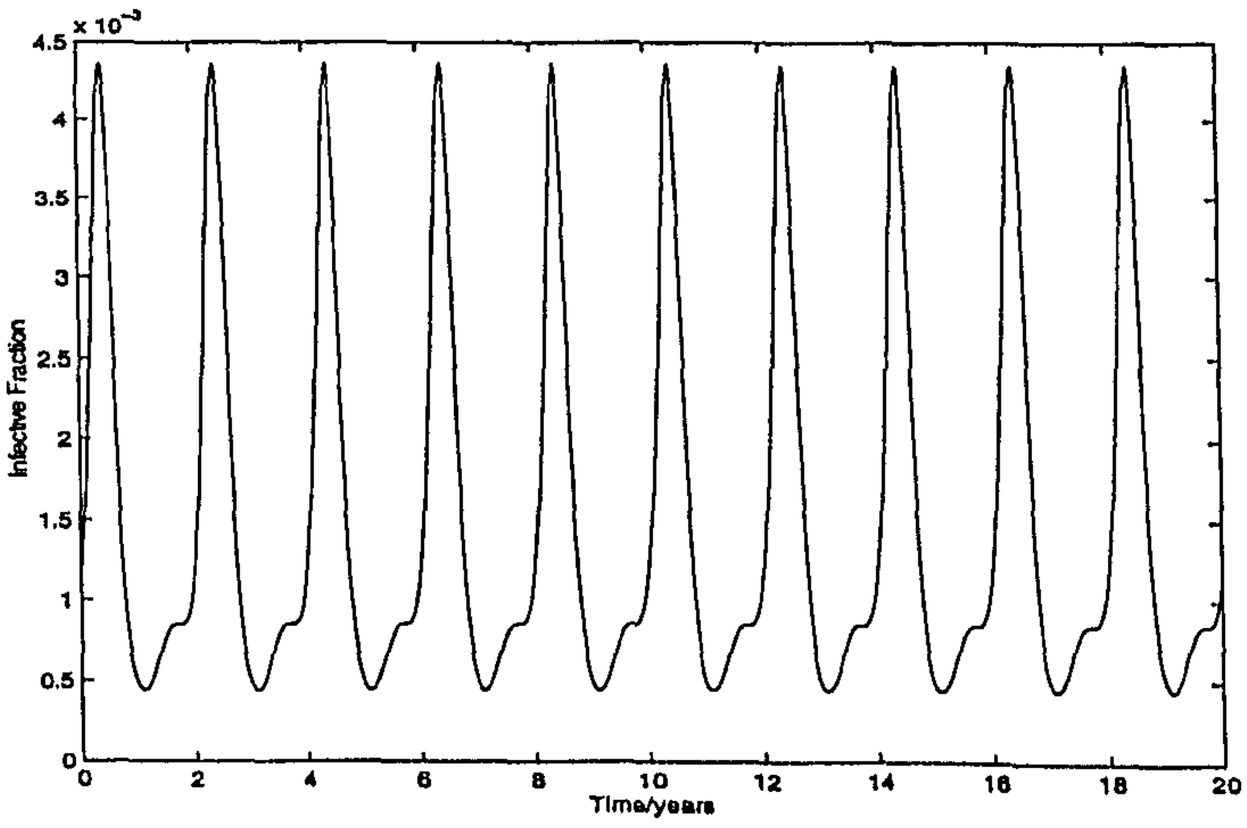

Figure 3.12: The infective fraction *versus* time using the second-order method with $N\beta_0 = 270$, $\delta = 0.08$ and (a) $\ell = 0.01$, (b) $\ell = 0.05$, (c) $\ell = 0.005$.

3.9 Conclusions

Three first-order schemes and a second-order finite-difference scheme have been developed for the numerical integration of the *SIR* whooping cough model given by the non-linear system of equations (3.3.6) and (3.3.7). The stability properties of the methods showed good agreement with the qualitative analysis of the ODE system. Numerical experiments showed that the first-order methods, $\mathcal{M}_2$, $\mathcal{M}_3$ and a second-order method gave the correct behaviour for larger value of a time step, ℓ, than Euler method ($\mathcal{M}_1$). Moreover, the first-order method, $\mathcal{M}_2$, shows superior stability properties in the sense that the method never produces overflow and convergence takes place for all ℓ.

The seasonal *SIR* model implies the modelling of periodic behaviour and even chaos. This model is also solved numerically using three first-order and a second-order methods. The second-order method showed more accuracy and produced solutions to the seasonal *SIR* model which were similar to those reported in Duncan *et al.* [10]. The first-order methods are sensitive to the step length used and using a very small time step seems to be necessary to obtain the correct cycles.

Chapter 4

The dynamics of one-dimensional whooping cough model

4.1 Introduction

The *SIR* whooping cough model which consists of two non-linear ordinary differential equations (ODEs) was considered in the previous chapter. It is assumed that the population is mixing thoroughly, so that there is no distinction between individuals in one place and those in another. When this is not so, the disease may spread faster in some part than in others and it is necessary to allow the variables to depend on space as well as time. It would thus seem natural to extend the model by including diffusional effects, allowing for investigation of the spatial spread of whooping cough epidemic. In this chapter a spatially-structured (reaction-diffusion) equation will be studied and three numerical methods developed for the numerical solution of the spatial spread of whooping cough in one space dimension. The population considered here consists of two parts, susceptibles and infectives. Let $S(z,t)$ and $I(z,t)$ denote the numbers of infected and susceptible individuals, where z and t denote the position in space and the time, respectively. In order to proceed, the epidemic is assumed to diffuse through space. As described in chapter 3, the transmission from susceptibles to infectives is assumed to be βSI where β is the transmissibility coefficient. This form means that βS is the number of susceptibles who catch the disease from each infective. Also, it is assumed that all births are into the susceptible class, and that births exactly balance deaths so that the total population size, N, is constant. With

these assumptions the whooping cough model with diffusion can be written as

$$\frac{\partial S}{\partial t} = \mu N - \mu S - \beta SI + \alpha \frac{\partial^2 S}{\partial z^2} \tag{4.1.1}$$

$$\frac{\partial I}{\partial t} = -(\mu + \nu)I + \beta SI + \alpha \frac{\partial^2 I}{\partial z^2} \tag{4.1.2}$$

where the parameters μ, ν and α denote the death rate, the rate of recovery from disease and the diffusivity of the population (which is assumed to be a non-negative constant and the same for both groups), respectively. Equations (4.1.1) and (4.1.2) are subject to the initial conditions

$$S(z,0) = S_0, \quad I(z,0) = I_0; \quad -L \leq z \leq L \tag{4.1.3}$$

and the boundary conditions are assumed to be

$$\frac{\partial S(\pm L,t)}{\partial z} = \frac{\partial I(\pm L,t)}{\partial z} = 0; \quad t > 0. \tag{4.1.4}$$

It will be assumed that the system {(4.1.1),(4.1.2)} is defined for $-L \leq z \leq L$, $t > 0$ and so, for this ranges, the initial/boundary-value problem {(4.1.1)-(4.1.4)} is symmetric about the line $z = 0$. Because of the symmetry it is enough to solve equations (4.1.1) and (4.1.2) which satisfy the initial conditions

$$S(z,0) = S_0, \quad I(z,0) = I_0; \quad 0 \leq z \leq L, \tag{4.1.5}$$

and the boundary conditions,

$$\frac{\partial S(0,t)}{\partial z} = \frac{\partial I(0,t)}{\partial z} = 0; \quad t > 0, \tag{4.1.6}$$

$$\frac{\partial S(L,t)}{\partial z} = \frac{\partial I(L,t)}{\partial z} = 0; \quad t > 0. \tag{4.1.7}$$

The discussion begins by analysing three numerical methods in §4.2, §4.3 and §4.4, respectively. In §4.5 the von Neumann method and maximum principle analysis will be used to analyse the stability of the methods and their implementations are given in §4.6. It is seen that the three methods are not expensive to implement, as the solution vector is obtained explicitly. The dynamics of whooping cough using two sets of initial conditions will be described in §4.7.

4.2 Discretization and Notations

A solution of the system of partial differential equations {(4.1.1),(4.1.2)} may be computed by finite-difference methods by discretizing the space interval $[0, L]$ into M sub-intervals each of width $h > 0$, and the time interval $t \geq 0$ is discretized in steps each of length $\ell > 0$. The open region $\Omega = [0, L] \times [t > 0]$ and its boundary $\partial\Omega$ consisting of the lines $z = 0$, $z = L$ and $t = 0$ are thus covered by a rectangular mesh, the mesh points having coordinates of the form $(z_m, t_n) = (mh, nl)$; $n = 0, 1, 2, \ldots$; $m = 0, 1, 2, \ldots, M$. The solutions of {(4.1.1),(4.1.2)} at the typical mesh point (z_m, t_n) are, of course, $S(z_m, t_n)$ and $I(z_m, t_n)$ which will be denoted by S_m^n and I_m^n, respectively. The theoretical solution of an approximating finite-difference method at the mesh point (z_m, t_n) will be denoted by X_m^n, Y_m^n, while the values actually obtained which may, for example, be subject to round-off errors at this mesh point will be denoted by $\widetilde{X}_m^n$ and $\widetilde{Y}_m^n$, respectively.

4.3 Numerical Methods

A family of numerical methods will be developed by approximating the time derivative in (4.1.1) and (4.1.2) by the first-order forward difference replacement

$$\frac{\partial u(z,t)}{\partial t} = \frac{u(z, t+\ell) - u(z,t)}{\ell} + O(\ell) \quad \text{as} \quad \ell \to 0, \tag{4.3.1}$$

and the space derivatives in (4.1.1) and (4.1.2) by the weighted approximant

$$\begin{aligned} \frac{\partial^2 u(z,t)}{\partial z^2} \approx\ & h^{-2}\Big[\theta\Big\{u(z-h, t+\ell) - 2u(z, t+\ell) + u(z+h, t+\ell)\Big\} \\ & +(1-\theta)\Big\{u(z-h,t) - 2u(z,t) + u(z+h,t)\Big\}\Big] \end{aligned} \tag{4.3.2}$$

in which $u(z,t) = S(z,t)$ or $I(z,t)$, $z = z_m$ $(m = 0, 1, \ldots, M)$, $t = t_n$ $(n = 0, 1, 2, \ldots)$ and θ, $0 \leq \theta \leq 1$, is a parameter. When $\theta = 0$, (4.3.2) is $O(h^2)$ as $h, \ell \to 0$ and is $O(h^2 + \ell)$ as $h, \ell \to 0$ otherwise.

The non-derivative terms in the right hand sides of (4.1.1) and (4.1.2) may be replaced in the following three ways

$$\text{(a)} \ -\mu X_m^n - \beta X_m^n Y_m^n \qquad \text{and} \qquad -(\mu+\nu)Y_m^n + \beta X_m^n Y_m^n \tag{4.3.3}$$

$$\text{(b)} \; -\mu X_m^{n+1} - \beta X_m^{n+1} Y_m^n \quad \text{and} \quad -(\mu+\nu) Y_m^{n+1} + \beta X_m^n Y_m^n \tag{4.3.4}$$

$$\text{(c)} \; -\mu \frac{(X_m^n + X_m^{n+1})}{2} - \beta \frac{(X_m^{n+1} Y_m^n + X_m^n Y_m^{n+1})}{2} \quad \text{and}$$

$$-(\mu+\nu) \frac{(Y_m^n + Y_m^{n+1})}{2} + \beta \frac{(X_m^{n+1} Y_m^n + X_m^n Y_m^{n+1})}{2}. \tag{4.3.5}$$

These approximations, together with the replacement for the time and space derivatives of S and I, give rise to three numerical methods, Method $A_1(\theta)$, Method $A_2(\theta)$ and Method $A_3(\theta)$ for the numerical solution of {(4.1.1)-(4.1.4)}. These methods are as follows:

Method $A_1(\theta)$, $0 \le \theta \le 1$:

$$\frac{X_m^{n+1} - X_m^n}{\ell} = \mu N - \mu X_m^n - \beta X_m^n Y_m^n + \theta \, \frac{X_{m-1}^{n+1} - 2X_m^{n+1} + X_{m+1}^{n+1}}{h^2}$$

$$+(1-\theta) \, \frac{X_{m-1}^n - 2X_m^n + X_{m+1}^n}{h^2}, \tag{4.3.6}$$

$$\frac{Y_m^{n+1} - Y_m^n}{\ell} = -(\mu+\nu) Y_m^n + \beta X_m^n Y_m^n + \theta \, \frac{Y_{m-1}^{n+1} - 2Y_m^{n+1} + Y_{m+1}^{n+1}}{h^2}$$

$$+(1-\theta) \, \frac{Y_{m-1}^n - 2Y_m^n + Y_{m+1}^n}{h^2}, \tag{4.3.7}$$

Method $A_2(\theta)$, $0 \le \theta \le 1$:

$$\frac{X_m^{n+1} - X_m^n}{\ell} = \mu N - \mu X_m^{n+1} - \beta X_m^{n+1} Y_m^n + \theta \, \frac{X_{m-1}^{n+1} - 2X_m^{n+1} + X_{m+1}^{n+1}}{h^2}$$

$$+(1-\theta) \, \frac{X_{m-1}^n - 2X_m^n + X_{m+1}^n}{h^2}, \tag{4.3.8}$$

$$\frac{Y_m^{n+1} - Y_m^n}{\ell} = -(\mu+\nu) Y_m^{n+1} + \beta X_m^n Y_m^n + \theta \, \frac{Y_{m-1}^{n+1} - 2Y_m^{n+1} + Y_{m+1}^{n+1}}{h^2}$$

$$+(1-\theta)\,\frac{Y_{m-1}^{n}-2Y_{m}^{n}+Y_{m+1}^{n}}{h^2}, \quad (4.3.9)$$

Method $A_3(\theta)$, $\theta = 1/2$:

$$\frac{X_m^{n+1}-X_m^n}{\ell} = \mu N - \mu\,\frac{(X_m^n+X_m^{n+1})}{2} - \beta\,\frac{(X_m^{n+1}Y_m^n + X_m^n Y_m^{n+1})}{2}$$

$$+\theta\,\frac{X_{m-1}^{n+1}-2X_m^{n+1}+X_{m+1}^{n+1}}{h^2} + (1-\theta)\,\frac{X_{m-1}^{n}-2X_m^{n}+X_{m+1}^{n}}{h^2}, \quad (4.3.10)$$

$$\frac{Y_m^{n+1}-Y_m^n}{\ell} = -(\mu+\nu)\,\frac{(Y_m^n+Y_m^{n+1})}{2} + \beta\,\frac{(X_m^{n+1}Y_m^n + X_m^n Y_m^{n+1})}{2}$$

$$+\theta\,\frac{Y_{m-1}^{n+1}-2Y_m^{n+1}+Y_{m+1}^{n+1}}{h^2} + (1-\theta)\,\frac{Y_{m-1}^{n}-2Y_m^{n}+Y_{m+1}^{n}}{h^2}. \quad (4.3.11)$$

It follows that equations (4.3.6)-(4.3.11) can be rewritten, equivalently, as

Method $A_1(\theta)$, $0 \le \theta \le 1$:

$$-p\theta X_{m-1}^{n+1} + (1+2p\theta)X_m^{n+1} - p\theta X_{m+1}^{n+1} = p(1-\theta)X_{m-1}^n$$
$$+\{1-\ell\mu-\ell\beta Y_m^n - 2p(1-\theta)\}X_m^n + p(1-\theta)X_{m+1}^n + \ell\mu N, \quad (4.3.12)$$

$$-p\theta Y_{m-1}^{n+1} + (1+2p\theta)Y_m^{n+1} - p\theta Y_{m+1}^{n+1} = p(1-\theta)Y_{m-1}^n$$
$$+\{1-(\mu+\nu)\ell+\ell\beta X_m^n - 2p(1-\theta)\}Y_m^n + p(1-\theta)Y_{m+1}^n, \quad (4.3.13)$$

Method $A_2(\theta)$, $0 \le \theta \le 1$:

$$-p\theta X_{m-1}^{n+1} + (1+\mu\ell+\ell\beta Y_m^n + 2p\theta)X_m^{n+1} - p\theta X_{m+1}^{n+1} = p(1-\theta)X_{m-1}^n$$
$$+\{1-2p(1-\theta)\}X_m^n + p(1-\theta)X_{m+1}^n + \ell\mu N, \quad (4.3.14)$$

$$-p\theta Y_{m-1}^{n+1} + (1+(\mu+\nu)\ell+2p\theta)Y_m^{n+1} - p\theta Y_{m+1}^{n+1} = p(1-\theta)Y_{m-1}^n$$
$$+\{1+\ell\beta X_m^n - 2p(1-\theta)\}Y_m^n + p(1-\theta)Y_{m+1}^n, \quad (4.3.15)$$

Method $A_3(\theta)$, $\theta = 1/2$:

$$-\frac{1}{2}pX_{m-1}^{n+1} + (1 + \frac{1}{2}\mu\ell + \frac{1}{2}\ell\beta Y_m^n + p)X_m^{n+1} - \frac{1}{2}pX_{m+1}^{n+1} + \frac{1}{2}\ell\beta X_m^n Y_m^{n+1}$$
$$= \frac{1}{2}pX_{m-1}^n + \{1 - \frac{1}{2}\ell\mu - p\}X_m^n + \frac{1}{2}pX_{m+1}^n + \ell\mu N, \qquad (4.3.16)$$

$$-\frac{1}{2}pY_{m-1}^{n+1} + (1 + \frac{1}{2}(\mu+\nu)\ell - \frac{1}{2}\ell\beta X_m^n + p)Y_m^{n+1} - \frac{1}{2}pY_{m+1}^{n+1} - \frac{1}{2}\ell\beta Y_m^n X_m^{n+1}$$
$$= \frac{1}{2}pY_{m-1}^n + \{1 - \frac{1}{2}(\mu+\nu)\ell - p\}Y_m^n + \frac{1}{2}pY_{m+1}^n, \qquad (4.3.17)$$

where $p = \alpha\ell/h^2$, $m = 0, 1, 2, \ldots, M$ and $n = 0, 1, 2, \ldots$.

4.4 Local Truncation Errors

Consider again the use of (4.3.1) and (4.3.2) in (4.1.1) and (4.1.2). The local truncation errors associated with (4.3.12), (4.3.14) and (4.3.16) may be obtained from (4.3.6), (4.3.8) and (4.3.10) and are given by

$$\mathcal{L}_S[S(z,t), I(z,t) : h, \ell] = \ell^{-1}[S(z,t+\ell) - S(z,t)]$$
$$-\alpha\theta h^{-2}\{S(z-h,t+\ell) - 2S(z,t+\ell) + S(z+h,t+\ell)\}$$
$$-(1-\theta)\alpha h^{-2}\{S(z-h,t) - 2S(z,t) + S(z+h,t)\}$$
$$-\mu N + a\{\mu + \beta I(z,t+p\ell)\}S(z,t+q\ell)$$
$$+b\{\mu + \beta I(z,t)\}S(z,t+\ell)$$
$$-\Big[\frac{\partial S(z,t)}{\partial t} - \mu N + \mu S(z,t) + \beta S(z,t)I(z,t) - \alpha\frac{\partial^2 S}{\partial z^2}\Big] \qquad (4.4.1)$$

where

(a) for family $A_1(\theta)$, $a = 1$, $b = p = q = 0$,

(b) for family $A_2(\theta)$, $a = q = 1$, $b = p = 0$,

(c) for family $A_3(\theta)$, $a = b = 0.5$, $p = 1$, $q = 0$.

The local truncation errors associated with (4.3.13), (4.3.15) and (4.3.17) may be written down from (4.3.7), (4.3.9) and (4.3.11) and are given by

$$\begin{aligned}\mathcal{L}_I[S(z,t),I(z,t):h,\ell] &= \ell^{-1}[I(z,t+\ell)-I(z,t)]\\ &-\alpha\theta h^{-2}\{I(z-h,t+\ell)-2I(z,t+\ell)+I(z+h,t+\ell)\}\\ &-(1-\theta)\alpha h^{-2}\{I(z-h,t)-2I(z,t)+I(z+h,t)\}\\ &+c\{(\mu+\nu)I(z,t+r\ell)-\beta S(z,t+s\ell)I(z,t)\}\\ &+d\{(\mu+\nu)-\beta S(z,t)\}I(z,t+\ell)\\ &-\left[\frac{\partial I(z,t)}{\partial t}+(\mu+\nu)I(z,t)-\beta S(z,t)I(z,t)-\alpha\frac{\partial^2 I}{\partial z^2}\right] \qquad (4.4.2)\end{aligned}$$

in which

(a) for family $A_1(\theta)$, $c=1,\ d=r=s=0,$

(b) for family $A_2(\theta)$, $c=r=1,\ d=s=0,$

(c) for family $A_3(\theta)$, $c=d=0.5,\ r=0,\ s=1.$

Using Taylor's series, the local truncation errors for the three methods, as $h,l\to 0$, are given by

(i) for family $A_1(\theta)$:

$$\mathcal{L}_S[S(z,t),I(z,t);h,\ell]=-\frac{1}{12}\alpha h^2\frac{\partial^4 S}{\partial z^4}+\ell\left[\frac{1}{2}\frac{\partial^2 S}{\partial t^2}-\alpha\theta\frac{\partial^3 S}{\partial z^2\partial t}\right]+\ldots, \qquad (4.4.3)$$

$$\mathcal{L}_I[S(z,t),I(z,t);h,\ell]=-\frac{1}{12}\alpha h^2\frac{\partial^4 I}{\partial z^4}+\ell\left[\frac{1}{2}\frac{\partial^2 I}{\partial t^2}-\alpha\theta\frac{\partial^3 I}{\partial z^2\partial t}\right]+\ldots, \qquad (4.4.4)$$

(ii) for family $A_2(\theta)$:

$$\begin{aligned}\mathcal{L}_S[S(z,t),I(z,t);h,\ell] &= -\frac{1}{12}\alpha h^2\frac{\partial^4 S}{\partial z^4}+\ell\left[\frac{1}{2}\frac{\partial^2 S}{\partial t^2}+\mu\frac{\partial S}{\partial t}+\beta I\frac{\partial S}{\partial t}-\alpha\theta\frac{\partial^3 S}{\partial z^2\partial l}\right]\\ &+\ldots, \qquad (4.4.5)\end{aligned}$$

$$\begin{aligned}\mathcal{L}_I[S(z,t),I(z,t);h,\ell] &= -\frac{1}{12}\alpha h^2\frac{\partial^4 I}{\partial z^4}+\ell\left[\frac{1}{2}\frac{\partial^2 I}{\partial t^2}+(\mu+\nu)\frac{\partial I}{\partial t}-\alpha\theta\frac{\partial^3 I}{\partial z^2\partial t}\right]\\ &+\ldots. \qquad (4.4.6)\end{aligned}$$

(iii) for family $A_3(\theta)$:

$$\begin{aligned}\mathcal{L}_S[S(z,t),I(z,t);h,\ell] &= -\frac{1}{12}\alpha h^2\frac{\partial^4 S}{\partial z^4}\\ &+\frac{1}{2}\Big[\frac{\partial^2 S}{\partial t^2}+\mu\frac{\partial S}{\partial t}+\beta I\frac{\partial S}{\partial t}+\beta S\frac{\partial I}{\partial t}-2\alpha\theta\frac{\partial^3 S}{\partial z^2\partial t}\Big]\ell\\ &+\Big[\frac{1}{6}\frac{\partial^3 S}{\partial t^3}+\frac{1}{4}\mu\frac{\partial^2 S}{\partial t^2}+\frac{1}{4}\beta I\frac{\partial^2 S}{\partial t^2}+\frac{1}{4}\beta S\frac{\partial^2 I}{\partial t^2}-\frac{1}{2}\alpha\theta\frac{\partial^4 S}{\partial z^2\partial t^2}\Big]\ell^2\\ &+\ldots,\end{aligned}\tag{4.4.7}$$

$$\begin{aligned}\mathcal{L}_I[S(z,t),I(z,t);h,\ell] &= -\frac{1}{12}\alpha h^2\frac{\partial^4 I}{\partial z^4}\\ &+\frac{1}{2}\Big[\frac{\partial^2 I}{\partial t^2}+(\mu+\nu)\frac{\partial I}{\partial t}-\beta S\frac{\partial I}{\partial t}-\beta I\frac{\partial S}{\partial t}-2\alpha\theta\frac{\partial^3 I}{\partial z^2\partial t}\Big]\ell\\ &+\Big[\frac{1}{6}\frac{\partial^3 I}{\partial t^3}+\frac{1}{4}(\mu+\nu)\frac{\partial^2 I}{\partial t^2}-\frac{1}{4}\beta S\frac{\partial^2 I}{\partial t^2}-\frac{1}{4}\beta I\frac{\partial^2 S}{\partial t^2}-\frac{1}{2}\alpha\theta\frac{\partial^4 I}{\partial z^2\partial t^2}\Big]\ell^2\\ &+\ldots.\end{aligned}\tag{4.4.8}$$

Equations (4.4.3), (4.4.4), (4.4.5) and (4.4.6) verify that both families $A_1(\theta)$ and $A_2(\theta)$ are $O(h^2+\ell)$ as $h,\ell\to 0$. Nevertheless, differentiating (4.1.1) and (4.1.2) with respect to t shows that when $\theta=\frac{1}{2}$ the term in ℓ vanishes in (4.4.7) and (4.4.8), leaving

$$\begin{aligned}\mathcal{L}_S[S(z,t),I(z,t);h,\ell] &= -\frac{\alpha h^2}{12}\frac{\partial^4 S}{\partial z^4}\\ &+\Big[\frac{1}{6}\frac{\partial^3 S}{\partial t^3}+\frac{1}{4}\mu\frac{\partial^2 S}{\partial t^2}+\frac{1}{4}\beta I\frac{\partial^2 S}{\partial t^2}+\frac{1}{4}\beta S\frac{\partial^2 I}{\partial t^2}-\frac{1}{4}\alpha\frac{\partial^4 S}{\partial z^2\partial t^2}\Big]\ell^2+\ldots\end{aligned}\tag{4.4.9}$$

$$\begin{aligned}\mathcal{L}_I[S(z,t),I(z,t);h,\ell] &= -\frac{\alpha h^2}{12}\frac{\partial^4 I}{\partial z^4}\\ &+\Big[\frac{1}{6}\frac{\partial^3 I}{\partial t^3}+\frac{1}{4}(\mu+\nu)\frac{\partial^2 I}{\partial t^2}-\frac{1}{4}\beta S\frac{\partial^2 I}{\partial t^2}-\frac{1}{4}\beta I\frac{\partial^2 S}{\partial t^2}-\frac{1}{4}\alpha\frac{\partial^4 I}{\partial z^2\partial t^2}\Big]\ell^2+\ldots\end{aligned}\tag{4.4.10}$$

which are $O(h^2+\ell^2)$ as $h,\ell\to 0$. It may be concluded that the family $A_3(\theta)$ is a second-order method provided $\theta=\frac{1}{2}$.

4.5 Stability Analyses

The von Neumann or Fourier series method of analysing stability will be used to gain some insight into the stability of the families $A_1(\theta)$ and $A_2(\theta)$. These methods seek the condition(s) under which small errors of the forms

$$Z^n_{x,m} := X^n_m - \widetilde{X}^n_m = e^{\gamma n\ell} e^{i\delta mh} \tag{4.5.1}$$

and

$$Z^n_{y,m} := Y^n_m - \widetilde{Y}^n_m = e^{\psi n\ell} e^{i\phi mh}, \tag{4.5.2}$$

where γ, ψ, δ and ϕ are real, $i = \sqrt{-1}$ and $\widetilde{X}^n_m$, $\widetilde{Y}^n_m$ are perturbed numerical solutions, necessary conditions for the errors not to grow as $n \to \infty$ are (see Smith [10])

$$|e^{\gamma\ell}| \leq 1 + M_x\ell \quad \text{and} \quad |e^{\psi\ell}| \leq 1 + M_y\ell \tag{4.5.3}$$

where M_x and M_y are non-negative constants independent of h, ℓ. The conditions in (4.5.3) make no allowance for growing solutions if $M_x = 0$ and $M_y = 0$.

Method $A_1(\theta)$:

Substituting Z_x into (4.3.12) leads to the (local) stability equation

$$\{1 + 4p\theta \sin^2 \frac{\delta h}{2}\}\xi_x = 1 - 4p(1-\theta)\sin^2 \frac{\delta h}{2} - \mu\ell - \ell\beta Y^n_m, \tag{4.5.4}$$

where $\xi_x = e^{\gamma\ell}$ and Y^n_m is treated as a (local) constant. The von Neumann necessary condition for stability is $|\xi_x| < 1$, that is, the stability restrictions are

$$\begin{aligned} 0 \leq \theta < 1/2, \qquad & p \leq \frac{2 - \ell(\mu + \beta Y^n_m)}{4(1-2\theta)}, \\ \theta = 1/2, \qquad & \ell(\mu + \beta Y^n_m) \leq 2, \\ 1/2 < \theta \leq 1, \qquad & p \geq \frac{\ell(\mu + \beta Y^n_m) - 2}{4(2\theta - 1)}. \end{aligned} \tag{4.5.5}$$

Substituting Z_y into (4.3.13) gives the (local) stability equation

$$\{1 + 4p\theta \sin^2 \frac{\phi h}{2}\}\xi_y = 1 - 4p(1-\theta)\sin^2 \frac{\phi h}{2} - (\mu + \nu)\ell + \beta\ell X^n_m, \tag{4.5.6}$$

where $\xi_y = e^{\psi\ell}$ and X_m^n is treated as a (local) constant. The von Neumann necessary condition for stability is $|\xi_y| < 1$, that is, the stability restrictions are

$$\begin{aligned}
0 \le \theta < 1/2, \qquad & p \le \frac{2 - \ell(\mu + \nu - \beta X_m^n)}{4(1-2\theta)} && \text{and} \quad p \ge \frac{-(\mu + \nu - \beta X_m^n)\ell}{4}, \\
\theta = 1/2, \qquad & \beta\ell X_m^n \ge (\mu + \nu)\ell - 2 && \text{and} \quad p \ge \frac{-(\mu + \nu - \beta X_m^n)\ell}{4}, \\
1/2 < \theta \le 1, \qquad & p \ge \frac{-2 + (\mu + \nu - \beta X_m^n)\ell}{4(2\theta - 1)} && \text{and} \quad p \ge \frac{-(\mu + \nu - \beta X_m^n)\ell}{4}.
\end{aligned} \tag{4.5.7}$$

Method $A_2(\theta)$: Substituting Z_x into (4.3.14) leads to the stability equation

$$\{1 + \ell\mu + \ell\beta Y_m^n + 4p\theta \sin^2 \frac{\delta h}{2}\}\xi_x = 1 - 4p(1-\theta)\sin^2 \frac{\delta h}{2}, \tag{4.5.8}$$

from which it may be deduced that, for stability,

$$\begin{aligned}
0 \le \theta < 1/2, \qquad & p \le \frac{2 + \ell\mu + \ell\beta Y_m^n}{4(1-2\theta)}, \\
\theta = 1/2, \qquad & \beta\ell Y_m^n \ge -2 - \mu\ell, \\
1/2 < \theta \le 1, \qquad & p \ge \frac{-(2 + \mu\ell + \ell\beta Y_m^n)}{4(2\theta - 1)}.
\end{aligned} \tag{4.5.9}$$

Substituting Z_y into (4.3.15) gives to the stability equation

$$\{1 + (\mu + \nu)\ell + 4p\theta \sin^2 \frac{\phi h}{2}\}\xi_y = 1 - 4p(1-\theta)\sin^2 \frac{\phi h}{2} + \ell\beta X_m^n, \tag{4.5.10}$$

with the consequent stability restrictions

$$\begin{aligned}
0 \le \theta < 1/2, \qquad & p \le \frac{2 + (\mu + \nu)\ell + \ell\beta X_m^n}{4(1-2\theta)} && \text{and} \quad p \ge \frac{-(\mu + \nu)\ell + \ell\beta X_m^n}{4}, \\
\theta = 1/2, \qquad & \beta\ell X_m^n \le -2 - (\mu + \nu)\ell && \text{and} \quad p \ge \frac{-(\mu + \nu)\ell + \ell\beta X_m^n}{4}, \\
1/2 < \theta \le 1, \qquad & p \ge \frac{-(2 + (\mu + \nu)\ell + \ell\beta X_m^n)}{4(2\theta - 1)} && \text{and} \quad p \ge \frac{-(\mu + \nu)\ell + \ell\beta X_m^n}{4}.
\end{aligned} \tag{4.5.11}$$

For the second-order method, $A_3(\theta = \frac{1}{2})$, the von Neumann method fails to give a criterion for stability since it is not possible to find $\xi_x = e^{\gamma\ell}$ and $\xi_y = e^{\psi\ell}$ explicitly (see for example Al-Showaikh [2]). Therefore, the maximum principle may be used instead to discuss the stability of the second-order method.

In order to investigate the convergence of the method $A_3(\theta = \frac{1}{2})$ equations (4.1.1) and (4.1.2) may be written as

$$\begin{aligned}\frac{1}{2}\alpha\left(\frac{\partial^2 S}{\partial z^2}+\frac{\partial^2 S}{\partial z^2}\right) &= \frac{\partial S}{\partial t}-\mu N+\frac{1}{2}(\mu+\beta I)S+\frac{1}{2}(\mu+\beta I)S \\ &= \frac{\partial S}{\partial t}-\mu N+G_1(z,t,S,I)+G_2(z,t,S,I), \qquad (4.5.12)\end{aligned}$$

$$\begin{aligned}\frac{1}{2}\alpha\left(\frac{\partial^2 I}{\partial z^2}+\frac{\partial^2 I}{\partial z^2}\right) &= \frac{\partial I}{\partial t}+\frac{1}{2}[(\mu+\nu)-\beta S]I+\frac{1}{2}[(\mu+\nu)-\beta S]I \\ &= \frac{\partial I}{\partial t}+G_3(z,t,S,I)+G_4(z,t,S,I), \qquad (4.5.13)\end{aligned}$$

with initial and boundary conditions

$$S(z,0)=S_0, \quad I(z,0)=I_0; \quad 0\le z\le L \qquad (4.5.14)$$

$$\frac{\partial S(z,t)}{\partial z}=\frac{\partial I(z,t)}{\partial z}=0; \quad \text{at } z=0 \text{ and } z=L,\ t>0. \qquad (4.5.15)$$

Assume that a solution of {(4.5.12),(4.5.13), (4.5.14), (4.5.15)} exists in the closed region $[\Omega: 0\le z\le L, 0\le t\le T]$ such that $\frac{\partial^4 S}{\partial z^4}$, $\frac{\partial^4 I}{\partial z^4}$, $\frac{\partial^2 S}{\partial t^2}$ and $\frac{\partial^2 I}{\partial t^2}$ exist and are bounded in Ω. Moreover, assume that functions G_1, G_2, G_3 and G_4 are boundedly differentiable with respect to S and I.

The difference equation to be studied as an approximation to (4.5.12) is ($\theta = 1/2$)

$$\begin{aligned}\frac{1}{2}\alpha\nabla_z^2(X_m^{n+1}+X_m^n) &= \nabla_t X_m^n-\mu N+\frac{1}{2}(\mu+\beta Y_m^{n+1})X_m^n \\ &\quad +\frac{1}{2}(\mu+\beta Y_m^n)X_m^{n+1}, \quad n\ge 0, \qquad (4.5.16)\end{aligned}$$

where

$$\nabla_z^2 X_m^n = \frac{X_{m-1}^n-2X_m^n+X_{m+1}^n}{h^2}, \qquad (4.5.17)$$

$$\nabla_t X_m^n = \frac{X_m^{n+1}-X_m^n}{\ell}. \qquad (4.5.18)$$

It is easy to see that

$$\frac{\partial S_m^{n+1}}{\partial t} = \frac{S_m^{n+1}-S_m^n}{\ell}+\frac{1}{2}\ell\,\overline{\frac{\partial^2 S_m^{n+1}}{\partial t^2}}, \qquad (4.5.19)$$

$$\frac{1}{2}\nabla_z^2(S_m^{n+1}+S_m^n) = \frac{1}{2}\frac{\partial^2 S_m^{n+1}}{\partial z^2}+\frac{1}{2}\frac{\partial^2 S_m^n}{\partial z^2}+\frac{1}{24}h^2\left(\overline{\frac{\partial^4 S_m^{n+1}}{\partial z^4}}+\overline{\frac{\partial^4 S_m^n}{\partial z^4}}\right), \tag{4.5.20}$$

$$G_1(z_m,t_{n+1},S_m^n,I_m^{n+1}) = G_1(z_m,t_{n+1},S_m^n,I_m^n)+(I_m^{n+1}-I_m^n)\overline{\frac{\partial G_1}{\partial I}}$$

$$= \frac{1}{2}(\mu+\beta I_m^n)S_m^n+(I_m^{n+1}-I_m^n)\overline{\frac{\partial G_1}{\partial S}}, \tag{4.5.21}$$

$$G_2(z_m,t_{n+1},S_m^{n+1},I_m^n) = G_2(z_m,t_{n+1},S_m^n,I_m^n)+(S_m^{n+1}-S_m^n)\overline{\frac{\partial G_2}{\partial S}}$$

$$= \frac{1}{2}(\mu+\beta I_m^n)S_m^n+(S_m^{n+1}-S_m^n)\overline{\frac{\partial G_2}{\partial S}}, \tag{4.5.22}$$

where the barred derivatives are evaluated at intermediate argument values as called for by the mean value theorem.

Substituting (4.5.19), (4.5.20), (4.5.21), (4.5.22) into (4.5.12) gives

$$\frac{1}{2}\alpha\nabla_z^2(S_m^{n+1}+S_m^n) = \nabla_t S_m^n-\mu N+\frac{1}{2}(\mu+\beta I_m^{n+1})S_m^n+\frac{1}{2}(\mu+\beta I_m^n)S_m^{n+1}$$

$$+\left\{\frac{1}{24}\alpha h^2\left(\overline{\frac{\partial^4 S_m^{n+1}}{\partial z^4}}+\overline{\frac{\partial^4 S_m^n}{\partial z^4}}\right)+\frac{1}{2}\ell\,\overline{\frac{\partial^2 S_m^{n+1}}{\partial t^2}}-(I_m^{n+1}-I_m^n)\overline{\frac{\partial G_1}{\partial I}}\right.$$

$$\left.-(S_m^{n+1}-S_m^n)\overline{\frac{\partial G_2}{\partial S}}\right\}. \tag{4.5.23}$$

The assumptions on S and I above require the boundedness of all the derivatives appearing inside the bracket along with $(S_m^{n+1}-S_m^n)$ and $(I_m^{n+1}-I_m^n)$ in the region $0\le z\le L$, $0\le t\le T$. Hence, in this region,

$$\frac{1}{2}\alpha\nabla_z^2(S_m^{n+1}+S_m^n) = \nabla_t S_m^n-\mu N+\frac{1}{2}(\mu+\beta I_m^{n+1})S_m^n+\frac{1}{2}(\mu+\beta I_m^n)S_m^{n+1}$$

$$+g_m^n \tag{4.5.24}$$

with

$$g_m^n = O(h^2+\ell). \tag{4.5.25}$$

Let

$$Z_{1m}^n = S_m^n - X_m^n, \tag{4.5.26}$$

$$Z_{2m}^n = I_m^n - Y_m^n, \tag{4.5.27}$$

then, subtracting (4.5.16) from (4.5.24) yields

$$\frac{1}{2}\alpha\,\nabla_z^2\,(Z_{1m}^{n+1} + Z_{1m}^n) = \nabla_t\, Z_{1m}^n + \frac{1}{2}(\mu + \beta I_m^{n+1})S_m^n - \frac{1}{2}(\mu + \beta Y_m^{n+1})X_m^n$$
$$+\frac{1}{2}(\mu + \beta I_m^n)S_m^{n+1} - \frac{1}{2}(\mu + \beta Y_m^n)X_m^{n+1} + g_m^n \tag{4.5.28}$$

with Z_{1m}^{n+1}, Z_{1m}^n vanishing on the boundary. As

$$G_1(z_m, t_{n+1}, S_m^n, I_m^{n+1}) = G_1(z_m, t_{n+1}, X_m^n, Y_m^{n+1}) + (S_m^n - X_m^n)\,\overline{\frac{\partial G_1}{\partial S}}$$
$$+(I_m^{n+1} - Y_m^{n+1})\,\overline{\frac{\partial G_1}{\partial I}}, \tag{4.5.29}$$

$$G_2(z_m, t_{n+1}, S_m^{n+1}, I_m^n) = G_2(z_m, t_{n+1}, X_m^{n+1}, Y_m^n) + (S_m^{n+1} - X_m^{n+1})\,\overline{\frac{\partial G_2}{\partial S}}$$
$$+(I_m^n - Y_m^n)\,\overline{\frac{\partial G_2}{\partial I}}, \tag{4.5.30}$$

thus,

$$\frac{1}{2}\alpha\,\nabla_z^2\,(Z_{1m}^{n+1} + Z_{1m}^n) = \nabla_t\, Z_{1m}^n + \frac{1}{2}\,\overline{\frac{\partial G_1}{\partial S}}\,Z_{1m}^n + \frac{1}{2}\,\overline{\frac{\partial G_2}{\partial S}}\,Z_{1m}^{n+1} + \frac{1}{2}\,\overline{\frac{\partial G_1}{\partial I}}\,Z_{2m}^{n+1}$$
$$+\frac{1}{2}\,\overline{\frac{\partial G_2}{\partial I}}\,Z_{2m}^n + g_m^n. \tag{4.5.31}$$

Assume that Z_{2m}^n, Z_{2m}^{n+1} are bounded. Then equation (4.5.31) may be written in the form

$$\frac{1}{2}\alpha\,\nabla_z^2\,(Z_{1m}^{n+1} + Z_{1m}^n) \le \nabla_t\, Z_{1m}^n + \frac{1}{2}\,M_{1S}\,(Z_{1m}^{n+1} + Z_{1m}^n) + \frac{1}{2}\,M_{1I}\,(Z_{2m}^n + Z_{2m}^{n+1})$$
$$+\,g_m^n \tag{4.5.32}$$

where

$$M_{1S} = \max\Big\{\overline{\frac{\partial G_1}{\partial S}}, \overline{\frac{\partial G_2}{\partial S}}\Big\}, \qquad M_{1I} = \max\Big\{\overline{\frac{\partial G_1}{\partial I}}, \overline{\frac{\partial G_2}{\partial I}}\Big\}.$$

It is known that g_m^n is bounded and Z_{1m}^n and Z_{1m}^{n+1} vanish on the boundary. Hence, by Theorem 2.15, X_m^n and X_m^{n+1} converge uniformly to S_m^n and S_m^{n+1}.

The difference equation to be studied as an approximation to (4.5.13) is ($\theta = 1/2$)

$$\begin{aligned}\frac{1}{2}\alpha\nabla_z^2(Y_m^{n+1}+Y_m^n) &= \nabla_t Y_m^n + \frac{1}{2}[(\mu+\nu)-\beta X_m^{n+1}]Y_m^n \\ &\quad + \frac{1}{2}[(\mu+\nu)-\beta X_m^n]Y_m^{n+1}, \quad n \geq 0 \end{aligned} \tag{4.5.33}$$

where ∇_z^2 and ∇_t are defined as in (4.5.17).

It is seen that

$$\frac{\partial I_m^{n+1}}{\partial t} = \frac{I_m^{n+1}-I_m^n}{\ell} + \frac{1}{2}\ell\,\overline{\frac{\partial^2 I_m^{n+1}}{\partial t^2}}, \tag{4.5.34}$$

$$\frac{1}{2}\nabla_z^2(I_m^{n+1}+I_m^n) = \frac{1}{2}\frac{\partial^2 I_m^{n+1}}{\partial z^2} + \frac{1}{2}\frac{\partial^2 I_m^n}{\partial z^2} + \frac{1}{24}h^2\left(\overline{\frac{\partial^4 I_m^{n+1}}{\partial z^4}} + \overline{\frac{\partial^4 I_m^n}{\partial z^4}}\right), \tag{4.5.35}$$

$$\begin{aligned} G_3(z_m, t_{n+1}, S_m^{n+1}, I_m^n) &= G_3(z_m, t_{n+1}, S_m^n, I_m^n) + (S_m^{n+1}-S_m^n)\overline{\frac{\partial G_3}{\partial S}} \\ &= \frac{1}{2}[(\mu+\nu)-\beta S_m^n]I_m^n + (S_m^{n+1}-S_m^n)\overline{\frac{\partial G_3}{\partial S}}, \end{aligned} \tag{4.5.36}$$

$$\begin{aligned} G_4(z_m, t_{n+1}, S_m^n, I_m^{n+1}) &= G_4(z_m, t_{n+1}, S_m^n, I_m^n) + (I_m^{n+1}-I_m^n)\overline{\frac{\partial G_4}{\partial I}} \\ &= \frac{1}{2}[(\mu+\nu)-\beta S_m^n]I_m^n + (I_m^{n+1}-I_m^n)\overline{\frac{\partial G_4}{\partial S}}, \end{aligned} \tag{4.5.37}$$

where the barred derivatives are evaluated at intermediate argument values as called for by the mean value theorem.

Substituting (4.5.34), (4.5.35), (4.5.36), (4.5.37) into (4.5.13) gives

$$\begin{aligned}\frac{1}{2}\alpha\nabla_z^2(I_m^{n+1}+I_m^n) &= \nabla_t I_m^n + \frac{1}{2}[(\mu+\nu)-\beta S_m^{n+1}]I_m^n + \frac{1}{2}[(\mu+\nu)-\beta S_m^n]I_m^{n+1} \\ &\quad + \left\{\frac{1}{24}\alpha h^2\left(\overline{\frac{\partial^4 I_m^{n+1}}{\partial z^4}} + \overline{\frac{\partial^4 I_m^n}{\partial z^4}}\right) + \frac{1}{2}\ell\,\overline{\frac{\partial^2 I_m^{n+1}}{\partial t^2}} - (S_m^{n+1}-S_m^n)\overline{\frac{\partial G_3}{\partial S}}\right. \\ &\quad \left. -(I_m^{n+1}-I_m^n)\overline{\frac{\partial G_4}{\partial I}}\right\}. \end{aligned} \tag{4.5.38}$$

The assumptions on S and I above require the boundedness of all the derivatives appearing inside the bracket along with $(S_m^{n+1}-S_m^n)$ and $(I_m^{n+1}-I_m^n)$ in the region

$0 \leq z \leq L$, $0 \leq t \leq T$. Hence, in this region,

$$\begin{aligned} \frac{1}{2}\alpha \nabla_z^2 (I_m^{n+1} + I_m^n) &= \nabla_t I_m^n + \frac{1}{2}[(\mu+\nu) - \beta S_m^{n+1}] I_m^n + \frac{1}{2}[(\mu+\nu) - \beta S_m^n] I_m^{n+1} \\ &\quad + g_m^n \end{aligned} \tag{4.5.39}$$

with

$$g_m^n = O(h^2 + \ell). \tag{4.5.40}$$

Subtracting (4.5.33) from (4.5.39) and using (4.5.26), gives

$$\begin{aligned} \frac{1}{2}\alpha \nabla_z^2 (Z_{2m}^{n+1} + Z_{2m}^n) &= \nabla_t Z_{2m}^n + \frac{1}{2}[(\mu+\nu) - \beta S_m^{n+1}] I_m^n - \frac{1}{2}[(\mu+\nu) - \beta X_m^{n+1}] Y_m^n \\ &\quad + \frac{1}{2}[(\mu+\nu) - \beta S_m^n] I_m^{n+1} - \frac{1}{2}[(\mu+\nu) - \beta X_m^n] Y_m^{n+1} + g_m^n \end{aligned} \tag{4.5.41}$$

with Z_{2m}^{n+1}, Z_{2m}^n vanishing on the boundary. As

$$\begin{aligned} G_3(z_m, t_{n+1}, S_m^{n+1}, I_m^n) &= G_3(z_m, t_{n+1}, X_m^{n+1}, Y_m^n) + (S_m^{n+1} - X_m^{n+1}) \overline{\frac{\partial G_3}{\partial S}} \\ &\quad + (I_m^n - Y_m^n) \overline{\frac{\partial G_3}{\partial I}}, \end{aligned} \tag{4.5.42}$$

$$\begin{aligned} G_4(z_m, t_{n+1}, S_m^n, I_m^{n+1}) &= G_4(z_m, t_{n+1}, X_m^n, Y_m^{n+1}) + (S_m^n - X_m^n) \overline{\frac{\partial G_4}{\partial S}} \\ &\quad + (I_m^{n+1} - Y_m^{n+1}) \overline{\frac{\partial G_4}{\partial I}}, \end{aligned} \tag{4.5.43}$$

thus equation (4.5.41) becomes

$$\begin{aligned} \frac{1}{2}\alpha \nabla_z^2 (Z_{2m}^{n+1} + Z_{2m}^n) &= \nabla_t Z_{2m}^n + \frac{1}{2} \overline{\frac{\partial G_3}{\partial S}} Z_{1m}^{n+1} + \frac{1}{2} \overline{\frac{\partial G_4}{\partial S}} Z_{1m}^n + \frac{1}{2} \overline{\frac{\partial G_3}{\partial I}} Z_{2m}^n \\ &\quad + \frac{1}{2} \overline{\frac{\partial G_4}{\partial I}} Z_{2m}^{n+1} + g_m^n. \end{aligned} \tag{4.5.44}$$

Let $M_{1S} = \max\left\{ \overline{\frac{\partial G_3}{\partial S}}, \overline{\frac{\partial G_4}{\partial S}} \right\}$ and $M_{2I} = \max\left\{ \overline{\frac{\partial G_3}{\partial I}}, \overline{\frac{\partial G_4}{\partial I}} \right\}$. Then equation (4.5.45) can be written in the form

$$\begin{aligned} \frac{1}{2}\alpha \nabla_z^2 (Z_{2m}^{n+1} + Z_{2m}^n) &\leq \nabla_t Z_{2m}^n + \frac{1}{2} M_{2S} (Z_{1m}^{n+1} + Z_{1m}^n) + \frac{1}{2} M_{2I} (Z_{2m}^n + Z_{2m}^{n+1}) \\ &\quad + g_m^n \end{aligned} \tag{4.5.45}$$

Assume that Z_{1m}^n, Z_{1m}^{n+1} are bounded. Since Z_{1m}^n and Z_{1m}^{n+1} vanish on the boundary, it follows, by Theorem 2.15, that Y_m^n and Y_m^{n+1} converge to I_m^n and I_m^{n+1} uniformly.

4.6 Implementation

Because of symmetry, it is enough to treat only the region $z \geq 0$. This provides considerable saving in storage and CPU time. This imposes the conditions

$$\frac{\partial S(0,t)}{\partial z} = 0 \quad \text{and} \quad \frac{\partial I(0,t)}{\partial z} = 0; \quad t > 0 \tag{4.6.1}$$

on the new boundary $z = 0$. The derivative $\partial S/\partial z$ in (4.1.4) may be approximated by the second-order, central-difference replacement

$$\frac{\partial S(z,t)}{\partial z} = \frac{S(z+h,t) - S(z-h,t)}{2h} + O(h^2) \tag{4.6.2}$$

with a similar replacement being made to $\partial I/\partial z$. The implementation of the boundary conditions (4.1.4), yields, on $z = 0$ and $z = L$,

$$X_1^n = X_{-1}^n,\ Y_1^n = Y_{-1}^n \quad \text{and} \quad X_{M+1}^n = X_{M-1}^n,\ Y_{M+1}^n = Y_{M-1}^n\ (n = 0, 1, 2, \ldots) \tag{4.6.3}$$

to second order thus introducing the exterior grid points $(z_{-1}, t_n) = (-h, n\ell)$ and $(z_{M+1}, t_n) = ((M+1)h, n\ell)$.

Let $\mathbf{X}^{n+1} = [X_0^{n+1}, X_1^{n+1}, \ldots, X_M^{n+1}]^T$ and $\mathbf{Y}^{n+1} = [Y_0^{n+1}, Y_1^{n+1}, \ldots, Y_M^{n+1}]^T$ where T denotes transpose. The modification to the formulae of the three families of numerical methods, and their implications, are as follows.

Method $A_1(\theta)$:

Taking $m = 0,\ M$ in (4.3.12) and (4.3.13) and using (4.6.3) gives

$m = 0,$

$$\begin{aligned}(1+2p\theta)X_0^{n+1} - 2p\theta X_1^{n+1} &= \{1 - \ell\mu - \ell\beta Y_0^n - 2p(1-\theta)\}X_0^n \\ &\quad + 2p(1-\theta)X_1^n + \ell\mu N, \end{aligned} \tag{4.6.4}$$

$$\begin{aligned}(1+2p\theta)Y_0^{n+1} - 2p\theta Y_1^{n+1} &= \{1 - (\mu+\nu)\ell + \ell\beta X_0^n - 2p(1-\theta)\}Y_0^n \\ &\quad + 2p(1-\theta)Y_1^n, \end{aligned} \tag{4.6.5}$$

and $m = M$,

$$-2p\theta X_{M-1}^{n+1} + (1+2p\theta)X_M^{n+1} = -2p(1-\theta)X_{M-1}^n + \{1-\ell\mu-\ell\beta Y_M^n - 2p(1-\theta)\}X_M^n + \ell\mu N, \quad (4.6.6)$$

$$-2p\theta Y_{M-1}^{n+1} + (1+2p\theta)Y_M^{n+1} = 2p(1-\theta)Y_{M-1}^n + \{1-(\mu+\nu)\ell + \ell\beta X_M^n - 2p(1-\theta)\}Y_M^n. \quad (4.6.7)$$

The solution vectors $\mathbf{X}^{n+1}$ and $\mathbf{Y}^{n+1}$ may be obtained using the following parallel algorithm:

$$\textbf{Processor 1}: \text{Solve} \quad E_1\mathbf{X}^{n+1} = F_1\mathbf{X}^n + \mathbf{q} \quad \text{for} \quad \mathbf{X}^{n+1}, \quad (4.6.8)$$

$$\textbf{Processor 2}: \text{Solve} \quad E_1\mathbf{Y}^{n+1} = G_1\mathbf{Y}^n \quad \text{for} \quad \mathbf{Y}^{n+1}, \quad (4.6.9)$$

where E_1 is a constant, tridiagonal matrix of order $M+1$ given by

$$E_1 = \begin{bmatrix} 1+2p\theta & -2p\theta & 0 & \cdots & 0 \\ -p\theta & 1+2p\theta & -p\theta & & \vdots \\ \vdots & \ddots & \ddots & \ddots & 0 \\ 0 & & -p\theta & 1+2p\theta & -p\theta \\ 0 & \cdots & 0 & -2p\theta & 1+2p\theta \end{bmatrix}, \quad (4.6.10)$$

and $\mathbf{q} = [\ell\mu N, \ldots, \ell\mu N]^T$ is a constant vector of order $M+1$. The square matrices F_1 and G_1 are also of order $M+1$ and are given by

$$F_1 = \begin{bmatrix} f_0 & 2p(1-\theta) & 0 & \cdots & 0 \\ p(1-\theta) & f_1 & p(1-\theta) & & \vdots \\ 0 & \ddots & \ddots & \ddots & 0 \\ \vdots & & p(1-\theta) & f_{M-1} & p(1-\theta) \\ 0 & \cdots & 0 & 2p(1-\theta) & f_M \end{bmatrix}, \quad (4.6.11)$$

where $f_i^n = 1 - \ell\mu - \ell\beta Y_i^n - 2p(1-\theta)$, $i = 0, 1, 2, \ldots, M$,

$$G_1 = \begin{bmatrix} g_0 & 2p(1-\theta) & 0 & \cdots & 0 \\ p(1-\theta) & g_1 & p(1-\theta) & & \vdots \\ 0 & \ddots & \ddots & \ddots & 0 \\ \vdots & & p(1-\theta) & g_{M-1} & p(1-\theta) \\ 0 & \cdots & 0 & 2p(1-\theta) & g_M \end{bmatrix}, \tag{4.6.12}$$

where $g_i = 1 - (\mu+\nu)\ell + \ell\beta X_i^n - 2p(1-\theta)$, $i = 0, 1, 2, \ldots, M$.

Method $A_2(\theta)$:

Taking $m = 0,\ M$ in (4.3.14) and (4.3.15) and using (4.6.3) gives

$m = 0$,

$$(1 + \mu\ell + \ell\beta Y_0^n + 2p\theta)X_0^{n+1} - 2p\theta X_1^{n+1} = \{1 - 2p(1-\theta)\}X_0^n + 2p(1-\theta)X_1^n + \ell\mu N, \tag{4.6.13}$$

$$(1 + (\mu+\nu)\ell + 2p\theta)Y_0^{n+1} - 2p\theta Y_1^{n+1} = \{1 + \ell\beta X_0^n - 2p(1-\theta)\}Y_0^n + 2p(1-\theta)Y_1^n, \tag{4.6.14}$$

and $m = M$,

$$-2p\theta X_{M-1}^{n+1} + (1 + \mu\ell + \ell\beta Y_M^n + 2p\theta)X_M^{n+1} = 2p(1-\theta)X_{M-1}^n + \{1 - 2p(1-\theta)\}X_M^n + \ell\mu N \tag{4.6.15}$$

$$-2p\theta Y_{M-1}^{n+1} + (1 + (\mu+\nu)\ell + 2p\theta)Y_M^{n+1} = 2p(1-\theta)Y_{M-1}^n + \{1 + \ell\beta X_M^n - 2p(1-\theta)\}Y_M^n. \tag{4.6.16}$$

In this method the solution vectors $\mathbf{X}^{n+1}$ and $\mathbf{Y}^{n+1}$ may be obtained using the parallel algorithm:

$$\textbf{Processor 1}: \text{Solve} \quad O_1\mathbf{X}^{n+1} = P_1\mathbf{X}^n + \mathbf{q} \quad \text{for} \quad \mathbf{X}^{n+1}, \tag{4.6.17}$$

$$\textbf{Processor 2}: \text{Solve} \quad Q_1\mathbf{Y}^{n+1} = R_1\mathbf{Y}^n \quad \text{for} \quad \mathbf{Y}^{n+1}, \tag{4.6.18}$$

where P_1 and Q_1 are constant, tridiagonal matrices of order $M+1$ given by

$$P_1 = \begin{bmatrix} a & 2p(1-\theta) & 0 & \cdots & 0 \\ p(1-\theta) & a & p(1-\theta) & & \vdots \\ \vdots & \ddots & \ddots & \ddots & 0 \\ 0 & & p(1-\theta) & a & p(1-\theta) \\ 0 & \cdots & 0 & 2p(1-\theta) & a \end{bmatrix} \tag{4.6.19}$$

and

$$Q_1 = \begin{bmatrix} q & -2p\theta & 0 & \cdots & 0 \\ -p\theta & q & -p\theta & & \vdots \\ \vdots & \ddots & \ddots & \ddots & 0 \\ 0 & & -p\theta & q & -p\theta \\ 0 & \cdots & 0 & -2p\theta & q \end{bmatrix} \tag{4.6.20}$$

with $a = 1-2p(1-\theta)$ and $q = 1+(\mu+\nu)\ell+2p\theta$, respectively. The matrix O_1 is a tridiagonal matrix of order $M+1$ given by

$$O_1 = \begin{bmatrix} b_0 & -2p\theta & 0 & \cdots & 0 \\ -p\theta & b_1 & -p\theta & & \vdots \\ \vdots & \ddots & \ddots & \ddots & 0 \\ 0 & & -p\theta & b_{M-1} & -p\theta \\ 0 & \cdots & 0 & -2p\theta & b_M \end{bmatrix}, \tag{4.6.21}$$

where $b_i = 1+\mu\ell+\ell\beta Y_i^n+2p\theta$, $i = 0,1,\ldots,M$. The matrix

$$R_1 = \begin{bmatrix} r_0 & 2p(1-\theta) & 0 & \cdots & 0 \\ p(1-\theta) & r_1 & p(1-\theta) & & \vdots \\ \vdots & \ddots & \ddots & \ddots & 0 \\ 0 & & p(1-\theta) & r_{M-1} & p(1-\theta) \\ 0 & \cdots & 0 & 2p(1-\theta) & r_M \end{bmatrix}, \qquad (4.6.22)$$

with $r_i = 1 + \ell\beta X_i^n - 2p(1-\theta)$, $i = 0, 1, 2, \ldots, M$, is also a tridiagonal matrix of order $M+1$.

Method $A_3(\theta = 1/2)$:

Taking $m = 0$, M in (4.3.16) and (4.3.17) and using (4.6.3) gives,

$m = 0$

$$(1 + \frac{1}{2}\mu\ell + \frac{1}{2}\ell N\beta Y_0^n + p)X_0^{n+1} - pX_1^{n+1} + \frac{1}{2}\ell N\beta X_0^n Y_0^{n+1}$$
$$= \{1 - \frac{1}{2}\ell\mu - p\}X_0^n + pX_1^n + \ell\mu N, \qquad (4.6.23)$$

$$(1 + \frac{1}{2}(\mu+\nu)\ell - \frac{1}{2}\ell\beta X_0^n + p)Y_0^{n+1} - pY_1^{n+1} - \frac{1}{2}\ell\beta Y_0^n X_0^{n+1}$$
$$= \{1 - \frac{1}{2}(\mu+\nu)\ell - p\}Y_0^n + pY_1^n, \qquad (4.6.24)$$

and, for $m = M$,

$$-pX_{M-1}^{n+1} + (1 + \frac{1}{2}\mu\ell + \frac{1}{2}\ell\beta Y_M^n + p)X_M^{n+1} + \frac{1}{2}\ell\beta X_M^n Y_M^{n+1}$$
$$= pX_{M-1}^n + \{1 - \frac{1}{2}\ell\mu - p\}X_M^n + \ell\mu N \qquad (4.6.25)$$

$$-pY_{M-1}^{n+1} + (1 + \frac{1}{2}(\mu+\nu)\ell - \frac{1}{2}\ell\beta X_M^n + p)Y_M^{n+1} - \frac{1}{2}\ell\beta Y_M^n X_M^{n+1}$$
$$= pY_{M-1}^n + \{1 - \frac{1}{2}(\mu+\nu)\ell - p\}Y_M^n. \qquad (4.6.26)$$

As described above, the linear algebraic systems given by {(4.6.8),(4.6.9)} and {(4.6.17),(4.6.18)} which represent the first-order methods $A_1(\theta)$ and $A_2(\theta)$, respectively, can be solved using parallel computation (using a computer with two processor). In parallel computation, the vectors $\mathbf{X}^{n+1}$ and $\mathbf{Y}^{n+1}$ can be obtained simultaneously and thus the time taken to solve the PDEs will be reduced significantly.

For the algebraic systems {(4.3.16),(4.3.17),(4.6.23),(4.6.25),(4.6.24),(4.6.26)} which represents the second-order method $A_3(\theta)$ with $\theta = \frac{1}{2}$, the implementation is different because of the appearance of the elements of $\mathbf{Y}^{n+1}$ in {(4.3.16),(4.6.23),(4.6.25)} and the elements of $\mathbf{X}^{n+1}$ in {(4.3.17),(4.6.24),(4.6.26)}; the vectors $\mathbf{X}^{n+1}$ and $\mathbf{Y}^{n+1}$ will be obtained simultaneously by solving a linear algebraic system of order $2M+2$ at each time step.

Let $\mathbf{U}^{n+1} = [(\mathbf{X}^{n+1})^T, (\mathbf{Y}^{n+1})^T]^T$ and $\mathbf{U}^n = [(\mathbf{X}^n)^T, (\mathbf{Y}^n)^T]^T$, where T denotes transpose, then it is seen that the system {(4.3.16),(4.3.17),(4.6.23),(4.6.25),(4.6.24), (4.6.26)} may be written in matrix-vector form as

$$\mathbf{W}^n\mathbf{U}^{n+1} = \mathbf{M}\,\mathbf{U}^n + \mathbf{b} \tag{4.6.27}$$

in which

$$\mathbf{W}^n = \begin{bmatrix} \mathbf{A}^n & \vdots & \mathbf{B}^n \\ \cdots & \cdots & \cdots \\ \mathbf{C}^n & \vdots & \mathbf{D}^n \end{bmatrix} \quad \text{and} \quad \mathbf{M} = \begin{bmatrix} \mathbf{E} & \vdots & \mathbf{0} \\ \cdots & \cdots & \cdots \\ \mathbf{0} & \vdots & \mathbf{F} \end{bmatrix}.$$

The vector $\mathbf{b}$ is a columm-vector of order $2M+2$ and is given by

$$\mathbf{b} = \left[\mathbf{q}_1^T, \mathbf{q}_2^T\right]^T$$

where $\mathbf{q}_1 = [\ell\mu N, \ldots, \ell\mu N]$ is a constant vector of order $M+1$ and $\mathbf{q}_2$ is a zero vector of order $M+1$. The matrices $\mathbf{W}^n$ and $\mathbf{M}$ are both of order $2M+2$ and their sub-matrices of order $M+1$ are given by

$$\mathbf{A}^n = \begin{bmatrix} A_0^n & -p & 0 & \cdots & 0 \\ -\frac{1}{2}p & A_1^n & -\frac{1}{2}p & & \vdots \\ 0 & \ddots & \ddots & \ddots & 0 \\ \vdots & & -\frac{1}{2}p & A_{M-1}^n & -\frac{1}{2}p \\ 0 & \cdots & 0 & -p & A_M^n \end{bmatrix}, \tag{4.6.28}$$

where $A_i^n = 1 + \frac{1}{2}\mu\ell + \frac{1}{2}\ell\beta Y_i^n + p$, $i = 0, 1, 2, \ldots, M$,

$$\mathbf{D}^n = \begin{bmatrix} D_0^n & -p & 0 & \cdots & 0 \\ -\frac{1}{2}p & D_1^n & -\frac{1}{2}p & & \vdots \\ 0 & \ddots & \ddots & \ddots & 0 \\ \vdots & & -\frac{1}{2}p & D_{M-1}^n & -\frac{1}{2}p \\ 0 & \cdots & 0 & -p & D_M^n \end{bmatrix}, \tag{4.6.29}$$

where $D_i^n = 1 + \frac{1}{2}(\mu+\nu)\ell - \frac{1}{2}\ell\beta X_i^n + p$, $i = 0, 1, 2, \ldots, M$,

$$\mathbf{E} = \begin{bmatrix} E & p & 0 & \cdots & 0 \\ \frac{1}{2}p & E & \frac{1}{2}p & & \vdots \\ \vdots & \ddots & \ddots & \ddots & 0 \\ 0 & & \frac{1}{2}p & E & \frac{1}{2}p \\ 0 & \cdots & 0 & p & E \end{bmatrix}, \tag{4.6.30}$$

where $E = 1 + \frac{1}{2}\mu\ell - p$,

$$\mathbf{F} = \begin{bmatrix} F & p & 0 & \cdots & 0 \\ \frac{1}{2}p & F & \frac{1}{2}p & & \vdots \\ 0 & \ddots & \ddots & \ddots & 0 \\ \vdots & & \frac{1}{2}p & F & \frac{1}{2}p \\ 0 & \cdots & 0 & p & F \end{bmatrix}, \tag{4.6.31}$$

where $F = 1 - \frac{1}{2}(\mu+\nu)\ell - p$,

$$\mathbf{B}^n = diag\{\frac{1}{2}\ell\beta X_i^n\},\ i = 0, 1, 2, \ldots, M \tag{4.6.32}$$

and

$$\mathbf{C}^n = diag\{-\frac{1}{2}\ell\beta Y_i^n\},\ i = 0, 1, 2, \ldots, M. \tag{4.6.33}$$

Further research reveals that it is possible to compute $\mathbf{X}^{n+1}$ and $\mathbf{Y}^{n+1}$ in parallel on an architecture with two processor; that is made possible because $\mathbf{B}^n$ and $\mathbf{C}^n$ are diagonal matrices so that it is easy to find the inverse matrices of $\mathbf{B}^n$ and $\mathbf{C}^n$, so equation (4.6.27) may be split to give

$$\mathbf{A}^n\mathbf{X}^{n+1} + \mathbf{B}^n\mathbf{Y}^{n+1} = \mathbf{E}\,\mathbf{X}^n + \mathbf{q}_1, \tag{4.6.34}$$

$$\mathbf{C}^n\mathbf{X}^{n+1} + \mathbf{D}^n\mathbf{Y}^{n+1} = \mathbf{F}\,\mathbf{Y}^n \tag{4.6.35}$$

which can be solved simultaneously for $\mathbf{X}^{n+1}$ and $\mathbf{Y}^{n+1}$ using the following parallel algorithm:

Processor 1 : Solve

$$(\mathbf{D}^n(\mathbf{B}^n)^{-1}\mathbf{A}^n - \mathbf{C}^n)\mathbf{X}^{n+1} = \mathbf{D}^n(\mathbf{B}^n)^{-1}\mathbf{E}\,\mathbf{X}^n - \mathbf{F}\,\mathbf{Y}^n + \mathbf{D}^n(\mathbf{B}^n)^{-1}\,\mathbf{q}_1$$

for $\mathbf{X}^{n+1}$ (4.6.36)

Processor 2 : Solve

$$(\mathbf{A}^n(\mathbf{C}^n)^{-1}\mathbf{D}^n - \mathbf{B}^n)\mathbf{Y}^{n+1} = -\mathbf{E}\,\mathbf{X}^n + \mathbf{A}^n(\mathbf{C}^n)^{-1}\mathbf{F}\,\mathbf{Y}^n - \mathbf{q}_1$$

for $\mathbf{Y}^{n+1}$ (4.6.37)

Equations (4.6.36) and (4.6.37) again can be solved using parallel computation, each processor solving a linear algebraic system of order $N+1$ at each time step.

4.7 Numerical experiments

To test the behaviour of the three methods, the solution of (4.1.1)-(4.1.4) was computed for susceptible and infectious individuals, respectively. Throughout the numerical experiments, the set of parameters given in (2.8.1) for μ and ν with $N = 25\times10^6$ and the infection rate, β, chosen to be $\beta = 5\times10^{-5}$. In the following numerical experiments, Experiments A and B, two sets of initial conditions are distributed over the interval $0 \le z \le 1$ given the functions $S(z,0)$ and $I(z,0)$.

Experiment A

In this experiment, the space step was given the value $h = 0.025$ so that $M = 39$. Hat-shaped initial distributions are used for S and I and are given by

$$S(z_i,0) = \begin{cases} 81250i & , 0 \le i \le \dfrac{M+1}{2} \\ 81250(M+1-i) & , \dfrac{M+1}{2} \le i \le M+1, \end{cases}$$

$$I(z_i,0) = \begin{cases} 187.5i & , 0 \le i \le \dfrac{M+1}{2} \\ 187.5(N+1-i) & , \dfrac{M+1}{2} \le i \le M+1. \end{cases}$$

In this case, the maximum value of each class of individuals is concentrated at the middle of the interval $0 \le z \le 1$ and the numbers decrease linearly to zero at the boundaries $z = 0$ and $z = 1$, see Figures 4.1.

For this experiment, numerical simulations were carried out to see the behaviour of the three suggested methods, $A_1(\theta)$, $A_2(\theta)$ with $\theta = 0,\ \frac{1}{2},\ 1$ and $A_3(\theta)$ with $\theta = \frac{1}{2}$, for the different values of the diffusion rate, α. The stability intervals of the numerical methods are obtained for $\alpha = 0.001,\ 0.01,\ 0.04$ and are summarized in Table 4.1. In the case of method $A_1(\theta)$ with $\theta = 0$, negative values of susceptible individuals, S, and infectious individuals, I, occurred for $\ell > 0.0334$ with $\alpha = 0.001$ while contrived oscillations were exhibited in the numerical solution as ℓ was increased beyond the value 0.0245 with $\alpha = 0.01$ and the value 0.0065 with $\alpha = 0.04$. The method produced overflow for $\ell > 0.0467$ with $\alpha = 0.001$, for $\ell > 0.0257$ with $\alpha = 0.01$ and for $\ell > 0.0077$ with $\alpha = 0.04$. Using $\theta = \frac{1}{2}$ and $\theta = 1$ negative values of susceptible and infectious individuals began as ℓ was increased above the values in the stability interval (see Table 4.1) with overflow occurring as ℓ was increased further.

Using Method $A_2(\theta)$ with $\theta = 0$ negative values did not arise in the numerical solution. It is seen that the method gave the qualitatively correct behaviour for $\ell < 0.3250$ with $\alpha = 0.001$, for $\ell < 0.0319$ with $\alpha = 0.01$ and for $\ell < 0.0076$ with $\alpha = 0.04$ after which oscillations and overflow occurred as ℓ was increased further. Using $\theta = \frac{1}{2}$ with $\alpha = 0.001$ the method never produced overflow and always converge

α	θ	Interval of Stability		
		Method $A_1(\theta)$	Method $A_2(\theta)$	Method $A_3(\theta)$
0.001	0	(0, 0.0334)	(0, 0.3245)	(0, 0.0358)
	$\frac{1}{2}$	(0, 0.0334)	(0, ∞)	
	1	(0, 0.0280)	(0, ∞)	
0.01	0	(0, 0.0245)	(0, 0.0319)	(0, 0.0387)
	$\frac{1}{2}$	(0, 0.0326)	(0, 7.5)	
	1	(0, 0.0317)	(0, ∞)	
0.04	0	(0, 0.0065)	(0, 0.0076)	(0, 0.0420)
	$\frac{1}{2}$	(0, 0.0339)	(0, 2.8)	
	1	(0, 0.0445)	(0, ∞)	

Table 4.1: Stability intervals of the methods

to the correct steady-state for all $\ell > 0$. For $\alpha = 0.01$ and $\alpha = 0.04$ the method did not produce overflow but negative values of infectious occurred before approaching to the correct behaviour as ℓ was increased beyond the value 7.5 with $\alpha = 0.01$ and the value 2.8 with $\alpha = 0.04$. Using $\theta = 1$ with $\alpha = 0.001$, $\alpha = 0.01$ and $\alpha = 0.04$, the qualitatively correct behaviour was observed for an arbitrarily large time step ℓ.

Using Method $A_3(\theta)$ with $\theta = \frac{1}{2}$ contrived oscillations did not arise in the numerical solution but negative values of susceptible and infectious individuals were observed as ℓ was increased above the value 0.0358 with $\alpha = 0.001$, the value 0.0387 with $\alpha = 0.01$ and the value 0.0420 with $\alpha = 0.04$ with overflow occurring for $\ell = 0.0579$ ($\alpha = 0.001$), for $\ell = 0.0895$ ($\alpha = 0.01$) and for $\ell > 0.2507$ ($\alpha = 0.04$), respectively.

The method $A_3(\theta)$ ($\theta = \frac{1}{2}$) was chosen to compute further numerical results. The space and time steps were given the value $h = 0.025$, $\ell = 0.001$ and the diffusive rate was given the values $\alpha = 0.005$, 0.01, 0.03, 0.04, 0.06, 0.09. The numerical results are depicted in Figures 4.2-4.7. These show that the dynamic behaviour of whooping cough changes as α is increased. It is found that the number of susceptibles are less than the number of infectious individuals near the middle of the interval for $\alpha = 0.005$, $\alpha = 0.01$ and $\alpha = 0.03$ (Figures 4.2-4.4). As α is increased, the number of susceptibles becomes larger than the number of infectious individuals and the number

of infectious individuals spreads on the z-axis, see Figures 4.5-4.7. Figure 4.8 (a) and (b) give the three-dimensional plots of susceptible and infectious individuals for $0 \leq z \leq 1$.

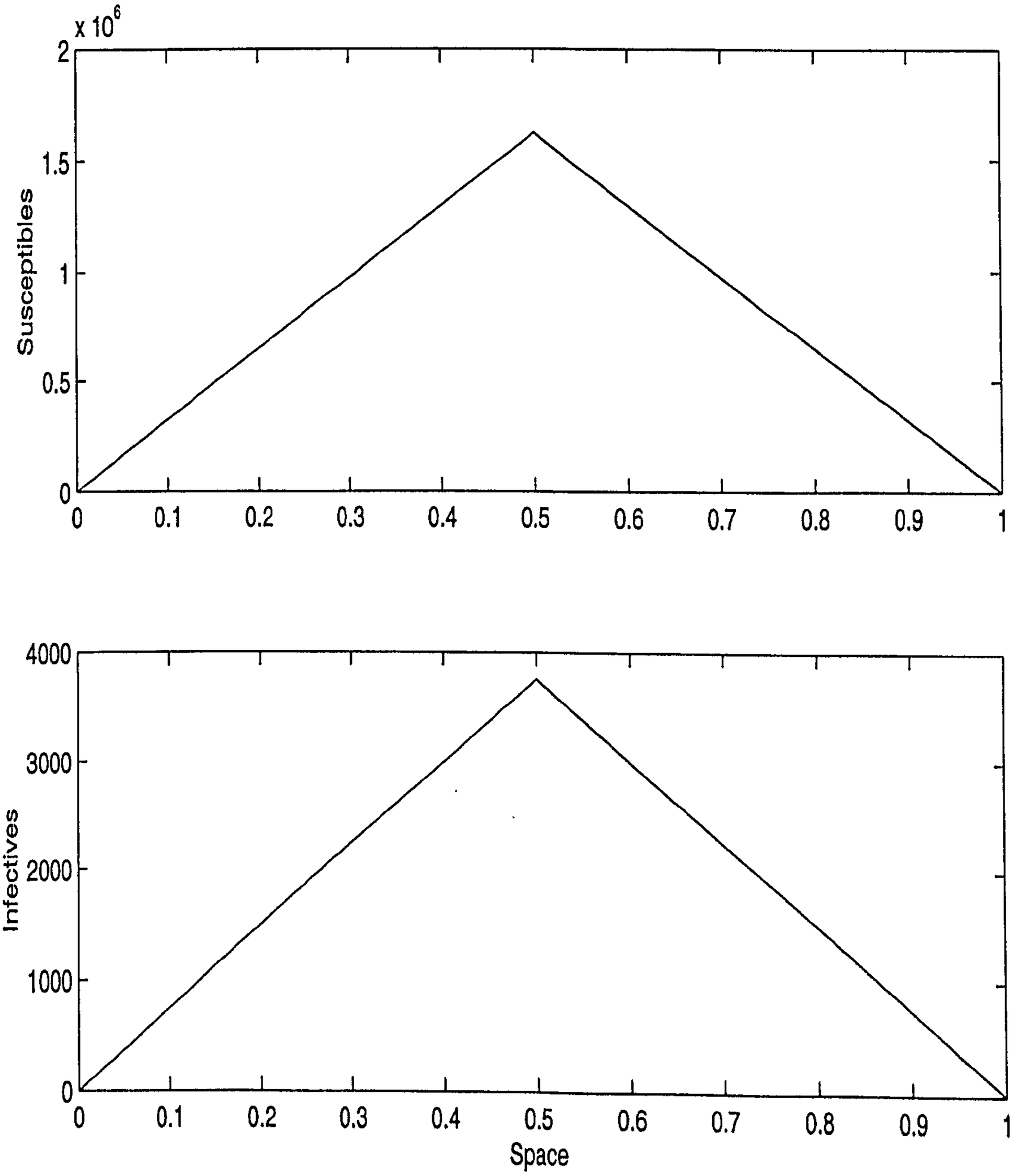

Figure 4.1: Experiment A, initial distributions of susceptibles and infectives.

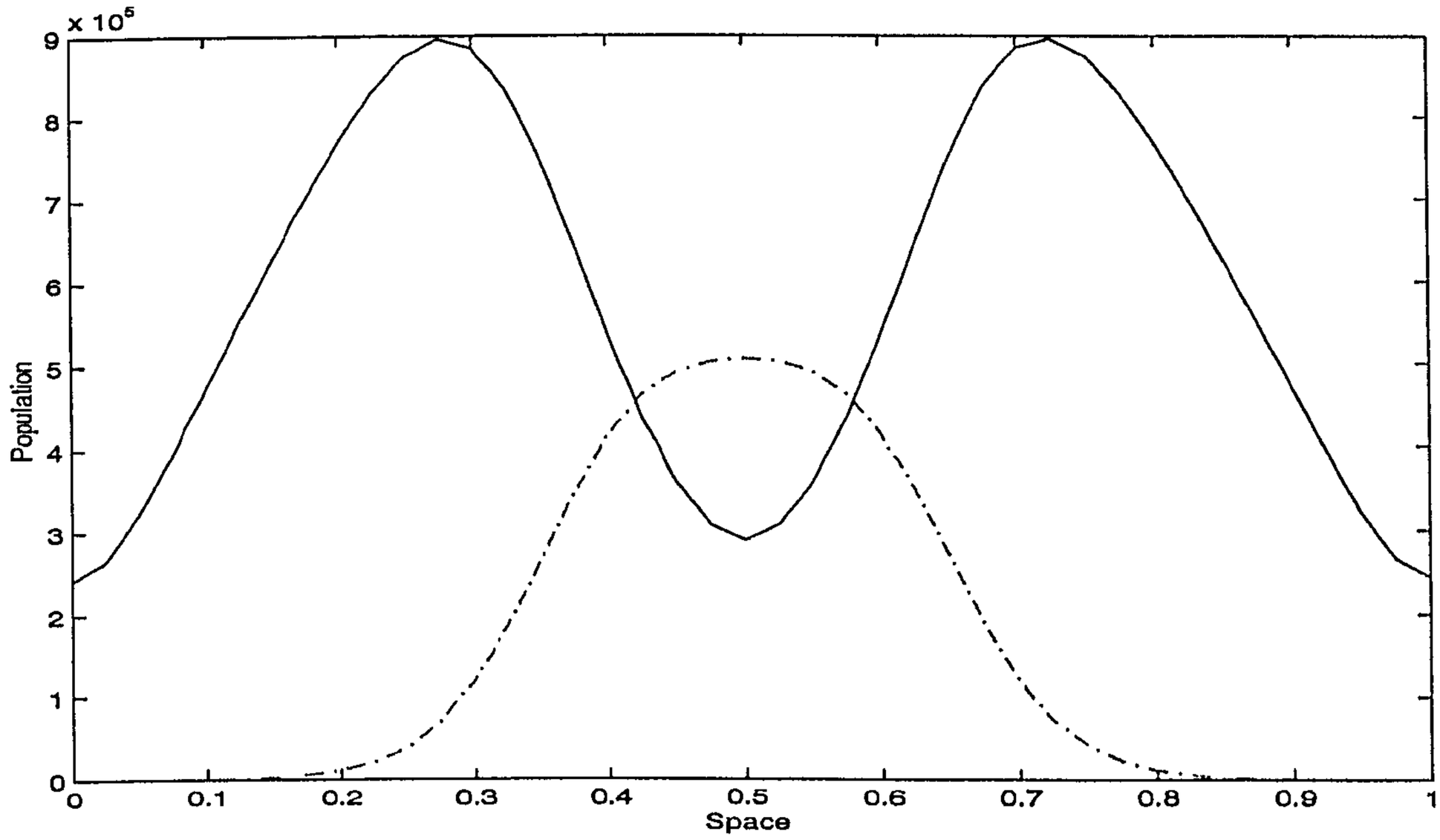

Figure 4.2: Experiment A, dynamics of whooping cough using $A_3(\theta = \frac{1}{2})$ at time $t = 0.15$, $\alpha = 0.005$, $\ell = 0.001$ and $h = 0.025$; susceptibles $(-)$ and infectives $(\cdot - \cdot)$.

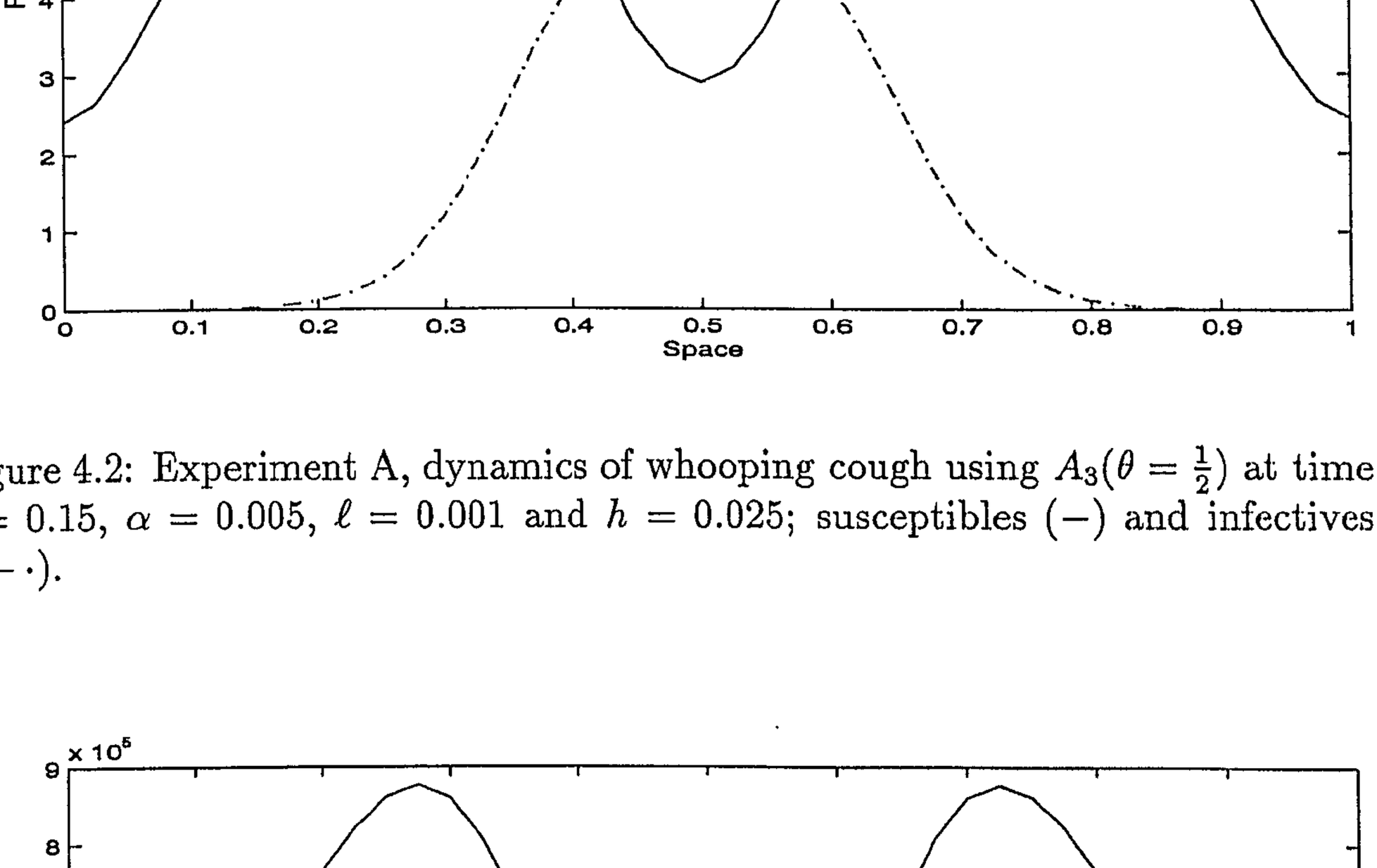

Figure 4.3: Experiment A, dynamics of whooping cough using $A_3(\theta = \frac{1}{2})$ at time $t = 0.15$, $\alpha = 0.01$, $\ell = 0.001$ and $h = 0.025$; susceptibles $(-)$ and infectives $(\cdot - \cdot)$.

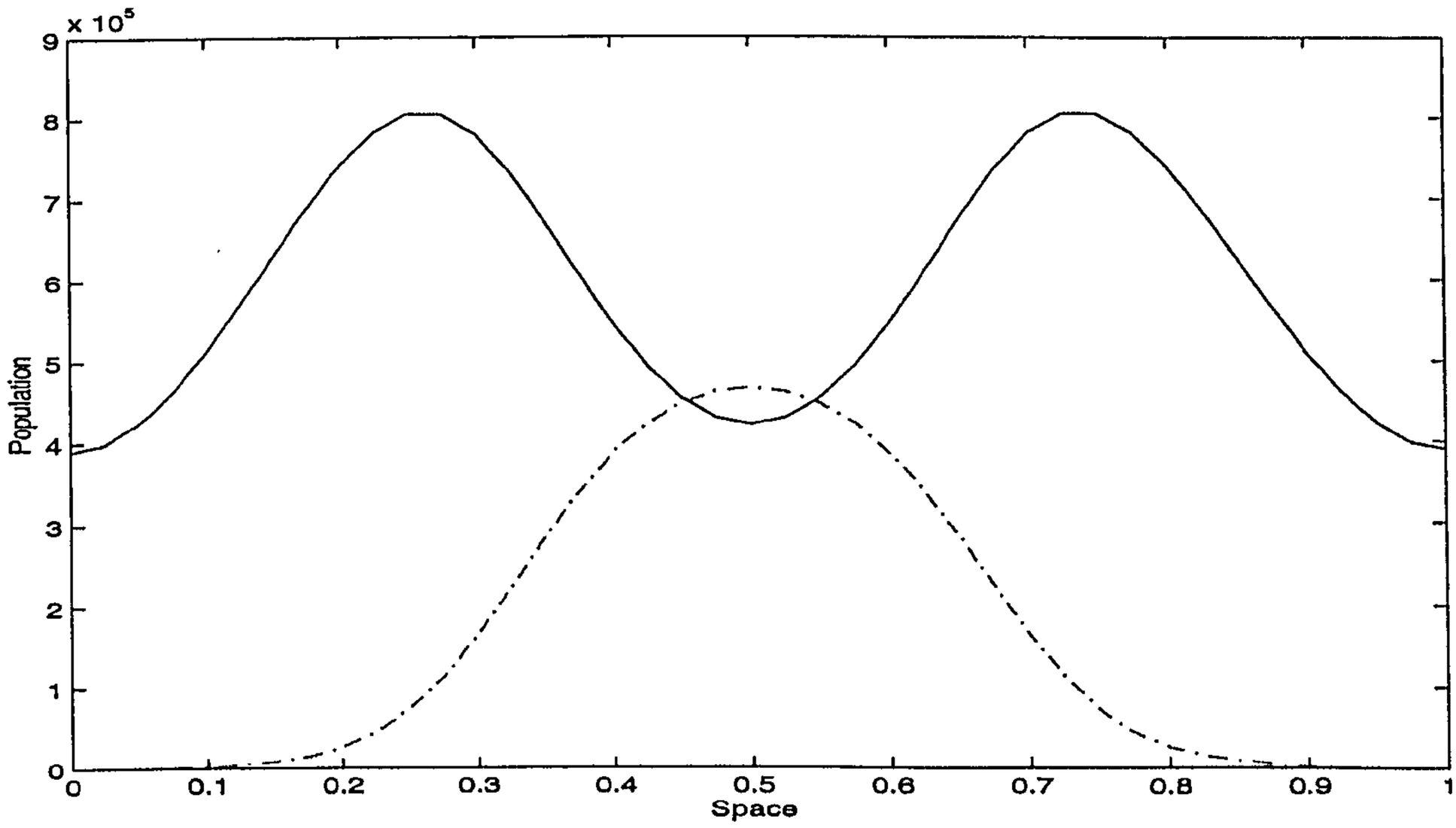

Figure 4.4: Experiment A, dynamics of whooping cough using $A_3(\theta = \frac{1}{2})$ at time $t = 0.15$, $\alpha = 0.03$, $\ell = 0.001$ and $h = 0.025$; susceptibles $(-)$ and infectives $(\cdot - \cdot)$.

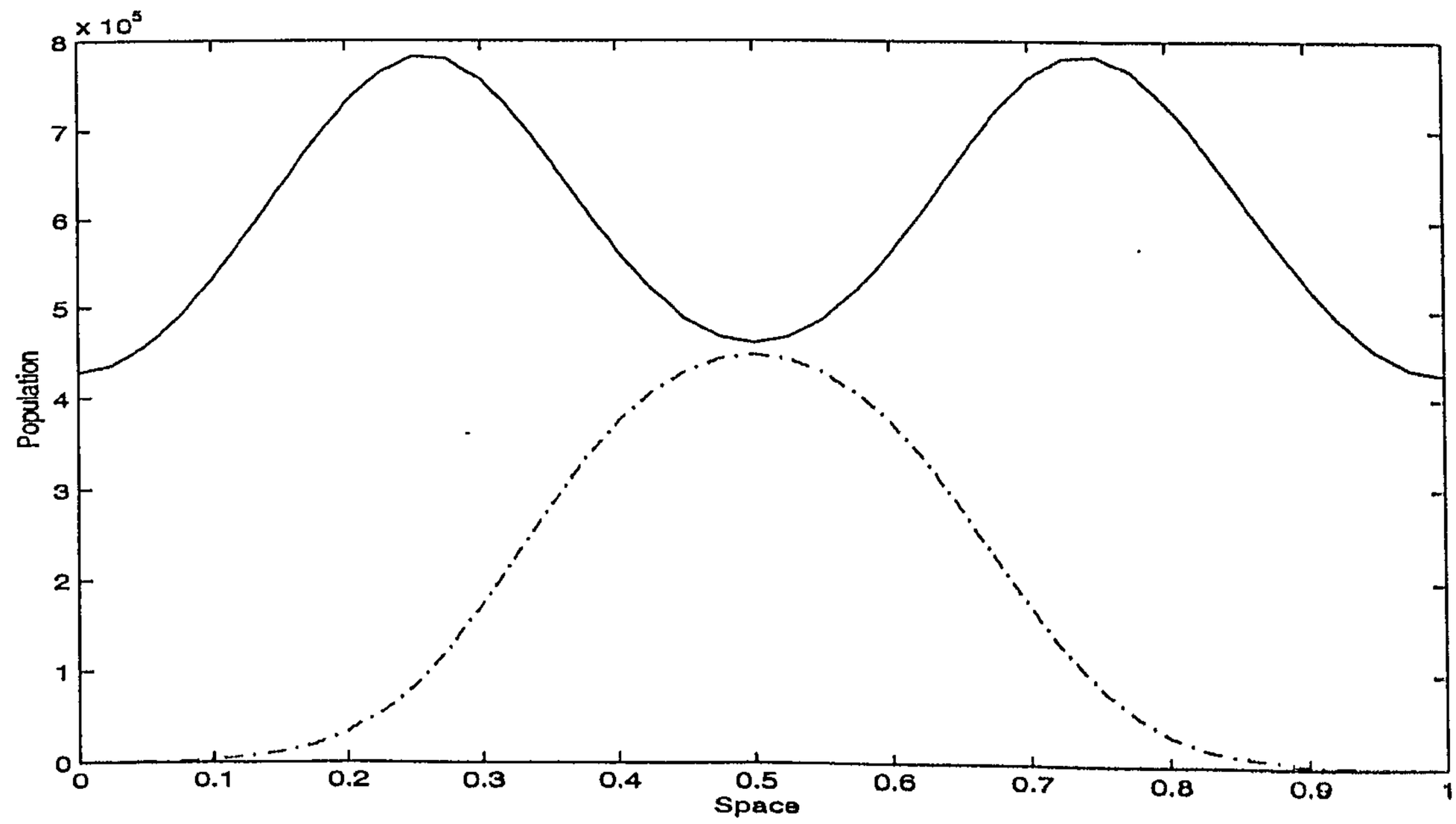

Figure 4.5: Experiment A, dynamics of whooping cough using $A_3(\theta = \frac{1}{2})$ at time $t = 0.15$, $\alpha = 0.04$, $\ell = 0.001$ and $h = 0.025$; susceptibles $(-)$ and infectives $(\cdot - \cdot)$.

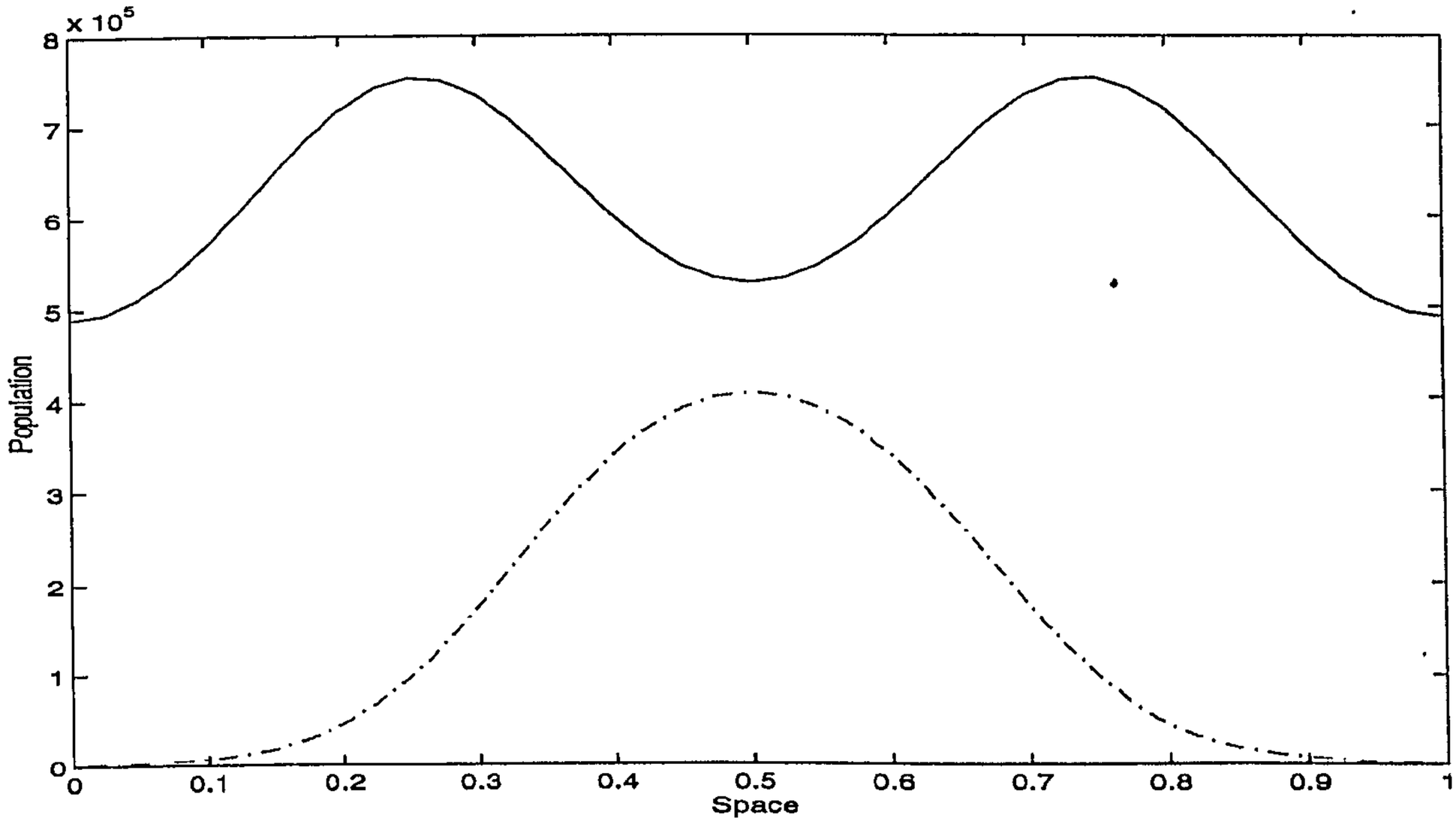

Figure 4.6: Experiment A, dynamics of whooping cough using $A_3(\theta = \frac{1}{2})$ at time $t = 0.15$, $\alpha = 0.06$, $\ell = 0.001$ and $h = 0.025$; susceptibles $(-)$ and infectives $(\cdot - \cdot)$.

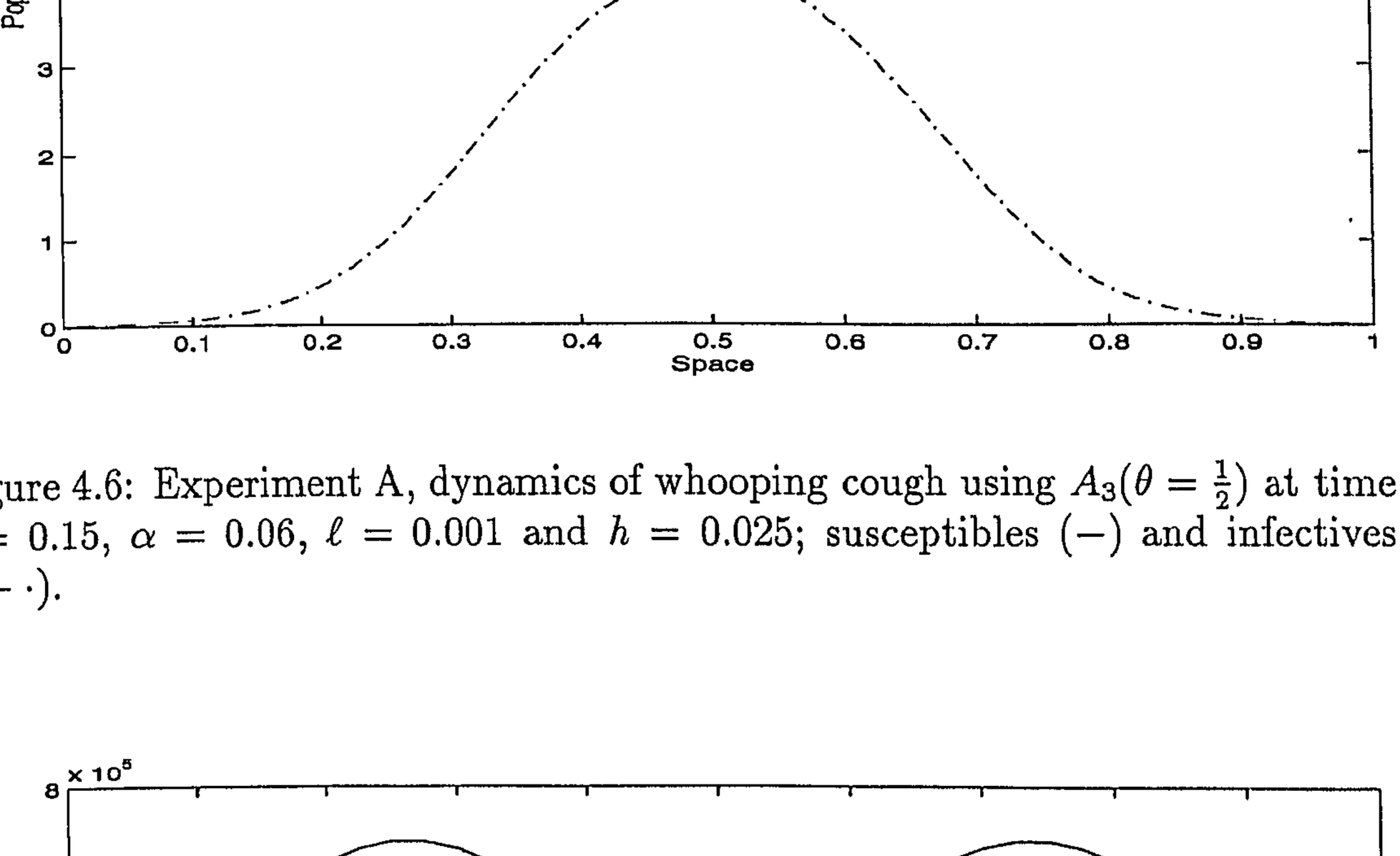

Figure 4.7: Experiment A, dynamics of whooping cough using $A_3(\theta = \frac{1}{2})$ at time $t = 0.15$, $\alpha = 0.09$, $\ell = 0.001$ and $h = 0.025$; susceptibles $(-)$ and infectives $(\cdot - \cdot)$.

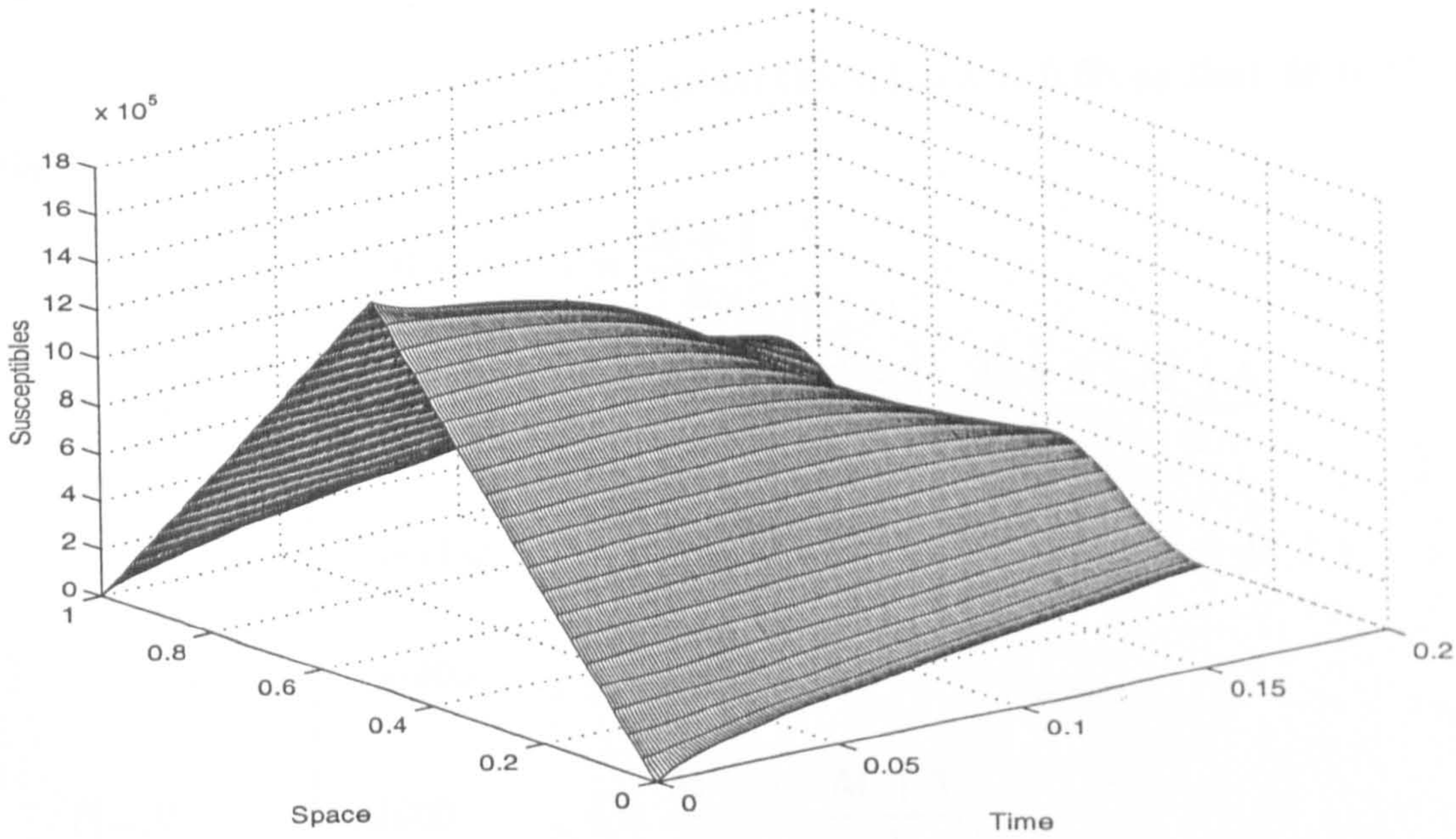

(a)

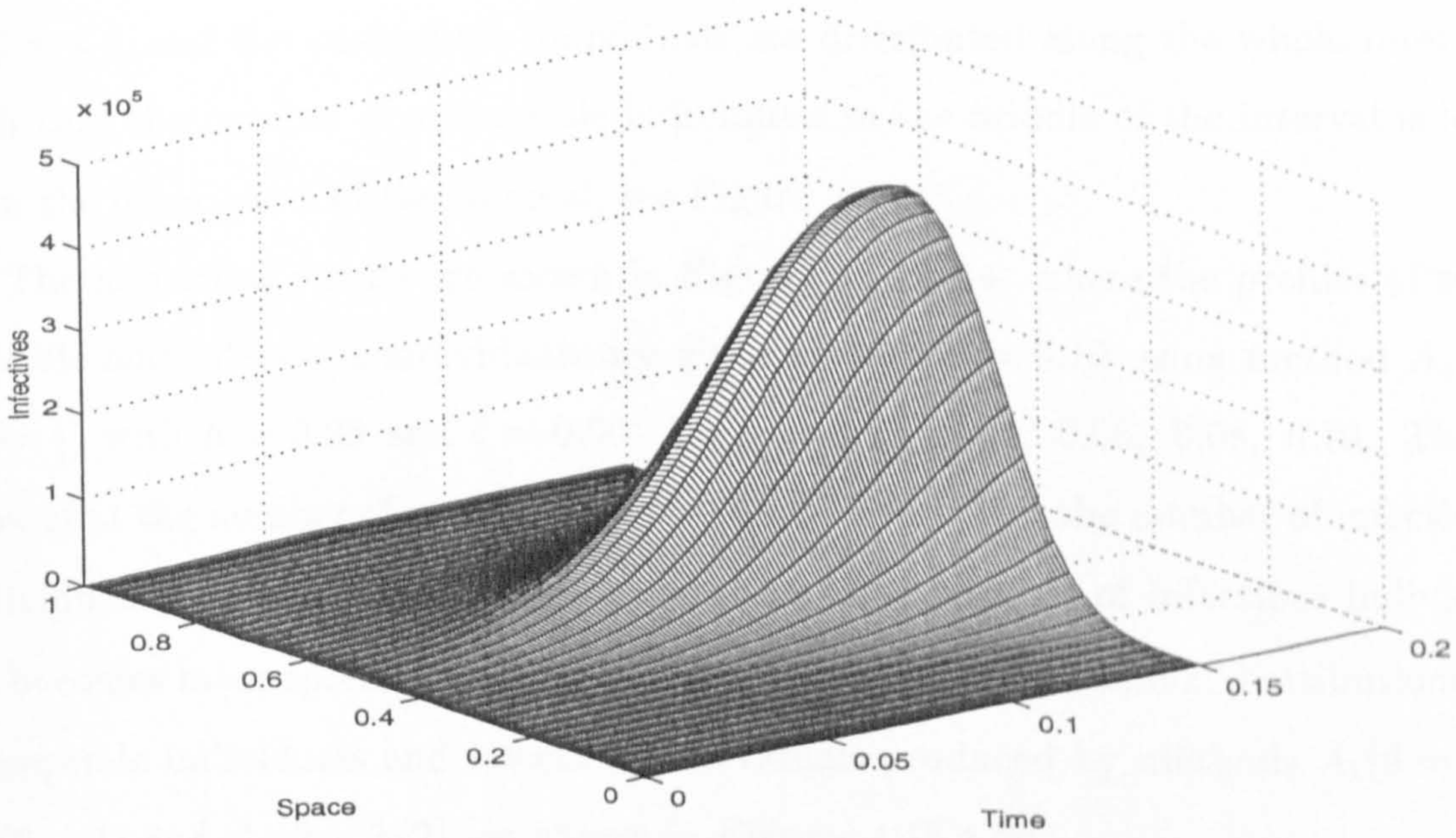

(b)

Figure 4.8: Experiment A, three-dimensional distribution of susceptibles and infectives for $\alpha = 0.001$ using $A_2(\theta = 1)$ with $h = 0.025$ and $\ell = 0.015$: (a) profiles for susceptibles and (b) profiles for infectives.

Experiment B

In this experiment, the space step was given the value $h = 0.05$ so that $M = 19$, the initial conditions are of the form

$$S(z_i,0) = \begin{cases} 1390480 & , i = \dfrac{M+1}{2} \\ 1590480 & , i = \dfrac{M-3}{2}, \dfrac{M-1}{2}, \dfrac{M+3}{2}, \dfrac{M+5}{2} \\ 1690480 & , 0 \le i \le \dfrac{M-5}{2} \quad \& \quad \dfrac{M+5}{2} \le i \le M+1 \end{cases}$$

$$I(z_i,0) = \begin{cases} 108000 & , i = \dfrac{M+1}{2} \\ 23000 & , i = \dfrac{M-1}{2}, \dfrac{M+3}{2} \\ 0 & , 0 \le i \le \dfrac{M-1}{2} \quad \& \quad \dfrac{M+3}{2} \le i \le M+1. \end{cases}$$

where the infectious individuals are concentrated in the middle of the interval $0 \le z \le 1$ and the susceptible individuals are distributed along the whole interval such that the number of susceptible individuals in the middle of the interval is less than the other parts of the interval, see Figure 4.9.

The numerical results are shown in Figures 4.10-4.14, where the profiles of susceptible and infectious individuals are given at time $t = 0.10$ using method $A_3(\theta)$ $(\theta = \frac{1}{2})$ with $h = 0.05$ and $\ell = 0.001$ for $\alpha = 0.01,\ 0.04,\ 0.06,\ 0.08,\ 0.10$. These show that the number of susceptible individuals is less than the number of infectious individuals near the middle of the interval and the number of infectious individuals becomes more spread-out as α increases. The three-dimensional distributions of susceptible individuals and infectious individuals produced by methods $A_1(\theta = 1)$, $A_2(\theta = 1)$ and $A_3(\theta = 1/2)$ are shown in Figures 4.15-4.20.

From experiments A and B, it can be seen that the dynamics of whooping cough depends on the initial distribution and the diffusion rate.

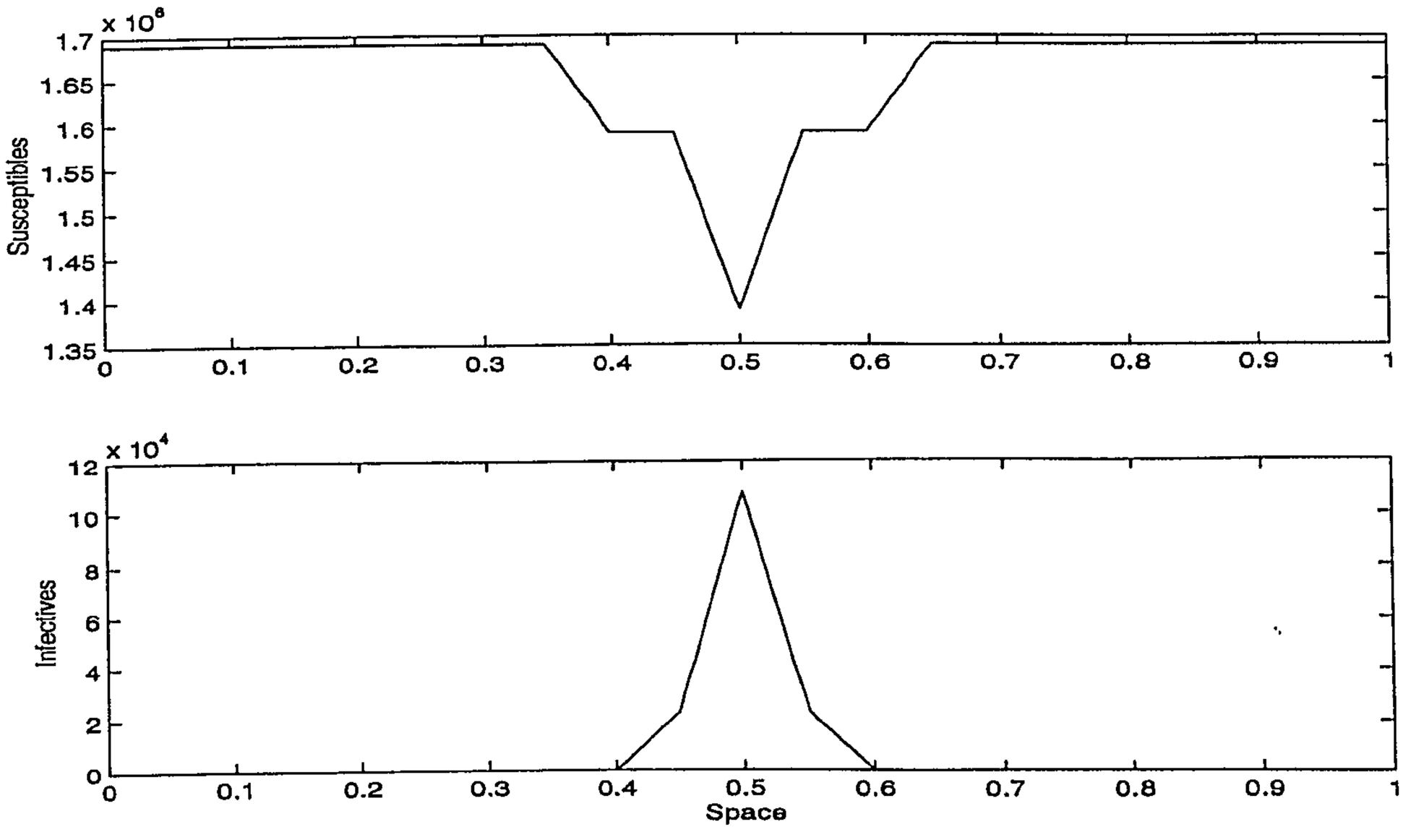

Figure 4.9: Experiment B, initial distributions of susceptibles and infectives.

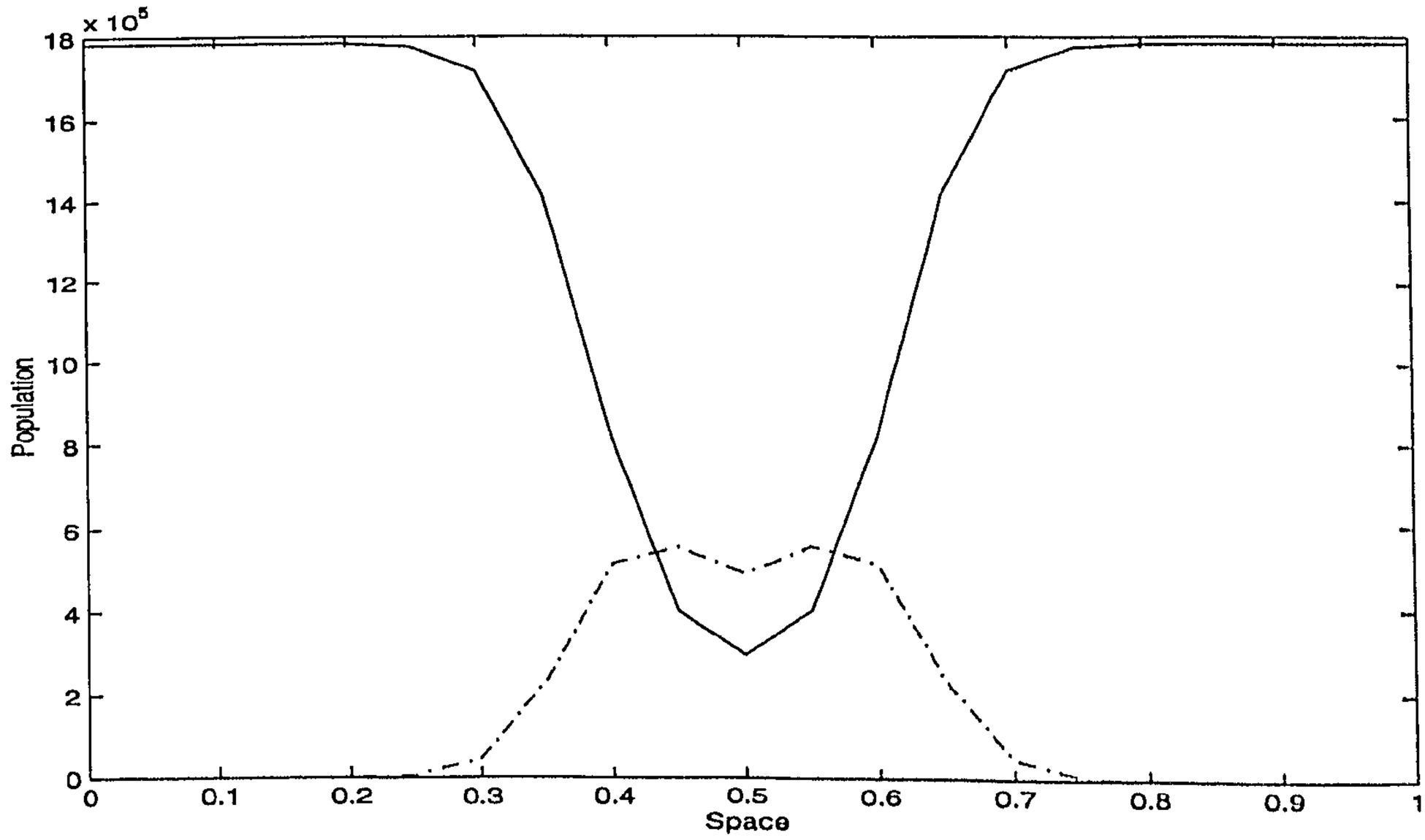

Figure 4.10: Experiment B, dynamics of whooping cough using $A_3(\theta = \frac{1}{2})$ at time $t = 0.1$, $\alpha = 0.01$, $\ell = 0.001$ and $h = 0.05$; susceptibles $(-)$ and infectives $(\cdot - \cdot)$.

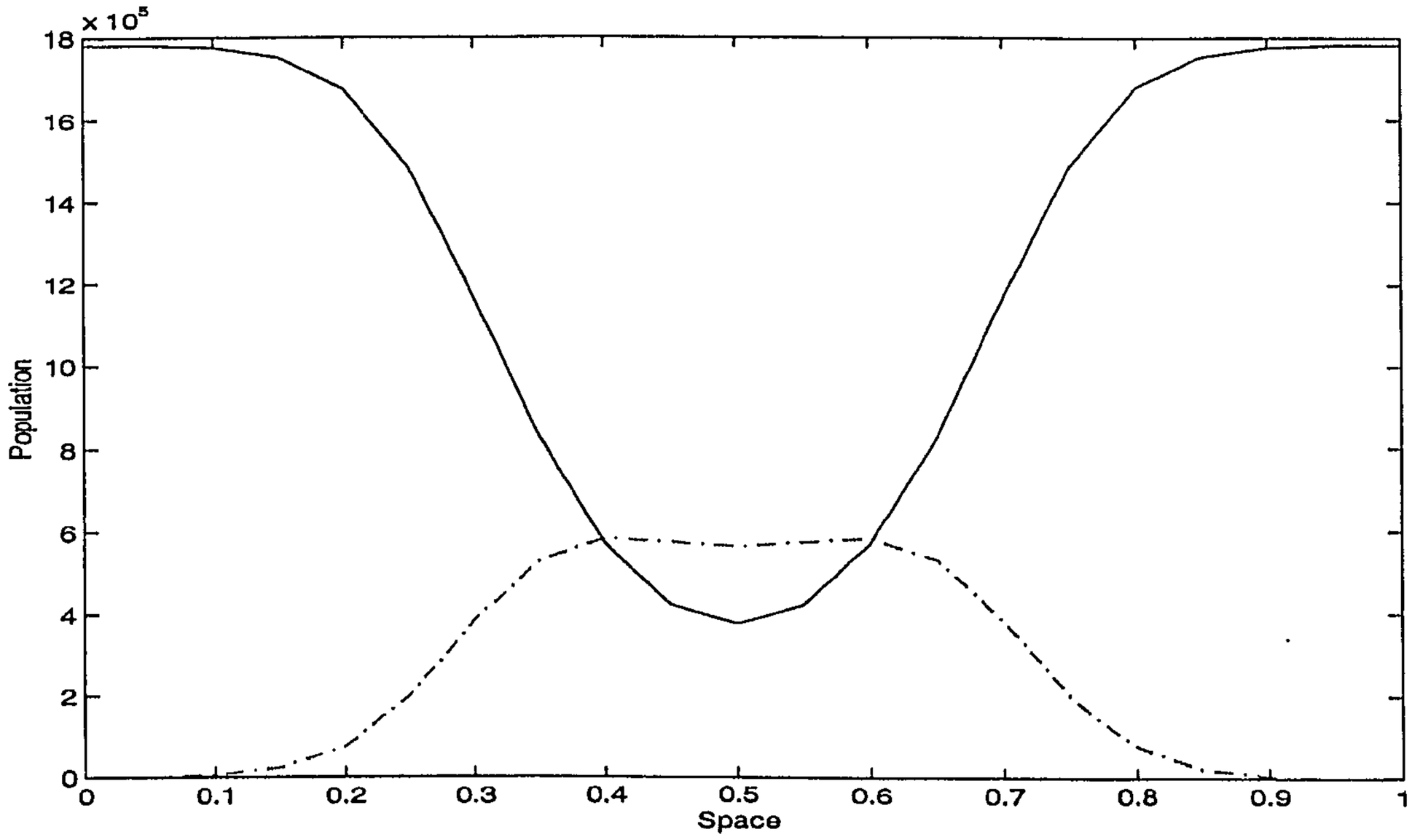

Figure 4.11: Experiment B, dynamics of whooping cough using $A_3(\theta = \frac{1}{2})$ at time $t = 0.1$, $\alpha = 0.04$, $\ell = 0.001$ and $h = 0.05$; susceptibles $(-)$ and infectives $(\cdot - \cdot)$.

Figure 4.12: Experiment B, dynamics of whooping cough using $A_3(\theta = \frac{1}{2})$ at time $t = 0.1$, $\alpha = 0.06$, $\ell = 0.001$ and $h = 0.05$; susceptibles $(-)$ and infectives $(\cdot - \cdot)$.

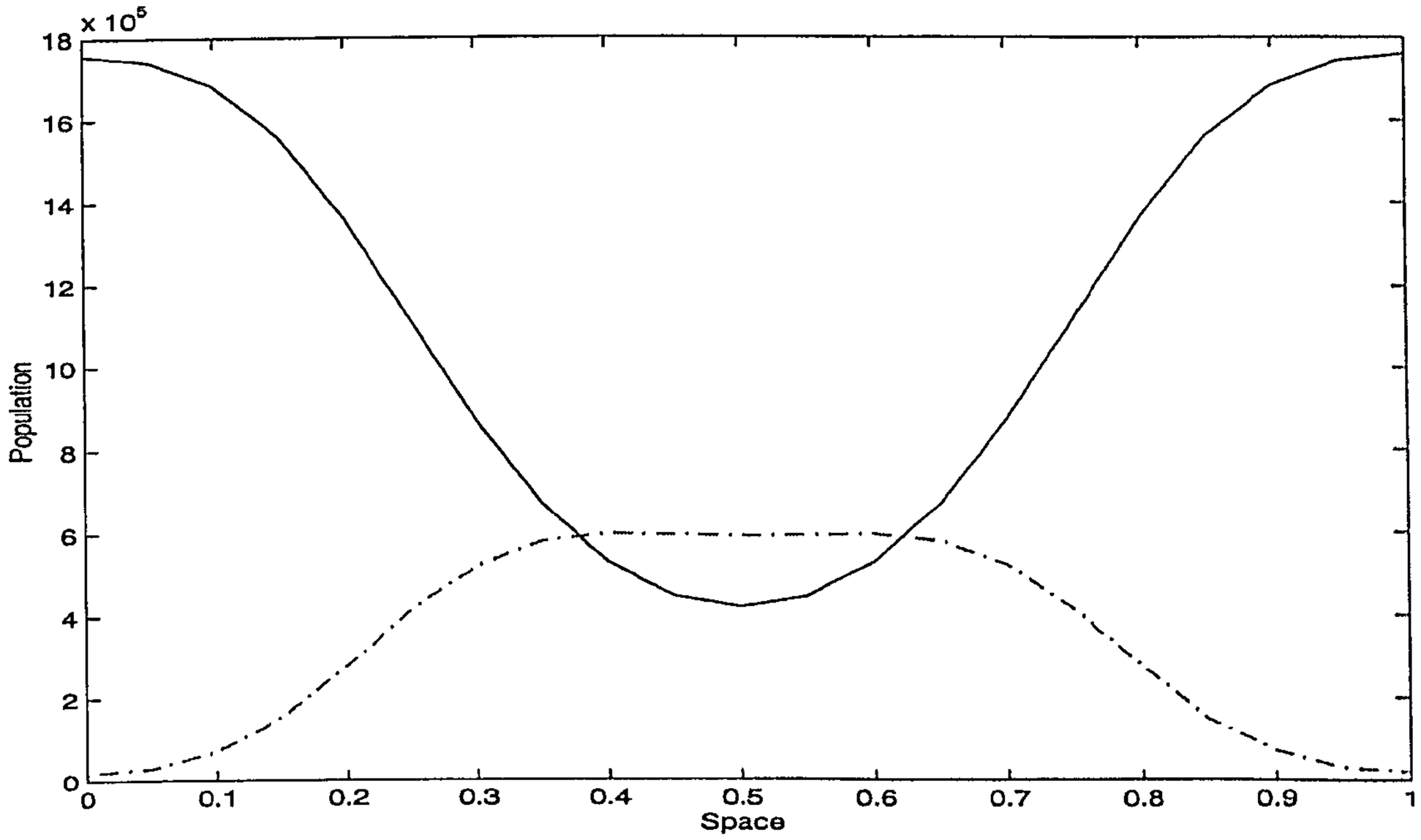

Figure 4.13: Experiment B, dynamics of whooping cough using $A_3(\theta = \frac{1}{2})$ at time $t = 0.1$, $\alpha = 0.08$, $\ell = 0.001$ and $h = 0.05$; susceptibles $(-)$ and infectives $(\cdot - \cdot)$.

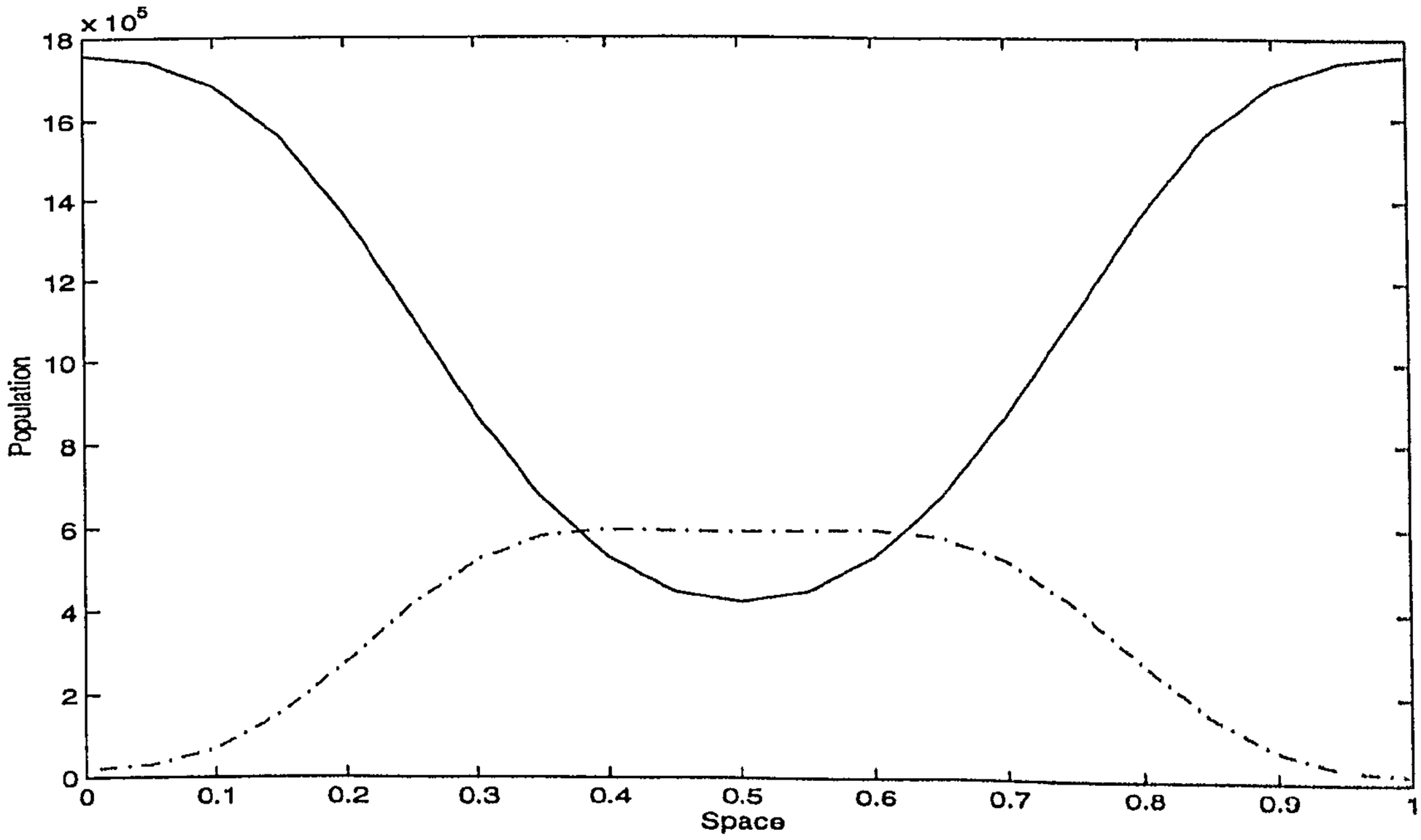

Figure 4.14: Experiment B, dynamics of whooping cough using $A_3(\theta = \frac{1}{2})$ at time $t = 0.1$, $\alpha = 0.10$, $\ell = 0.001$ and $h = 0.05$; susceptibles $(-)$ and infectives $(\cdot - \cdot)$.

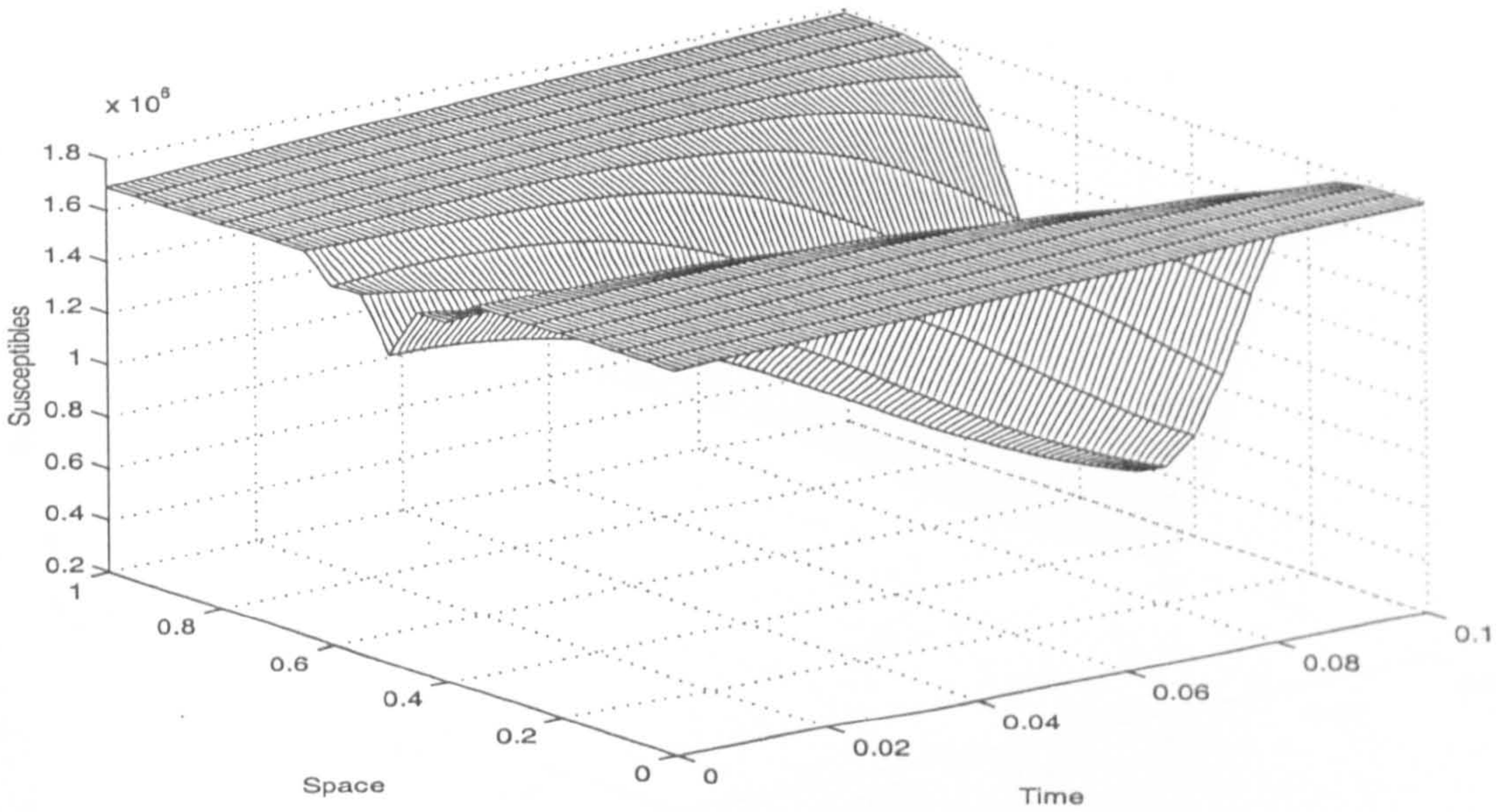

Figure 4.15: Experiment B, three-dimensional distribution of susceptibles using $A_1(\theta = 1)$; $\alpha = 0.04$, $\ell = 0.001$ and $h = 0.025$.

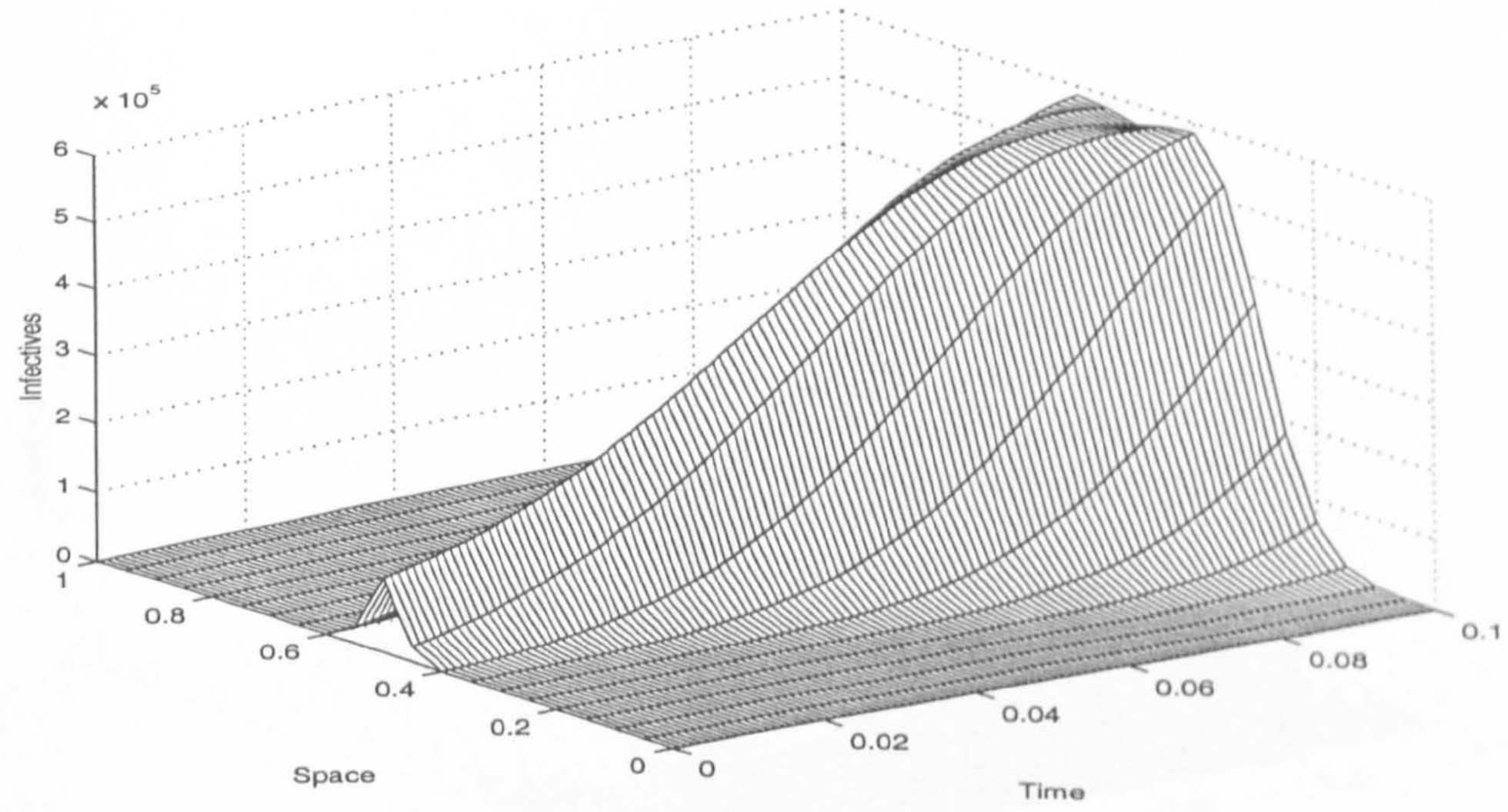

Figure 4.16: Experiment B, three-dimensional distribution of infectives using $A_1(\theta = 1)$; $\alpha = 0.04$, $\ell = 0.001$ and $h = 0.025$.

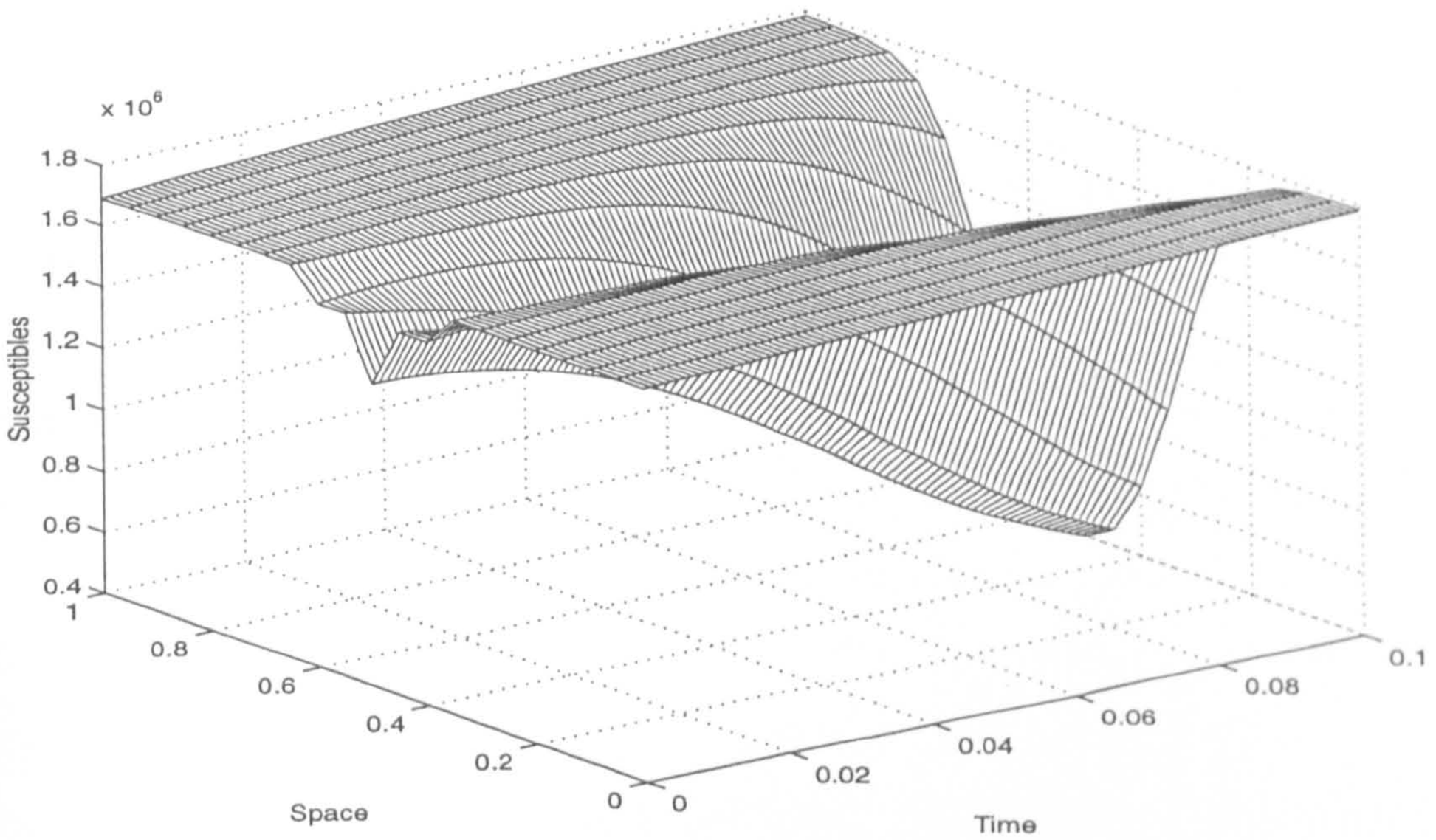

Figure 4.17: Experiment B, three-dimensional distribution of susceptibles using $A_2(\theta = 1)$; $\alpha = 0.04$, $\ell = 0.001$ and $h = 0.025$.

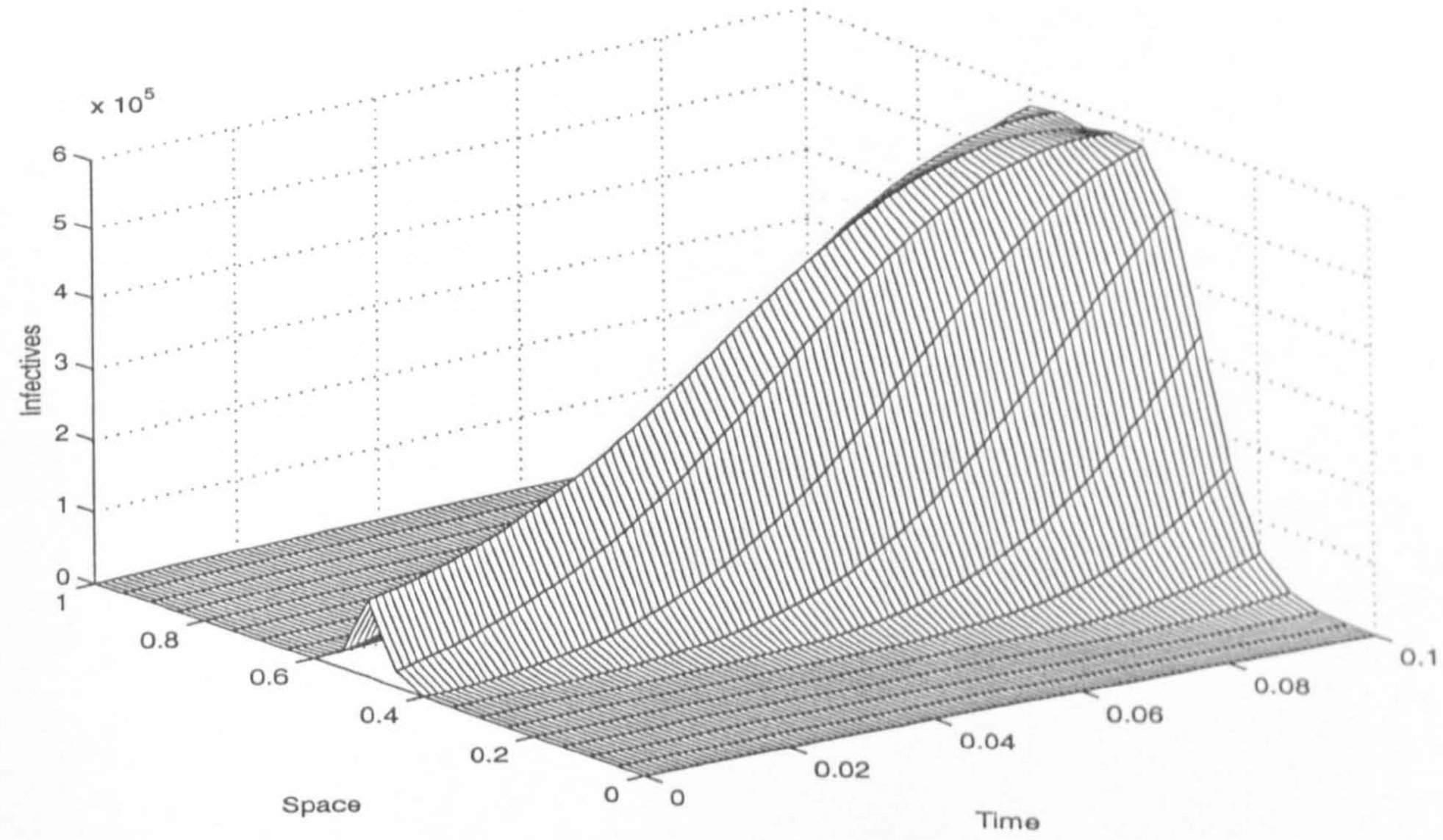

Figure 4.18: Experiment B, three-dimensional distribution of infectives using $A_2(\theta = 1)$; $\alpha = 0.04$, $\ell = 0.001$ and $h = 0.025$.

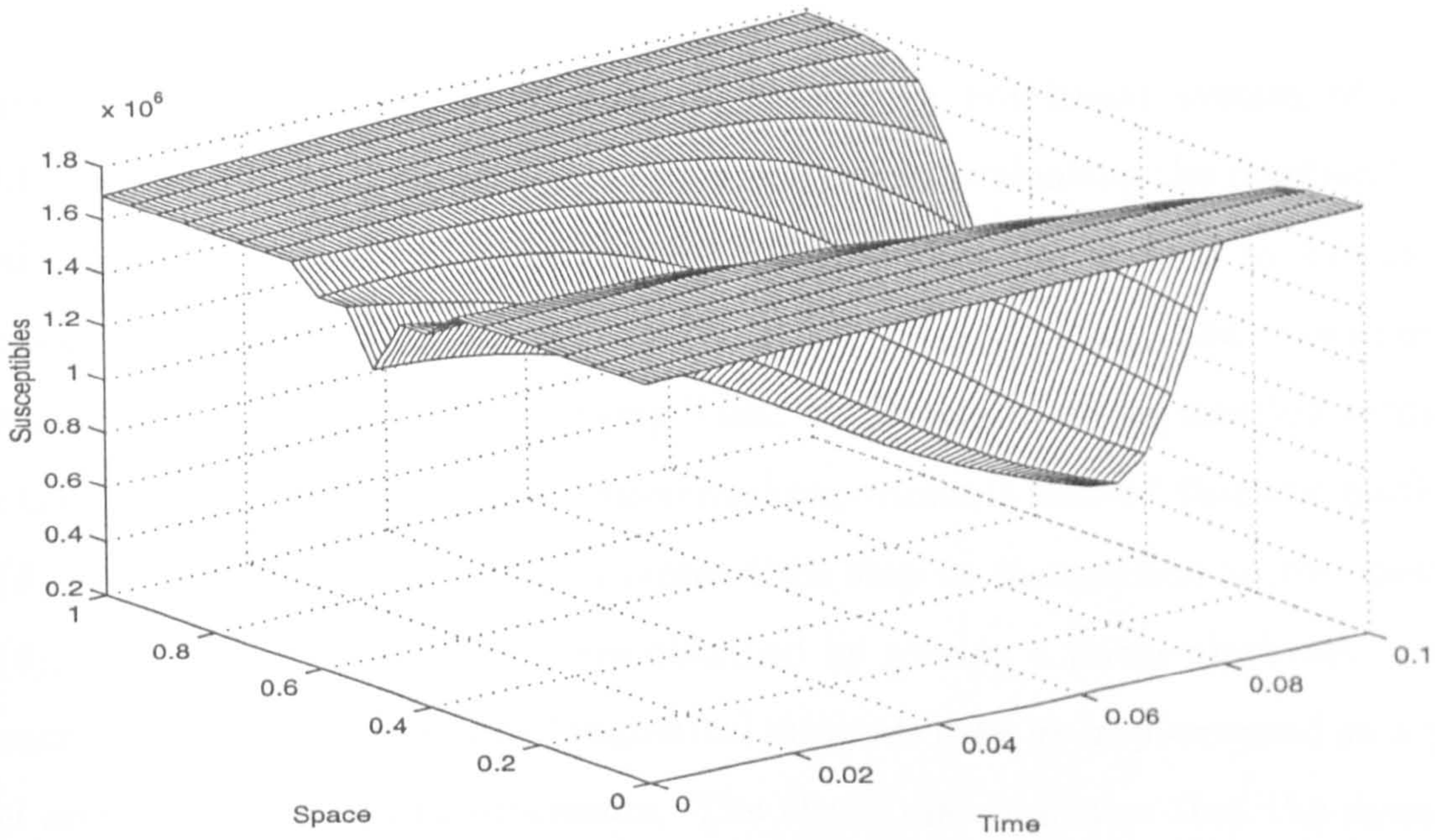

Figure 4.19: Experiment B, three-dimensional distribution of susceptibles using $A_3(\theta = \frac{1}{2})$; $\alpha = 0.04$, $\ell = 0.001$ and $h = 0.025$.

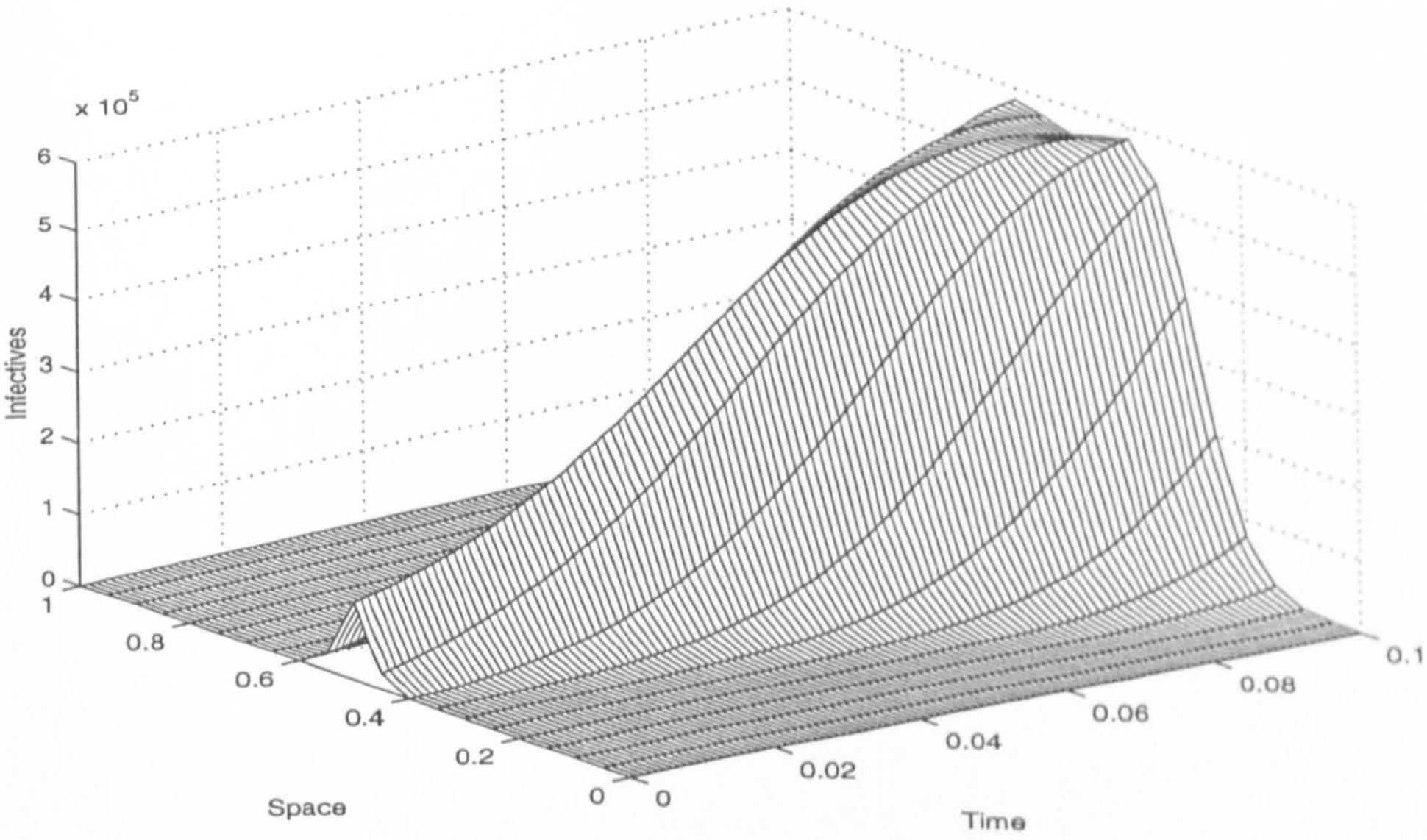

Figure 4.20: Experiment B, three-dimensional distribution of infectives using $A_3(\theta = \frac{1}{2})$; $\alpha = 0.04$, $\ell = 0.001$ and $h = 0.025$.

4.8 Conclusion

Three numerical methods have been use to solve a non-linear system of PDEs {(4.1.1)-(4.1.4)}. The first method $A_1(\theta)$ is derived by evaluating the reaction terms at the time level $t = t_n$ whereas the method $A_2(\theta)$ can be derived by evaluating the reaction terms at the time level $t = t_n$ and $t = t_{n+1}$. Finally, the second-order method $A_3(\theta = 1/2)$ is derived by using linear combinations of the reaction terms at the time level $t = t_n$ and $t = t_{n+1}$. Numerical experiments showed that the methods $A_2(\theta)$ and $A_3(\theta)$ allow the use of a larger time step in comparison to the method $A_1(\theta)$. The numerical solutions were obtained by solving a linear algebraic system at each time step. The families of numerical methods may be implemented on a parallel architecture using two processors. The study also indicates that the dynamic behaviour of whooping cough depends on the initial distributions and the diffusion rate.

Chapter 5

One-dimensional Whooping Cough Dynamics of Convection Type

5.1 Introduction

In this chapter, a one-dimensional model of whooping cough of hyperbolic type will be considered to explain the spatial spread of epidemics in the absence of diffusional effects as described in Chapter 4. It is assumed that the spread of whooping cough with migratory effects, i.e. convection, might be in wave form. Let $S(z,t)$ and $I(z,t)$ denote the numbers of susceptible and infectious individuals and z and t denote the position in space and the time, respectively. The convective velocity, denoted by ρ, is assumed to be equal for both groups. The convective whooping cough equations are then

$$\frac{\partial S}{\partial t} + \rho\frac{\partial S}{\partial z} = \mu N - \mu S - \beta SI, \tag{5.1.1}$$

$$\frac{\partial I}{\partial t} + \rho\frac{\partial I}{\partial z} = -(\mu+\nu)I + \beta SI, \tag{5.1.2}$$

with initial conditions given by

$$S(z,0) = f(z), \quad I(z,0) = g(z); \quad -L \leq z \leq L. \tag{5.1.3}$$

Assume that equations (5.1.1) and (5.1.2) are defined for $-L \leq z \leq L$ and the functions $f(z)$ and $g(z)$ are continuous on $-L \leq z \leq L$. It will be also assumed that, for this range, the system $\{$(5.1.1)-(5.1.3)$\}$ is symmetric about the line $z = 0$.

This imposes

$$\frac{\partial S}{\partial z}(0,t) = 0 \quad \text{and} \quad \frac{\partial I}{\partial z}(0,t) = 0; \quad t > 0 \tag{5.1.4}$$

as the boundary conditions and the initial conditions are given by

$$S(z,0) = f(z) \quad \text{and} \quad I(z,0) = g(z); \quad 0 \leq z \leq L. \tag{5.1.5}$$

The parameters μ, ν and β are positive and are defined as in previous chapters. The convection rate ρ is assumed to be a positive constant. A family of numerical methods based on finite-difference approximations are derived in § 5.2 to solve the system {(5.1.1),(5.1.2)} for $0 \leq z \leq L$, $t > 0$ subject to (5.1.4) and (5.1.5). The local truncation errors and the stability restrictions of these numerical methods are analysed in § 5.3. The results of some numerical experiments are discussed in § 5.4.

5.2 Numerical Methods

A solution of the system of partial differential equations {(5.1.1),(5.1.2)} may be computed by finite-difference techniques, by dividing the space interval $[0, L]$ into M sub-intervals each of width h so that $Mh = L$. The z-coordinates of the M points of this discretization are $z_m = mh\,(m = 0, 1, 2, \ldots, M)$; clearly, z_0 is the coordinate of every point on the t-axis. The time interval $t \geq 0$ is discretized in steps each of length $\ell > 0$. The solutions of {(5.1.1)-(5.1.3)} at the typical mesh point (z_m, t_n) are, of course, $S(z_m, t_n)$ and $I(z_m, t_n)$ which will be denoted by S_m^n and I_m^n, while the solutions of the approximating finite-difference method at the grid point $(z_m, t_n) = (mh, n\ell)$; $n = 0, 1, 2, \ldots$; $m = 0, 1, 2, \ldots, M$, will be denoted by X_m^n and Y_m^n, respectively. The values actually obtained, which may be subject to round-off errors, will be denoted by $\widetilde{X_m^n}$ and $\widetilde{Y_m^n}$.

A family of numerical methods will be developed by approximating the time derivatives in (5.1.1) and (5.1.2) by the first-order forward-difference replacement

$$\frac{\partial u(z,t)}{\partial t} = \frac{u(z,t+\ell) - u(z,t)}{\ell} + O(\ell) \text{ as } \ell \to 0, \tag{5.2.1}$$

and the space derivatives in (5.1.1) and (5.1.2) by the weighted approximant

$$\frac{\partial u}{\partial z} \approx \frac{\theta\{u(z,t+\ell)-u(z-h,t+\ell)\}+(1-\theta)\{u(z,t)-u(z-h,t)\}}{h} \tag{5.2.2}$$

in which $u(z,t)$ represents $X(z,t)$ or $Y(z,t)$ and $0 \leq \theta \leq 1$ is a parameter. The terms on the right-hand sides of (5.1.1) and (5.1.2) may be replaced in the following ways

$$\text{(i)} \quad -(\mu+\beta Y_m^n)X_m^n \quad \text{and} \quad \{\beta X_m^n-(\mu+\nu)\}Y_m^n, \tag{5.2.3}$$

$$\text{(ii)} \quad -(\mu+\beta Y_m^n)X_m^{n+1} \quad \text{and} \quad \beta X_m^n Y_m^n-(\mu+\nu)Y_m^{n+1}. \tag{5.2.4}$$

These approximations, together with the replacement for the derivatives of S and I result in the numerical methods, $\mathcal{M}_1(\theta)$ and $\mathcal{M}_2(\theta)$, for the numerical solution of {(5.1.1),(5.1.2)}:

Method $\mathcal{M}_1(\theta)$, $0 \leq \theta \leq 1$

$$\begin{aligned}-\rho r\theta X_{m-1}^{n+1}+(1+\rho r\theta)X_m^{n+1} &= \rho r(1-\theta)X_{m-1}^n \\ &\quad +\{1-\rho r(1-\theta)-\ell(\mu+\beta Y_m^n)\}X_m^n+\ell\mu N,\end{aligned} \tag{5.2.5}$$

$$\begin{aligned}-\rho r\theta Y_{m-1}^{n+1}+(1+\rho r\theta)Y_m^{n+1} &= \rho r(1-\theta)Y_{m-1}^n \\ &\quad +\{1-\rho r(1-\theta)-\ell(\mu+\nu-\beta X_m^n)\}Y_m^n,\end{aligned} \tag{5.2.6}$$

Method $\mathcal{M}_2(\theta)$, $0 \leq \theta \leq 1$

$$\begin{aligned}-\rho r\theta X_{m-1}^{n+1}+\left\{1+\rho r\theta+\ell(\mu+\beta Y_m^n)\right\}X_m^{n+1} &= \rho r(1-\theta)X_{m-1}^n \\ &\quad +\{1-\rho r(1-\theta)\}X_m^n+\ell\mu N,\end{aligned} \tag{5.2.7}$$

$$\begin{aligned}-\rho r\theta Y_{m-1}^{n+1}+\left\{1+\rho r\theta+\ell(\mu+\nu)\right\}Y_m^{n+1} &= \rho r(1-\theta)Y_{m-1}^n \\ &\quad +\{1-\rho r(1-\theta)+\ell\beta X_m^n\}Y_m^n,\end{aligned} \tag{5.2.8}$$

where $r=\ell/h$. The families of methods $\mathcal{M}_1(\theta)$ and $\mathcal{M}_2(\theta)$ are explicit for $\theta=0$ and implicit for $0<\theta\leq 1$. The methods {(5.2.5),(5.2.6)} and {(5.2.7),(5.2.8)} may be

applied with $m = 1, 2, \ldots, M$; for $m = 0$ they require some modification. Because of symmetry, only the region $z \geq 0$ will be considered. This imposes the conditions

$$\frac{\partial S}{\partial z}(0,t) = 0 \quad \text{and} \quad \frac{\partial I}{\partial z}(0,t) = 0; \quad t > 0,$$

so that, to second order,

$$X_1^n = X_{-1}^n \quad \text{and} \quad Y_1^n = Y_{-1}^n \quad (n = 0, 1, 2, \ldots). \tag{5.2.9}$$

Thus, methods $\mathcal{M}_1(\theta)$ and $\mathcal{M}_2(\theta)$ can be rearranged and modified to give the following families of methods:

Method $\mathcal{M}_1(\theta)$

Taking $m = 0$,

$$\begin{aligned}(1+\rho r\theta)X_0^{n+1} - \rho r\theta X_1^{n+1} = \{1 - \rho r(1-\theta) - \ell(\mu + \beta Y_0^n)\}X_0^n \\ +\rho r(1-\theta)X_1^n + \ell\mu N,\end{aligned} \tag{5.2.10}$$

for $m = 1, 2, \ldots, M$,

$$\begin{aligned}-\rho r\theta X_{m-1}^{n+1} + (1+\rho r\theta)X_m^{n+1} = \rho r(1-\theta)X_{m-1}^n \\ +\{1 - \rho r(1-\theta) - \ell(\mu + \beta Y_m^n)\}X_m^n + \ell\mu N,\end{aligned} \tag{5.2.11}$$

and for $m = 0$,

$$\begin{aligned}(1+\rho r\theta)Y_0^{n+1} - \rho r\theta Y_1^{n+1} = \{1 - \rho r(1-\theta) - \ell(\mu + \nu - \beta X_0^n)\}Y_0^n \\ +\rho r(1-\theta)Y_1^n,\end{aligned} \tag{5.2.12}$$

for $m = 1, 2, \ldots, M$,

$$\begin{aligned}-\rho r\theta Y_{m-1}^{n+1} + (1+\rho r\theta)Y_m^{n+1} = \rho r(1-\theta)Y_{m-1}^n \\ +\{1 - \rho r(1-\theta) - \ell(\mu + \nu - \beta X_m^n)\}Y_m^n.\end{aligned} \tag{5.2.13}$$

Method $\mathcal{M}_2(\theta)$

Taking $m = 0$,

$$\left\{1 + \rho r\theta + \ell(\mu + \beta Y_0^n)\right\}X_0^{n+1} - \rho r\theta X_1^{n+1} = \{1 - \rho r(1-\theta)\}X_0^n + \rho r(1-\theta)X_1^n + \ell\mu N, \quad (5.2.14)$$

for $m = 1, 2, \ldots, M$,

$$-\rho r\theta X_{m-1}^{n+1} + \left\{1 + \rho r\theta + \ell(\mu + \beta Y_m^n)\right\}X_m^{n+1} = \rho r(1-\theta)X_{m-1}^n + \{1 - \rho r(1-\theta)\}X_m^n + \ell\mu N, \quad (5.2.15)$$

and for $m = 0$,

$$\left\{1 + \rho r\theta + \ell(\mu + \nu)\right\}Y_0^{n+1} - \rho r\theta Y_1^{n+1} = \{1 - \rho r(1-\theta) + \ell\beta X_0^n\}Y_0^n + \rho r(1-\theta)Y_1^n, \quad (5.2.16)$$

for $m = 1, 2, \ldots, M$,

$$-\rho r\theta Y_{m-1}^{n+1} + \left\{1 + \rho r\theta + \ell(\mu + \nu)\right\}Y_m^{n+1} = \rho r(1-\theta)Y_{m-1}^n + \{1 - \rho r(1-\theta) + \ell\beta X_m^n\}Y_m^n. \quad (5.2.17)$$

5.3 Analyses of the methods

5.3.1 Local Truncation Errors

The local truncation error associated with (5.2.5) is given by

$$\mathcal{L}_S[S(z,t), I(z,t) : h, \ell] = \frac{S(z,t+\ell) - S(z,t)}{\ell} + \rho\theta\,\frac{S(z,t+\ell) - S(z-h,t+\ell)}{h} + \rho(1-\theta)\,\frac{S(z,t) - S(z-h,t)}{h} - \mu N + \{\mu + \beta I(z,t)\}S(z,t) - \left[\frac{\partial x(z,t)}{\partial t} + \rho\frac{\partial x(z,t)}{\partial z} - \mu N + \mu S(z,t) + \beta S(z,t)I(z,t)\right]. \quad (5.3.1)$$

Expanding $S(z-h,t)$, $S(z,t+\ell)$, $S(z-h,t+\ell)$ as Taylor series about (z,t) gives

$$\mathcal{L}_S[S(z,t), I(z,t); h, \ell] = \left\{\frac{1}{2}\frac{\partial^2 S}{\partial z^2} + \rho\theta\frac{\partial^2 S}{\partial z \partial t}\right\}\ell - \frac{1}{2}\rho h\frac{\partial^2 S}{\partial z^2} - \frac{1}{2}\rho\theta\ell h\frac{\partial^3 S}{\partial z^2 \partial t} + \left\{\frac{1}{6}\frac{\partial^3 S}{\partial t^3} + \frac{1}{2}\rho\theta\frac{\partial^3 S}{\partial z \partial t^2}\right\}\ell^2 + \ldots, \quad (5.3.2)$$

which is $O(h+\ell)$ as $h, \ell \to 0$.

The local truncation error associated with (5.2.6) is given by

$$\mathcal{L}_I[S(z,t), I(z,t) : h, \ell] = \frac{I(z,t+\ell) - I(z,t)}{\ell} + \rho\theta \frac{I(z,t+\ell) - I(z-h,t+\ell)}{h}$$
$$+\rho(1-\theta)\frac{I(z,t) - I(z-h,t)}{h} + \{(\mu+\nu) - \beta S(z,t)\}I(z,t)$$
$$-\left[\frac{\partial I(z,t)}{\partial t} + \rho\frac{\partial I(z,t)}{\partial z} + (\mu+\nu)I(z,t) - \beta S(z,t)I(z,t)\right]. \qquad (5.3.3)$$

Expanding $I(z-h,t)$, $I(z,t+\ell)$, $I(z-h,t+\ell)$ as Taylor series about (z,t) leads to

$$\mathcal{L}_I[S(z,t), I(z,t); h, \ell] = \left\{\frac{1}{2}\frac{\partial^2 I}{\partial t^2} + \rho\theta\frac{\partial^2 I}{\partial z \partial t}\right\}\ell - \frac{1}{2}\rho h\frac{\partial^2 I}{\partial z^2} - \frac{1}{2}\rho\theta\ell h\frac{\partial^3 I}{\partial z^2 \partial t}$$
$$+\left\{\frac{1}{6}\frac{\partial^3 I}{\partial t^3} + \frac{1}{2}\rho\theta\frac{\partial^3 I}{\partial z \partial t^2}\right\}\ell^2 + \ldots, \qquad (5.3.4)$$

which is $O(h+\ell)$ as $h, \ell \to 0$.

Similarly, the local truncation errors associated with (5.2.7) and (5.2.8) are given by

$$\mathcal{L}_S[S(z,t), I(z,t); h, \ell] = \left\{\frac{1}{2}\frac{\partial^2 S}{\partial z^2} + (\mu+\beta I)\frac{\partial S}{\partial t} + \rho\theta\frac{\partial^2 S}{\partial z \partial t}\right\}\ell - \frac{1}{2}\rho h\frac{\partial^2 S}{\partial z^2}$$
$$-\frac{1}{2}\rho\theta\ell h\frac{\partial^3 S}{\partial z^2 \partial t} + \left\{\frac{1}{6}\frac{\partial^3 S}{\partial t^3} + \frac{1}{2}(\mu+\beta I)\frac{\partial^2 S}{\partial t^2} + \frac{1}{2}\rho\theta\frac{\partial^3 S}{\partial z \partial t^2}\right\}\ell^2$$
$$+\ldots, \qquad (5.3.5)$$

$$\mathcal{L}_I[S(z,t), I(z,t); h, \ell] = \left\{\frac{1}{2}\frac{\partial^2 I}{\partial t^2} + (\mu+\nu)\frac{\partial I}{\partial t} + \rho\theta\frac{\partial^2 I}{\partial z \partial t}\right\}\ell - \frac{1}{2}\rho h\frac{\partial^2 I}{\partial z^2}$$
$$-\frac{1}{2}\rho\theta\ell h\frac{\partial^3 I}{\partial z^2 \partial t} + \left\{\frac{1}{6}\frac{\partial^3 I}{\partial t^3} + \frac{1}{2}(\mu+\nu)\frac{\partial^2 I}{\partial t^2} + \frac{1}{2}\rho\theta\frac{\partial^3 I}{\partial z \partial t^2}\right\}\ell^2$$
$$+\ldots, \qquad (5.3.6)$$

which are $O(h+\ell)$ as $h, \ell \to 0$. These reveal that the families of methods $\mathcal{M}_1(\theta)$ and $\mathcal{M}_2(\theta)$ are first-order in time as well as in space for $0 \leq \theta \leq 1$.

5.3.2 Stability Analyses

The von Neumann or Fourier series method of analysing stability will be used to analyse the stability properties of the methods. This method of analysing stability is based on considering small errors Z_m^n of the forms

$$Z_{x,m}^n = e^{\gamma n\ell} e^{i\delta mh} \quad \text{and} \quad Z_{y,m}^n = e^{\psi n\ell} e^{i\phi mh}; \quad \gamma, \psi, \delta, \phi \in \mathbb{R}, \tag{5.3.7}$$

with $i = \sqrt{-1}$. The von Neumann necessary condition for the error not to grow as $n \to \infty$ is

$$|e^{\gamma\ell}| \leq 1 + M_x\,\ell \quad \text{and} \quad |e^{\psi\ell}| \leq 1 + M_y\,\ell, \tag{5.3.8}$$

where M_x and M_y are non-negative constants independent of h, ℓ.

Method $\mathcal{M}_1$

Substituting Z_x into (5.2.5) and dividing by $e^{\gamma nl} e^{i\delta mh}$ leaves

$$\xi_x = \frac{1 - \rho r(1-\theta) - \ell(\mu + \beta Y_m^n) + \rho r(1-\theta)e^{-i\delta h}}{1 + \rho r\theta - \rho r\theta e^{-i\delta h}}, \tag{5.3.9}$$

where $\xi_x = e^{\gamma\ell}$ and Y_m^n is treated as a constant. This gives the stability condition

$$|\xi_x|^2 = \frac{(1-A)^2 + \{4\rho^2 r^2(1-\theta)^2 - 4\rho r(1-\theta)(1-A)\}\sin^2\frac{\delta h}{2}}{1 + (4\rho^2 r^2\theta^2 + 4\rho r\theta)\sin^2\frac{\delta h}{2}}, \tag{5.3.10}$$

where $A = \ell(\mu + \beta Y_m^n)$. If $4\rho^2 r^2(1-\theta)^2 - 4\rho r(1-\theta)(1-A) \geq 0$ then

$$\begin{aligned} |\xi_x|^2 &\leq \frac{(1-A)^2 + 4\rho^2 r^2(1-\theta)^2 - 4\rho r(1-\theta)(1-A)}{1 + 4\rho^2 r^2\theta^2 + 4\rho r\theta} \\ &= \left\{\frac{1 - A - 2\rho r(1-\theta)}{1 + 2\rho r\theta}\right\}^2, \end{aligned} \tag{5.3.11}$$

so that

$$|\xi_x| \leq \left|\frac{1 - A - 2\rho r(1-\theta)}{1 + 2\rho r\theta}\right|. \tag{5.3.12}$$

It follows that $|\xi_x| \leq 1$ leads to the stability restrictions

$$0 \leq \theta < 1/2, \qquad r \leq \frac{2-A}{2\rho(1-2\theta)} \quad \text{and} \quad r \geq \frac{1-A}{\rho(1-\theta)} \quad \text{and} \quad A < 1,$$

$$\begin{aligned}
\theta = 1/2, \qquad & r \geq \frac{2}{\rho}(1-A) \qquad \text{and} \quad A < 1, \\
1/2 < \theta < 1, \qquad & r \geq \frac{A-2}{2\rho(2\theta-1)} \quad \text{and} \quad r \geq \frac{1-A}{\rho(1-\theta)} \quad \text{and} \quad A < 1, \\
\theta = 1, \qquad & r \geq \frac{A-2}{2\rho(2\theta-1)} \quad \text{and} \quad A \geq 1.
\end{aligned} \tag{5.3.13}$$

Substituting, next, Z_y into (5.2.6) gives

$$|\xi_y|^2 = \frac{(1+B-C)^2 + \{4\rho^2 r^2(1-\theta)^2 - 4\rho r(1-\theta)(1+B-C)\}\sin^2\frac{\phi h}{2}}{1+(4\rho^2 r^2\theta^2 + 4\rho r\theta)\sin^2\frac{\phi h}{2}}, \tag{5.3.14}$$

where $\xi_y = e^{\psi\ell}$, $B = \ell\beta X_m^n$, $C = \ell(\mu+\nu)$ and X_m^n is treated as a constant.

Similarly, if $4\rho^2 r^2(1-\theta)^2 - 4\rho r(1-\theta)(1+B-C) \geq 0$ then

$$|\xi_y| \leq \left|\frac{1+B-C-2\rho r(1-\theta)}{1+2\rho r\theta}\right|. \tag{5.3.15}$$

The consequent stability restrictions are

$$\begin{aligned}
0 \leq \theta < 1/2, \qquad & \frac{B-C}{2\rho} \leq r \leq \frac{2+B-C}{2\rho(1-2\theta)} \text{ and } r \geq \frac{1+B-C}{\rho(1-\theta)} \quad \text{and} \quad C < 1+B, \\
\theta = 1/2, \qquad & r \geq \frac{2}{\rho}(1+B-C) \qquad \text{and} \quad C < 1+B, \\
1/2 < \theta < 1, \qquad & r \geq \frac{C-B-2}{2\rho(2\theta-1)} \quad \text{and} \quad r \geq \frac{1+B-C}{\rho(1-\theta)} \quad \text{and} \quad C < 1+B, \\
\theta = 1, \qquad & r \geq \frac{C-B-2}{2\rho(2\theta-1)} \quad \text{and} \quad C \geq 1+B.
\end{aligned} \tag{5.3.16}$$

Method $\mathcal{M}_2$

Substituting Z_x into (5.2.7) leads to

$$|\xi_x|^2 = \frac{1+\{4\rho^2 r^2(1-\theta)^2 - 4\rho r(1-\theta)\}\sin^2\frac{\delta h}{2}}{(1+A)^2 + \{4\rho^2 r^2\theta^2 + 4\rho r\theta(1+A)\}\sin^2\frac{\delta h}{2}}, \tag{5.3.17}$$

where $\xi_x = e^{\gamma\ell}$, $A = \ell(\mu+\beta Y_m^n)$ and Y_m^n is treated as a constant. If $4\rho^2 r^2(1-\theta)^2 - 4\rho r(1-\theta) \geq 0$ then

$$|\xi_x| \leq \left|\frac{1-2\rho r(1-\theta)}{1+A+2\rho r\theta}\right|. \tag{5.3.18}$$

The following stability restrictions are obtained

$$0 \leq \theta < 1/2, \qquad r \leq \frac{A+2}{2\rho(1-2\theta)} \quad \text{and} \quad r \geq \frac{1}{\rho(1-\theta)},$$

$$\begin{aligned} \theta = 1/2, \qquad & r \geq \frac{2}{\rho}, \\ 1/2 < \theta < 1, \qquad & r \geq \frac{1}{\rho(1-\theta)}, \\ \theta = 1, \qquad & r < \infty. \end{aligned} \tag{5.3.19}$$

Substituting, next, Z_y into (5.2.8) gives

$$|\xi_y|^2 = \frac{(1+B)^2 + \{4\rho^2 r^2(1-\theta)^2 - 4\rho r(1-\theta)(1+B)\}\sin^2\frac{\phi h}{2}}{(1+C)^2 + \{4\rho^2 r^2\theta^2 + 4\rho r\theta(1+C)\sin^2\frac{\phi h}{2}} \tag{5.3.20}$$

where $\xi_y = e^{\psi\ell}$, $B = \ell\beta X_m^n$, $C = \ell(\mu+\nu)$ and X_m^n is treated as a constant. If $4\rho^2 r^2(1-\theta)^2 - 4\rho r(1-\theta)(1+B) \geq 0$,

$$|\xi_y| \leq \left|\frac{(1+B) - 2\rho r(1-\theta)}{(1+C) + 2\rho r\theta}\right|. \tag{5.3.21}$$

and the consequent stability restrictions are

$$\begin{aligned} 0 \leq \theta < 1/2, \qquad & \frac{B-C}{2\rho} \leq r \leq \frac{2+B+C}{2\rho(1-2\theta)} \quad \text{and} \quad r \geq \frac{1+B}{\rho(1-\theta)}, \\ \theta = 1/2, \qquad & r \geq \frac{B-C}{2\rho} \quad \text{and} \quad r \geq \frac{2+2B}{\rho}, \\ 1/2 < \theta < 1, \qquad & r \geq \frac{B-C}{2\rho} \quad \text{and} \quad r \geq \frac{1+B}{\rho(1-\theta)}, \\ \theta = 1, \qquad & r \geq \frac{B-C}{2\rho}. \end{aligned} \tag{5.3.22}$$

5.4 Numerical experiments

In order to examine the behaviour of the families of computational methods $\mathcal{M}_1$ and $\mathcal{M}_2$, the solution of the system {(5.1.1),(5.1.2)} with

$$S(z,0) = 3125000(1.0-z), \quad I(z,0) = 750(1.0-z); \quad 0 \leq z \leq 1, \tag{5.4.1}$$

was computed for the numbers of susceptible and infective individuals. The space interval $0 \leq z \leq 1$ was divided into 40 subintervals each of width $h = 0.025$, so that $M = 40$. The set of parameters given in (2.8.1) for μ and ν were used with $N = 25 \times 10^6$ and the infection rate, β, chosen to be $\beta = 5 \times 10^{-5}$.

Numerical experiments were carried out using Methods $\mathcal{M}_1$ and $\mathcal{M}_2$ with the convection rate $\rho = 0.5$. Method $\mathcal{M}_1$ gave the correct numerical solutions for $\ell < 0.0096$

with $\theta = \frac{1}{2}$ and for $\ell < 0.0102$ with $\theta = 1$. Some negative values of susceptibles were seen for $0.0096 < \ell < 0.00198$ with $\theta = \frac{1}{2}$ and for $0.0102 < \ell < 0.0198$ with $\theta = 1$ and overflow were produced as ℓ increased further. In the case of method $\mathcal{M}_2(\theta)$ with $\theta = \frac{1}{2}$, 1, the correct numerical solutions are observed for all $\ell > 0$.

The solutions were computed using Methods $\mathcal{M}_1$ and $\mathcal{M}_2$ with, first of all, $\rho = 0.5$. The time step is chosen to be 0.001 and the parameter θ was given the values 1/2 and 1. These are exhibited in Figures 5.1-5.7 and different angle views of Figures 5.1 and 5.3 are shown in Figures 5.2 and 5.4, respectively. It was seen that the number of susceptibles decreases whereas the number of infectives increase near $z = 0$ as time increases. Tables 5.1 and 5.2 display an example of the closeness of the results for infectives using Methods $\mathcal{M}_1$ and $\mathcal{M}_2$ with $\theta = \frac{1}{2}$ and $\theta = 1$, at time $t = 0.1$. Using $\theta = 1$, the number of infectious individuals is seen to decay more than when $\theta = \frac{1}{2}$ is used, as z increases. The solution obtained using Method $\mathcal{M}_2$ converges to the steady-state solution a little faster than the solution obtained using Method $\mathcal{M}_1$. The numerical experiments were then repeated using Method $\mathcal{M}_2$ with $\theta = 1$ for $\rho = 1$ and $\rho = 1.5$, respectively, for testing the effect of ρ. It was seen that the shapes of the surfaces are unaffected by change in ρ. As ρ increases, the number of susceptibles at ρ given point in space becomes smaller while the number of infectives at the given point is higher, see figures 5.8 (a), (b).

Table 5.1: The numbers of infectious individuals at time $t = 0.1$ using Method $\mathcal{M}_1$ with $\rho = 0.5$, $\ell = 0.001$, $\theta = \frac{1}{2}$ and $\theta = 1$

Space, z	$\theta = \frac{1}{2}$	$\theta = 1$
0.0	1420776	1420824
0.1	1435798	1433374
0.2	1403630	1401060
0.3	1131709	1133351
0.4	586624	592227
0.5	178783	181742
0.6	38873	39576
0.7	7121	7238
0.8	1144	1159
0.9	152	154
1.0	12	12

Table 5.2: The numbers of infectious individuals at time $t = 0.1$ using Method $\mathcal{M}_2$ with $\rho = 0.5$, $\ell = 0.001$, $\theta = \frac{1}{2}$ and $\theta = 1$

Space, z	$\theta = \frac{1}{2}$	$\theta = 1$
0.0	1538493	1538554
0.1	1539110	1536651
0.2	1444385	1442571
0.3	1087553	1090311
0.4	526072	531437
0.5	156573	159084
0.6	34534	35124
0.7	6507	6607
0.8	1079	1093
0.9	148	149
1.0	12	12

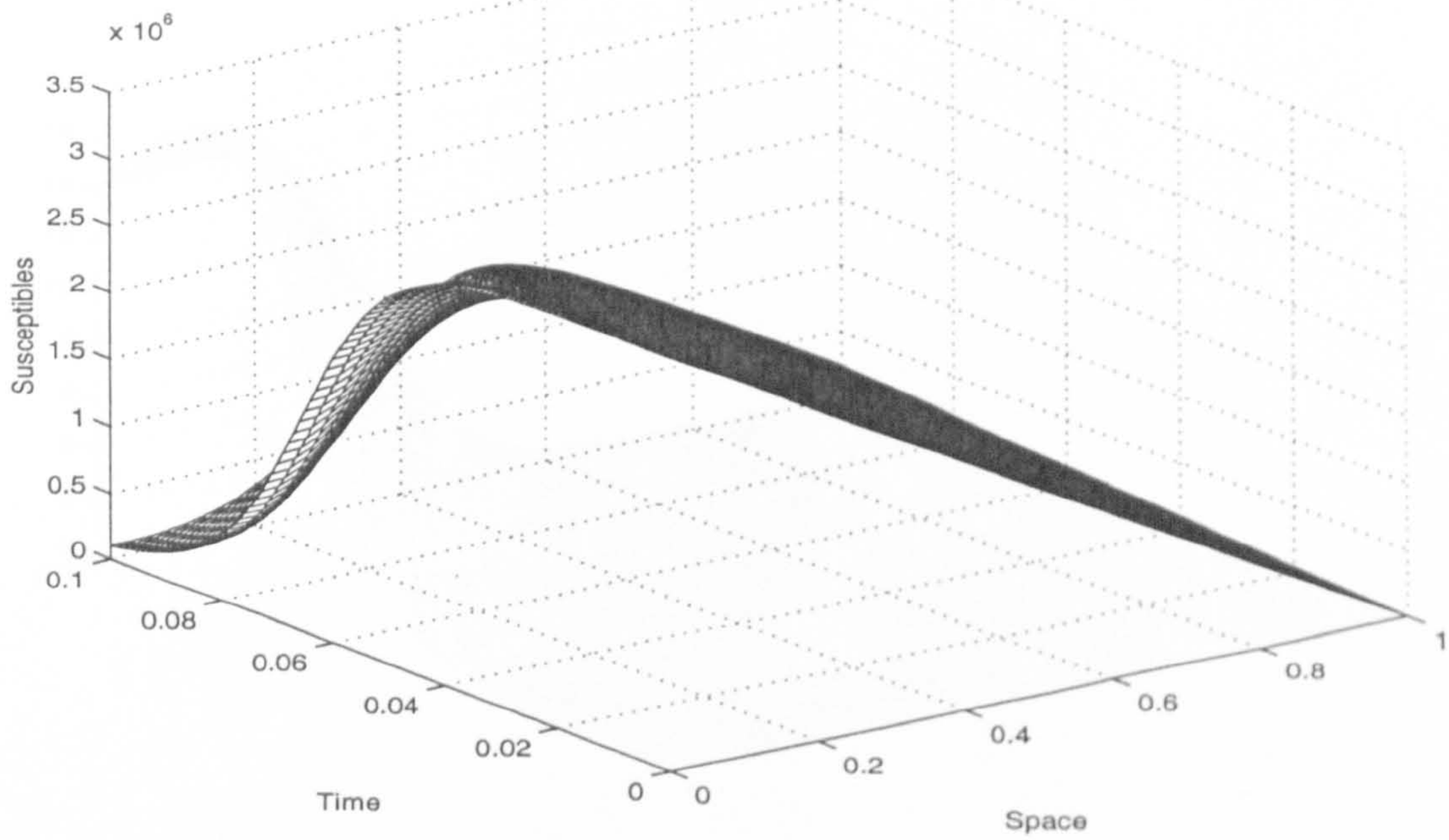

Figure 5.1: Three-dimensional distribution of susceptibles using Method $\mathcal{M}_1$ with $\theta = \frac{1}{2}$, $\rho = 0.5$, $\ell = 0.001$ and $h = 0.025$.

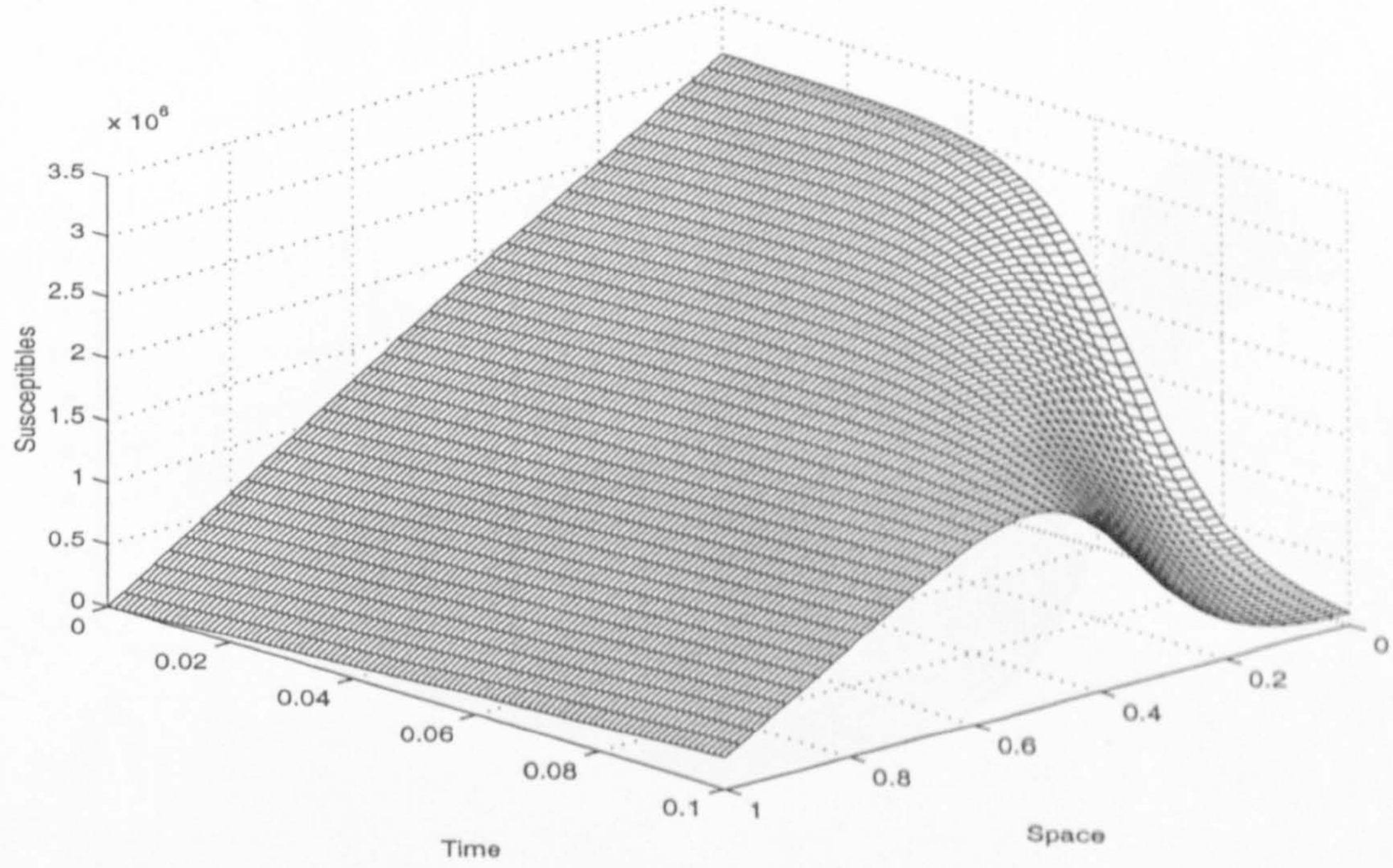

Figure 5.2: Different angle view of Figure 5.1; view([135,30])

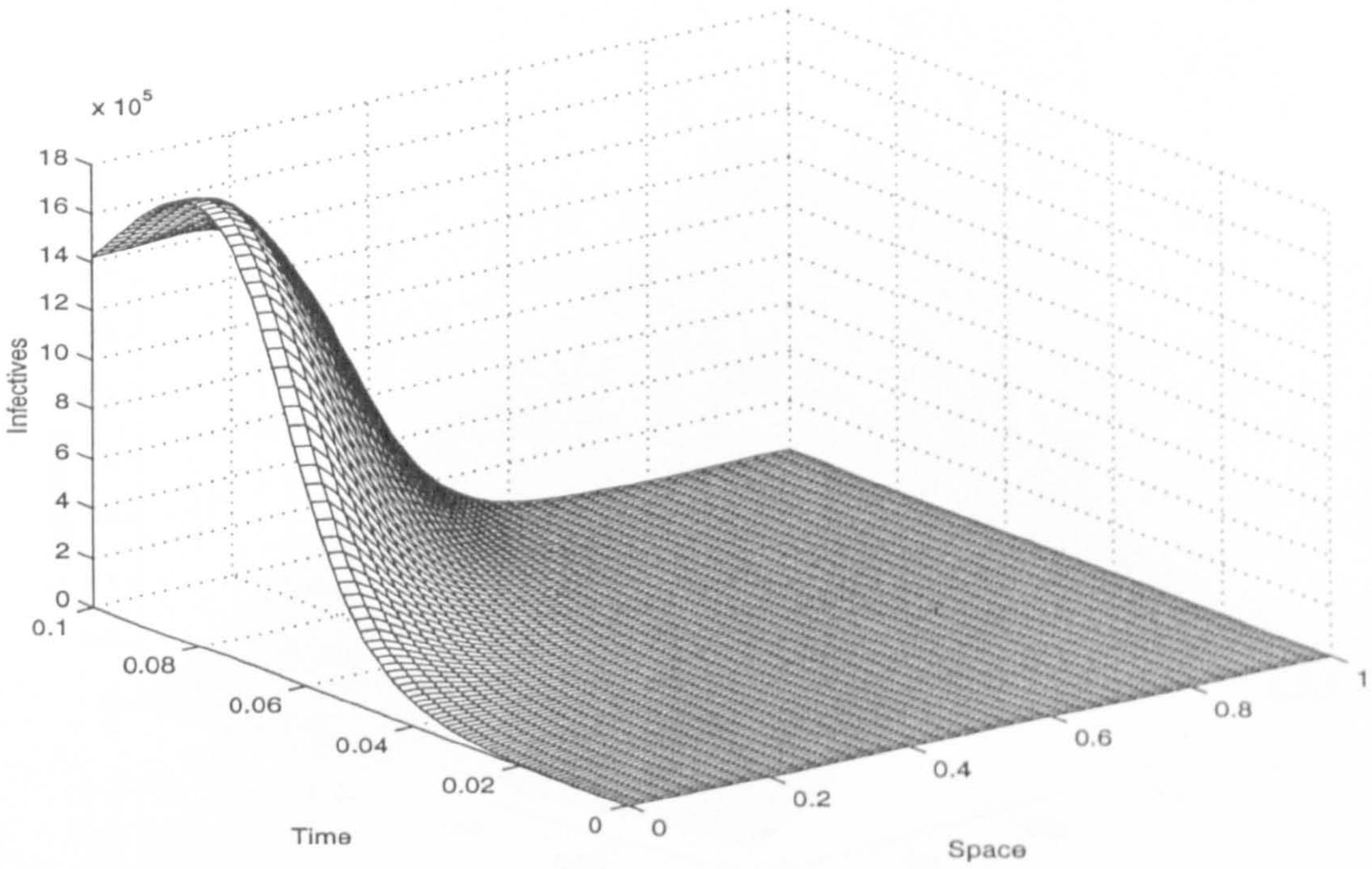

Figure 5.3: Three-dimensional distribution of infectives using Method $\mathcal{M}_1$ with $\theta = \frac{1}{2}$, $\rho = 0.5$, $\ell = 0.001$ and $h = 0.025$.

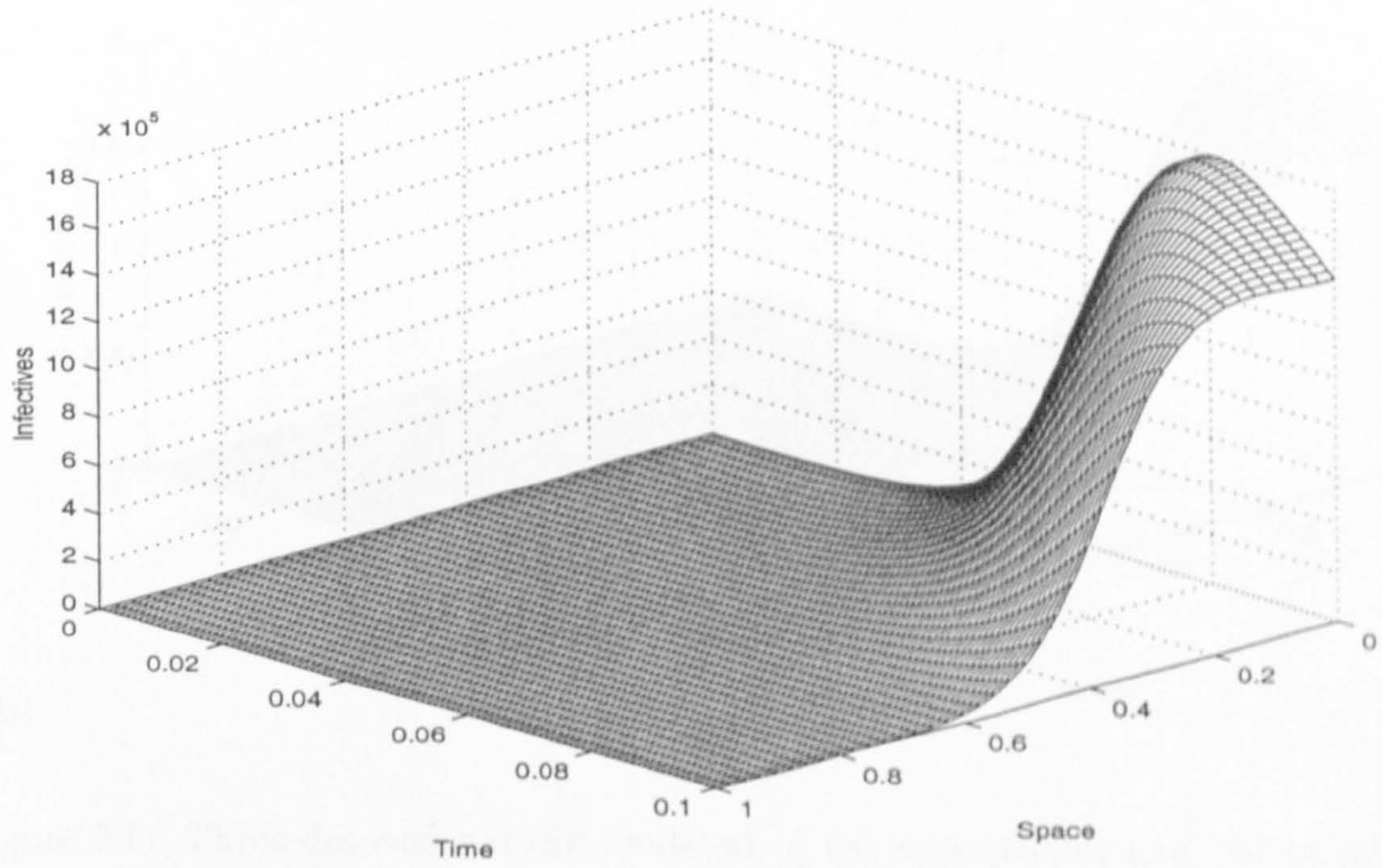

Figure 5.4: Different angle view of Figure 5.3; view([135,30])

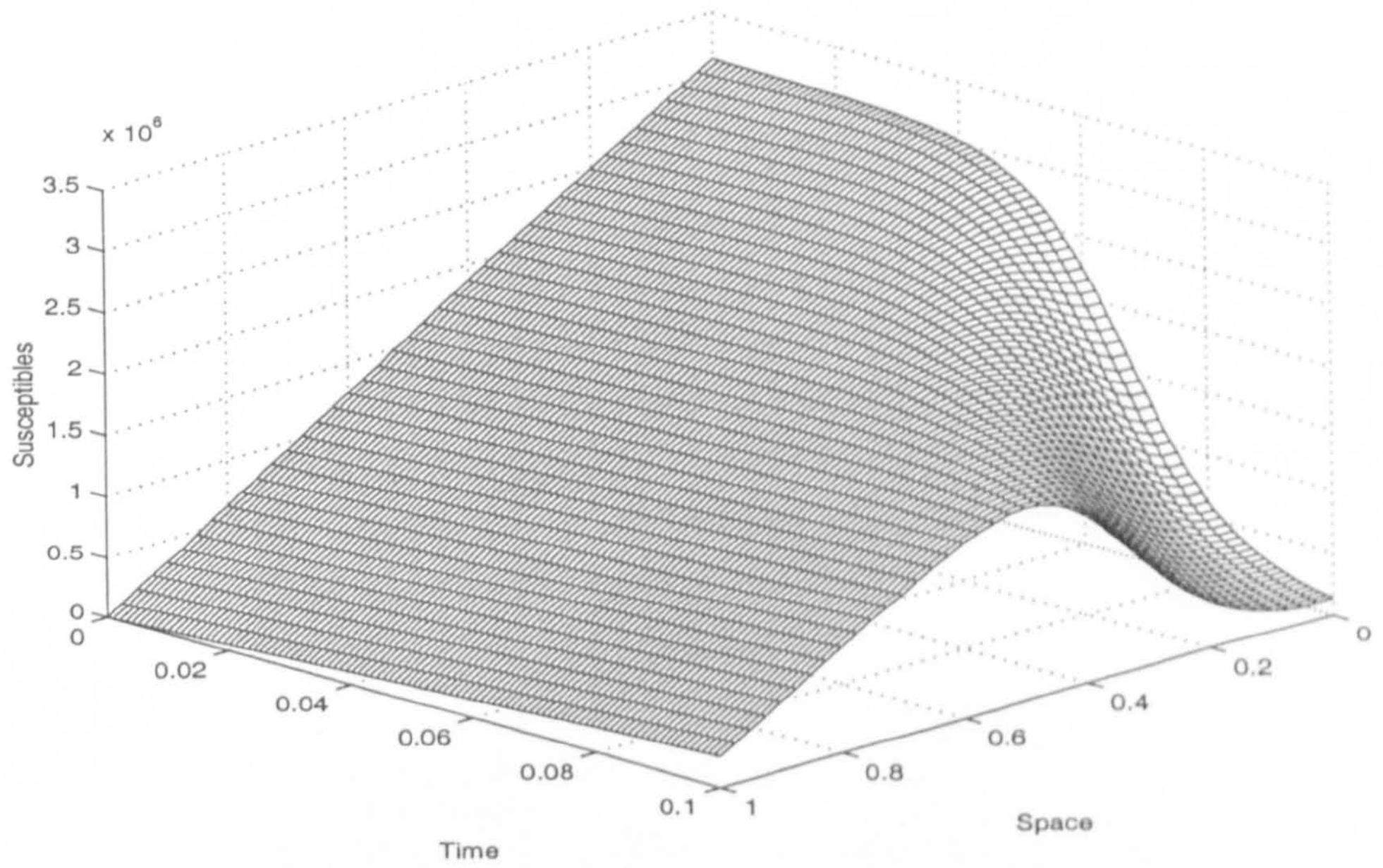

(a)

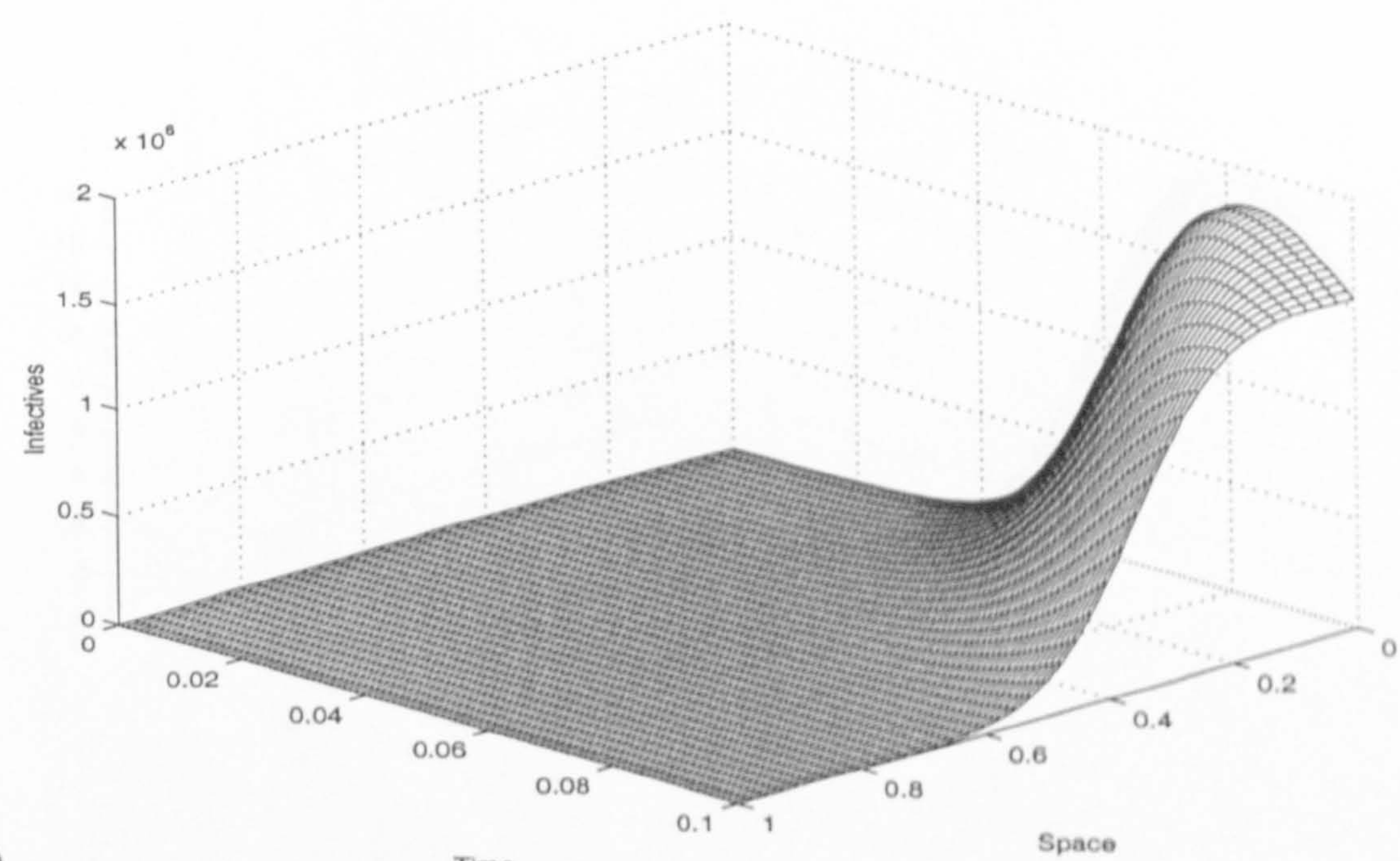

(b)

Figure 5.5: Three-dimensional distributions of (a) susceptibles and (b) infectives using Method $\mathcal{M}_2$ with $\theta = \frac{1}{2}$, $\rho = 0.5$, $\ell = 0.001$ and $h = 0.025$.

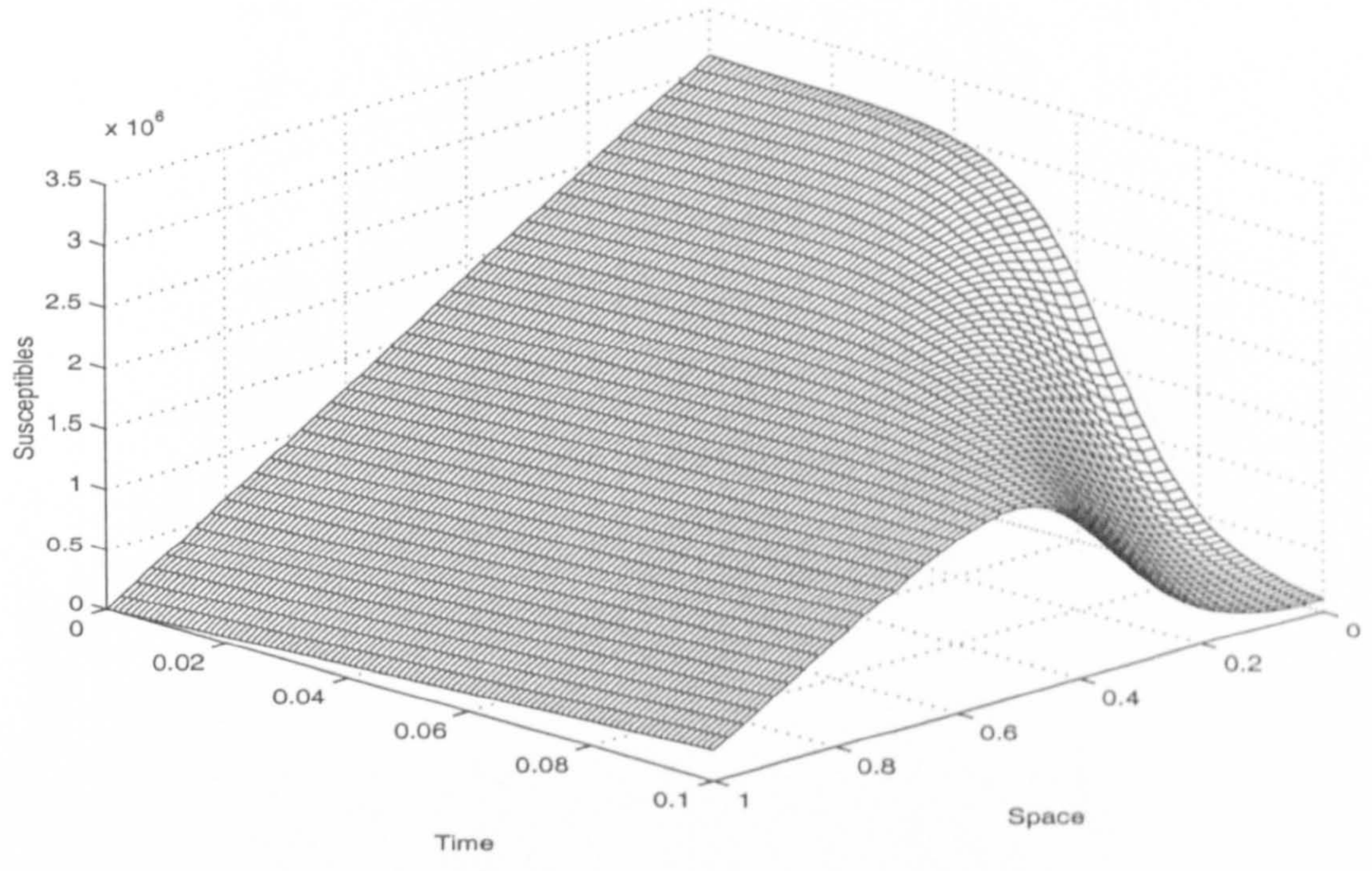

(a)

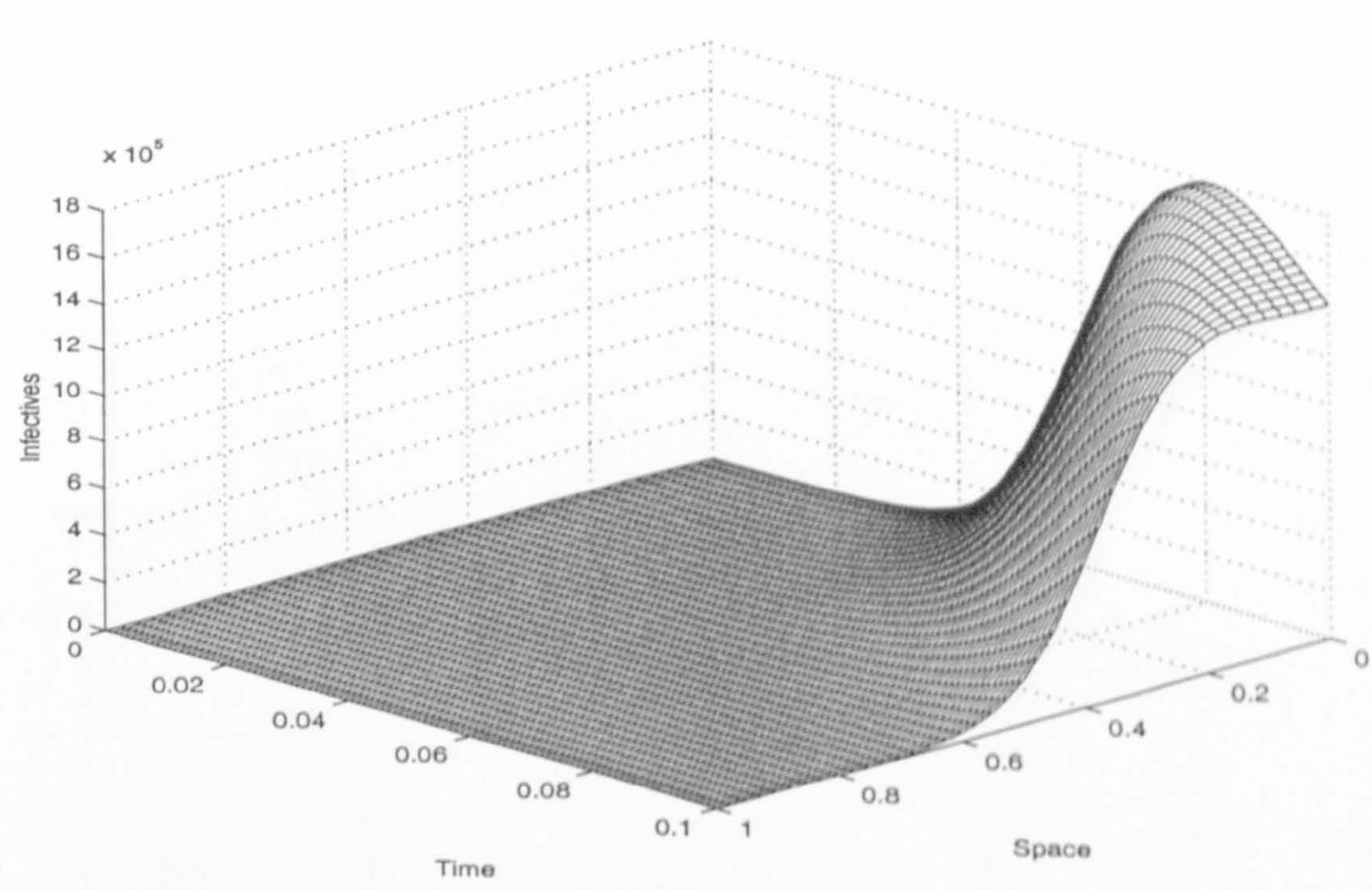

(b)

Figure 5.6: Three-dimensional distributions of (a) susceptibles and (b) infectives using Method $\mathcal{M}_1$ with $\theta = 1$, $\rho = 0.5$, $\ell = 0.001$ and $h = 0.025$.

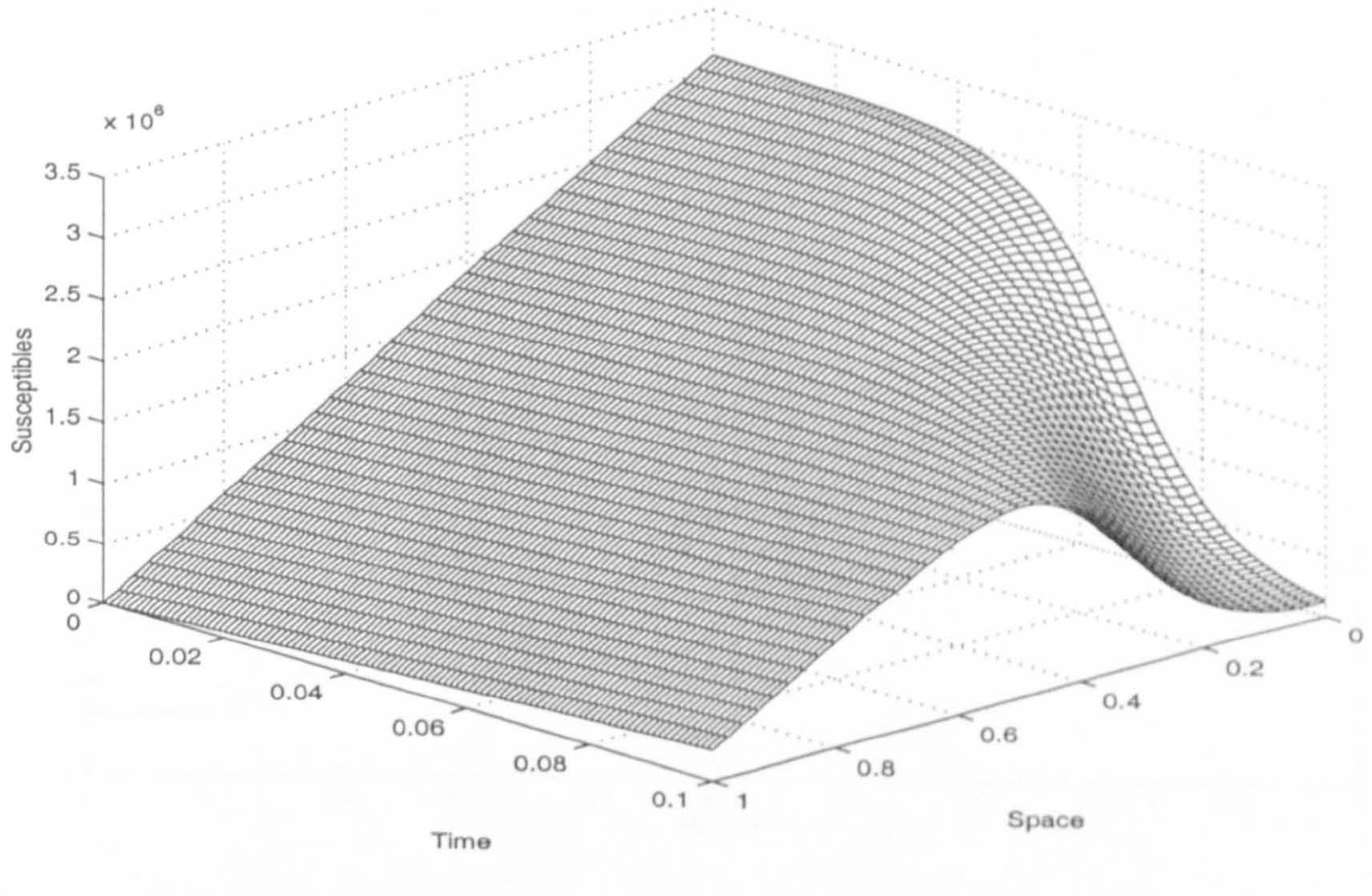

(a)

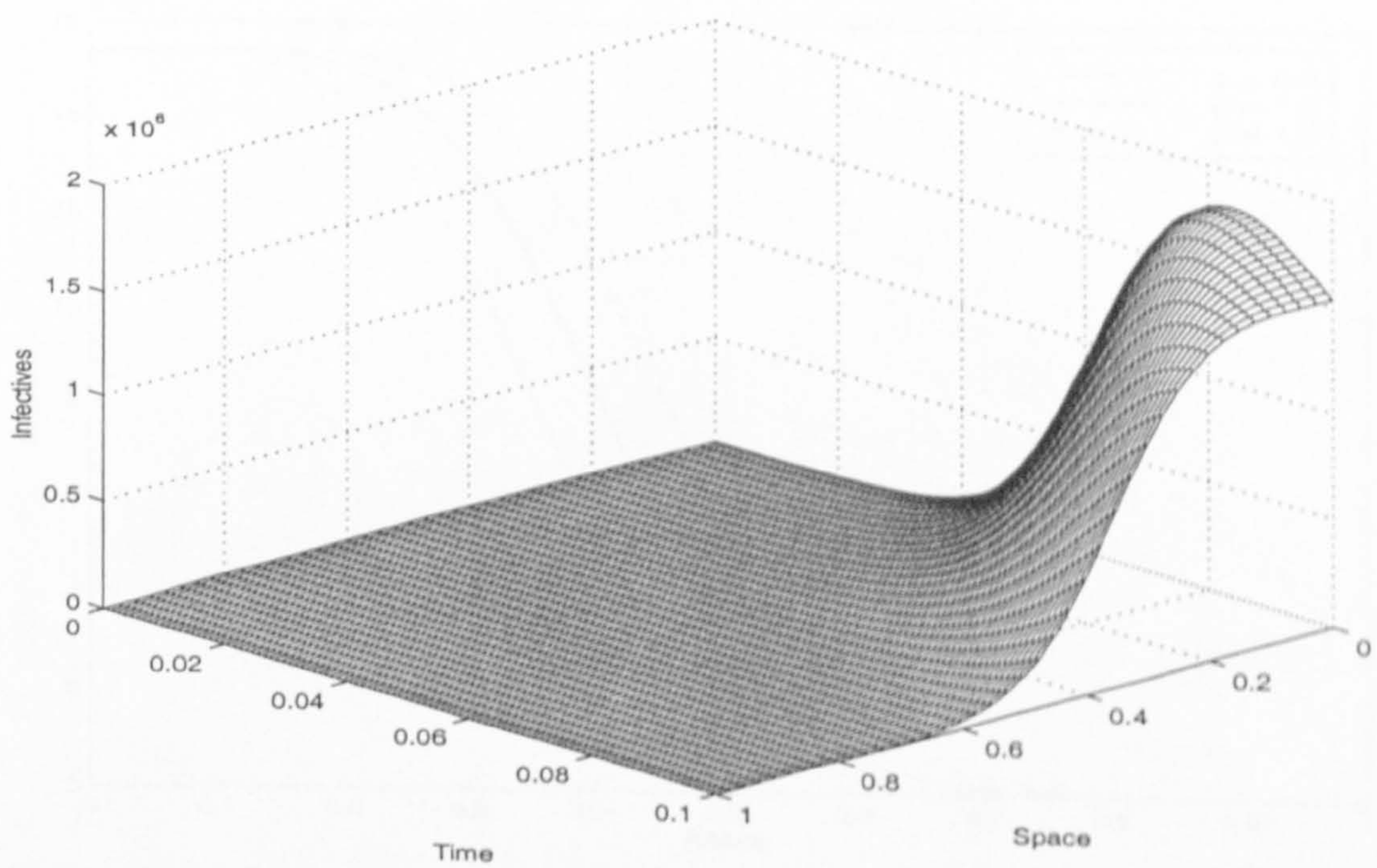

(b)

Figure 5.7: Three-dimensional distributions of (a) susceptibles and (b) infectives using Method $\mathcal{M}_2$ with $\theta = 1$, $\rho = 0.5$, $\ell = 0.001$ and $h = 0.025$.

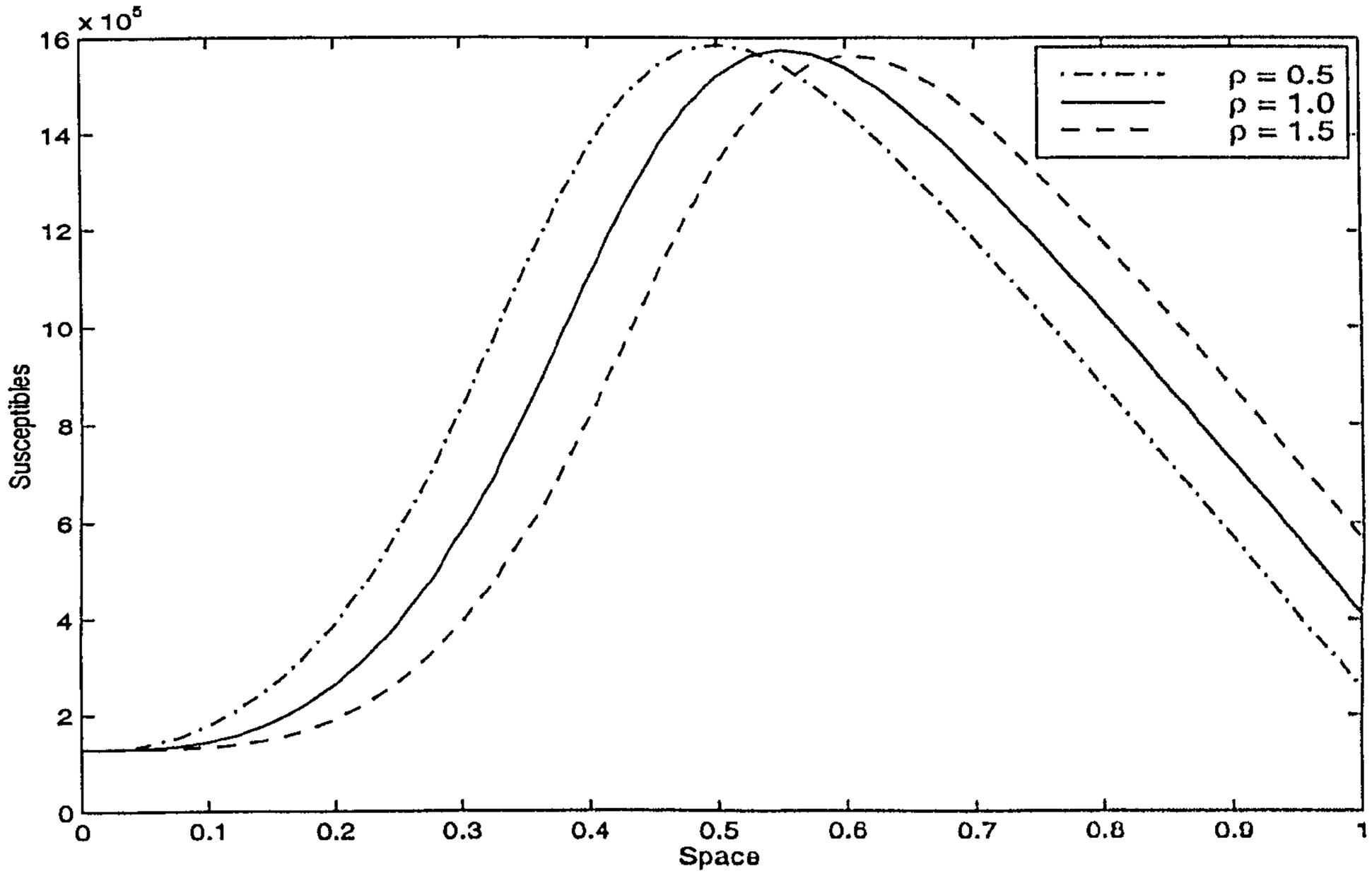

(a)

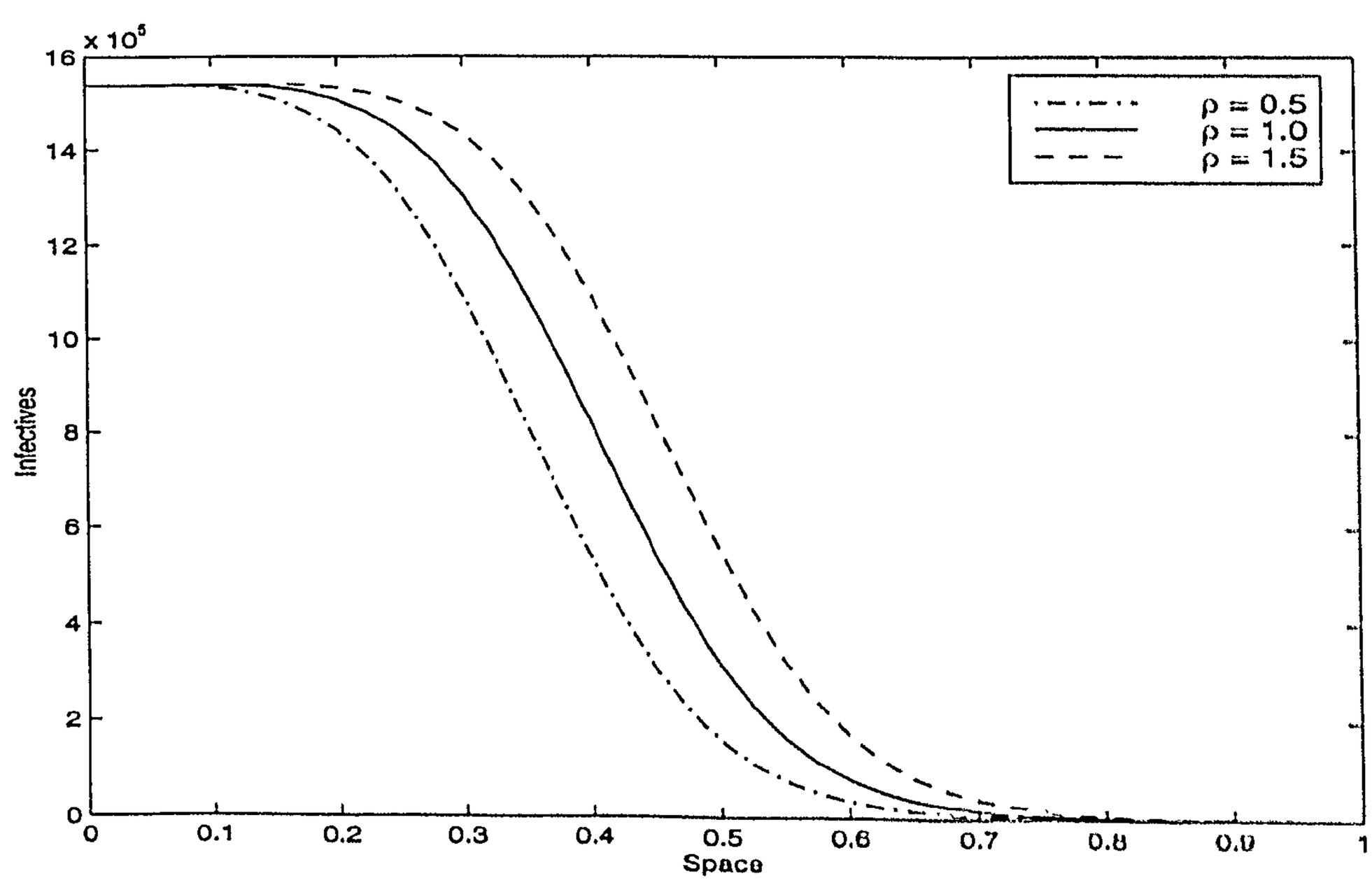

(b)

Figure 5.8: Solution profiles using Method $\mathcal{M}_2$ at time $t = 0.1$ with $\theta = 1$, $h = 0.025$, $\ell = 0.001$ and $\rho = 0.5, 1.0, 1.5$; (a) the number of susceptible individuals, (b) the number of infective individuals.

Chapter 6

Diffusion-Convection Whooping Cough Model

6.1 Introduction

The initial/boundary-value problem for whooping cough dynamics of diffusion-convection type is studied in this chapter. The system is the class of non-linear parabolic equations given by

$$\frac{\partial S}{\partial t} + \rho\frac{\partial S}{\partial z} = \mu N - \mu S - \beta SI + \alpha\frac{\partial^2 S}{\partial z^2}, \tag{6.1.1}$$

$$\frac{\partial I}{\partial t} + \rho\frac{\partial I}{\partial z} = \beta SI - (\mu+\nu)I + \alpha\frac{\partial^2 I}{\partial z^2} \tag{6.1.2}$$

in which $S = S(z,t)$ and $I = I(z,t)$ are the numbers of susceptible and infectious individuals, respectively, at time t and distance z from the origin; $\alpha > 0$ and $\rho > 0$ are, respectively, the diffusion and convection rates. The parameters μ, ν, β and N are as before.

The initial conditions are of the form

$$S(z,0) = f(z) \quad \text{and} \quad I(z,0) = g(z); \quad 0 \le z \le L \tag{6.1.3}$$

and the boundary conditions are

$$\begin{aligned} &\frac{\partial S}{\partial z}(0,t) = \frac{\partial I}{\partial z}(0,t) = 0; \quad t > 0, \\ &\frac{\partial S}{\partial z}(L,t) = \frac{\partial I}{\partial z}(L,t) = 0; \quad t > 0. \end{aligned} \tag{6.1.4}$$

The object of this chapter is to study the solution of the system {(6.1.1)-(6.1.4)}, which is a composite of Chapters 4 and 5. A second-order finite-difference method is used to compute the solution of this problem and its local truncation errors are given in §6.2. The implementation of the method, analysis of stability and the results of some numerical experiments are reported in §6.3, §6.4 and §6.5, respectively.

6.2 Numerical Methods

The interval $0 \leq z \leq L$ is divided into M sub-intervals each of width h so that $Mh = L$ and the time variable t is discretized in steps of length ℓ. The open region $\Omega = [0 < z < L,\, t > 0]$; the closure of Ω will be denoted by $\overline{\Omega}$ and its boundary $\partial\Omega$ consisting of the segments $\partial\Omega_0\,(0 < z < L,\, t = 0)$, $\partial\Omega_1\,(z = 0,\, t > 0)$ and $\partial\Omega_2\,(z = L, t > 0)$ have thus been covered by a rectangular mesh having coordinates of the form (z_m, t_n) where $z_m = mh$ $(m = 0, 1, 2, \ldots, M-1, M)$ and $t_n = n\ell$ $(n = 0, 1, 2, \ldots)$. The solutions of {(6.1.1),(6.1.2)} at the typical point (z_m, t_n) are, of course, $S(z_m, t_n)$, and $I(z_m, t_n)$; these may be denoted by S_m^n and I_m^n, respectively. The theoretical solution of numerical approximations to {(6.1.1),(6.1.2)} at the same mesh point will be denoted by X_m^n and Y_m^n, while the values actually obtained by computation, which may be subject to round-off errors, will be denoted by $\widetilde{X_m^n}$ and $\widetilde{Y_m^n}$.

To integrate the differential equation numerically using the finite-difference method, the time and space derivatives in {(6.1.1),(6.1.2)} are approximated as follows

$$\frac{\partial\varphi}{\partial t} \approx \frac{\varphi(z, t+\ell) - \varphi(z,t)}{\ell} \tag{6.2.1}$$

$$\begin{aligned}\frac{\partial\varphi}{\partial z} \approx\ & \theta\left\{\frac{\varphi(z+h, t+\ell) - \varphi(z-h, t+\ell)}{2h}\right\} \\ & +(1-\theta)\left\{\frac{\varphi(z+h,t) - \varphi(z-h,t)}{2h}\right\}\end{aligned} \tag{6.2.2}$$

$$\frac{\partial^2\varphi}{\partial z^2} \approx \theta\left\{\frac{\varphi(z-h, t+\ell) - 2\varphi(z, t+\ell) + \varphi(z+h, t+\ell)}{h^2}\right\}$$

$$+(1-\theta)\left\{\frac{\varphi(z-h,t)-2\varphi(z,t)+\varphi(z+h,t)}{h^2}\right\} \tag{6.2.3}$$

in which $0 \leq \theta \leq 1$ and $\varphi = \varphi(z,t)$ will be represented $X = X(z,t)$ and $Y = Y(z,t)$.

A family of numerical methods can be derived by taking a linear combination of the non-linear terms at times t_n and t_{n+1}, giving

$$\begin{aligned}
&\frac{1}{\ell}\{X_m^{n+1}-X_m^n\}+\frac{\rho\,\theta}{2h}\{X_{m+1}^{n+1}-X_{m-1}^{n+1}\}+\frac{\rho}{2h}(1-\theta)\{X_{m+1}^n-X_{m-1}^n\}=\mu N\\
&-\mu\{a_1X_m^{n+1}+(1-a_1)X_m^n\}-b_1\,\beta\,X_m^{n+1}Y_m^n-c_1\,\beta\,X_m^nY_m^{n+1}-(1-b_1-c_1)\beta X_m^nY_m^n\\
&\quad+\frac{\alpha\,\theta}{h^2}\{X_{m-1}^{n+1}-2X_m^{n+1}+X_{m+1}^{n+1}\}+\frac{\alpha}{h^2}(1-\theta)\{X_{m-1}^n-2X_m^n+X_{m+1}^n\}
\end{aligned} \tag{6.2.4}$$

and

$$\begin{aligned}
&\frac{1}{\ell}\{Y_m^{n+1}-Y_m^n\}+\frac{\rho\,\theta}{2h}\{Y_{m+1}^{n+1}-Y_{m-1}^{n+1}\}+\frac{\rho}{2h}(1-\theta)\{Y_{m+1}^n-Y_{m-1}^n\}\\
&\qquad=a_2\,\beta X_m^{n+1}Y_m^n+b_2\,\beta X_m^nY_m^{n+1}+(1-a_2-b_2)\beta X_m^nY_m^n\\
&\qquad-(\mu+\nu)\{c_2Y_m^{n+1}+(1-c_2)Y_m^n\}+\frac{\alpha\,\theta}{h^2}\{Y_{m-1}^{n+1}-2Y_m^{n+1}+Y_{m+1}^{n+1}\}\\
&\qquad+\frac{\alpha}{h^2}(1-\theta)\{Y_{m-1}^n-2Y_m^n+Y_{m+1}^n\}.
\end{aligned} \tag{6.2.5}$$

Equations (6.2.4) and (6.2.5) then may be rearranged to yield

$$\begin{aligned}
&-\Big\{\frac{1}{2}\rho r\theta+\alpha p\theta\Big\}X_{m-1}^{n+1}+\Big[1+2\alpha p\theta+a_1\mu\ell+b_1\beta\ell Y_m^n\Big]X_m^{n+1}+\Big\{\frac{1}{2}\rho r\theta-\alpha p\theta\Big\}X_{m+1}^{n+1}\\
&\qquad+c_1\beta\ell X_m^nY_m^{n+1}=\Big\{(1-\theta)(\frac{1}{2}\rho r+\alpha p)\Big\}X_{m-1}^n\\
&\qquad\qquad+\Big[1-2(1-\theta)\alpha p-(1-a_1)\mu\ell-(1-b_1-c_1)\beta\ell Y_m^n\Big]X_m^n\\
&\qquad\qquad+\Big\{(1-\theta)(\alpha p-\frac{1}{2}\rho r)\Big\}X_{m+1}^n+\mu N\ell
\end{aligned} \tag{6.2.6}$$

and

$$\begin{aligned}
&-\Big\{\frac{1}{2}\rho r\theta+\alpha p\theta\Big\}Y_{m-1}^{n+1}+\Big[1+2\alpha p\theta+c_2(\mu+\nu)\ell-b_2\beta\ell X_m^n\Big]Y_m^{n+1}\\
&\qquad+\Big\{\frac{1}{2}\rho r\theta-\alpha p\theta\Big\}Y_{m+1}^{n+1}-a_2\beta\ell Y_m^nX_m^{n+1}=\Big\{(1-\theta)(\frac{1}{2}\rho r+\alpha p)\Big\}Y_{m-1}^n\\
&\qquad\qquad+\Big[1-2(1-\theta)\alpha p-(1-c_2)(\mu+\nu)\ell+(1-a_2-b_2)\beta\ell X_m^n\Big]Y_m^n,\\
&\qquad\qquad+\Big\{(1-\theta)(\alpha p-\frac{1}{2}\rho r)\Big\}Y_{m+1}^n
\end{aligned} \tag{6.2.7}$$

where $r = \ell/h$ and $p = \ell/h^2$.

The local truncation error associated with (6.2.6) at the point $(z,t) = (z_m, t_n)$ follows from (6.2.4) and is given by

$$\begin{aligned}
\mathcal{L}_S[S(z,t), I(z,t) : h, l] \doteq\ & \ell^{-1}\{S(z,t+\ell) - S(z,t)\} \\
& +(2h)^{-1}\,\rho\,\theta\{S(z+h,t+\ell) - S(z-h,t+\ell)\} \\
& +(2h)^{-1}\,\rho\,(1-\theta)\{S(z+h,t) - S(z-h,t)\} - \mu N \\
& +\mu\{a_1 S(z,t+\ell) + (1-a_1)S(z,t)\} + b_1\,\beta\,S(z,t+\ell)I(z,t) \\
& +c_1\,\beta\,S(z,t)I(z,t+\ell) + (1-b_1-c_1)\beta S(z,t)I(z,t) \\
& -h^{-2}\,\alpha\,\theta\{S(z-h,t+\ell) - 2S(z,t+\ell) + S(z+h,t+\ell)\} \\
& -h^{-2}\,\alpha\,(1-\theta)\{S(z-h,t) - 2S(z,t) + S(z+h,t)\} \qquad (6.2.8)
\end{aligned}$$

Expanding $S(z,t+\ell)$, $S(z\pm h,t+\ell)$, $S(z\pm h,t)$ and $I(z,t+\ell)$ as Taylor series about (z,t) leads to

$$\begin{aligned}
\mathcal{L}_S[S(z,t), I(z,t) : h, l] = {} & h^2\Big\{\frac{\rho}{6}\frac{\partial^3 S}{\partial z^3} - \frac{\alpha}{12}\frac{\partial^4 S}{\partial z^4}\Big\} + \frac{1}{6}\rho\theta h^2\ell\frac{\partial^4 S}{\partial z^3\partial t} \\
& +\ell\Big\{\frac{1}{2}\frac{\partial^2 S}{\partial t^2} + \theta(\rho\frac{\partial^2 S}{\partial z\partial t} - \alpha\frac{\partial^3 S}{\partial z^2\partial t}) + (a_1\mu + b_1\beta I)\frac{\partial S}{\partial t} + c_1\beta S\frac{\partial I}{\partial t}\Big\} \\
& +\ell^2\Big\{\frac{1}{6}\frac{\partial^3 S}{\partial t^3} + \frac{1}{2}\theta\Big[\rho\frac{\partial^3 S}{\partial z\partial^2 t} - \alpha\frac{\partial^4 S}{\partial z^2\partial t^2}\Big] + (\frac{1}{2}a_1\mu + \frac{1}{2}b_1\beta I)\frac{\partial^2 S}{\partial t^2} \\
& +\frac{1}{2}c_1\beta S\frac{\partial^2 I}{\partial t^2}\Big\} + \ldots, \qquad (6.2.9)
\end{aligned}$$

as $h, \ell \to 0$.

The local truncation error associated with (6.2.7) at the point $(z,t) = (z_m, t_n)$ may be written down from (6.2.5) and is given by

$$\begin{aligned}
\mathcal{L}_I[S(z,t), I(z,t) : h, l] = {} & \ell^{-1}\{I(z,t+\ell) - I(z,t)\} \\
& +(2h)^{-1}\,\rho\,\theta\{I(z+h,t+\ell) - I(z-h,t+\ell)\} \\
& +(2h)^{-1}\,\rho\,(1-\theta)\{I(z+h,t) - I(z-h,t)\} - a_2\,\beta S(z,t+\ell)I(z,t) \\
& -b_2\,\beta S(z,t)I(z,t+\ell) - (1-a_2-b_2)\beta S(z,t)I(z,t) \\
& +(\mu+\nu)\{c_2 I(z,t+\ell) + (1-c_2)I(z,t)\} \\
& -h^{-2}\,\alpha\,\theta\{I(z-h,t+\ell) - 2I(z,t+\ell) + I(z+h,t+\ell)\} \\
& -h^{-2}\,\alpha\,(1-\theta)\{I(z-h,t) - 2I(z,t) + I(z+h,t)\} \qquad (6.2.10)
\end{aligned}$$

After expanding $I(z,t+\ell)$, $I(z\pm h,t+\ell)$, $I(z\pm h,t)$ and $S(z,t+\ell)$ using Taylor's expansion, about the point (z,t), equation (6.2.10) becomes

$$\begin{aligned}\mathcal{L}_I[S(z,t),I(z,t):h,l] &= h^2\Big\{\frac{\rho}{6}\frac{\partial^3 I}{\partial z^3}-\frac{\alpha}{12}\frac{\partial^4 I}{\partial z^4}\Big\}+\frac{1}{6}\rho\theta h^2\ell\frac{\partial^4 I}{\partial z^3\partial t}\\ &+\ell\Big\{\frac{1}{2}\frac{\partial^2 I}{\partial t^2}+\theta(\rho\frac{\partial^2 I}{\partial z\partial t}-\alpha\frac{\partial^3 I}{\partial z^2\partial t})+c_2(\mu+\nu)\frac{\partial I}{\partial t}-a_2\beta I\frac{\partial S}{\partial t}-b_2\beta S\frac{\partial I}{\partial t}\Big\}\\ &+\ell^2\Big\{\frac{1}{6}\frac{\partial^3 I}{\partial t^3}+\frac{1}{2}\theta\Big[\rho\frac{\partial^3 I}{\partial z\partial^2 t}-\alpha\frac{\partial^4 I}{\partial z^2\partial t^2}\Big]+\frac{1}{2}c_2(\mu+\nu)\frac{\partial^2 I}{\partial t^2}-\frac{1}{2}a_2\beta I\frac{\partial^2 S}{\partial t^2}\\ &-\frac{1}{2}b_2\beta S\frac{\partial^2 I}{\partial t^2}\Big\}+\ldots,\end{aligned}\tag{6.2.11}$$

as $h,\ell\to 0$. The above analyses of the local truncation errors show that the finite-difference scheme {(6.2.6),(6.2.7)} is always second-order accurate in space, and it can be second-order accurate in time if the combination $(a_i,b_i,c_i)=(\frac{1}{2},\frac{1}{2},\frac{1}{2})$, $i=1,2$, is used with $\theta=\frac{1}{2}$.

Then, a second-order method for solving the system (6.1.1)-(6.1.4) will be given by

$$\begin{aligned}&-\Big(\frac{1}{4}\rho r+\frac{1}{2}\alpha p\Big)X_{m-1}^{n+1}+\Big[1+\alpha p+\frac{1}{2}\mu\ell+\frac{1}{2}\beta\ell Y_m^n\Big]X_m^{n+1}+\Big(\frac{1}{4}\rho r-\frac{1}{2}\alpha p\Big)X_{m+1}^{n+1}\\ &+\frac{1}{2}\beta\ell X_m^n Y_m^{n+1}=\Big(\frac{1}{4}\rho r+\frac{1}{2}\alpha p\Big)X_{m-1}^n+\Big[1-\alpha p-\frac{1}{2}\mu\ell\Big]X_m^n\\ &+\Big(\frac{1}{2}\alpha p-\frac{1}{4}\rho r\Big)X_{m+1}^n+\mu N\ell,\end{aligned}\tag{6.2.12}$$

$$\begin{aligned}&-\Big(\frac{1}{4}\rho r+\frac{1}{2}\alpha p\Big)Y_{m-1}^{n+1}+\Big[1+\alpha p+\frac{1}{2}(\mu+\nu)\ell-\frac{1}{2}\beta\ell X_m^n\Big]Y_m^{n+1}+\Big(\frac{1}{4}\rho r-\frac{1}{2}\alpha p\Big)Y_{m+1}^{n+1}\\ &-\frac{1}{2}\beta\ell Y_m^n X_m^{n+1}=\Big(\frac{1}{4}\rho r+\frac{1}{2}\alpha p\Big)Y_{m-1}^n+\Big[1-\alpha p-\frac{1}{2}(\mu+\nu)\ell\Big]Y_m^n\\ &+\Big(\frac{1}{2}\alpha p-\frac{1}{4}\rho r\Big)Y_{m+1}^n.\end{aligned}\tag{6.2.13}$$

The method {(6.2.12),(6.2.13)} may be applied for $m=1,2,3,\ldots,M-1$. In the case $m=0$ and $m=M$, they require some modification. Applying the boundary conditions (6.1.4), would yield to second order,

$$X_1=X_{-1},\ X_{M+1}=X_{M-1}\quad\text{and}\quad Y_1=Y_{-1},\ Y_{M+1}=Y_{M-1}$$

at time levels t_n and t_{n+1}, thus introducing the exterior grid points (z_{-1},t_{n+1}), (z_{-1},t_n), (z_{n+1},t_{n+1}), (z_{n+1},t_n). Then, for $m=0$

$$\left[1+\alpha p+\frac{1}{2}\mu\ell+\frac{1}{2}\beta\ell Y_0^n\right]X_0^{n+1}-\alpha pX_1^{n+1}+\frac{1}{2}\beta\ell X_0^nY_0^{n+1}$$
$$=\alpha pX_1^n+\left[1-\alpha p-\frac{1}{2}\mu\ell\right]X_0^n+\mu N\ell, \quad (6.2.14)$$

$$\left[1+\alpha p+\frac{1}{2}(\mu+\nu)\ell-\frac{1}{2}\beta\ell X_0^n\right]Y_0^{n+1}-\alpha pY_1^{n+1}-\frac{1}{2}\beta\ell Y_0^nX_0^{n+1}$$
$$=\left[1-\alpha p-\frac{1}{2}(\mu+\nu)\ell\right]Y_0^n+\alpha pY_1^n. \quad (6.2.15)$$

The equations for $m=1,2,3,\ldots,M-1$ are unaffected. For $m=M$

$$-\alpha pX_{M-1}^{n+1}+\left[1+\alpha p+\frac{1}{2}\mu\ell+\frac{1}{2}\beta\ell Y_M^n\right]X_M^{n+1}+\frac{1}{2}\beta\ell X_M^nY_M^{n+1}$$
$$=\alpha pX_{M-1}^n+\left[1-\alpha p-\frac{1}{2}\mu\ell\right]X_M^n+\mu N\ell, \quad (6.2.16)$$

$$-\alpha pY_{M-1}^{n+1}+\left[1+\alpha p+\frac{1}{2}(\mu+\nu)\ell-\frac{1}{2}\beta\ell X_M^n\right]Y_M^{n+1}-\frac{1}{2}\beta\ell Y_M^nX_M^{n+1}$$
$$=\alpha pY_{M-1}^n+\left[1-\alpha p-\frac{1}{2}(\mu+\nu)\ell\right]Y_M^n. \quad (6.2.17)$$

6.3 Implementation

An algorithm for the implementation of the second-order method will be adapted from that described in Chapter 4. Because of the appearance of the terms containing X_m^{n+1} and Y_m^{n+1} in (6.2.12) and (6.2.13), respectively, the solution vectors $\mathbf{X}^{n+1}$, $\mathbf{Y}^{n+1}$ will be obtained simultaneously by solving a linear algebraic system of order $2(M+1)$ at each time step. Let $\mathcal{X}^{n+1}=[(\mathbf{X}^{n+1})^T,(\mathbf{Y}^{n+1})^T]^T$ and $\mathcal{X}^n=[(\mathbf{X}^n)^T,(\mathbf{Y}^n)^T]^T$, then equations (6.2.14)-(6.2.17) may be written in matrix-vector form as

$$\mathcal{W}^n\mathcal{X}^{n+1}=\mathcal{M}^n\mathcal{X}^n+\mathcal{B} \quad (6.3.1)$$

in which

$$\mathcal{W}^n=\begin{bmatrix}\mathcal{E}^n & \vdots & \mathcal{F}^n\\ \cdots & \cdots & \cdots\\ \mathcal{G}^n & \vdots & \mathcal{H}^n\end{bmatrix} \quad (6.3.2)$$

$$\mathcal{M}^n = \begin{bmatrix} \mathcal{J}^n & \vdots & O \\ \cdots & \cdots & \cdots \\ O & \vdots & \mathcal{K}^n \end{bmatrix}, \tag{6.3.3}$$

where O is the zero matrix of order $(M+1)$, and the vector $\mathcal{B}$ is the column-vector of order $2(M+1)$ given by

$$\mathcal{B} = \Big[\underbrace{\ell\mu N,\ \ldots,\ \ell\mu N}_{(M+1)\text{ times}},\ 0,\ \ldots,\ 0\Big]^T, \tag{6.3.4}$$

where T denotes transpose.

The matrices $\mathcal{W}^n$ and $\mathcal{M}^n$ are of order $2M+2$ and their sub-matrices of order $M+1$ are given by

$$\mathcal{E}^n = \begin{bmatrix} e_0 & -\alpha p & 0 & \cdots & 0 \\ -\frac{1}{4}\rho r - \frac{1}{2}\alpha p & e_1 & \frac{1}{4}\rho r - \frac{1}{2}\alpha p & & \vdots \\ 0 & \ddots & \ddots & \ddots & 0 \\ \vdots & & -\frac{1}{4}\rho r - \frac{1}{2}\alpha p & e_{M-1} & \frac{1}{4}\rho r - \frac{1}{2}\alpha p \\ 0 & \cdots & 0 & -\alpha p & e_M \end{bmatrix}, \tag{6.3.5}$$

where $e_i = 1 + \alpha p + \frac{1}{2}\mu\ell + \frac{1}{2}\beta\ell Y_i^n, \quad i = 0,1,2,\ldots,M,$

$$\mathcal{H}^n = \begin{bmatrix} h_0 & -\alpha p & 0 & \cdots & 0 \\ -\frac{1}{4}\rho r - \frac{1}{2}\alpha p & h_1 & \frac{1}{4}\rho r - \frac{1}{2}\alpha p & & \vdots \\ 0 & \ddots & \ddots & \ddots & 0 \\ \vdots & & -\frac{1}{4}\rho r - \frac{1}{2}\alpha p & h_{M-1} & \frac{1}{4}\rho r - \frac{1}{2}\alpha p \\ 0 & \cdots & 0 & -\alpha p & h_M \end{bmatrix}, \tag{6.3.6}$$

where $h_i = 1 + \alpha p + \frac{1}{2}(\mu+\nu)\ell - \frac{1}{2}\beta\ell X_i^n, \quad i = 0,1,2,\ldots,M,$

$$\mathcal{J}^n = \begin{bmatrix} j & \alpha p & 0 & \cdots & 0 \\ \frac{1}{4}\rho r + \frac{1}{2}\alpha p & j & -\frac{1}{4}\rho r + \frac{1}{2}\alpha p & & \vdots \\ 0 & \ddots & \ddots & \ddots & 0 \\ \vdots & & \frac{1}{4}\rho r + \frac{1}{2}\alpha p & j & -\frac{1}{4}\rho r + \frac{1}{2}\alpha p \\ 0 & \cdots & 0 & \alpha p & j \end{bmatrix}, \tag{6.3.7}$$

where $j = 1 - \alpha p - \frac{\ell}{2}\mu$,

$$\mathcal{K}^n = \begin{bmatrix} k & \alpha p & 0 & \cdots & 0 \\ \frac{1}{4}\rho r + \frac{1}{2}\alpha p & k & -\frac{1}{4}\rho r + \frac{1}{2}\alpha p & & \vdots \\ 0 & \ddots & \ddots & \ddots & 0 \\ \vdots & & \frac{1}{4}\rho r + \frac{1}{2}\alpha p & k & -\frac{1}{4}\rho r + \frac{1}{2}\alpha p \\ 0 & \cdots & 0 & \alpha p & k \end{bmatrix}, \tag{6.3.8}$$

where $k = 1 - \alpha p - \frac{\ell}{2}(\mu + \nu)$, and

$$\mathcal{F}^n = \text{diag}\{\frac{1}{2}\beta\ell X_i^n\} \quad i = 0, 1, 2, \ldots, M, \tag{6.3.9}$$

$$\mathcal{G}^n = \text{diag}\{-\frac{1}{2}\beta\ell Y_i^n\} \quad i = 0, 1, 2, \ldots, M \tag{6.3.10}$$

are diagonal matrices of order $M + 1$.

6.4 Stability Analysis

Throughout this section, the maximum principle analysis will be used to prove convergence of the numerical method developed in §6.2.

Equation (6.1.1) is written in the form

$$\begin{aligned} \frac{\alpha}{2}\left(\frac{\partial^2 S}{\partial z} + \frac{\partial^2 S}{\partial z}\right) &= \frac{\partial S}{\partial t} + \frac{\rho}{2}\left(\frac{\partial S}{\partial z} + \frac{\partial S}{\partial z}\right) - \mu N + \frac{1}{2}(\mu + \beta I)S + \frac{1}{2}(\mu + \beta I)S, \\ &= \frac{\partial S}{\partial t} + \frac{\rho}{2}\left(\frac{\partial S}{\partial z} + \frac{\partial S}{\partial z}\right) - \mu N + F_1(z, t, S, I) \\ &\quad + F_2(z, t, S, I), \end{aligned} \tag{6.4.1}$$

where F_1 and F_2 are assumed to be boundedly-differentiable with respect to S and I.

The solutions $S(z,t)$ and $I(z,t)$ are approximated by the functions $X(z,t)$ and $Y(z,t)$, respectively, defined on Ω, which agree with $S(z,t)$ and $I(z,t)$ on $\partial\Omega_i$, $i = 0, 1, 2$, and satisfy the following difference equation

$$\begin{aligned} \frac{\alpha}{2}\nabla_z^2(X_m^{n+1} + X_m^n) &= \nabla_t X_m^n + \frac{\rho}{2}\nabla_z(X_m^{n+1} + X_m^n) - \mu N + \frac{1}{2}(\mu + \beta Y_m^n)X_m^{n+1} \\ &\quad + \frac{1}{2}(\mu + \beta Y_m^{n+1})X_m^n, \quad n \geq 0, \end{aligned} \tag{6.4.2}$$

where

$$\begin{aligned}\nabla_z^2 X_m^n &= (X_{m-1}^n - 2X_m^n + X_{m+1}^n)/h^2,\\ \nabla_z X_m^n &= (X_{m+1}^n + X_{m-1}^n)/h,\\ \nabla_t X_m^n &= (X_m^{n+1} - X_m^n)/\ell.\end{aligned} \tag{6.4.3}$$

It is easy to see that

$$\frac{1}{2}\nabla_z^2(S_m^{n+1} + S_m^n) = \frac{1}{2}\frac{\partial^2 S_m^{n+1}}{\partial z^2} + \frac{1}{2}\frac{\partial^2 S_m^n}{\partial z^2} + \frac{h^2}{24}\left(\overline{\frac{\partial^4 S_m^{n+1}}{\partial z^4}} + \overline{\frac{\partial^4 S_m^n}{\partial z^4}}\right),$$

$$\frac{1}{2}\nabla_z(S_m^{n+1} + S_m^n) = \frac{1}{2}\frac{\partial S_m^{n+1}}{\partial z} + \frac{1}{2}\frac{\partial S_m^n}{\partial z} + \frac{h^2}{12}\left(\overline{\frac{\partial^3 S_m^{n+1}}{\partial z^3}} + \overline{\frac{\partial^3 S_m^n}{\partial z^3}}\right),$$

$$\nabla_t S_m^n = \frac{\partial S_m^{n+1}}{\partial z} - \frac{\ell}{2}\overline{\frac{\partial^2 S_m^{n+1}}{\partial t^2}},$$

$$F_1(z_m, t_{n+1}, S_m^{n+1}, I_m^n) = F_1(z_m, t_{n+1}, S_m^n, I_m^n) + (S_m^{n+1} - S_m^n)\overline{\frac{\partial F_1}{\partial S}} \tag{6.4.4}$$

$$= \tfrac{1}{2}(\mu + \beta I_m^n)S_m^n + (S_m^{n+1} - S_m^n)\overline{\frac{\partial F_1}{\partial S}},$$

$$F_2(z_m, t_{n+1}, S_m^n, I_m^{n+1}) = F_2(z_m, t_{n+1}, S_m^n, I_m^n) + (I_m^{n+1} - I_m^n)\overline{\frac{\partial F_2}{\partial I}}$$

$$= \tfrac{1}{2}(\mu + \beta I_m^n)S_m^n + (I_m^{n+1} - I_m^n)\overline{\frac{\partial F_2}{\partial I}},$$

where the barred derivatives are evaluated at intermediate argument values as called for by the mean value theorem. Substituting (6.4.4) into (6.4.1) yields

$$\begin{aligned}\frac{\alpha}{2}\nabla_z^2(S_m^{n+1} + S_m^n) &= \nabla_t S_m^n + \frac{\rho}{2}\nabla_z(S_m^{n+1} + S_m^n) - \mu N + \frac{1}{2}(\mu + \beta I_m^n)S_m^{n+1}\\ &+ \frac{1}{2}(\mu + \beta I_m^{n+1})S_m^n + \left\{\frac{\alpha h^2}{24}\left(\overline{\frac{\partial^4 S_m^{n+1}}{\partial z^4}} + \overline{\frac{\partial^4 S_m^n}{\partial z^4}}\right) + \frac{\ell}{2}\overline{\frac{\partial^2 S_m^{n+1}}{\partial t^2}}\right.\\ &- \frac{\rho h^2}{12}\left(\overline{\frac{\partial^3 S_m^{n+1}}{\partial z^3}} + \overline{\frac{\partial^3 S_m^n}{\partial z^3}}\right) - (S_m^{n+1} - S_m^n)\overline{\frac{\partial F_1}{\partial S}}\\ &- \left.(I_m^{n+1} - I_m^n)\overline{\frac{\partial F_2}{\partial I}}\right\}.\end{aligned} \tag{6.4.5}$$

The assumptions on S and I above require the boundedness of all the derivatives appearing inside the brackets along with $(S_m^{n+1} - S_m^n)$ and $(I_m^{n+1} - I_m^n)$ in the region

$\overline{\Omega}$. Hence, in this region,

$$\begin{aligned}\frac{\alpha}{2}\nabla_z^2(S_m^{n+1}+S_m^n) &= \nabla_t S_m^n + \frac{\rho}{2}\nabla_z(S_m^{n+1}+S_m^n) - \mu N + \frac{1}{2}(\mu+\beta I_m^n)S_m^{n+1} \\ &+ \frac{1}{2}(\mu+\beta I_m^{n+1})S_m^n + g_m^n \qquad (6.4.6)\end{aligned}$$

with

$$g_m^n = O(h^2+\ell). \qquad (6.4.7)$$

Let

$$Z_{1m}^n = S_m^n - X_m^n \quad \text{and} \quad Z_{2m}^n = I_m^n - Y_m^n. \qquad (6.4.8)$$

Subtracting (6.4.2) from (6.4.6), and using (6.4.8), gives

$$\begin{aligned}\frac{\alpha}{2}\nabla_z^2(Z_{1m}^{n+1}+Z_{1m}^n) &= \nabla_t Z_{1m}^n + \frac{\rho}{2}\nabla_z(Z_{1m}^{n+1}+Z_{1m}^n) + \frac{1}{2}(\mu+\beta I_m^n)S_m^{n+1} \\ &-\frac{1}{2}(\mu+\beta Y_m^n)X_m^{n+1} + \frac{1}{2}(\mu+\beta I_m^{n+1})S_m^n \\ &-\frac{1}{2}(\mu+\beta Y_m^{n+1})X_m^n + g_m^n. \qquad (6.4.9)\end{aligned}$$

As

$$\begin{aligned}F_1(z,t_{n+1},S_m^{n+1},I_m^n) &= F_1(z,t_{n+1},X_m^{n+1},Y_m^n) + \overline{\frac{\partial F_1}{\partial S}}(S_m^{n+1}-X_m^{n+1}) \\ &+\overline{\frac{\partial F_1}{\partial I}}(I_m^n - Y_m^n), \qquad (6.4.10)\\ F_2(z,t_{n+1},S_m^n,I_m^{n+1}) &= F_2(z,t_{n+1},X_m^n,Y_m^{n+1}) + \overline{\frac{\partial F_2}{\partial S}}(S_m^n-X_m^n) \\ &+\overline{\frac{\partial F_2}{\partial I}}(I_m^{n+1}-Y_m^{n+1}), \qquad (6.4.11)\end{aligned}$$

equation (6.4.9) can be rewritten in the form

$$\begin{aligned}\frac{\alpha}{2}\nabla_z^2(Z_{1m}^{n+1}+Z_{1m}^n) &= \nabla_t Z_{1m}^n + \frac{\rho}{2}\nabla_z(Z_{1m}^{n+1}+Z_{1m}^n) + \frac{1}{2}\overline{\frac{\partial F_1}{\partial S}}Z_{1m}^{n+1} + \frac{1}{2}\overline{\frac{\partial F_1}{\partial I}}Z_{2m}^n \\ &+\frac{1}{2}\overline{\frac{\partial F_2}{\partial S}}Z_{1m}^n + \frac{1}{2}\overline{\frac{\partial F_2}{\partial I}}Z_{2m}^{n+1} + g_m^n. \qquad (6.4.12)\end{aligned}$$

This may be written as

$$\begin{aligned}\frac{\alpha}{2}\nabla_z^2(Z_{1m}^{n+1}+Z_{1m}^n) &\le \nabla_t Z_{1m}^n + \frac{\rho}{2}\nabla_z(Z_{1m}^{n+1}+Z_{1m}^n) + M_{1S}\widehat{Z_{1m}^n} \\ &+M_{1I}\widehat{Z_{2m}^n} + g_m^n, \qquad (6.4.13)\end{aligned}$$

where

$$M_{1S} = \max\left\{ \overline{\frac{\partial F_1}{\partial S}}, \overline{\frac{\partial F_2}{\partial S}} \right\} \quad \text{and} \quad M_{1I} = \max\left\{ \overline{\frac{\partial F_1}{\partial I}}, \overline{\frac{\partial F_2}{\partial I}} \right\} \tag{6.4.14}$$

and

$$\widehat{Z_{1m}^n} = \frac{Z_{1m}^{n+1} + Z_{1m}^n}{2} \quad \text{and} \quad \widehat{Z_{2m}^n} = \frac{Z_{2m}^{n+1} + Z_{2m}^n}{2}. \tag{6.4.15}$$

Now, Z_{1m}^n and Z_{1m}^{n+1} vanish on $\partial\Omega_i$ $(i = 0, 1, 2)$. Assume that $\widehat{Z_{2m}^n}$ is bounded. It is known that g_m^n is bounded. Hence, by Theorem 2.15, X_m^{n+1} and X_m^n converge to S_m^{n+1} and S_m^n uniformly.

Similarly, equation (6.1.2) may be written in the form

$$\begin{aligned} \frac{\alpha}{2}\left(\frac{\partial^2 I}{\partial z} + \frac{\partial^2 I}{\partial z}\right) &= \frac{\partial I}{\partial t} + \frac{\rho}{2}\left(\frac{\partial I}{\partial z} + \frac{\partial I}{\partial z}\right) + \frac{1}{2}((\mu+\nu) - \beta S)I + \frac{1}{2}((\mu+\nu) - \beta S)I \\ &= \frac{\partial I}{\partial t} + \frac{\rho}{2}\left(\frac{\partial I}{\partial z} + \frac{\partial I}{\partial z}\right) + G_1(z,t,S,I) + G_2(z,t,S,I), \end{aligned} \tag{6.4.16}$$

where G_1 and G_2 are assumed to be boundedly-differentiable with respect to S and I.

The solutions $S(z,t)$ and $I(z,t)$ are approximated by the functions $X(z,t)$ and $Y(z,t)$, respectively, defined on Ω; they agree with $S(z,t)$ and $I(z,t)$ on $\partial\Omega_i$, $i = 0, 1, 2$ and satisfy the difference equation

$$\begin{aligned} \frac{\alpha}{2}\nabla_z^2(Y_m^{n+1} + Y_m^n) = \nabla_t Y_m^n + \frac{\rho}{2}\nabla_z(Y_m^{n+1} + Y_m^n) + \frac{1}{2}((\mu+\nu) - \beta X_m^n)Y_m^{n+1} \\ + \frac{1}{2}((\mu+\nu) - \beta X_m^{n+1})Y_m^n, \quad n \geq 0 \end{aligned} \tag{6.4.17}$$

where ∇_z^2, ∇_z and ∇_t are defined as in (6.4.3).

It is easy to show that

$$\frac{1}{2}\nabla_z^2(I_m^{n+1}+I_m^n)=\frac{1}{2}\frac{\partial^2 I_m^{n+1}}{\partial z^2}+\frac{1}{2}\frac{\partial^2 I_m^n}{\partial z^2}+\frac{h^2}{24}\left(\overline{\frac{\partial^4 I_m^{n+1}}{\partial z^4}}+\overline{\frac{\partial^4 I_m^n}{\partial z^4}}\right),$$

$$\frac{1}{2}\nabla_z(I_m^{n+1}+I_m^n)=\frac{1}{2}\frac{\partial I_m^{n+1}}{\partial z}+\frac{1}{2}\frac{\partial I_m^n}{\partial z}+\frac{h^2}{12}\left(\overline{\frac{\partial^3 I_m^{n+1}}{\partial z^3}}+\overline{\frac{\partial^3 I_m^n}{\partial z^3}}\right),$$

$$\nabla_t I_m^n=\frac{\partial I_m^{n+1}}{\partial z}-\frac{\ell}{2}\overline{\frac{\partial^2 I_m^{n+1}}{\partial t^2}},$$

$$\begin{aligned}
G_1(z_m,t_{n+1},S_m^n,I_m^{n+1}) &= G_1(z_m,t_{n+1},S_m^n,I_m^n)+(I_m^{n+1}-I_m^n)\overline{\frac{\partial G_1}{\partial I}} \qquad (6.4.18)\\
&= \frac{1}{2}(\mu+\nu-\beta S_m^n)I_m^n+(I_m^{n+1}-I_m^n)\overline{\frac{\partial G_1}{\partial I}},\\
G_2(z_m,t_{n+1},S_m^{n+1},I_m^n) &= G_2(z_m,t_{n+1},S_m^n,I_m^n)+(S_m^{n+1}-S_m^n)\overline{\frac{\partial G_2}{\partial S}}\\
&= \frac{1}{2}(\mu+\nu-\beta S_m^n)I_m^n+(S_m^{n+1}-S_m^n)\overline{\frac{\partial G_2}{\partial S}},
\end{aligned}$$

where the barred derivatives are evaluated at intermediate argument values as called for by the mean value theorem. Substituting (6.4.18) into (6.4.16) gives

$$\begin{aligned}
\frac{\alpha}{2}\nabla_z^2(I_m^{n+1}+I_m^n) &= \nabla_t I_m^n+\frac{\rho}{2}\nabla_z(I_m^{n+1}+I_m^n)+\frac{1}{2}((\mu+\nu)-\beta S_m^n)I_m^{n+1}\\
&+ \frac{1}{2}((\mu+\nu)-\beta S_m^{n+1})I_m^n+\left\{\frac{\alpha h^2}{24}\left(\overline{\frac{\partial^4 I_m^{n+1}}{\partial z^2}}+\overline{\frac{\partial^4 I_m^n}{\partial z^2}}\right)\right.\\
&+ \frac{\ell}{2}\overline{\frac{\partial^2 I_m^{n+1}}{\partial t^2}}-\frac{\rho h^2}{12}\left(\overline{\frac{\partial^3 I_m^{n+1}}{\partial z^3}}+\overline{\frac{\partial^3 I_m^n}{\partial z^3}}\right)-(I_m^{n+1}-I_m^n)\overline{\frac{\partial G_1}{\partial I}}\\
&- \left.(S_m^{n+1}-S_m^n)\overline{\frac{\partial G_2}{\partial S}}\right\}. \qquad (6.4.19)
\end{aligned}$$

The assumptions on S and I above require the boundedness of all the derivatives appearing inside the brackets along with $(S_m^{n+1}-S_m^n)$ and $(I_m^{n+1}-I_m^n)$ in the region $\overline{\Omega}$. Hence, in this region,

$$\begin{aligned}
\frac{\alpha}{2}\nabla_z^2(I_m^{n+1}+I_m^n) &= \nabla_t I_m^n+\frac{\rho}{2}\nabla_z(I_m^{n+1}+I_m^n)+\frac{1}{2}((\mu+\nu)-\beta S_m^{n+1})I_m^n\\
&+ \frac{1}{2}((\mu+\nu)-\beta S_m^n)I_m^{n+1}+g_m^n \qquad (6.4.20)
\end{aligned}$$

with

$$g_m^n=O(h^2+\ell). \qquad (6.4.21)$$

Subtracting (6.4.20) from (6.4.17) and using the definitions of the truncation errors in (6.4.8) gives

$$\begin{aligned}\frac{\alpha}{2}\nabla_z^2(Z_{2m}^{n+1}+Z_{2m}^n) &= \nabla_t Z_{2m}^n+\frac{\rho}{2}\nabla_z(Z_{2m}^{n+1}+Z_{2m}^n)+\frac{1}{2}((\mu+\nu)-\beta S_m^n)I_m^{n+1}\\ &\quad -\frac{1}{2}((\mu+\nu)-\beta X_m^n)Y_m^{n+1}+\frac{1}{2}((\mu+\nu)-\beta S_m^{n+1})I_m^n\\ &\quad -\frac{1}{2}((\mu+\nu)-\beta X_m^{n+1})Y_m^n+g_m^n. \qquad (6.4.22)\end{aligned}$$

As

$$\begin{aligned}G_1(z,t_{n+1},S_m^n,I_m^{n+1}) &= G_1(z,t_{n+1},X_m^n,Y_m^{n+1})+\overline{\frac{\partial G_1}{\partial S}}(S_m^n-X_m^n)\\ &\quad +\overline{\frac{\partial G_1}{\partial I}}(I_m^{n+1}-Y_m^{n+1}), \qquad (6.4.23)\\ G_2(z,t_{n+1},S_m^{n+1},I_m^n) &= G_2(z,t_{n+1},X_m^{n+1},Y_m^n)+\overline{\frac{\partial G_2}{\partial S}}(S_m^{n+1}-X_m^{n+1})\\ &\quad +\overline{\frac{\partial G_2}{\partial I}}(I_m^n-Y_m^n), \qquad (6.4.24)\end{aligned}$$

it follows that equation (6.4.22) may be written as

$$\begin{aligned}\frac{\alpha}{2}\nabla_z^2(Z_{2m}^{n+1}+Z_{2m}^n) &= \nabla_t Z_{2m}^n+\frac{\rho}{2}\nabla_z(Z_{2m}^{n+1}+Z_{2m}^n)+\frac{1}{2}\overline{\frac{\partial G_1}{\partial S}}Z_{1m}^n+\frac{1}{2}\overline{\frac{\partial G_1}{\partial I}}Z_{2m}^{n+1}\\ &\quad +\frac{1}{2}\overline{\frac{\partial G_2}{\partial S}}Z_{1m}^{n+1}+\frac{1}{2}\overline{\frac{\partial G_2}{\partial I}}Z_{2m}^n+g_m^n, \qquad (6.4.25)\end{aligned}$$

with Z_{2m}^n and Z_{2m}^{n+1} vanishing on $\partial\Omega_i$.

Let

$$M_{2S}=\max\left\{\overline{\frac{\partial G_1}{\partial S}},\overline{\frac{\partial G_2}{\partial S}}\right\} \quad \text{and} \quad M_{2I}=\max\left\{\overline{\frac{\partial G_1}{\partial I}},\overline{\frac{\partial G_2}{\partial I}}\right\}.$$

Then, equation (6.4.25) can be written as

$$\begin{aligned}\frac{\alpha}{2}\nabla_z^2(Z_{2m}^{n+1}+Z_{2m}^n) &\le \nabla_t Z_{2m}^n+\frac{\rho}{2}\nabla_z(Z_{2m}^{n+1}+Z_{2m}^n)+M_{2S}\widehat{Z_{1m}^n}\\ &\quad +M_{2I}\widehat{Z_{2m}^n}+g_m^n, \qquad (6.4.26)\end{aligned}$$

with $\widehat{Z_{1m}^n}$ and $\widehat{Z_{2m}^n}$ are defined as in (6.4.15).

Assume that $\widehat{Z_{1m}^n}$ is bounded. Since Z_{2m}^n and Z_{2m}^{n+1} vanish on $\partial\Omega_i$, it follows from Theorem 2.15 that Y_m^n and Y_m^{n+1} converge uniformly to I_m^n and I_m^{n+1}.

6.5 Numerical Results

Following Chapter 4, experiment A was carried out and method {(6.2.12),(6.2.13)} was used to solve the initial/boundary-value problem (6.1.1)-(6.1.4) thus monitoring the numbers of susceptible and infectious individuals, respectively. The parameters N, μ, ν and β are as in the previous chapters. The numerical experiments were carried out to see the behaviour of the numerical solutions for various values of the diffusion and convection rates.

Case $\alpha < \rho$

The diffusion and convection rates were chosen to be $\alpha = 0.01$, $\rho = 0.5$ and $\alpha = 0.1$, $\rho = 1.0$. The method {(6.2.12),(6.2.13)} produced positive solutions for $\ell < 0.0436$ with $\alpha = 0.01$, $\rho = 0.5$ and for $\ell < 0.0488$ with $\alpha = 0.1$, $\rho = 1.0$ leading to negative results, and to overflow as ℓ was increased further. The numerical results are depicted in Figures 6.1-6.4. These show that the behaviour of the whooping cough dynamics changed: that is, the symmetry about the line $x = 0.5$ was completely changed as t increased.

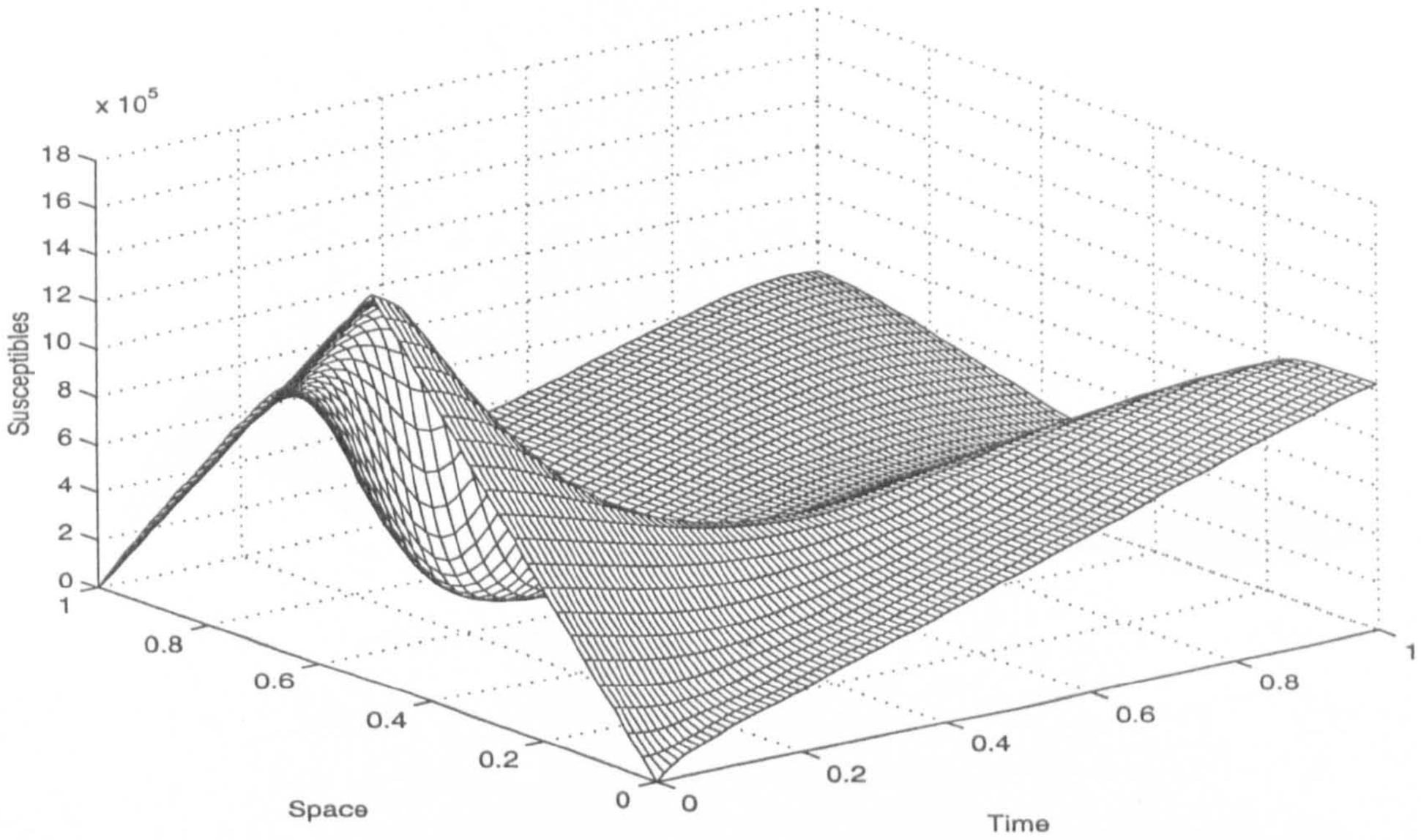

Figure 6.1: Three dimensional profile of susceptibles at $t = 1.0$; $\alpha = 0.01$, $\rho = 0.5$, $h = 0.025$ and $\ell = 0.01$.

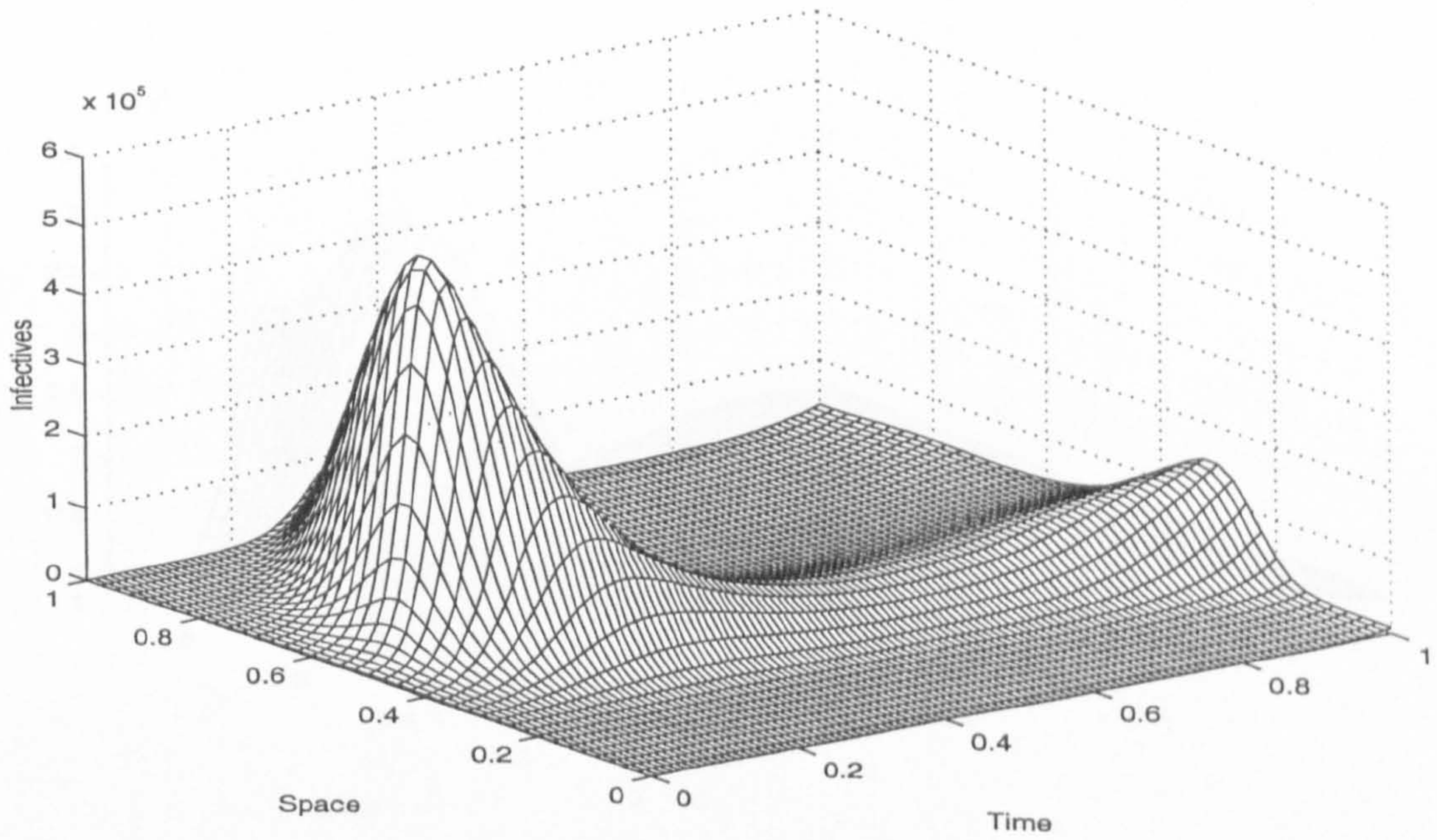

Figure 6.2: Three dimensional profile of infectives at $t = 1.0$; $\alpha = 0.01$, $\rho = 0.5$, $h = 0.025$ and $\ell = 0.01$.

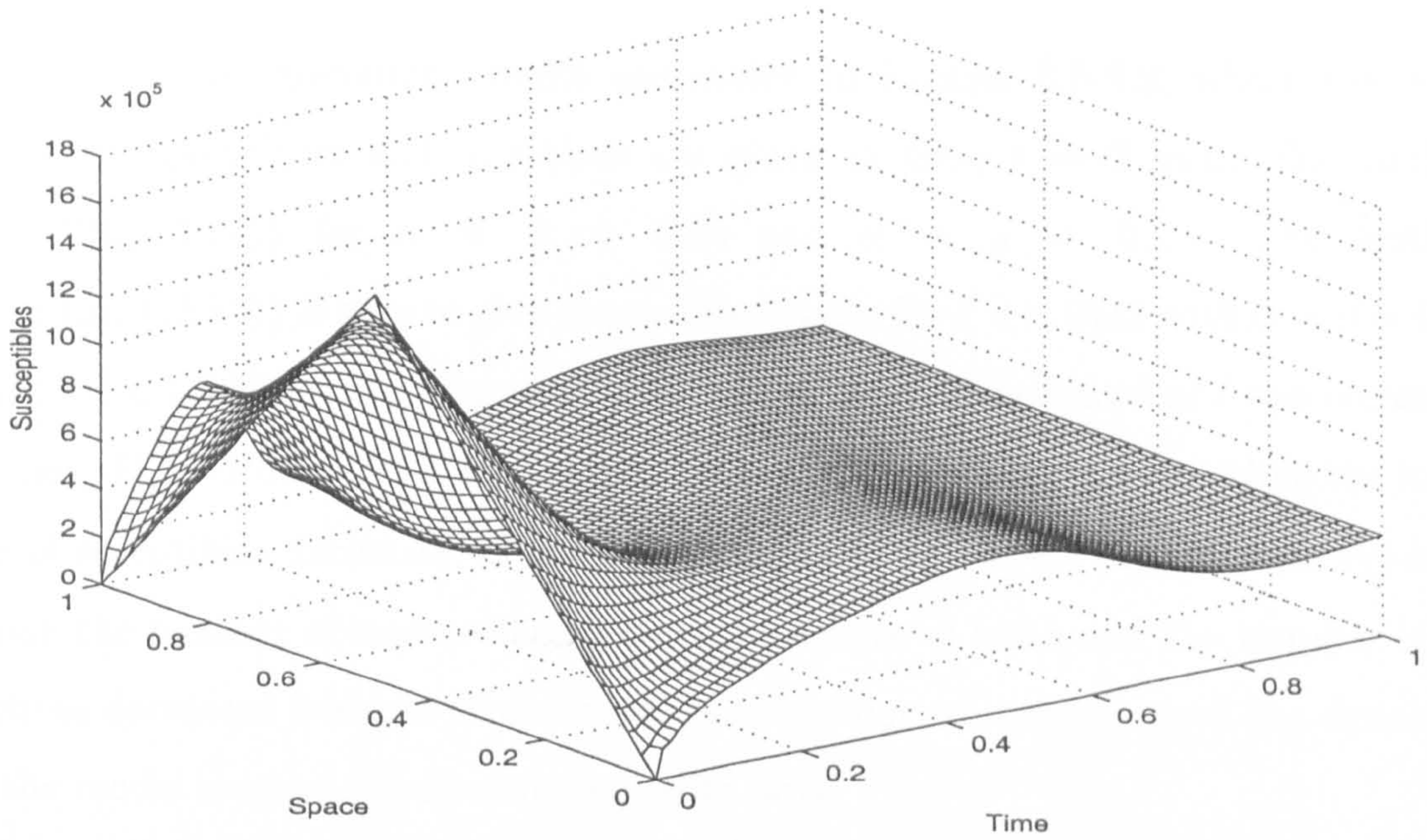

Figure 6.3: Three dimensional profile of susceptibles at $t = 1.0$; $\alpha = 0.1$, $\rho = 1.0$, $h = 0.025$ and $\ell = 0.01$.

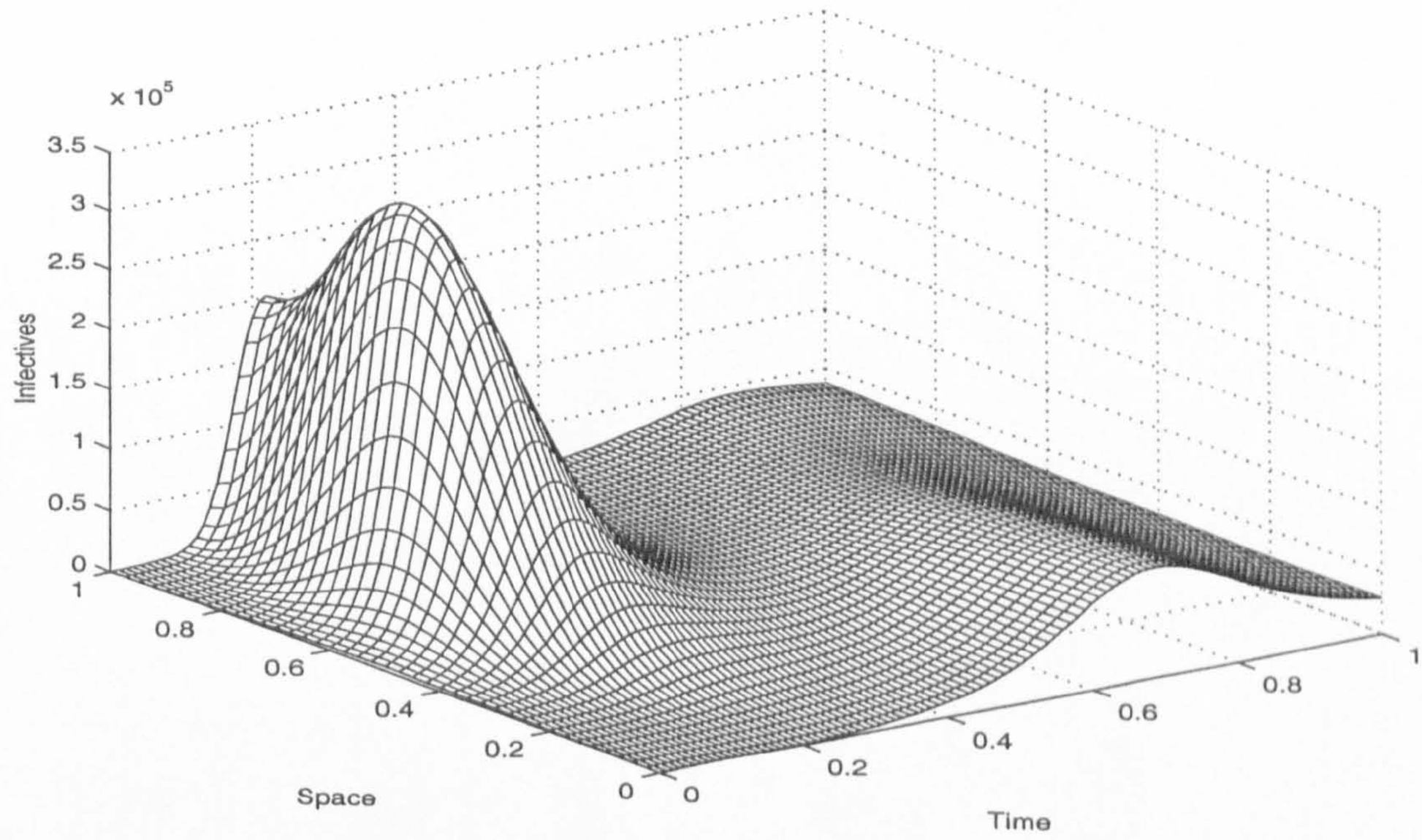

Figure 6.4: Three dimensional profile of infectives at $t = 1.0$; $\alpha = 0.1$, $\rho = 1.0$, $h = 0.025$ and $\ell = 0.01$.

Case $\alpha = \rho$

In this case the numerical results are shown in Figures 6.5-6.8, where the wave forms of susceptibles and infectives are given at time $t = 2$ using the method {(6.2.12),(6.2.13)} for $\alpha = \rho = 0.05$ and $\alpha = \rho = 0.1$. The method {(6.2.12),(6.2.13)} is seen to give reasonable results for $\ell < 0.0432$ with $\alpha = \rho = 0.05$ and for $\ell < 0.0461$ with $\alpha = \rho = 0.1$ after which overflow occurred as ℓ was increased further. Figures 6.5-6.8 show that the number of infectives increases while the number of suseptibles decreases. These are seen clearly at $t \approx 0.5$ (approximately) after which the number of susceptibles increased because of birth and the number of infectives decreased because of death. This behaviour continuous until the dynamics of the model reach a steady state as t gets large.

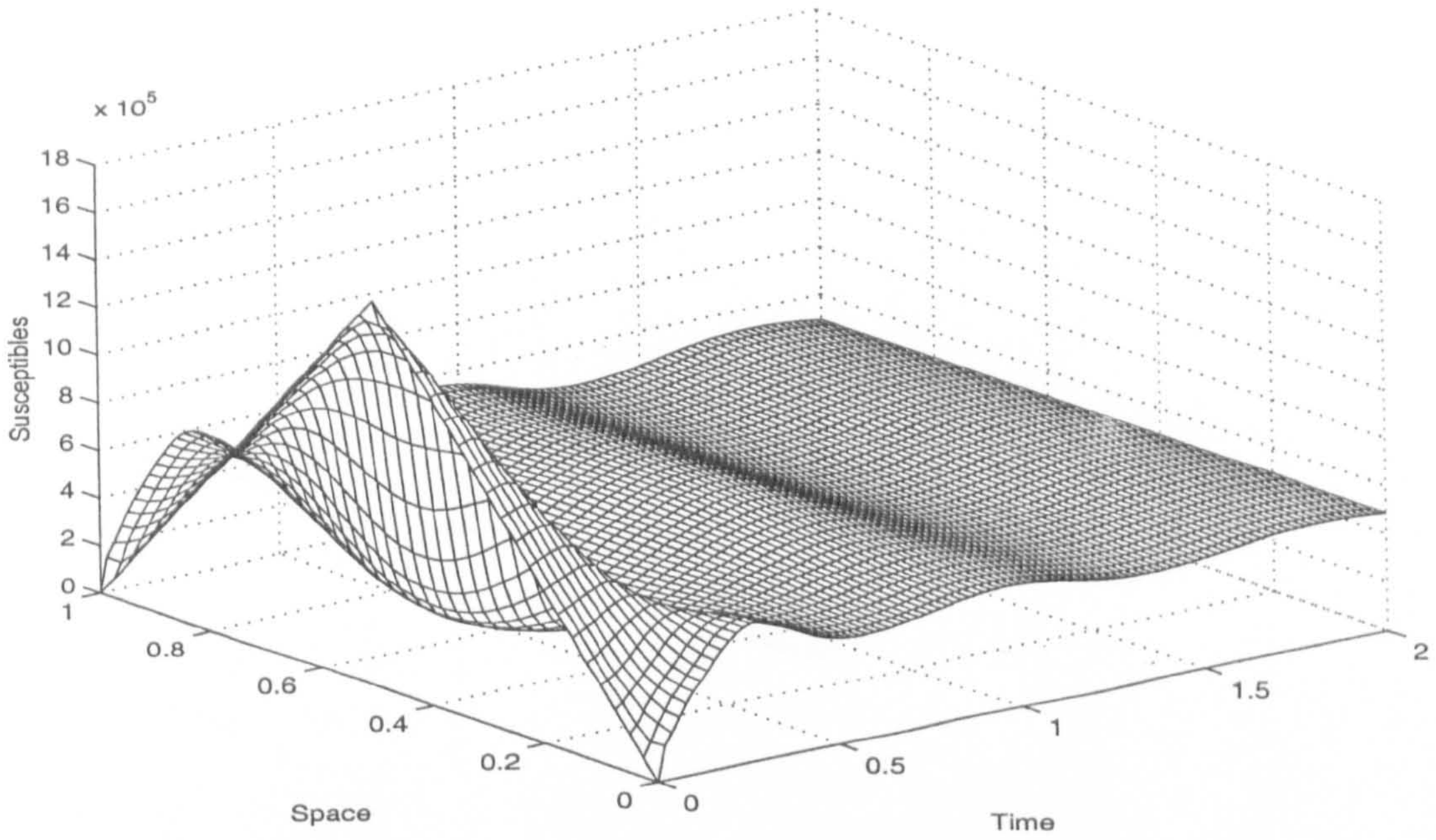

Figure 6.5: Three dimensional profile of susceptibles at $t = 2.0$; $\alpha = \rho = 0.05$, $h = 0.025$ and $\ell = 0.02$.

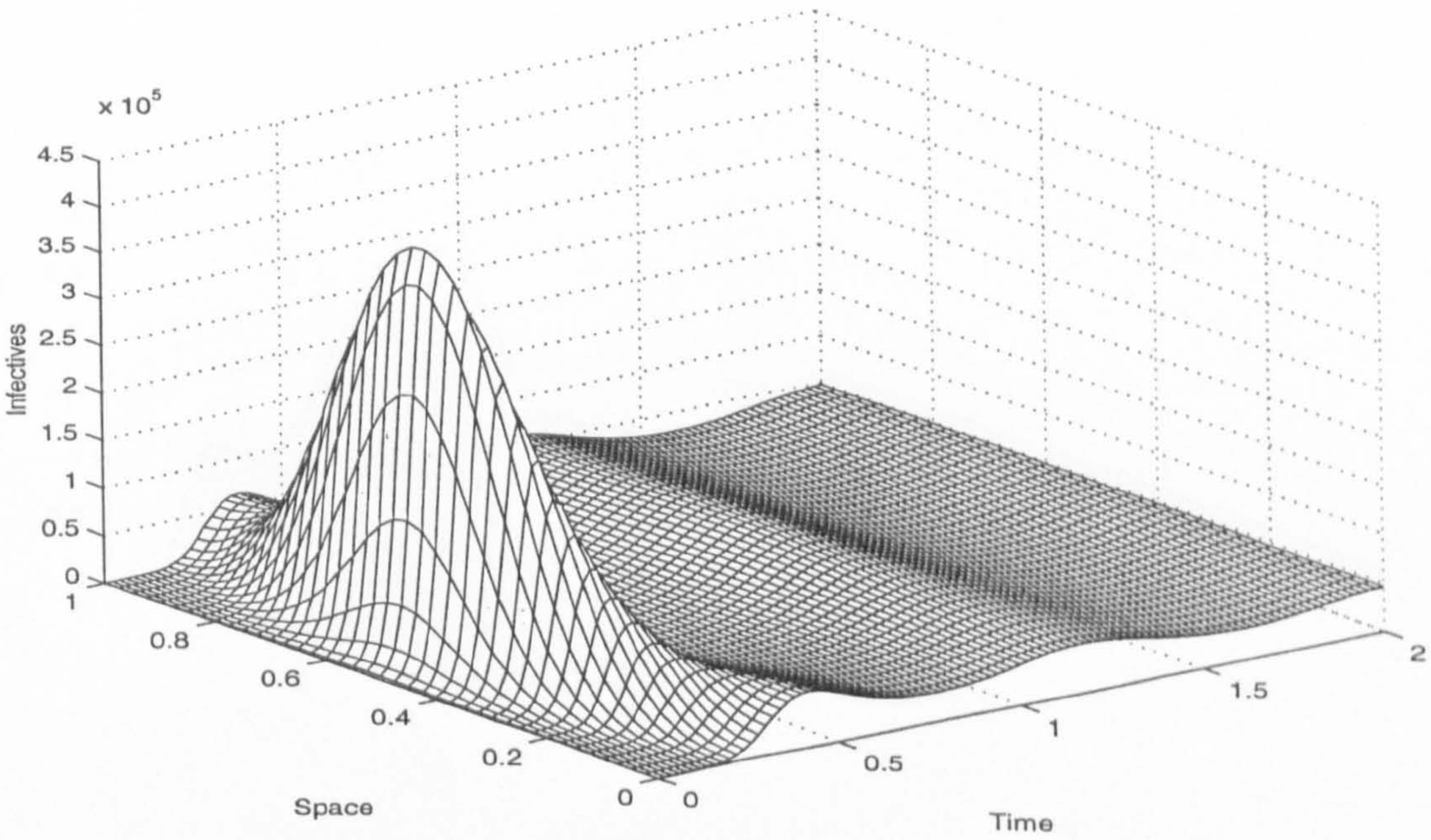

Figure 6.6: Three dimensional profile of infectives at $t = 2.0$; $\alpha = \rho = 0.05$, $h = 0.025$ and $\ell = 0.02$.

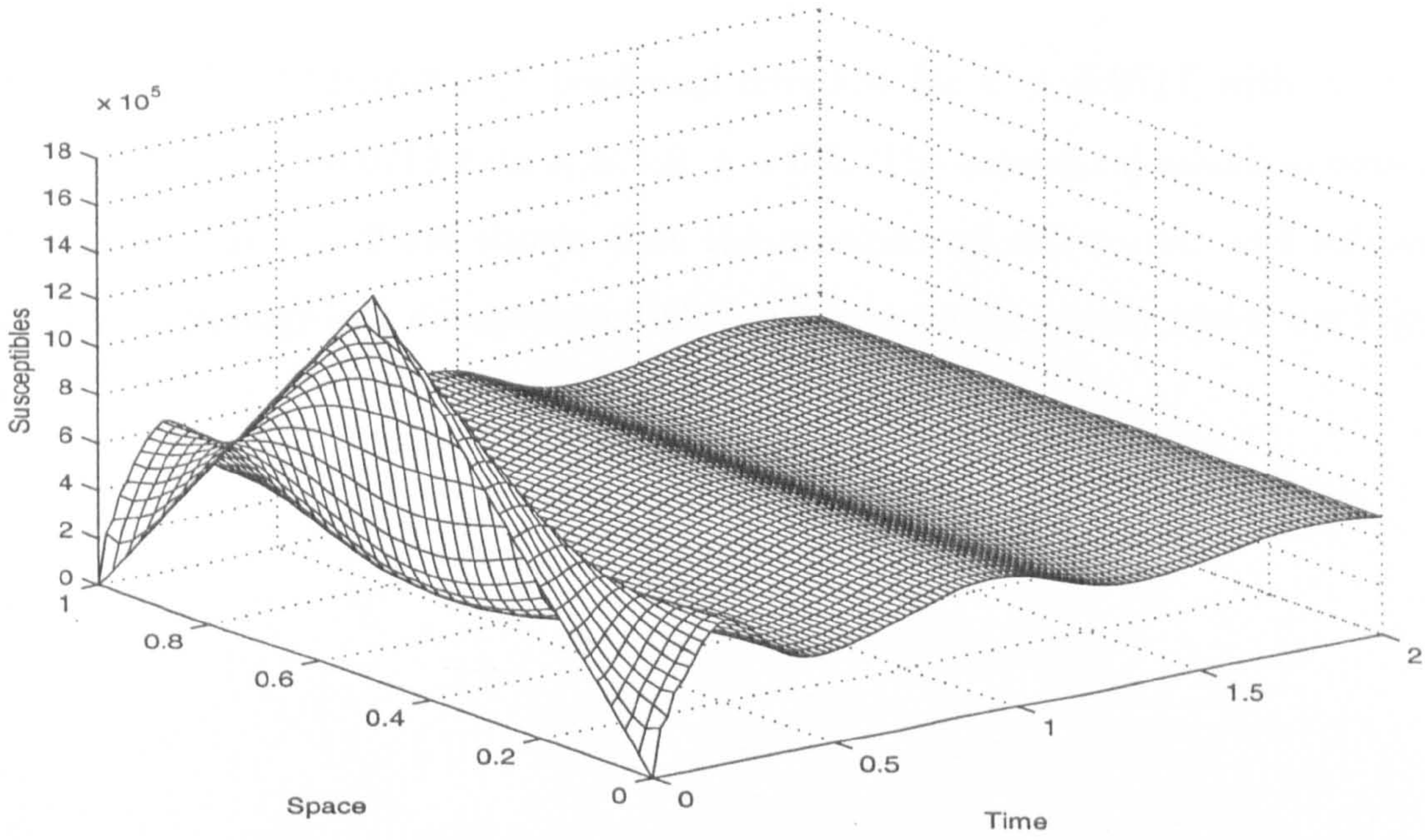

Figure 6.7: Three dimensional profile of susceptibles at $t = 2.0$; $\alpha = \rho = 0.1$, $h = 0.025$ and $\ell = 0.02$.

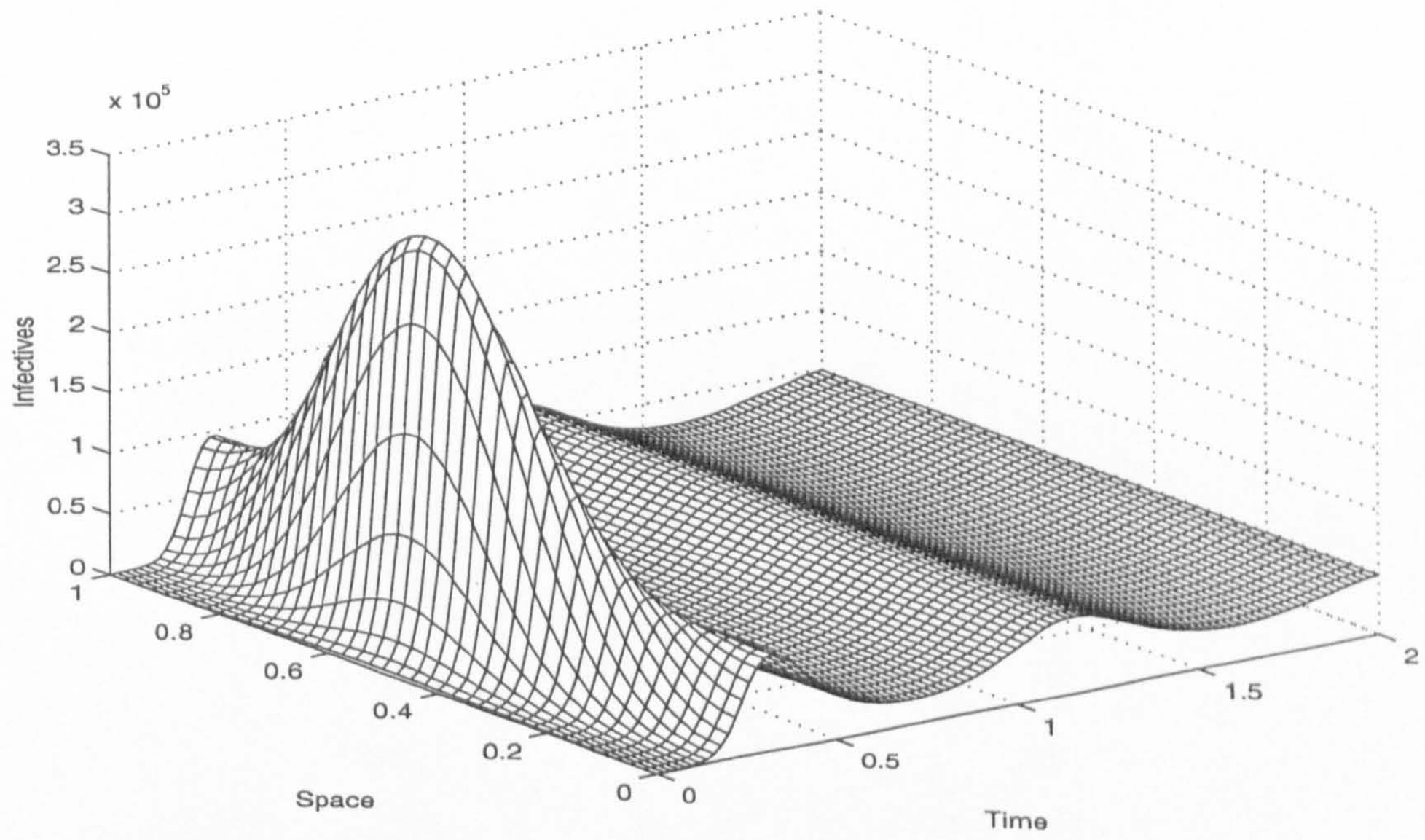

Figure 6.8: Three dimensional profile of infectives at $t = 2.0$; $\alpha = \rho = 0.1$, $h = 0.025$ and $\ell = 0.02$.

Case $\alpha > \rho$

The method {(6.2.12),(6.2.13)} produced overflow for $\ell > 0.0717$ with $\alpha = 1.0$, $\rho = 0.01$ and for $\ell > 0.0719$ with $\alpha = 1.0$, $\rho = 0.5$. The numerical solutions obtained with $\ell = 0.02$ at $t = 2$ are shown that the numbers of susceptible and infectious individuals converge in a damped oscillatory manner to the steady state, see Figures 6.9-6.12.

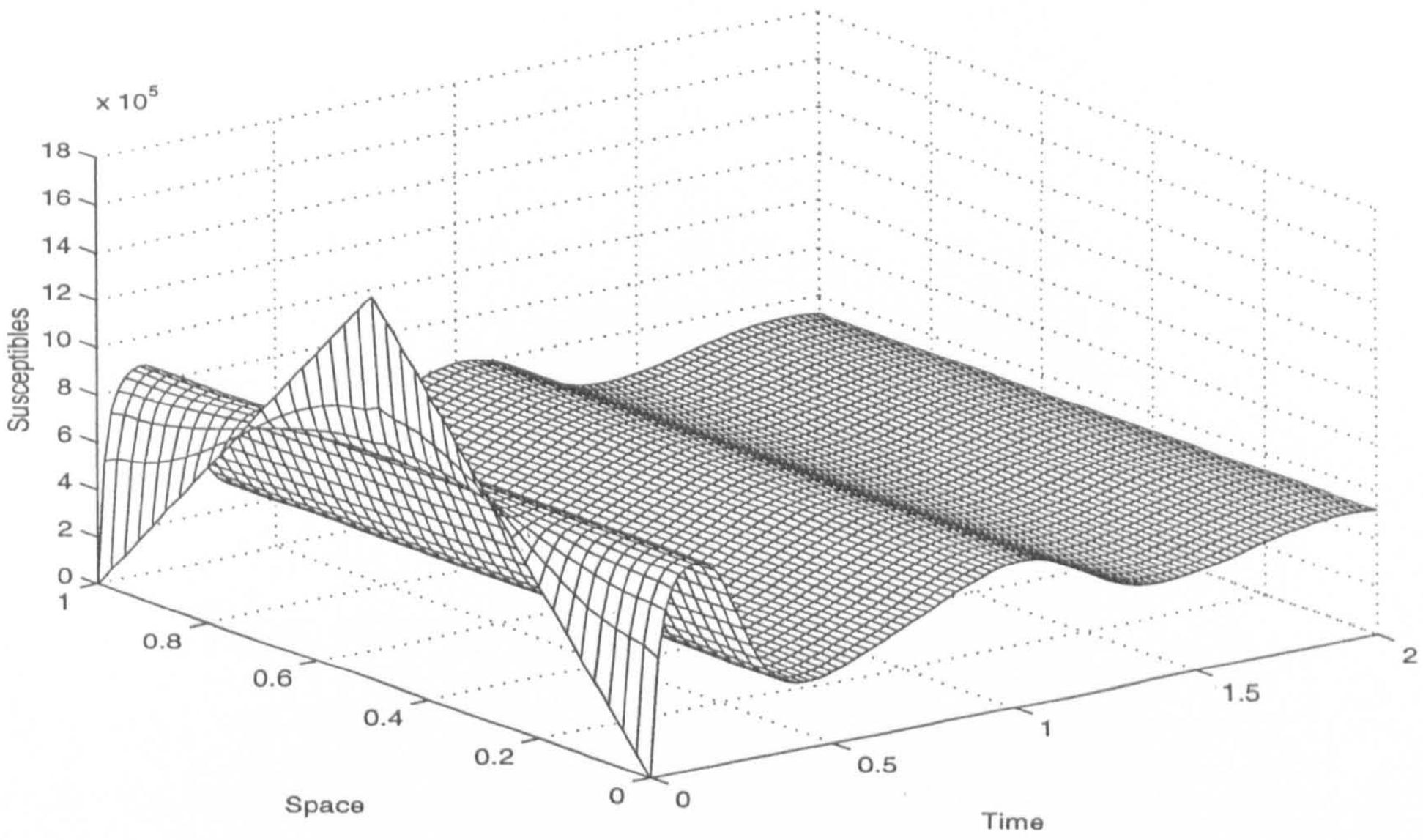

Figure 6.9: Three dimensional profile of susceptibles; $\alpha = 1.0$, $\rho = 0.01$, $h = 0.025$ and $\ell = 0.02$.

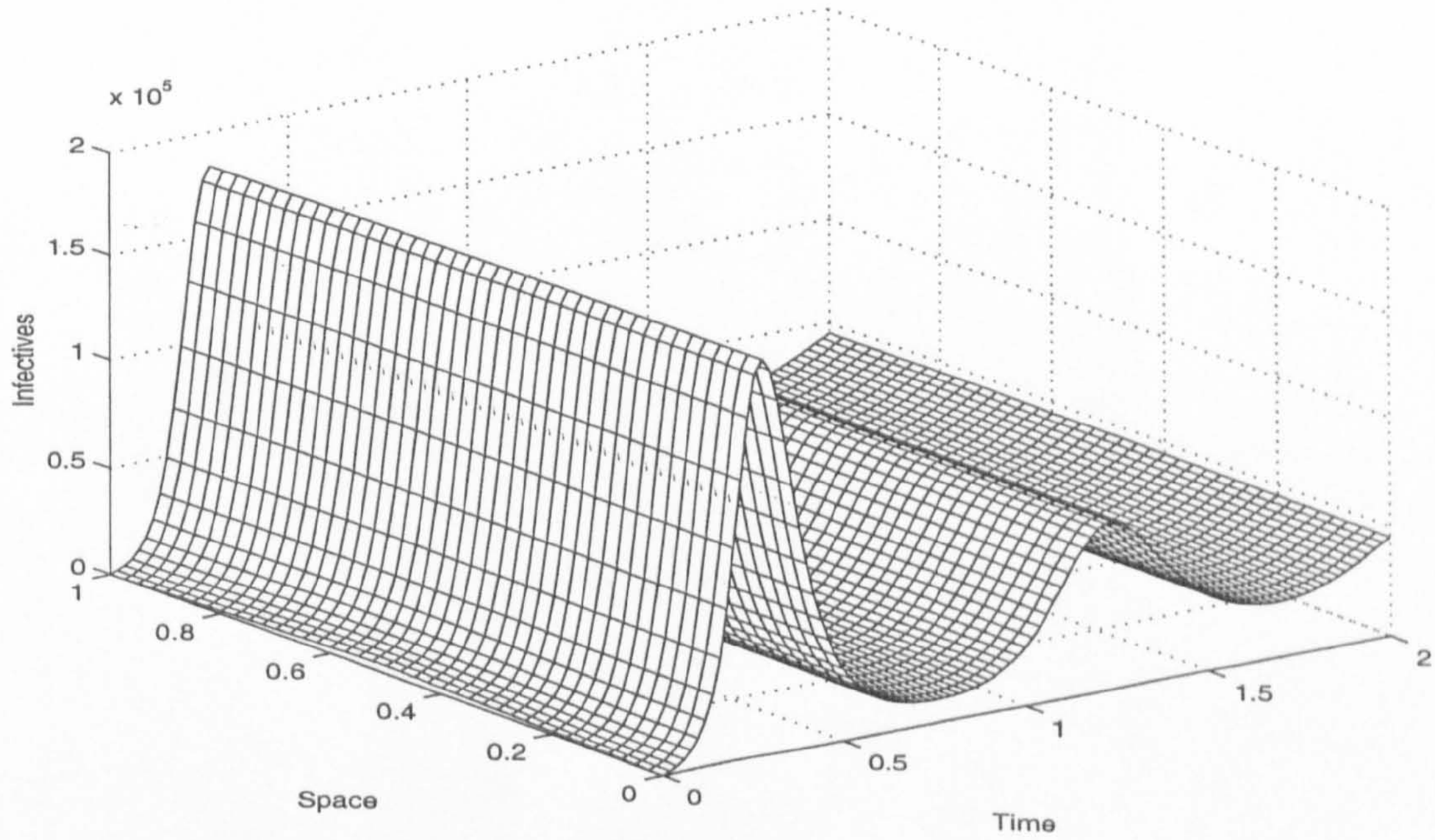

Figure 6.10: Three dimensional profile of infectives; $\alpha = 1.0$, $\rho = 0.01$, $h = 0.025$ and $\ell = 0.02$.

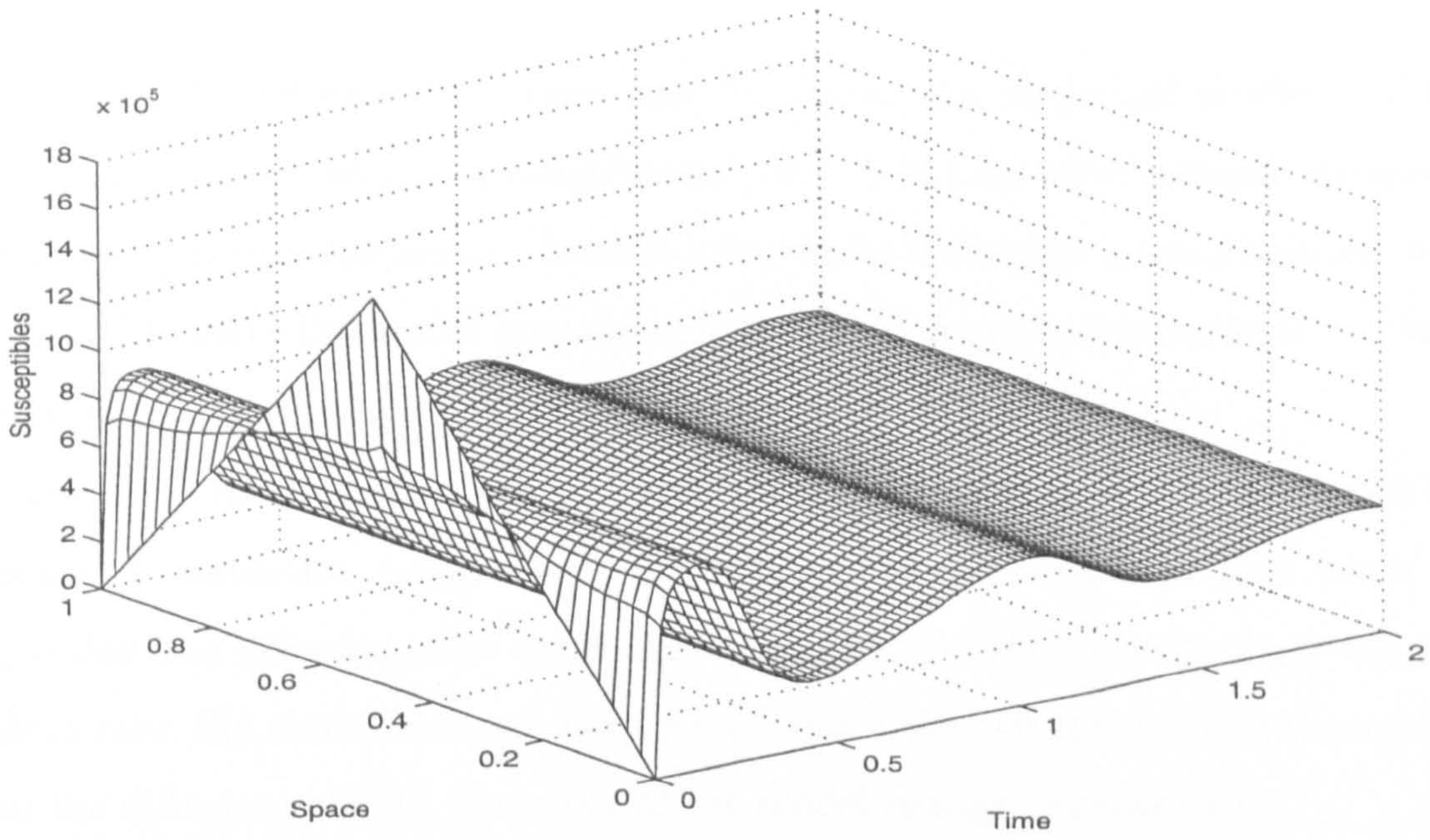

Figure 6.11: Three dimensional profile of susceptibles; $\alpha = 2.0$, $\rho = 1.00$, $h = 0.025$ and $\ell = 0.02$.

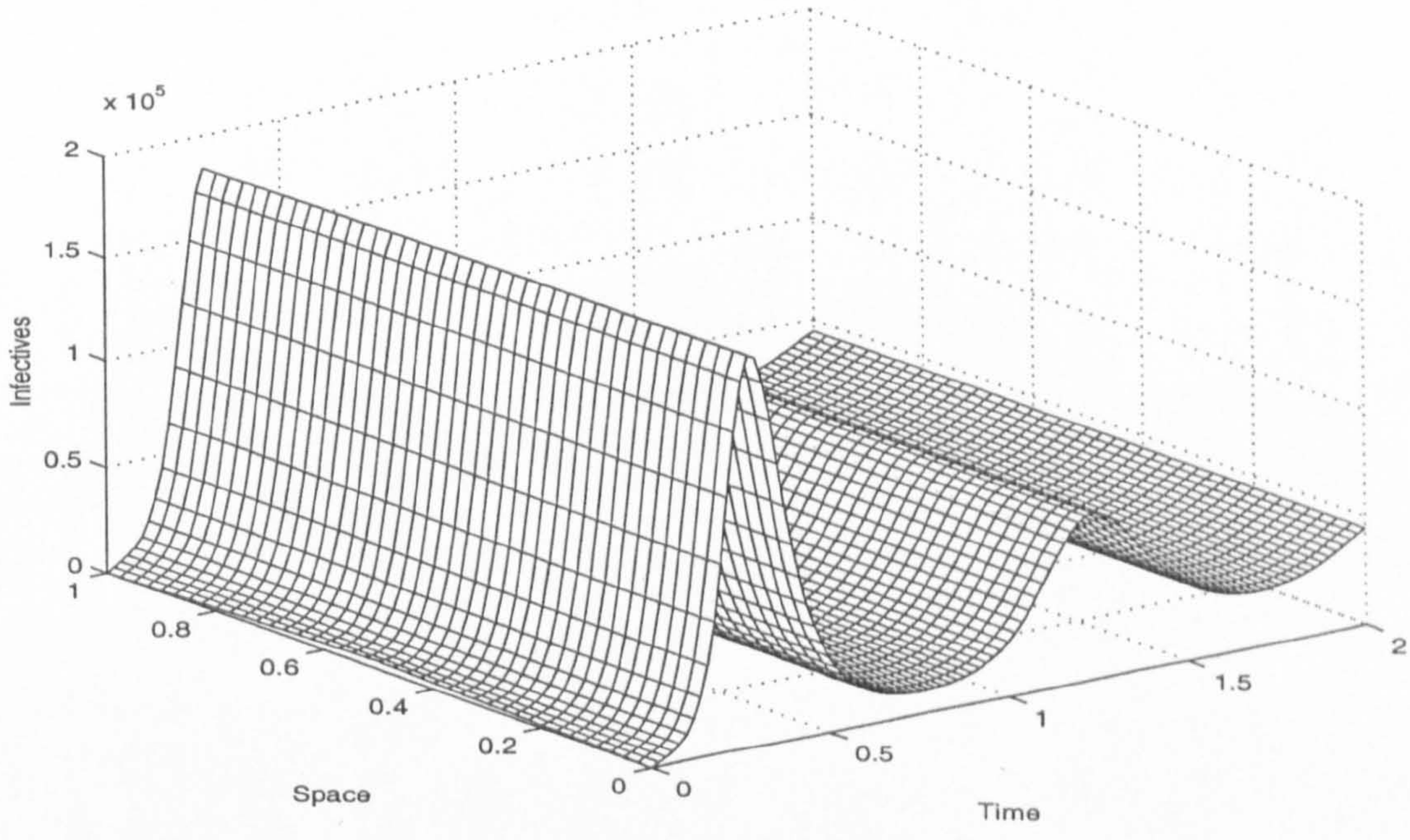

Figure 6.12: Three dimensional profile of infectives; $\alpha = 2.0$, $\rho = 1.00$, $h = 0.025$ and $\ell = 0.02$.

6.6 Summary

Finite-difference schemes have been used to obtain the numerical solutions of the diffusion-convection whooping cough model, (6.1.1)-(6.1.4), which models the spread of whooping cough epidemics. Second-order finite-difference approximations were developed to solve the model equations. The maximum principle analysis was used to analyse convergence.

The study indicates that the whooping cough dynamics is dependent on the diffusion and convection rates. It is seen from the results obtained that when the convection and diffusion rates are equal or the diffusion rate is larger than the convection rate, the model behaved as expected and when the convection rate was less than the diffusion rate the dynamics of the model change unexpectedly.

Chapter 7

Conclusions

In this thesis, mathematical modelling of the transmission dynamics of whooping cough has centred on the *SIR* compartmental model. The differential equations involved in this model usually cannot be solved analytically and thus numerical methods have been developed for their solution.

First- and second-order methods have been developed for the numerical solution of the model ODEs and PDEs. The second-order methods were developed by taking a linear combination of first-order methods. The proposed methods are characterized to be implicit. In each case, however, it is observed that the solution may be obtained explicitly. The *SIR* whooping cough model involving non-linear ODEs was studied and analysed in detail first of all. Stability analysis showed that there are two critical (equilibrium) points: one is trivial (no disease) and the other is non-trivial. A threshold condition determines which of these two critical points is stable. If the value of the basic reproductive number ($\mathcal{R}_0$ as described in Chapter 3) is greater than unity, the system settles down in the epidemic state. In this case, the equilibrium is approached *via* damped oscillations. Throughout the numerical simulations of the ODEs with $\mathcal{R}_0 < 1$ and $\mathcal{R}_0 > 1$, it was found that using a sufficiently small value of the time step, ℓ, with the first of the first-order methods (Euler method), the solutions obtained converged to the correct fixed point. For $\mathcal{R}_0 > 1$, the Euler method produced the solution moving to a stable limit cycle rather than to the stable non-trivial fixed point when the time step exceeds a certain value. As with most

problems solved using it, the Euler method required a severe restriction on the size of the time step.

To avoid chaotic or spurious solutions, while still permitting the use of a large time-step, alternative methods of first and second order have been proposed for the numerical solution of the *SIR* whooping cough model. It was seen that the proposed methods have superior stability properties to the Euler method to which they are compared. One of the alternative first-order methods, Method $\mathcal{M}_2$, showed superior convergence in the sense that the solution obtained converged to the fixed point for all $\ell > 0$. An alternative method, Method $\mathcal{M}_3$, of the same order converged to the fixed point faster than other proposed methods. This method induced chaotic behaviour in the numerical solutions for $\mathcal{R}_0 > 1$ whenever the parameter of time discretization exceeded a certain value. The second-order method showed more accuracy but this method is very restrictive on stepsize for $\mathcal{R}_0 > 1$ and converged to the trivial fixed point ($\mathcal{R}_0 < 1$) for large values of the stepsize. The proposed methods, however, converge to the correct fixed point for a sufficiently small time step.

The *SIR* whooping cough model has been extended to three systems of partial differential equations, namely reaction-diffusion, reaction-convection and reaction-convection-diffusion types as described in Chapters 4, 5 and 6, respectively. The development of numerical methods for solving the system of ordinary differential equations was adapted for the numerical solutions of those systems. In a series of numerical experiments, the spread of whooping cough in one dimension was discussed for $\mathcal{R}_0 > 1$. The study indicated that the whooping cough dynamics was dependent on the diffusion rate, the convection rate and the initial distributions. It is also seen that the numerical methods developed are economical and reliable in that the solutions are obtained by solving a single linear algebraic system at each time step as opposed to solving a non-linear system which is the case most of the time when solving non-linear PDEs. The chaos present in the proposed numerical methods was investigated and was avoided by choosing appropriate time steps.

As a conclusion, the model investigated in this thesis, called the *SIR* model (see Chapter 3), is seen to simulate the dynamics of whooping cough adequately in that it captures the essence of microparasitic interaction that builds the foundation of the disease. More sophisticated models are readily formulated but will usually still have the simple *SIR* model in their core. Hence it makes sense to understand the dynamics of this model before turning to more complicated and, hopefully, more realistic approaches. Furthermore, the qualitative properties of the *SIR* model can be derived analytically, the numerical methods can be tested easily on how good they approximated the true behaviour of the system. It may, therefore, be envisaged that the methods developed which perform well on the simple model will do so on a more sophisticated approach. Future work is to study the model for whooping cough transmission and vaccination and the model incorporating age structure.

References

[1] Ablowitz, M. J. & Herbst, B. M. On homoclinic structure and numerically induced chaos for the nonlinear Schrödinger equation, *SIAM J. Appl. Math.* **50**, 339-351 (1990).

[2] Al-Showaikh, F. N. M. *Ph. D. thesis,* Brunel University, 1998.

[3] Anderson, R. M. & May, R. M. *Infectious Diseases of Humans: Dynamics and Control,* Oxford University Press, 1992.

[4] Bolker, B. M. & Grenfell, B. T. Space, persistence and dynamics of measles epidemics. *Phil. Trans. R. Soc. Lond.* B **348**, 309-320 (1995).

[5] Burden, R. L. & Faires, J. D. *Numerical Analysis,* 6th ed., Brooks/Cole Pub. Co., Pacific Grove, 1997.

[6] Corless, R. M., Essex, C. & Neremberg, M. A. H. Numerical methods can suppress chaos. *Phys. Lett.* A **157**, 27-36 (1991).

[7] Dietz, K. The incidence of infectious diseases under the influence of seasonal fluctuations. In *Mathematical Models in Medicine,* Lecture Notes in Biomathematics, No. 11, Springer-Verlag, New York, pp.1-15, 1976.

[8] Douglas, J., Jr. On the numerical integration of quasi-linear parabolic differential equations. *Pacific Journal of Mathematics.* **6**, 35-42 (1956).

[9] Ducan, C. J., Duncan, S. R. & Scott, S. Whooping cough epidemics in London, 1701-1812: infection dynamics, seasonal forcing and the effects of malnutrition. *Proc. R. Soc. Lond.* B **263**, 445-450 (1996).

[10] Duncan, S. R., Scott, S. & Duncan, C. J. Modelling the different smallpox epidemics in England. *Phil. Trans. R. Soc. Lond.* B **346**, 407-419 (1994).

[11] Gleick, J. *Chaos: Making a New Science.* Sphere Books(Cardinal), London, 1988.

[12] Gray, P. & Scott, S. K. *Chemical Oscillations and Instability: Non-linear Chemical Kinetics.* Oxford Clarendon Press, 1994.

[13] Herges, Udo. S. *Ph. D. thesis,* Brunel University, 1995.

[14] Hethcote, H. W. Three basic epidemiological models. In: Levin, S. A., Hallam, T. G. and Gross, L. J. (eds) *Applied Mathematical Ecology,* Biomathematics vol 18, Springer-Verlag, New York, pp. 119-144, 1989.

[15] Lambert, J. D. *Numerical Methods for Ordinary Differential Systems: the Initial-Value Problem,* Wiley & Sons, New York, 1991.

[16] Lees, M. Approximate solutions of parabolic equations. *J. Soc. Indust. Appl. Math.* 7(2), 167-183 (1959).

[17] Luenberger, D. G. *Introduction to Dynamic Systems: Theory, Models and Applications.* Wiley & Sons, New York, 1979.

[18] London, W. P. & Yorke, J. A. Recurrent outbreaks of measles, chickenpox and mumps. I. Seasonal variation in contact rates. *Am. J. Epidemiol.* **98**, 453-468 (1973).

[19] Mitchell, A. R. & Griffiths, D. F. *The Finite Difference Method in Partial Differential Equations,* Wiley & Sons, New York, 1980.

[20] Olsen, L. F. & Schaffer, W. M. Chaos versus noisy periodicity: alternative hypotheses for childhood epidemics. *Science, Wash* **249**, 499-504 (1990).

[21] Piyawong, W. & Twizell, E. H. Technical Report TR/11/00, Department of Mathematical Sciences, Brunel University, Uxbridge, Middlesex, UB8 3PH, May 2000.

[22] Protter, M. H. & Weinberger, H. F. *Maximum Principles in Differential Equations.* Prentice-Hall, New Jersey, 1967.

[23] Rand, D. A. & Wilson, H. B. Chaotic stochasticity: a ubiquitous source of unpredictability in epidemics. *Proc. R. Soc. Lond.* B **246**, 179-184 (1991).

[24] Rose, M. E. On the integration of non-linear parabolic equations by implicit difference methods. *Quart. Appl. Math.* **15**, 237-248 (1956).

[25] Sandefur, J. T. *Discret Dynamical Systems: Theory and Applications.* Clarendon Press, Oxford, 1990.

[26] Schaffer, W. M. & Kott, M. Nearly one-dimensional dynamics in an epidemic. *J. Theor. Biol.* **112**, 403-427 (1985).

[27] Tidd, C. W., Olsen, L. F. & Schaffer, W. M. The case for chaos in childhood epidemics. II. Predicting historical epidemics from mathematical models. *Proc. R. Soc. Lond.* B **254**, 257-273 (1993).

[28] Twizell, E. H. *Computational Methods for Partial Differential Equations,* Ellis Horwood, Chichester, 1984.

[29] Twizell, E. H. *Numerical Methods, with Applications in the Biomedical Sciences,* Ellis Horwood, Chichester, 1988.

[30] Twizell, E. H., Wang, Y., & Price, W. G. Chaos-free numerical solutions of reaction-diffusion equations. *Proc. R. Soc. Lond.* A **430**, 541-576 (1990).

[31] Wiggins, S. *Introduction to Applied Nonlinear Dynamical Systems and Chaos.* Springer-Verlag, New York, 1990.

Bibliography

[1] Aron, J. L. & Schwartz, I. B. Seasonality and period-doubling bifurcations in an epidemic model. *J. Theor. Biol.* **110**, 665-679 (1984).

[2] Conte, S. D. & Carl de Boor. Conte, S. D. *Elementary Numerical Analysis : An Algorithmic Approach.* McGraw-Hill, London, 1980.

[3] Drazin, P. G. *Nonlinear Systems.* Cambridge University Press, 1992.

[4] Greenspan, G. & Casulli, V. *Numerical Analysis for Applied Mathematics, Science, and Engineering.* Addison-Wesley, California, 1988.

[5] Guckenheimer, J. & Holmes, P. *Nonlinear Oscillations, Dynamical Systems, and Bifurcations of Vector Fields.* Springer-Verlag, New York, 1983.

[6] Hethcote H. W. The mathematics of infectious diseases. *SIAM Review* **42**(4), 599-653 (2000).

[7] Jain, M. K. *Numerical Solution of Differential Equations.* 2sd ed., Wiley Eastern, New Delhi, 1984.

[8] Jordan, D. W. & Smith, P. *Nonlinear Ordinary Differential Equations.* 2nd ed., Clarendon Press, Oxford, 1987.

[9] Lapidus, L. & Pinder, G. F. *Numerical Solution of Partial Differential Equations in Science and Engineering.* Wiley & Sons, New York, 1982.

[10] Smith G. D. *Numerical Solution of Partial Differential Equations: Finite Difference Methods.* 3rd ed., Clarendon Press, Oxford, 1985.

[11] Smith, H. L. Subharmonic bifurcation in an S-I-R Epidemic model. *J. Math. Biol.* **17**, 163-177 (1983).

[12] Street, R. L. *The Analysis and Solution of Partial Differential Equations.* Brooks/Cole Pub. Co., California, 1973.

[13] Twizell, E. H., Wang, Y., Price, W. G. & Fakhr F. Finite-difference methods for solving the reaction-diffusion equations of a simple isothermal chemical system. *Numer. Meth. Part. Difft. Equations* **10**, 435-454 (1994).

[14] Verhulst, F. *Nonlinear Differential Equations and Dynamical Systems.* Springer-Verlag, New York, 1989.

[15] Wright, P. F. Pertussis in developing coutries: definition of the problem and prospects for control. *Rev. Infect. Dis.* **13**, S528-534 (1991).